GPO PRICE     $ _____

OTS PRICE(S) $ _____

Hard copy (HC) _4.00_

Microfiche (MF) _1.00_

# TECHNICAL   MEMORANDUM

## X-184

DECLASSIFIED BY AUTHORITY OF NASA
CLASSFICATION CHANGE NOTICES NO. 12
DATED 5-26-65 ITEM NO. 6

A WIND-TUNNEL INVESTIGATION OF THE CARRY LOADS AND MUTUAL

INTERFERENCE EFFECTS OF 1/40-SCALE MODELS OF THE

X-15 AND B-52 AIRPLANES IN COMBINATION

By Robert T. Taylor and William J. Alford, Jr.

Langley Research Center
Langley Field, Va.

DECLASSIFIED: EFFECTIVE 1-29-65
AUTHORITY F.G. DRCEKA (ATSS#1)
Memo dated 5-13-65; AFSDO 5439

# NATIONAL  AERONAUTICS  AND  SPACE  ADMINISTRATION

WASHINGTON                            December 1959

NATIONAL AERONAUTICS AND SPACE ADMINISTRATION

TECHNICAL MEMORANDUM X-184

A WIND-TUNNEL INVESTIGATION OF THE CARRY LOADS AND MUTUAL

INTERFERENCE EFFECTS OF 1/40-SCALE MODELS OF THE

X-15 AND B-52 AIRPLANES IN COMBINATION[*]

By Robert T. Taylor and William J. Alford, Jr.

SUMMARY

*26633*

A wind-tunnel investigation has been made of the aerodynamic charac-
teristics of a North American X-15 model and of a Boeing B-52 model under
conditions simulating launching of the X-15 from the B-52. Buffeting
data also were obtained on the right-hand horizontal-tail panel of the
B-52 model behind the X-15 model installation. The data are presented
without analysis; however, the reader is directed to NASA Memoran-
dum 6-8-59L which offers a brief analysis of the X-15 launch problem.

*Author*

INTRODUCTION

Past aerial launchings of research airplanes have been made from
the center-line location of the carrier airplane. In the case of the
X-15, B-52 combination, however, the carry location chosen is beneath
the 18-percent semispan of the right wing. The choice of such an asym-
metrical location raises questions as to the carry loads and launching
safety of the combination.

A wind-tunnel investigation was therefore undertaken in the Langley
high-speed 7- by 10-foot wind tunnel to determine the carry loads, the
mutual interference effects, and a qualitative measure of the B-52
horizontal-tail panel buffeting due to the installation of the X-15.

The purpose of the present paper is to present, without analysis,
the results of these wind-tunnel tests with some notes on the reduction
of the data. A brief analysis of the X-15 launch problem based on these
data is given in reference 1. The data of the present paper were used
in reference 1 to determine static stability derivatives and to estimate
damping derivatives in calculating the X-15 drop motion at the design
conditions of altitude and Mach number.

---

[*]Title, Unclassified.

## COEFFICIENTS AND SYMBOLS

The longitudinal data represented herein are about the stability axis and the lateral data are about the body axis. The positive sense of the coefficients and angles used in the paper are given in figure 1 (on the left for the X-15 and on the right for the B-52). The force and moment coefficients are based on the dimensions of the model for which the data are given.

$C_L$       lift coefficient, $\dfrac{\text{Lift}}{qS}$

$C_D$       drag coefficient, $\dfrac{\text{Drag}}{qS}$

$C_D'$       approximate drag coefficient, $\dfrac{\text{Approximate drag}}{qS}$

$C_m$       pitching-moment coefficient about $\bar{c}/5$ on X-15 or about $\bar{c}/4$ on B-52, $\dfrac{\text{Pitching moment}}{qS\bar{c}}$

$C_l$       rolling-moment coefficient about balance axial center line, $\dfrac{\text{Rolling moment}}{qSb}$

$C_n$       yawing-moment coefficient about $\bar{c}/5$ on X-15 or $\bar{c}/4$ on B-52, $\dfrac{\text{Yawing moment}}{qSb}$

$C_Y$       side-force coefficient, $\dfrac{\text{Side force}}{qS}$

$C_B$       B-52 horizontal-tail root bending-moment coefficient (positive root moment caused by upload at tip), $\dfrac{\text{Root bending moment}}{q\,\dfrac{St}{2}\,\dfrac{bt}{2}}$

$q$       free-stream dynamic pressure, $\frac{1}{2}\rho V^2$, lb/sq ft

$\rho$       free-stream density, slugs/cu ft

$\bar{c}_w$       mean aerodynamic chord of wing, ft

$\bar{c}_h$      mean aerodynamic chord of wing, ft

$r$      radius, in.

$V$      free-stream velocity, ft/sec

$c$      chord, ft

$\bar{c}$      mean aerodynamic chord, ft

$b$      wing span, ft

$b_t$      horizontal-tail span, ft

$R$      Reynolds number

$S$      wing area, sq ft

$S_t$      horizontal-tail area, sq ft

$\alpha$      B-52 angle of attack, deg

$\Delta\alpha$      X-15 incidence relative to B-52, deg

$\alpha'$      X-15 angle of attack, deg

$\beta$      angle of sideslip, deg

$\Delta\beta = \beta_{X-15} - \beta_{B-52}$

$\phi$      angle of bank, deg

$i_t$      B-52 horizontal-tail incidence, deg

$\delta_r$      X-15 vertical-tail deflection, deg

$\delta_e$      X-15 horizontal-tail deflection, deg

$\delta_B$      X-15 speed-brake deflection, deg

$M$      free-stream Mach number

$X,Y,Z$      airplane body axes

$z$      separation distance, measured normal to B-52 center line, in.

4

$\delta_a$        differential horizontal-tail deflection, $\delta_{e,R} - \delta_{e,L}$, deg

$\Delta M$       root-mean-square buffeting bending moment of right horizontal tail, in-lb upload at tip gives positive moment

$\delta_f$        deflection of outboard B-52 flap, deg

Subscripts:

X-15       refers to X-15 model

B-52       refers to B-52 model

R           right-hand tail panel

L           left-hand tail panel

w          wind axis

## MODEL AND APPARATUS

The investigation was made in the Langley high-speed 7- by 10-foot wind tunnel. The models used were 1/40-scale representations of the B-52 and X-15 airplanes. Sketches of the models and modification details are presented in figure 2. Photographs of the various model installations are shown in figure 3. With the X-15 in the captive condition (pylon mounted), data were taken from two six-component strain-gage balances, one in each model. In addition, buffeting data were recorded from a strain gage mounted on the root of the right-hand horizontal-tail panel of the B-52 model. It should be pointed out that no attempt was made to scale this panel structurally; however, an instantaneous reading pressure gage recording the pressure difference between the upper and lower surfaces was installed in the panel directly back of the X-15 model to assess the power content of the X-15 wake over the frequency range of interest.

During the tests to determine the aerodynamic characteristics of the X-15 (X-15 sting mounted) while traversing the flow field of the B-52, no aerodynamic and buffeting measurements were made on the B-52 model.

Further data were obtained on each model individually through the Mach number range.

## TESTS AND CORRECTIONS

The tests were made over a Mach number range from 0.40 to 0.85. The range of test Reynolds number for each model is presented in figure 4. The primary variables of the investigation included the angles of attack and sideslip of both models individually and in combination, and the angles of attack, sideslip, and bank of the X-15 in the presence of the B-52 at several separation distances. Tests to determine control effectiveness of the X-15 in the captive position were made to permit estimates of carry loads due to control deflection. Data also were obtained on both models separately in the tunnel. Additional data were obtained on the clean B-52 model with No. 60 carborundum grains applied at the position of estimated full-scale boundary-layer transition. This estimation was made by using the method of reference 2.

### Carry Tests

This series of tests was conducted with the X-15 model mounted on a 6-component strain-gage balance suspended beneath the pylon under the B-52 wing. The attitude of the X-15 with respect to the B-52 reference line was measured (wind-off) as $\alpha_0 = 2.25^O$, $\beta = 0^O$, and $\phi = 0^O$. The jet-boundary corrections applied to these data (ref. 3) are those induced by the B-52 model. When corrections for the effects of tunnel blockage (ref. 4) were applied to the data, the drag of both models was considered.

The drag of the B-52 model was corrected to the condition of free-stream static pressure at the model base. No base-pressure correction was applied to the X-15 data. Corrections to the model angle of attack due to support deflections have been applied to the data for both models.

### Separation Tests

During this series of tests the X-15 model was sting-mounted in the presence of the B-52. (See fig. 3(e).) As mentioned previously, no B-52 data were taken under these conditions. The blockage corrections for these tests were the same as the corrections applied to the data for the X-15 when pylon mounted. No jet-boundary corrections have been applied to these data. Also the base-pressure correction has not been applied to the X-15 data. Deviations of the X-15 angle of attack due to support deflection have been accounted for but corrections to the vertical displacement due to support flexibility are unknown and are therefore not applied. In this connection it should be pointed out that a fouling circuit was installed between the mating surfaces of the pylon and the X-15 fuselage to indicate when the X-15 model touched the pylon. No data were taken under such conditions.

### Tests of the X-15 and B-52 Separately

These tests concerned each model tested individually in the tunnel. In the case of the B-52 model, the support-deflection, blockage, jet-boundary and base-pressure corrections have been applied in the normal manner. The data taken on the X-15 model did not require correction for jet-boundary or blockage effects because of the relatively small size of the model. The data have been corrected for the effects of support deflection and the model drag has been corrected for the difference between actual test base pressure and free-stream static pressure.

### Reduction of the B-52 Tail-Panel Buffeting Data

The instantaneous output of both the root bending-moment gage and the pressure pickup were fed through appropriate instrumentation and recorded on tape. The harmonic content of these taped signals were subsequently analyzed over a frequency range from about 40 cycles per second to 750 cycles per second. A typical record so obtained is illustrated in the following sketch:
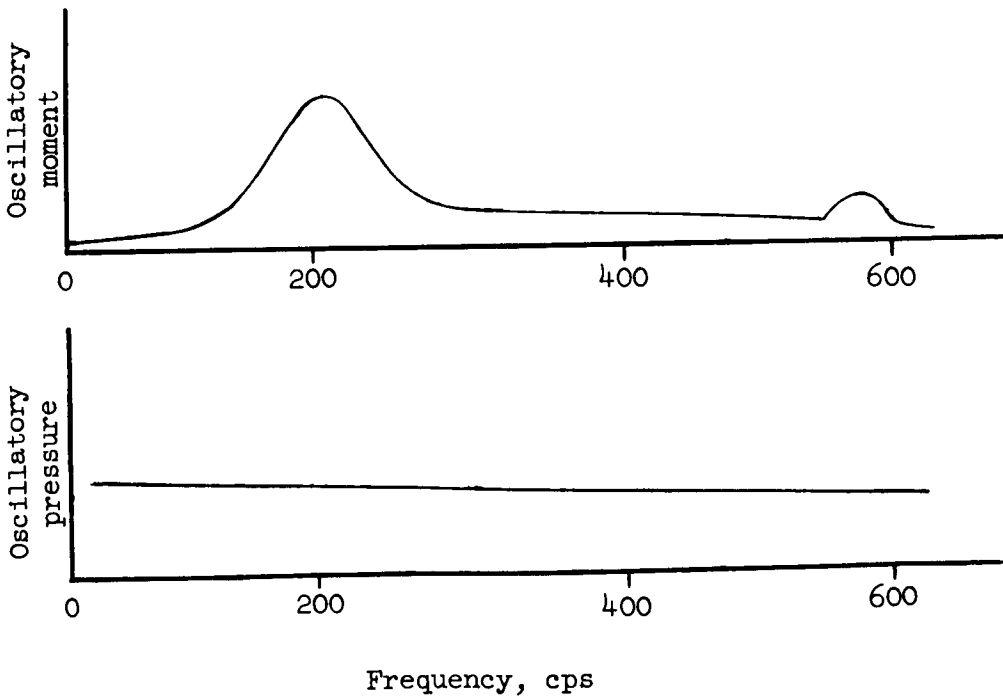
Frequency, cps

As will be noted, the oscillatory pressure input remains relatively constant throughout the frequency range of interest and therefore it is felt that no oscillating pressure inputs are being damped by the tail structure.

It is reasonable then to plot the root-mean-square values of the bending-moment gage against angle of attack as an indication of buffeting. Although these measurements are not intended to be quantitative, they should give an indication of the onset of the buffeting which from the engineering viewpoint is adequate. Figure 5 of reference 1 indicates remarkable agreement between these data and the flight buffeting boundary of the B-52 airplane.

## PRESENTATION OF RESULTS

The results of the wind-tunnel investigation on the aerodynamic characteristics of an X-15 model and of a B-52 model under conditions simulating launching of the X-15 from the B-52 are presented in the following figures:

The configuration constants for each figure are given in table I.

Langley Research Center,
    National Aeronautics and Space Administration,
        Langley Field, Va., August 20, 1959.

# REFERENCES

1. Alford, William J., Jr., and Taylor, Robert T.:  Aerodynamic Charac-
   teristics of the X-15/B-52 Combination.  NASA MEMO 6-8-59L, 1959.

2. Von Doenhoff, Albert E., and Horton, Elmer A.:  A Low-Speed Experi-
   mental Investigation of the Effect of a Sandpaper Type of Roughness
   on Boundary-Layer Transition.  NACA Rep. 1349, 1958.  (Supersedes
   NACA TN 3858.)

3. Gillis, Clarence L., Polhamus, Edward C., and Gray, Joseph L., Jr.:
   Charts for Determining Jet-Boundary Corrections for Complete Models
   in 7- by 10-Foot Closed Rectangular Wind Tunnels.  NACA WR L-123,
   1945.  (Formerly NACA ARR L5G31.)

4. Herriot, John G.:  Blockage Corrections for Three-Dimensional-Flow
   Closed-Throat Wind Tunnels, With Consideration of the Effect of
   Compressibility.  NACA Rep. 995, 1950.  (Supersedes NACA RM A7B28.)

TABLE I.- CONFIGURATION CONSTANTS

[Figures 41(a), 41(b), and 41(c) present data for fixes $A_1$, $B_2$, and $B_1$, respectively]

| $z$, in. | $\delta_f$, deg | $i_t$, deg | $\delta_a$, deg | $\delta_r$, deg | $\delta_e$, deg | $\delta_B$, deg | Pylon position | $\beta$, deg | $\Delta\alpha$, deg | $\Delta\beta$, deg | $\phi$, deg | Slot used | Transition | Buffet fairing | Forces and moments for B-52 | Forces and moments for X-15 | B-52 buffeting |
|---|---|---|---|---|---|---|---|---|---|---|---|---|---|---|---|---|---|
|  | 0 | -2 to 8 |  |  |  |  | Off | 0 |  |  |  | — | Off | Off | 5 |  |  |
|  | 0 | 3 |  |  |  |  | Off | -4 to 4 |  |  |  | — | Off | Off | 6 |  |  |
|  | 0 | -2 to 8 |  |  |  |  | Off | 0 |  |  |  | A | On | Off | 7 |  |  |
|  | 0 | -2 to 8 | -15 to 15 | -10 to 10 | -15 to 15 | 0 | Off | 0 | 0 | 0 | 0 | A | Off | Off | 8 |  |  |
|  | 0 | 3 | 0 | 0 | 0 | 0 | Off | 0 | 2°15' | 0 | 0 | A | Off | Off | 9 | 28 |  |
|  | 0 | 3 | 0 | 0 | 0 | 0 | Off | 0 | 2°15' | 0 | 0 | A | Off | Off | 20 |  |  |
|  | 0 | 3 | 0 | 0 | 0 | 0 | Off | 0 | 2°15' | 0 | 0 | A | Off | Off | 11 |  |  |
|  | 0 | 3 | -15 to 15 | -10 to 10 | -15 to 15 | 0 | Off | -4 | 2°15' | 0 | 0 | A | Off | Off | 12 |  |  |
|  | 0 | 3 | 0 | 0 | 0 | 35 | Off | 0 | 2°15' | 0 | 0 | A | Off | Off | 13 |  |  |
|  | 30 |  | 0 | 0 | 0 | 0 | On | 0 |  |  |  | A | Off | On | 14 |  |  |
|  | 0 |  |  |  |  | 0 | On | 0 | 2°15' | 0 | 0 | A | Off | On | 15 |  | 21 |
|  |  |  |  |  |  |  | On |  |  |  |  |  | Off | On | 16 |  | 22 |
|  | 30 |  |  |  |  |  | On | -4 | 2°15' | 0 | 0 | A | Off | Off | 17 |  | 23 |
|  | 0 |  | -15 to 15 | -10 to 10 | -15 to 15 | 0 | On | 0 | 2°15' | 0 | 0 | A | Off | Off | 18 |  | 24 |
|  | 0 |  | -15 to 15 | -10 to 10 | -15 to 15 | 0 | On | -4 | 2°15' | 0 | 0 | A | Off | On | 19 |  | 25 |
| 0 | 30 | Off | 0 | 0 | 0 | 35 | On | 0 |  |  |  | — | Off | Off |  |  |  |
| 0 | 0 | Off | 0 | 0 | 0 | 0 | On | -4 |  |  |  | — | Off | Off |  |  |  |
| 0 to 12 | 0 |  |  |  |  | 0 | On | 0 | 2°15' | 0 | 0 | A | Off | Off |  | 26 |  |
| 0 to 12 | 0 |  |  |  |  | 0 | On | 0 | 2°15' | 0 | 0 | A | Off | Off |  | 27 |  |
| 0 to 12 | 0 |  |  |  |  | 0 | On | 0 | 2°15' | 0 | 0 | A | Off | Off |  | 28 |  |
| 0 to 12 | 0 |  |  |  |  | 0 | On | 0 | 2°15' | 0 | 0 | A | Off | Off |  | 29 |  |
| 0 to 12 | 0 |  |  |  |  | 0 | On | 0 | 1°30' | 0 | 0 | A | Off | Off |  | 30 |  |
| 0 to 12 | 0 |  |  |  |  | 0 | On | 0 | 1°30' | 0 | 0 | A | Off | Off |  | 31 |  |
| 0 to 12 | 0 |  |  |  |  | 0 | On | 0 | 0 | 0 | 0 |  | Off | Off |  | 32 |  |
| 0 to 12 | 0 |  |  |  |  | 0 | On | 0 | 3°5' | 0 | 0 |  | Off | Off |  | 33 |  |
| 0 to 12 | 0 |  |  |  |  | 0 | On | 0 | 1°30' | 0 | 0 |  | Off | Off |  | 34 |  |
| 0 to 12 | 0 |  |  |  |  | 0 | On | 0 | 1°30' | 0 | 0 |  | Off | Off |  | 35 |  |
| 0 to 12 | 0 |  |  |  |  | 0 | On | 0 | 1°30' | 0 | 0 |  | Off | Off |  | 36 |  |
| 0 to 12 | 0 |  |  |  |  | 0 | On | 0 | 1°30' | 0 | 0 |  | Off | Off |  | 37 |  |
| 0 to 12 | 0 |  |  |  |  | 0 | On | 0 | 1°30' | 0 | 0 |  | Off | Off |  | 38 |  |
| 0 to 12 | 0 |  |  |  |  | 0 | On | 0 | 1°30' | 2°19' | 9°50' |  | Off | Off |  | 39 |  |
| 0 to 12 | 0 |  |  |  |  | 0 | On | 0 | 1°30' | -2°19' | -9°50' |  | Off | Off |  | 40 |  |
| 0 to 12 | 0 |  |  |  |  | 0 | On | 0 | 1°30' | 0 | 0 | A | Off | Off |  | 41(a) |  |
| 0 to 12 | 0 |  |  |  |  | 0 | On | 0 | 1°30' | 0 | 0 | B | Off | Off |  | 41(b) |  |
| 0 to 12 | 0 |  |  |  |  | 0 | On | 0 | 1°30' | 0 | 0 | — | Off | Off |  | 41(c) |  |
| 0 to 12 | 0 |  |  |  |  | 0 | On | 0 | 1°30' | 0 | 0 | — | Off | Off |  | 42 |  |
| 0 to 12 | 0 |  |  |  |  | 0 | On | 0 | 1°30' | 0 | 0 |  | Off | Off |  | 43 |  |

Figure 1.- System of axes used in the investigations. Positive directions of forces, moments, angles, and direction are indicated by arrows.
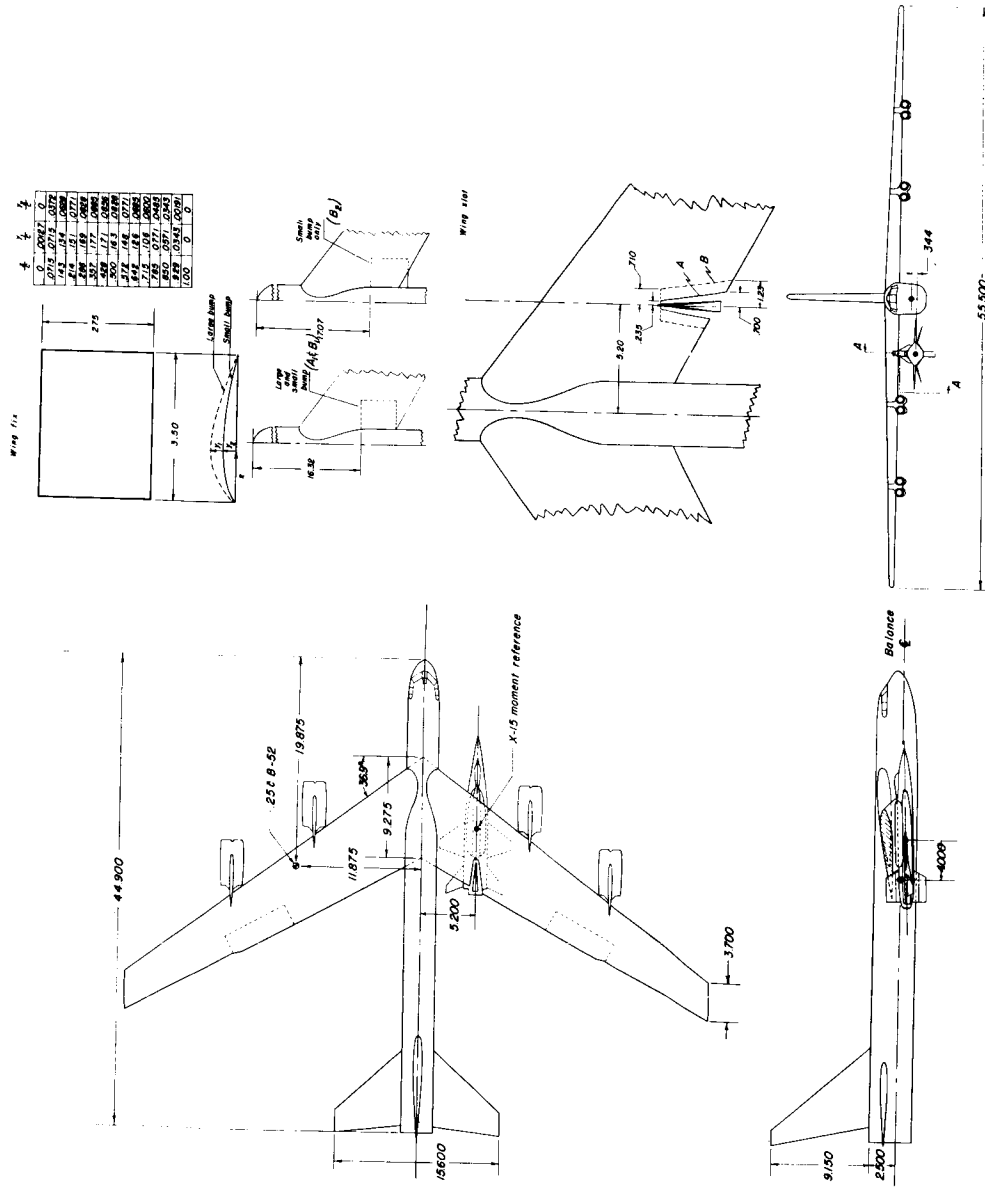
(a) General arrangement of B-52 and X-15 models with wing fix and cutout details.

Figure 2.- Model sketches. All dimensions in inches unless otherwise noted.

| | Wing | Horiz tail exposed | Vertical tail |
|---|---|---|---|
| Aspect ratio | 2.528 | 2.458 | 1.335 |
| Taper ratio | .200 | .305 | |
| $\Lambda c/4$ | 25°38' | 45° | 23°22' |

COORDINATES

| Wing | | Horizontal tail | |
|---|---|---|---|
| x/c % | y/c % | x/c % | y/c % |
| 0.00 | 0.00 | 0.00 | 0.00 |
| 0.50 | .044 | 0.50 | .54 |
| .75 | .049 | .75 | .58 |
| 1.25 | .059 | 1.25 | .65 |
| 2.50 | .077 | 2.50 | .80 |
| 5.00 | 1.06 | 5.00 | 1.05 |
| 7.50 | 1.27 | 7.50 | 1.27 |
| 10.00 | 1.46 | 10.00 | 1.45 |
| 15.00 | 1.76 | 15.00 | 1.77 |
| 20.00 | 2.00 | 20.00 | 1.99 |
| 25.00 | 2.18 | 25.00 | 2.17 |
| 30.00 | 2.31 | 30.00 | 2.32 |
| 35.00 | 2.41 | 35.00 | 2.46 |
| 40.00 | 2.48 | 40.00 | 2.50 |
| 45.00 | 2.50 | 45.00 | 2.50 |
| 50.00 | 2.48 | 50.00 | 2.46 |
| 60.00 | 2.43 | 60.00 | 2.35 |
| 65.00 | 2.35 | | |
| 67.00 | 2.08 | | |
| Str. line | | Str. line | |
| 100.00 | 0.50 | 100.00 | 0.51 |

(b) Sketch of X-15 model.

Figure 2.- Concluded.
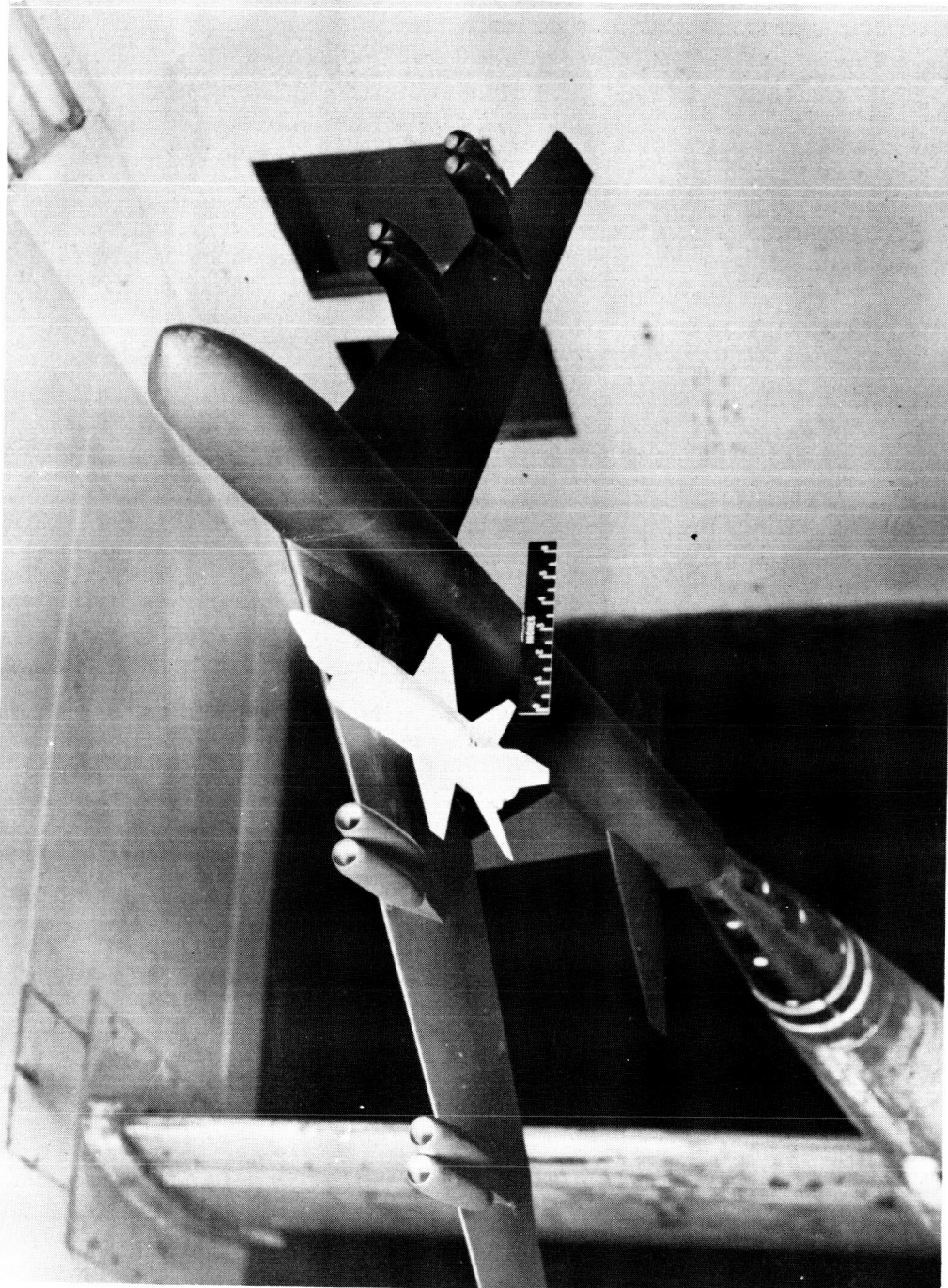
(a) Three-quarter front view of X-15 pylon mounted.     L-57-4309

Figure 3.- Photographs of the model mounted in the Langley high-speed 7- by 10-foot wind tunnel.
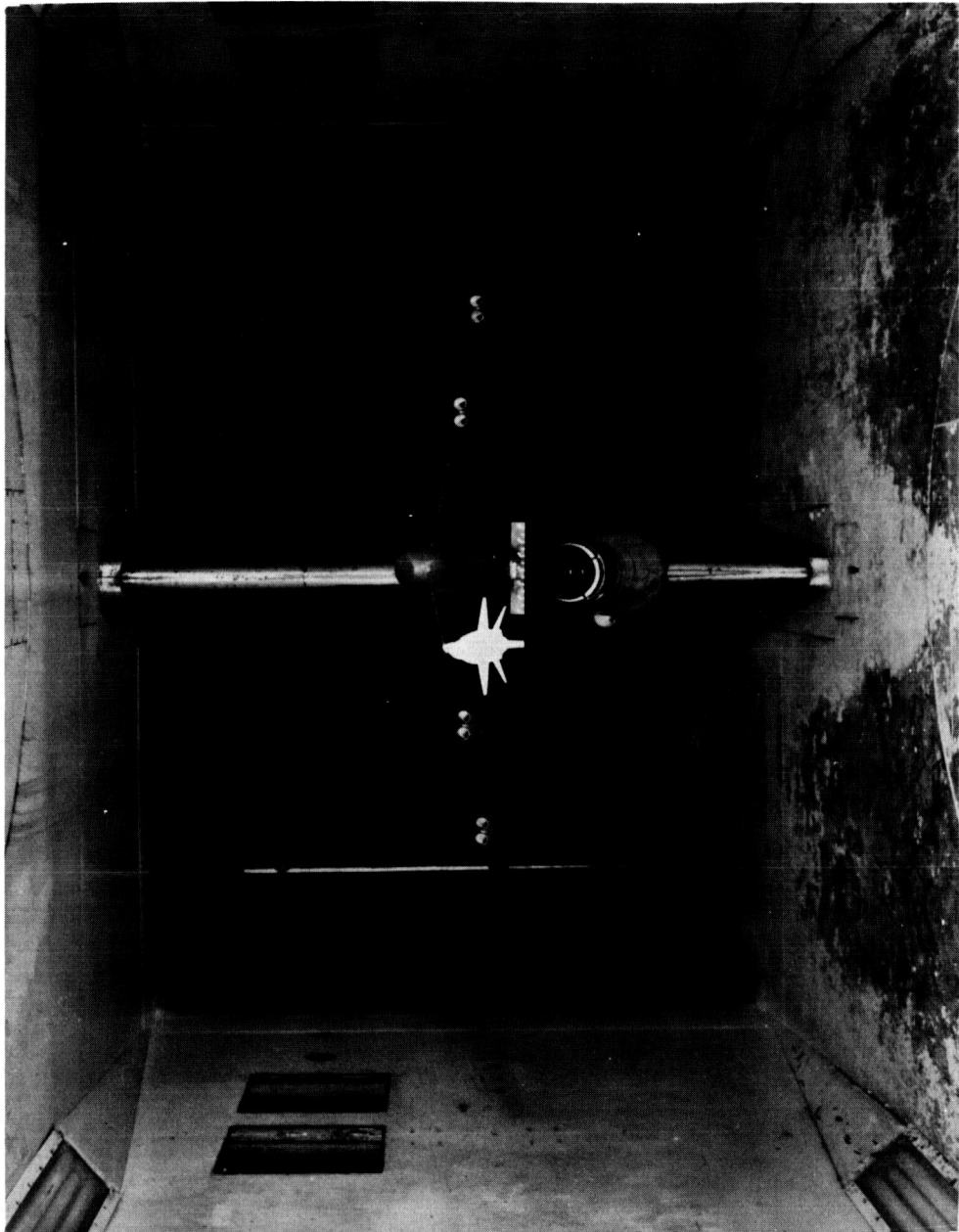
(b) Front view of X-15 pylon mounted.     L-57-4308

Figure 3.- Continued.

(c) Front view of X-15 detail.    L-57-4517

Figure 3.- Continued.
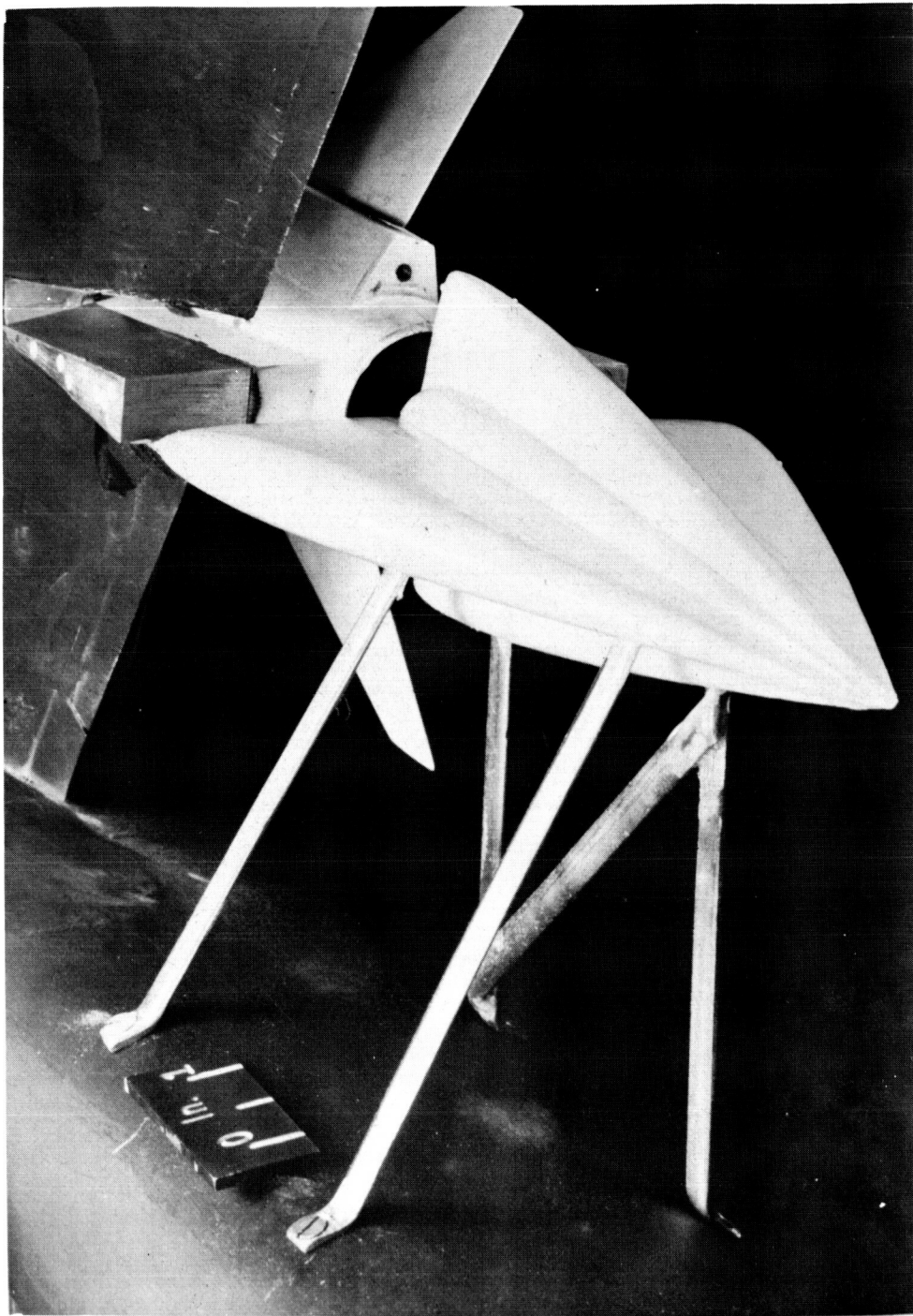
(d) Three-quarter rear view of buffet-fairing detail. L-57-4516

Figure 3.- Continued.
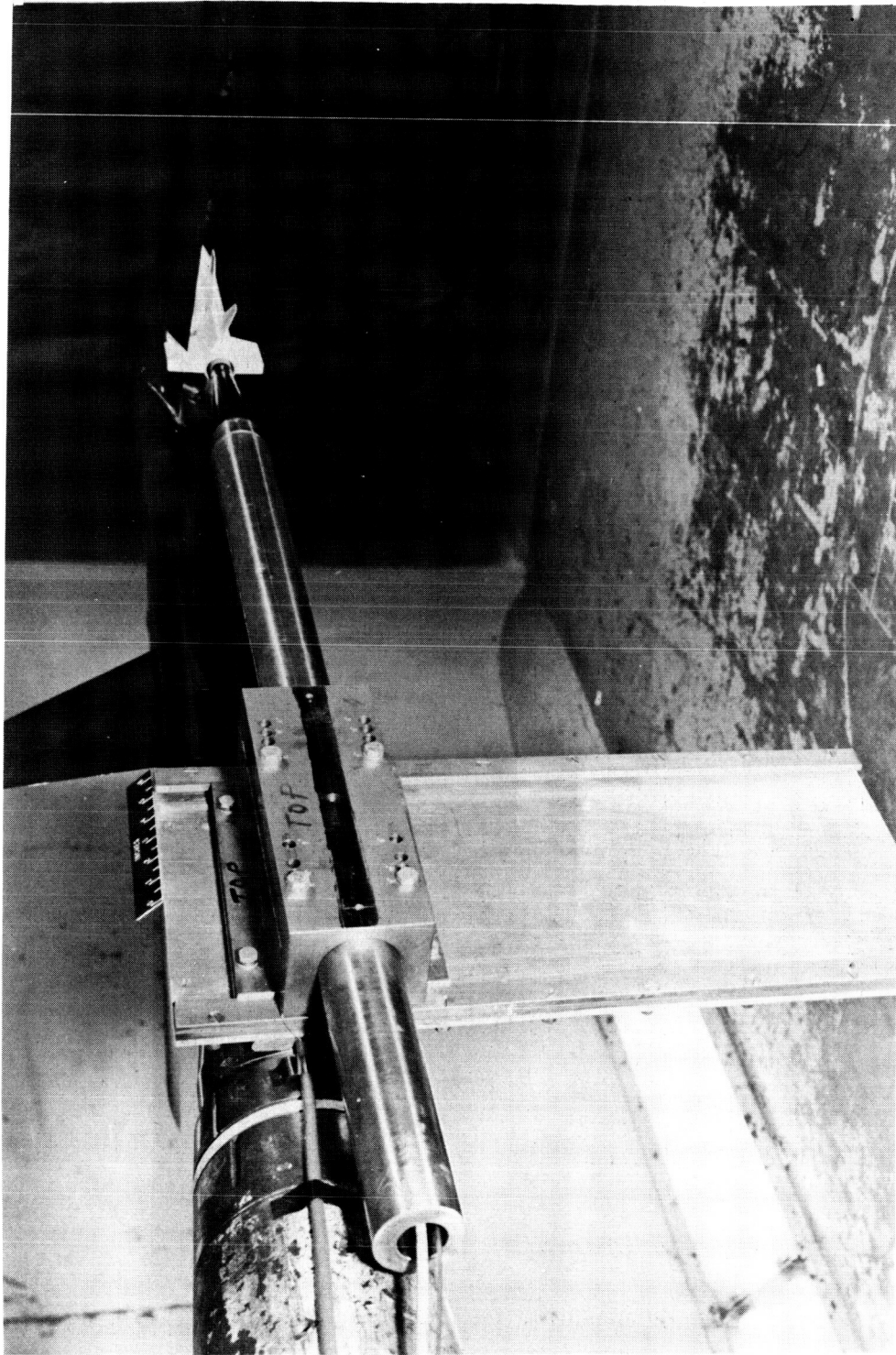
(e) Three-quarter rear view of sting-mount detail.   L-57-4684

Figure 3.- Concluded.
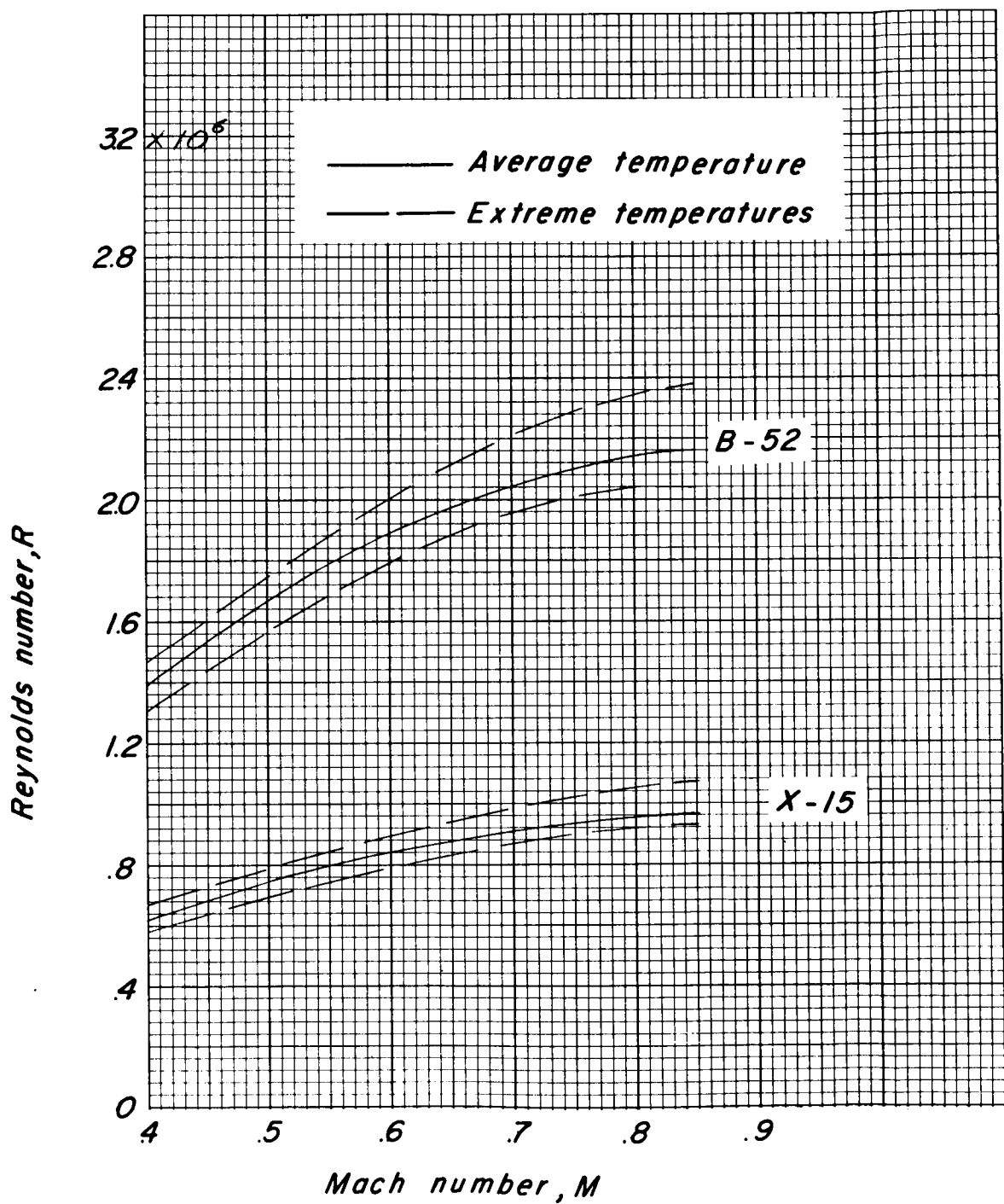
Figure 4.- Variation of Reynolds number with Mach number for B-52
and X-15 models.

(a)  $i_t = 3^o$.
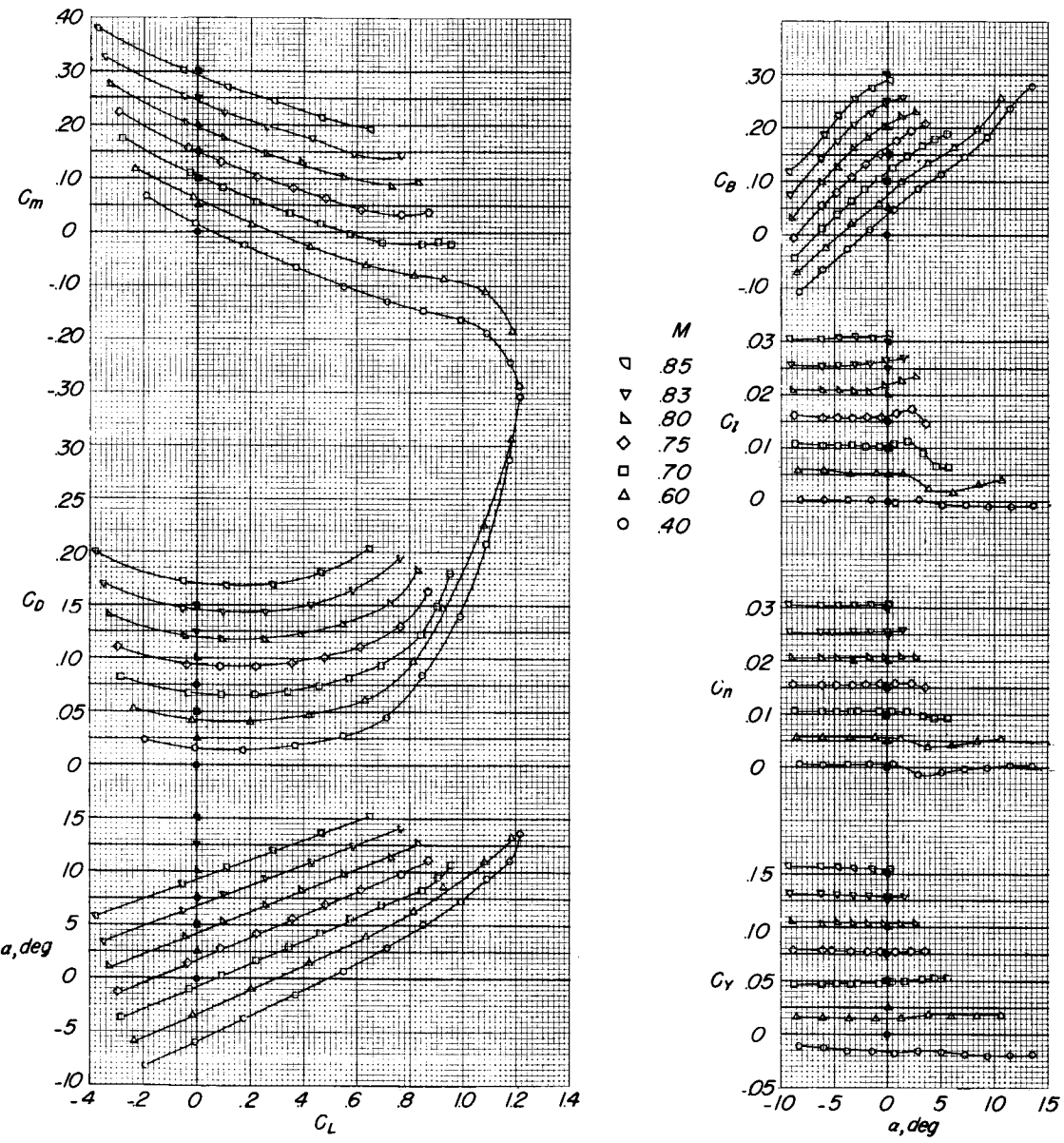
Figure 5.- Aerodynamic characteristics of the B-52 airplane model.  Original configuration; effect of tail incidence; $\beta = 0^o$.
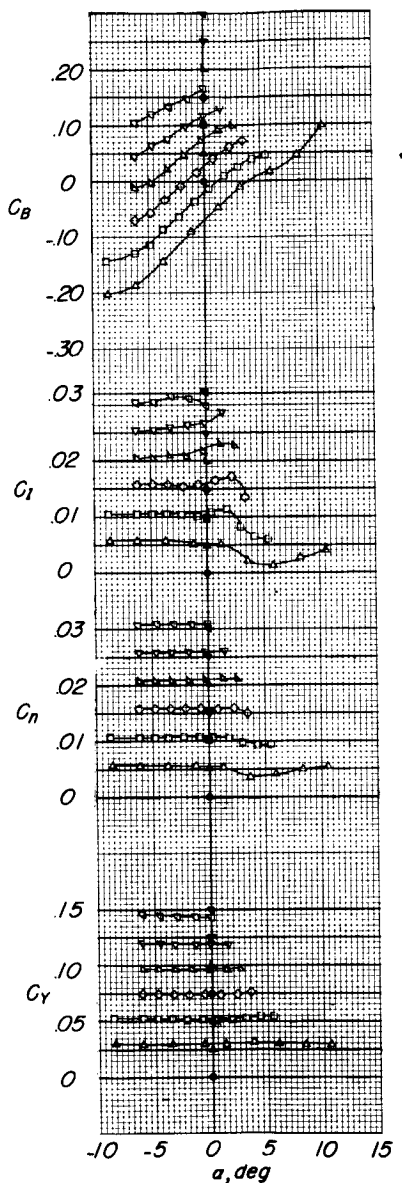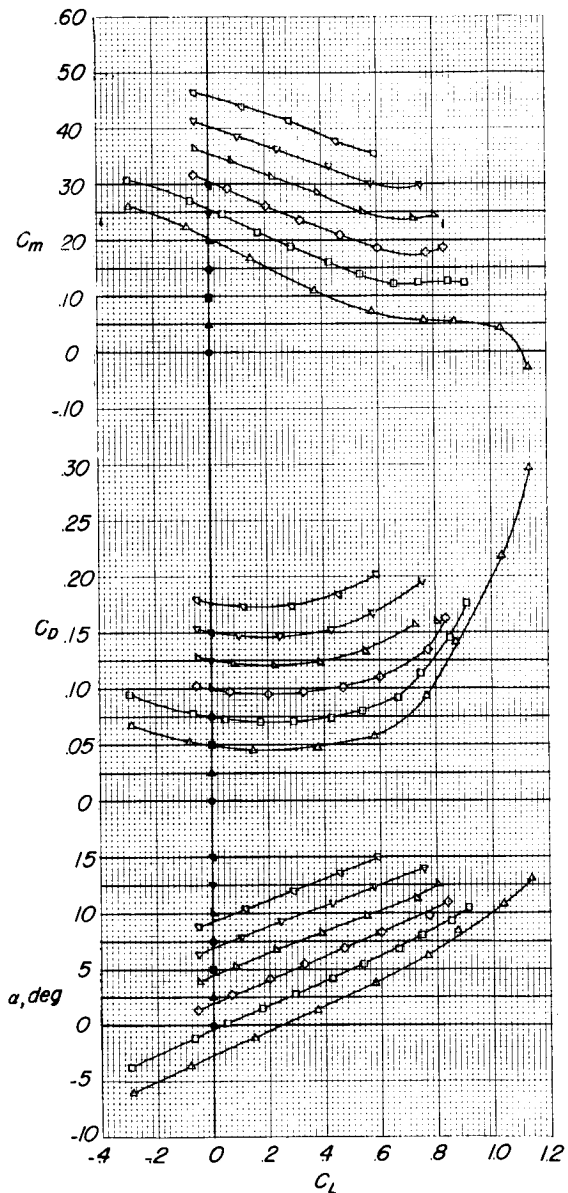
(b)  $i_t = -2^\circ$.

Figure 5.- Continued.

(c)  $i_t = 8°$.

Figure 5.- Continued.
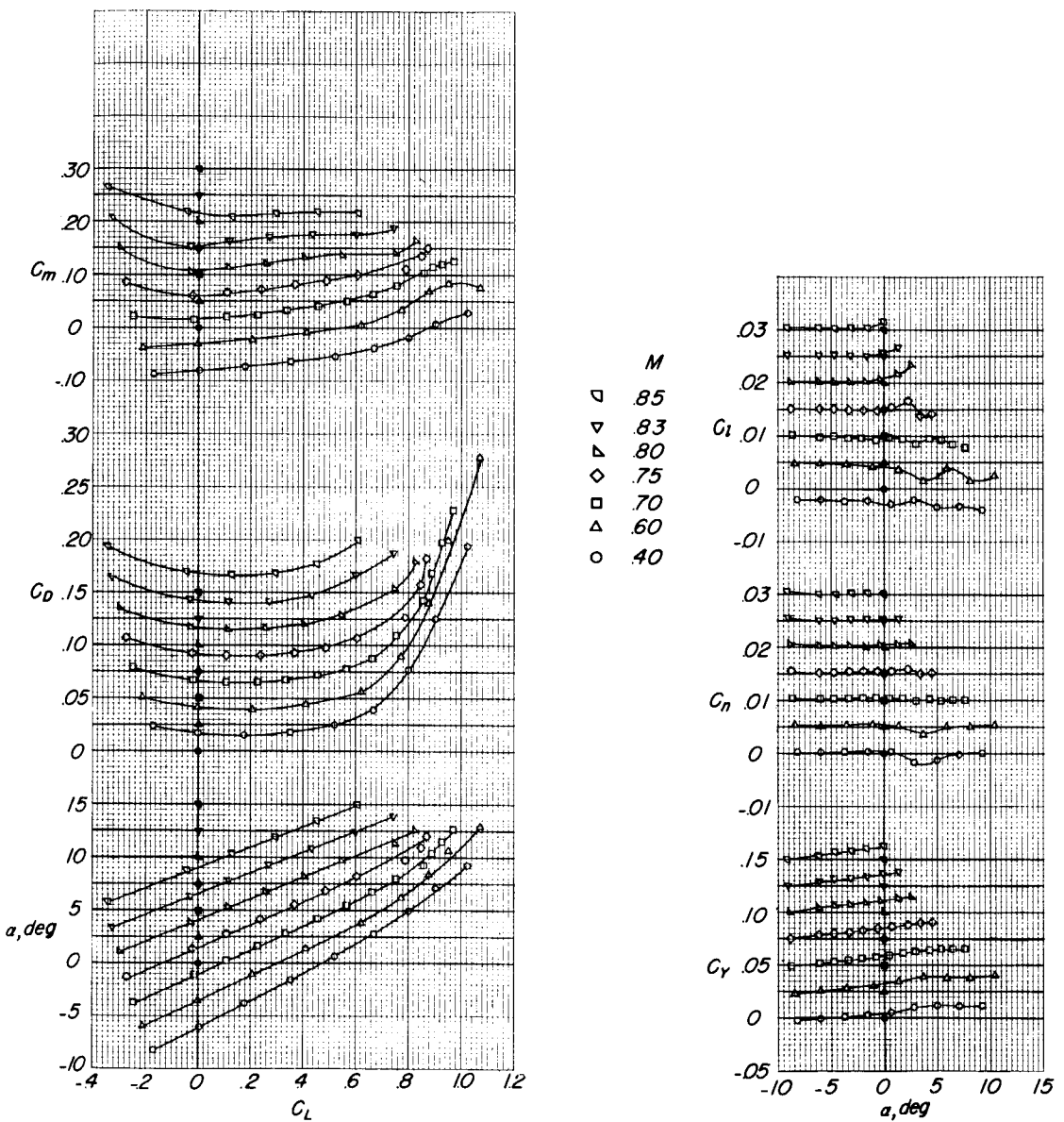
(d)  Horizontal tail off.

Figure 5.- Concluded.
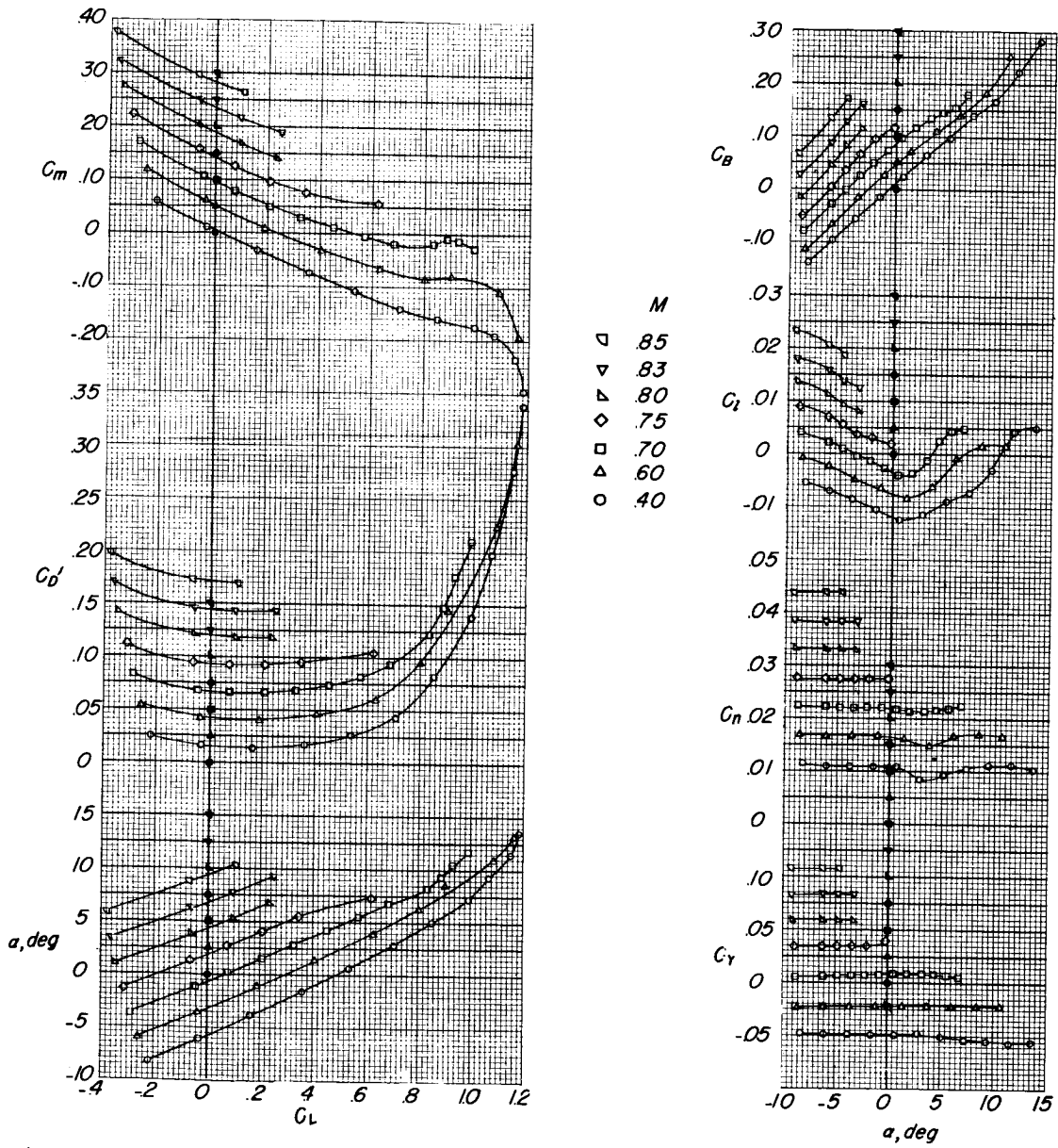
(a)  β = 4°.

Figure 6.- Aerodynamic characteristics of the B-52 airplane model.  Original configuration; effect of sideslip; $i_t$ = 3°.

24
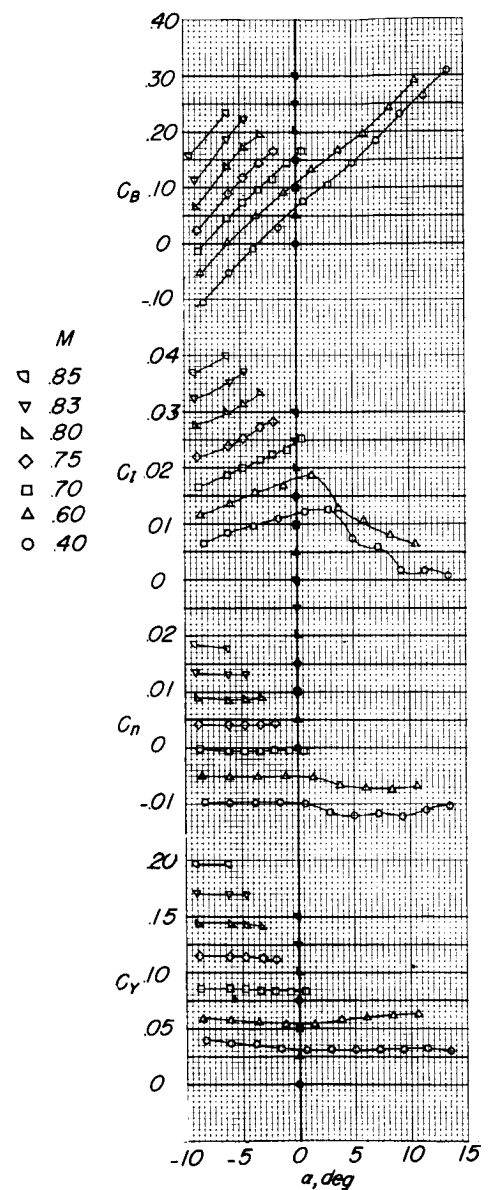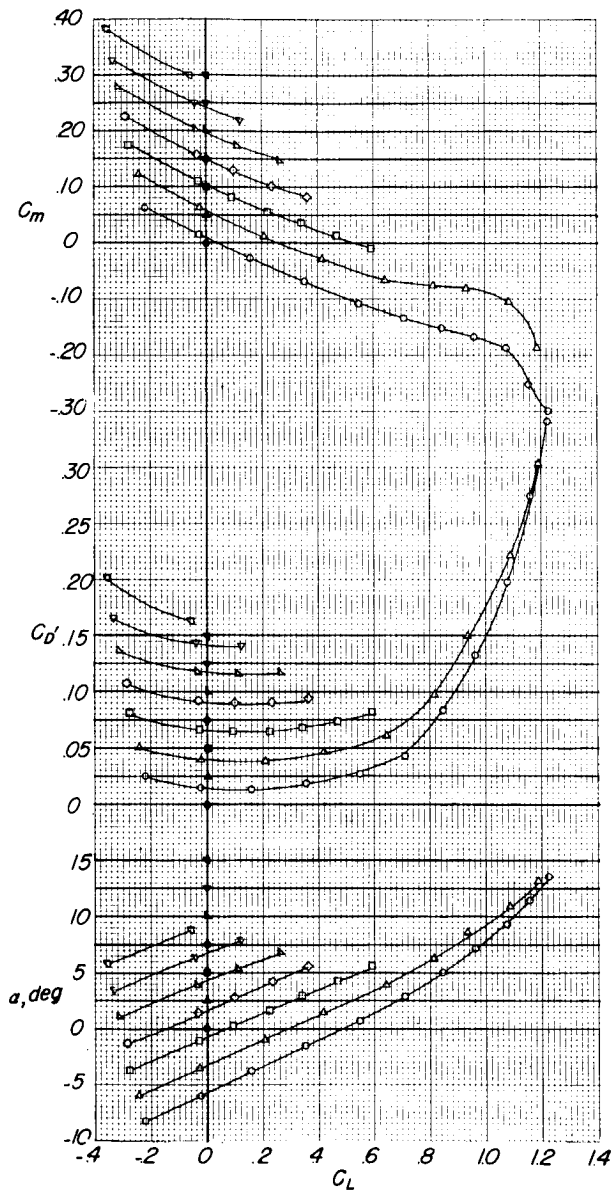


(b)  β = -4°.

Figure 6.- Concluded.
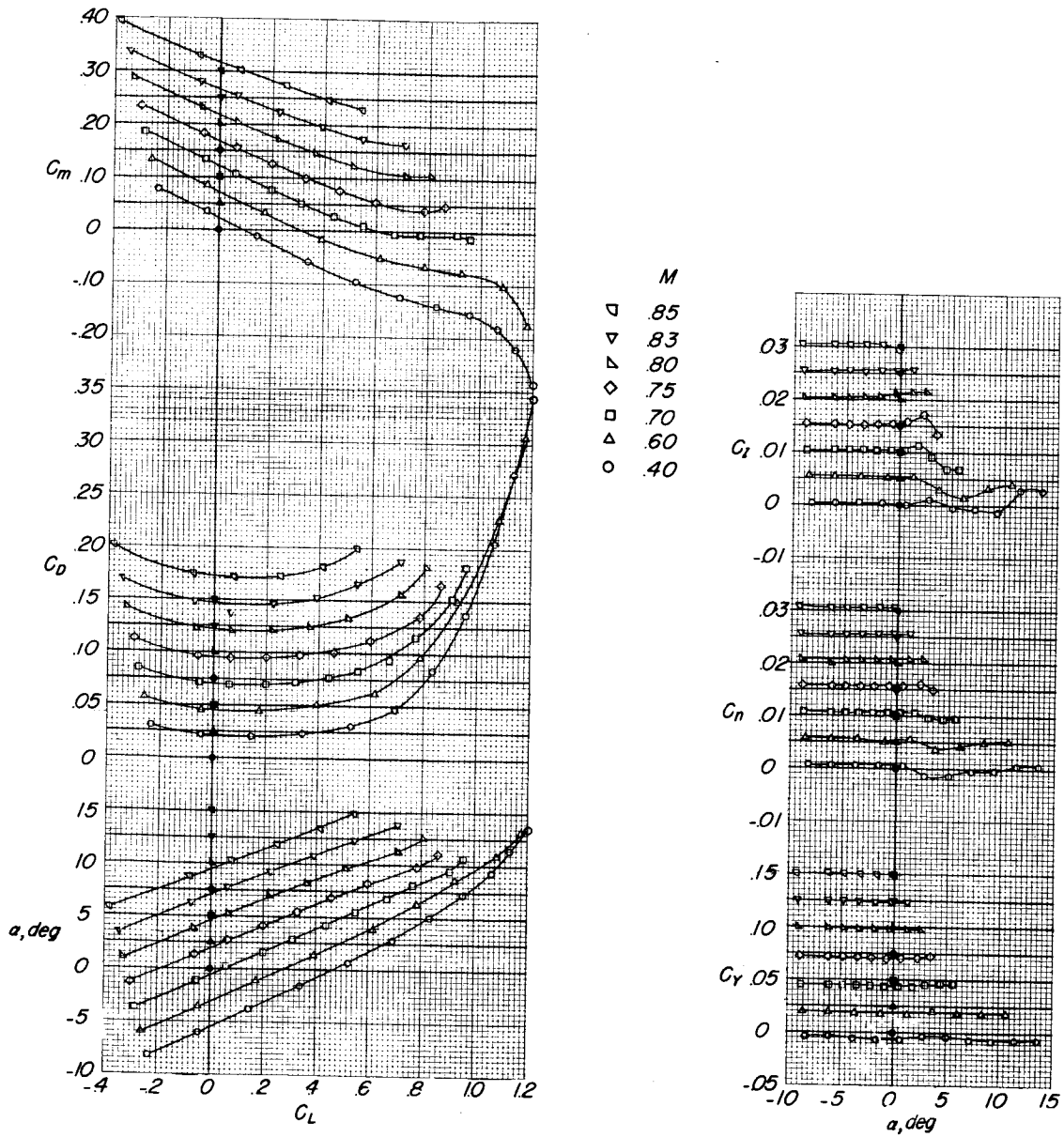
Figure 7.- Aerodynamic characteristics of the B-52 airplane model. Original configuration; transition strips installed; $i_t = 3°$; $\beta = 0°$.

(a)  $i_t = -2^O$.
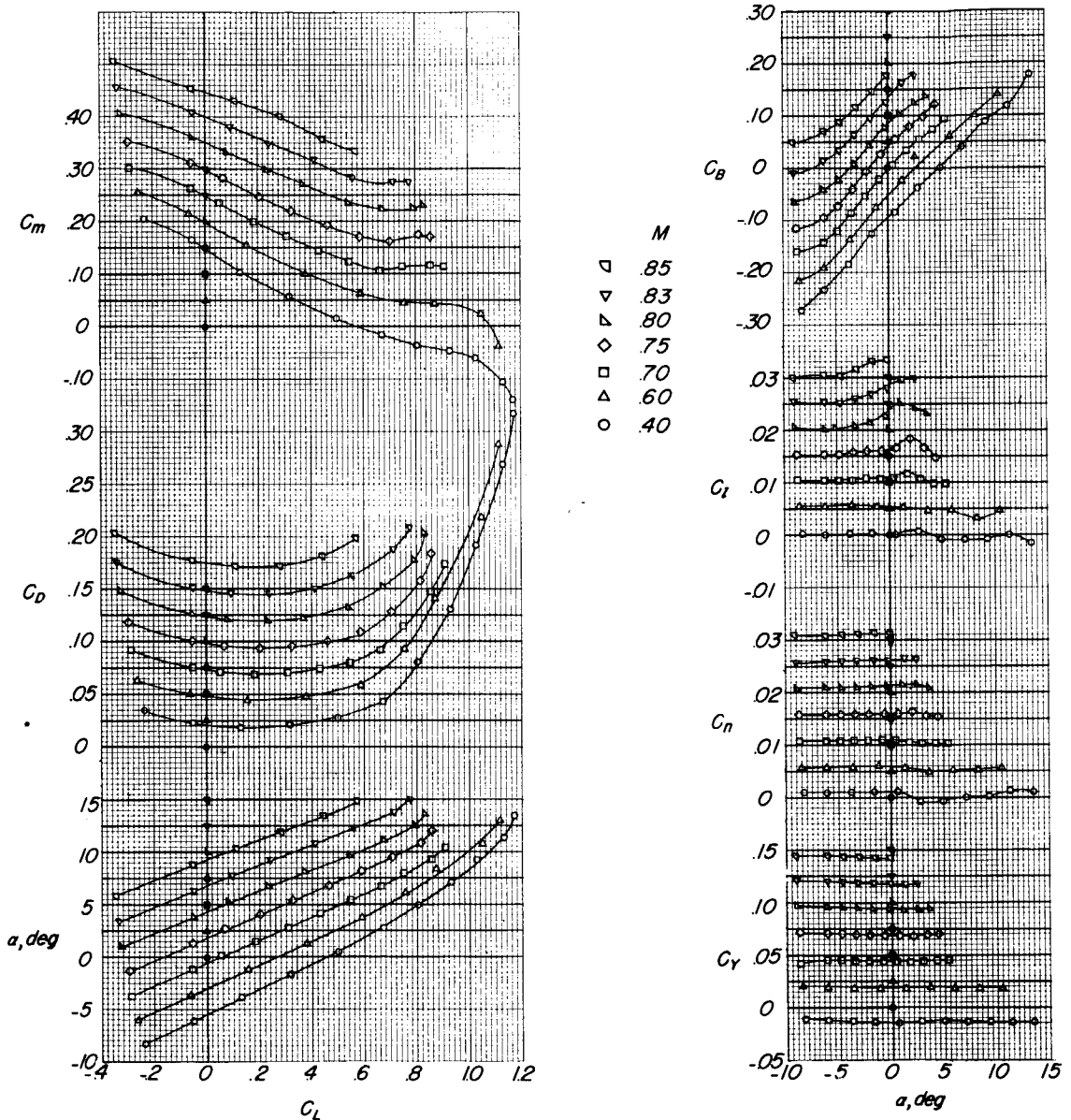
Figure 8.- Aerodynamic characteristics of the B-52 with small wing slot A.
Pylon off; X-15 off; $\delta_f = 0^O$; $\beta = 0^O$.

(b)  $i_t = 3^o$.
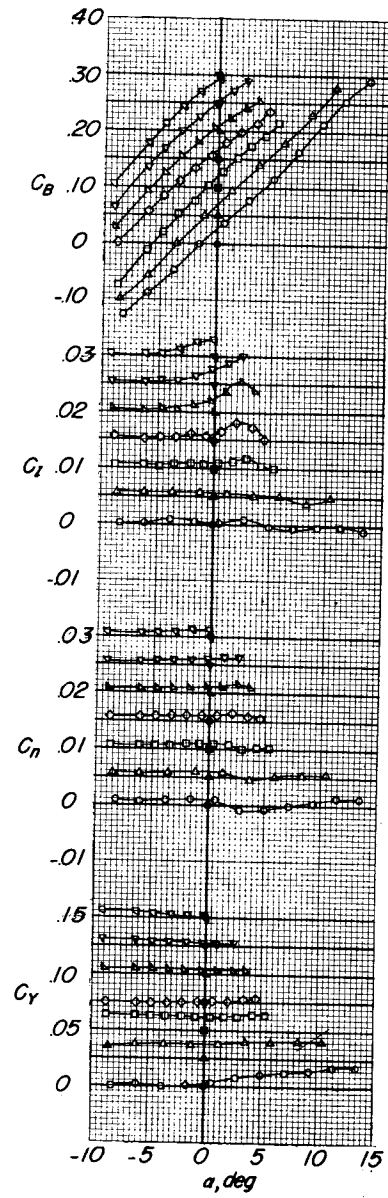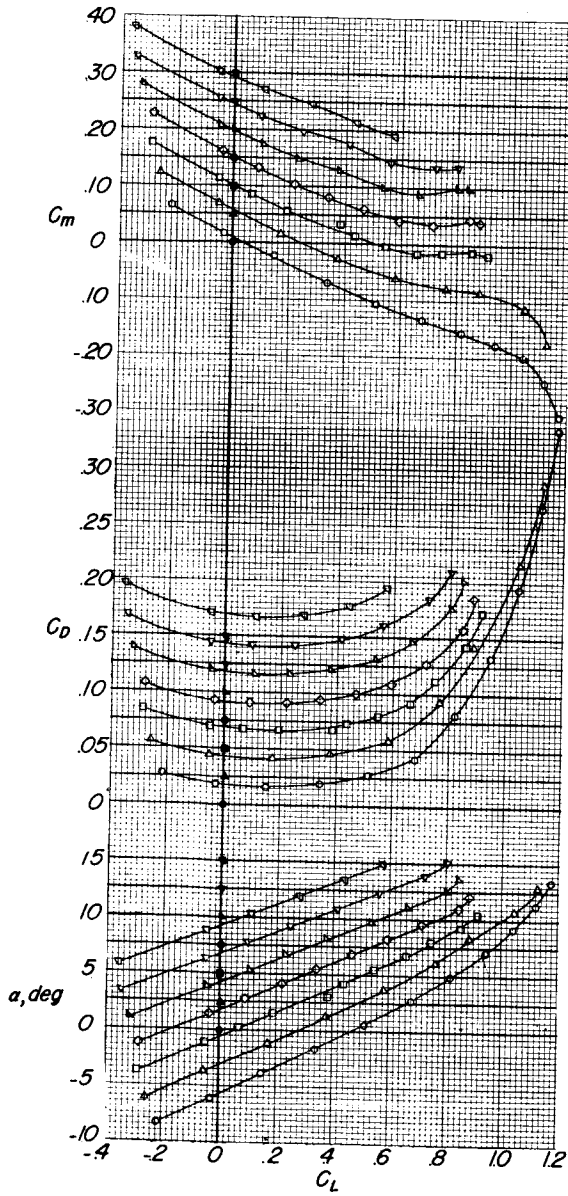
Figure 8.- Continued.
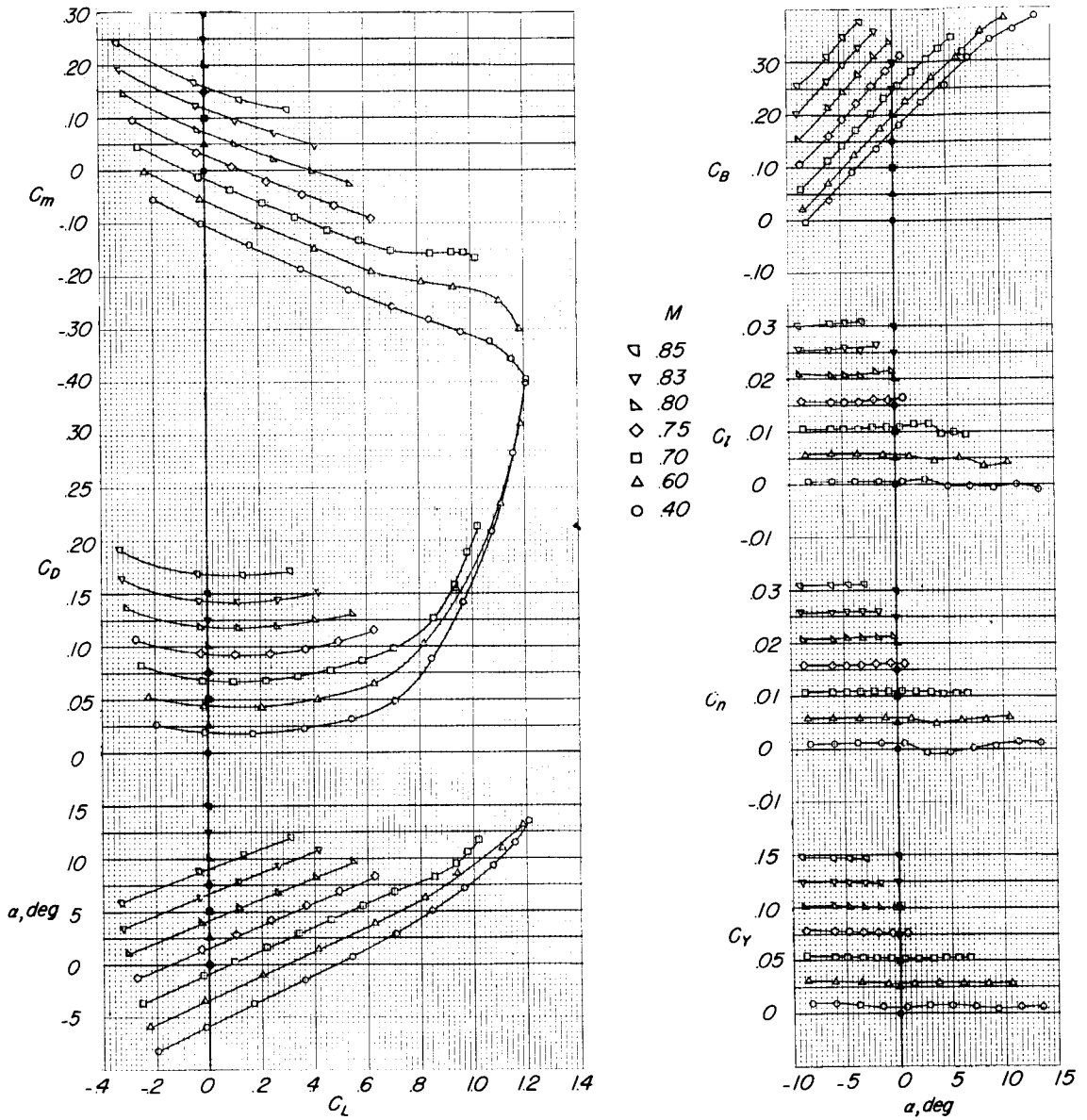
(c)  $i_t = 8°$.

Figure 8.- Concluded.

(a)   $i_t = 3^o$.
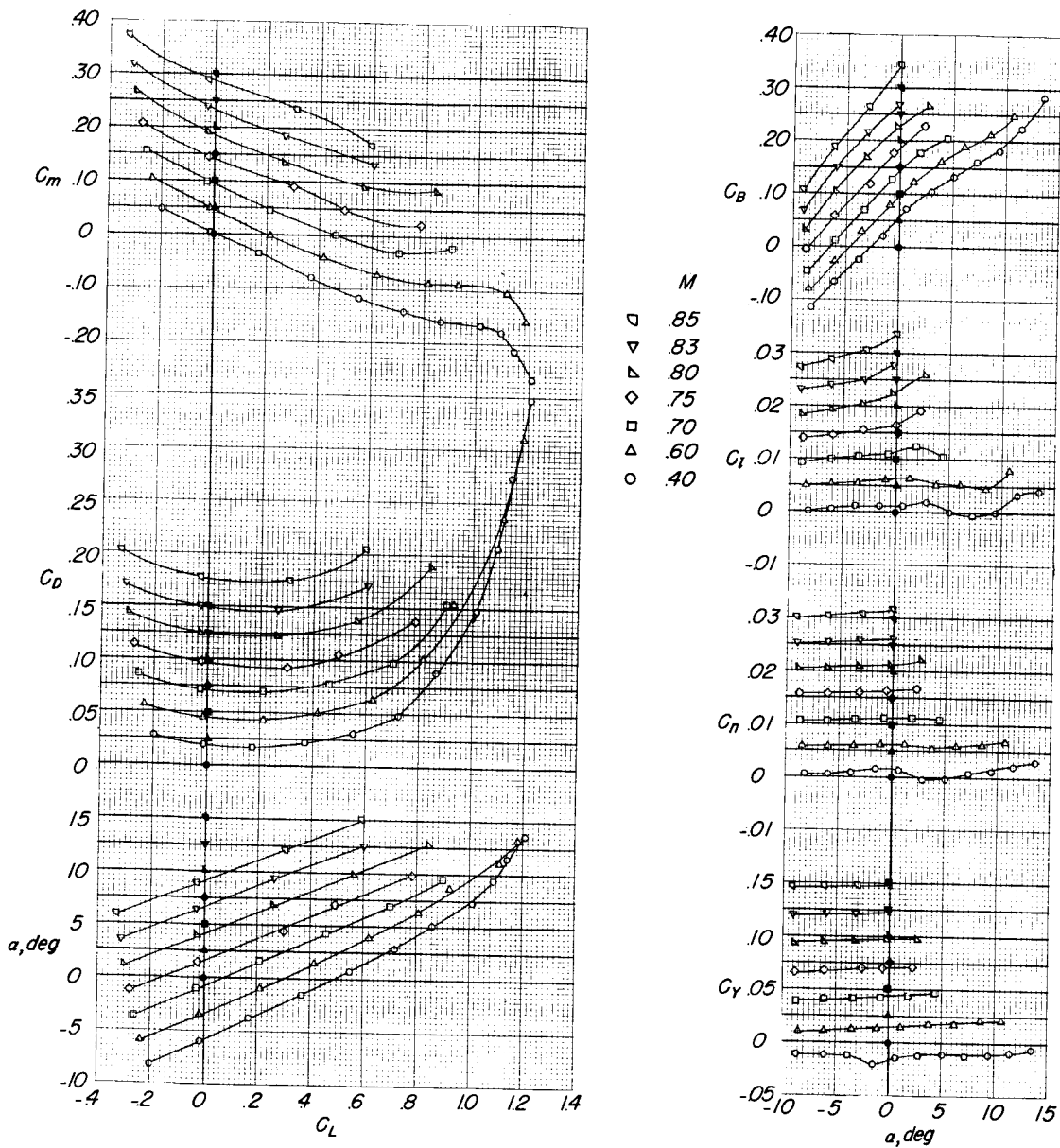
Figure 9.- Aerodynamic characteristics of the B-52 airplane model.  Wing slot A; X-15 pylon mounted; effect of B-52 stabilizer deflection; $\beta = 0^o$; $\delta_a = \delta_r = \delta_e = 0^o$.
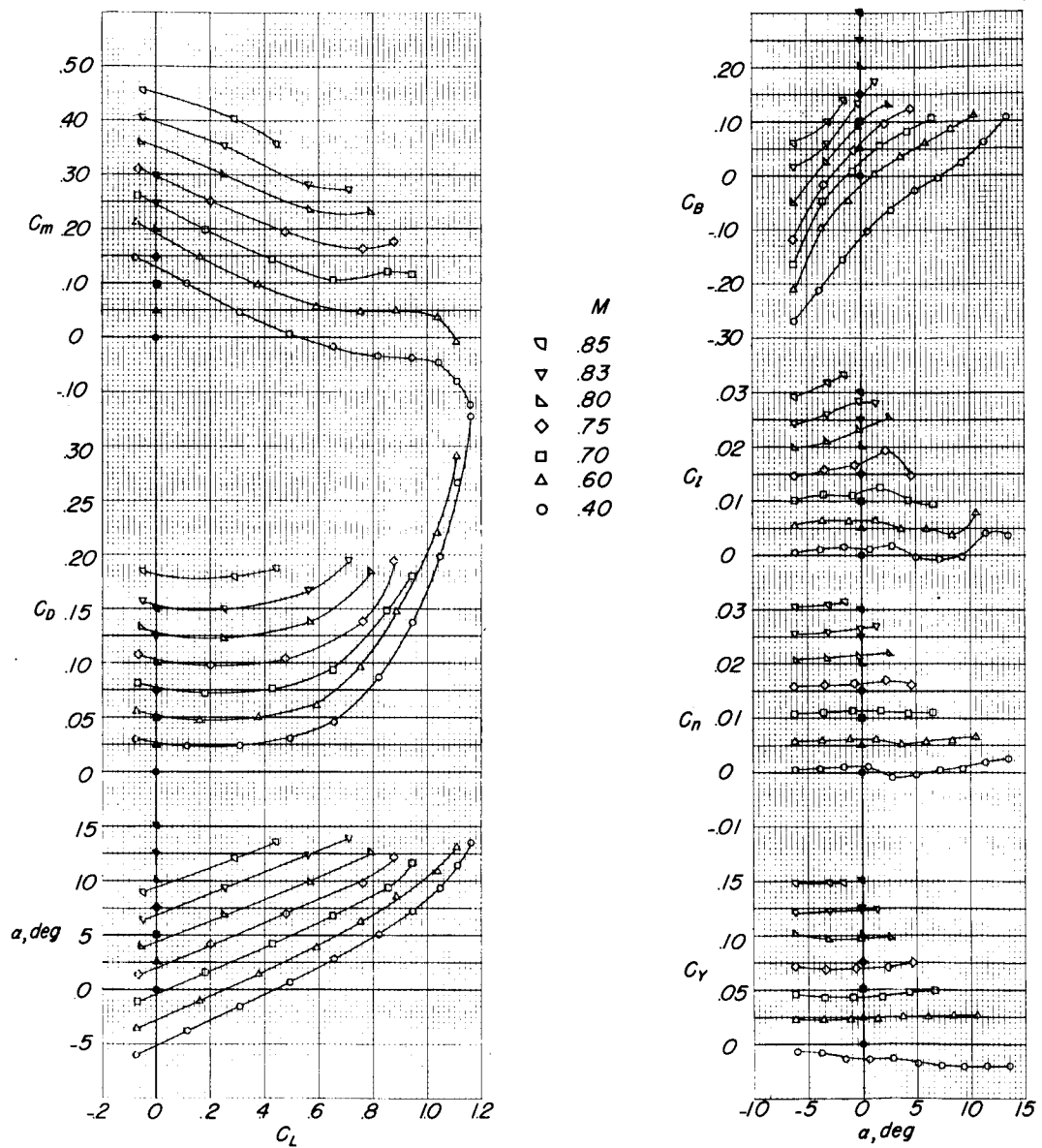
(b)  $i_t = -2^\circ$.

Figure 9.- Continued.
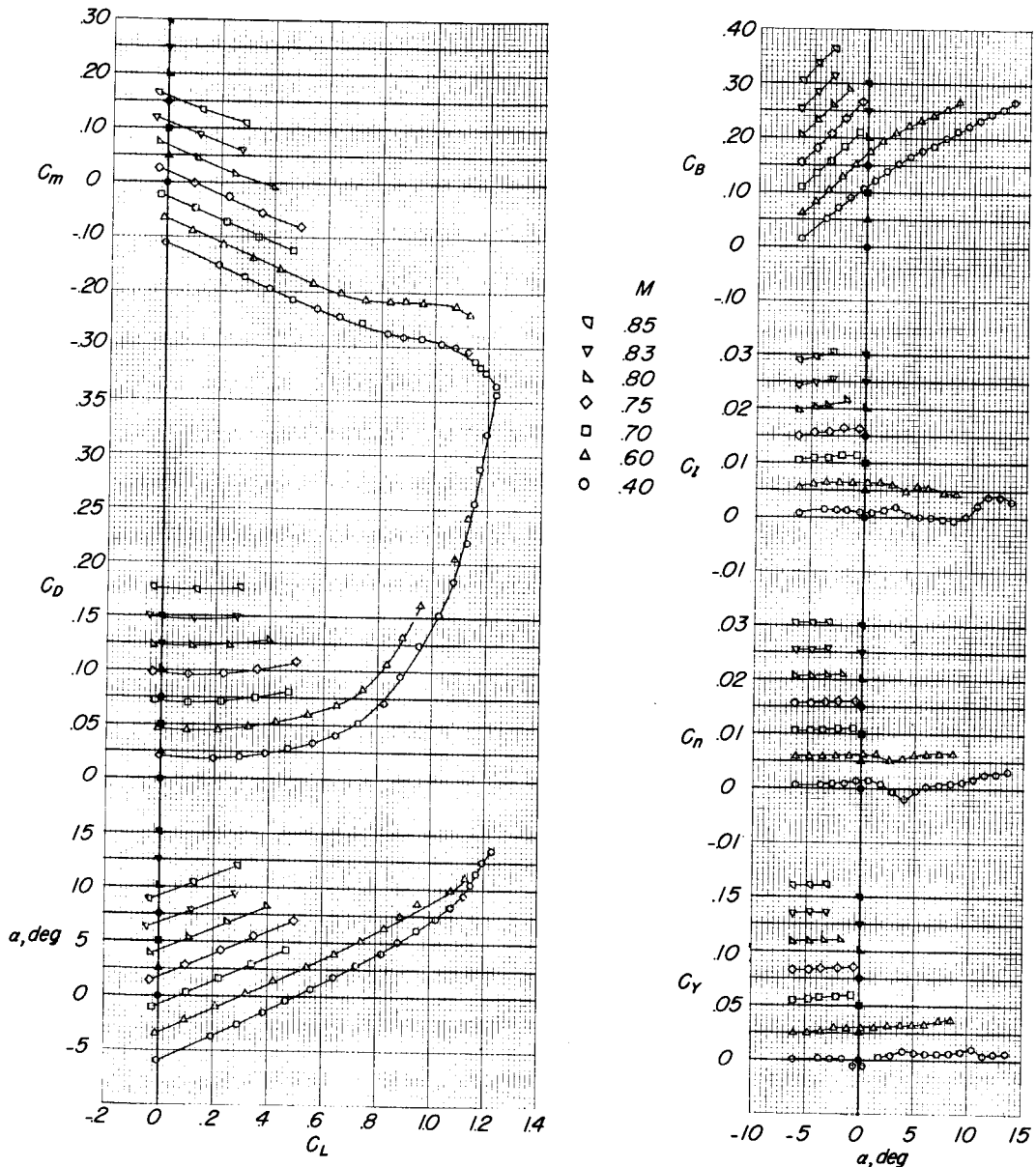
(c)  $i_t = 8°$.

Figure 9.- Continued.
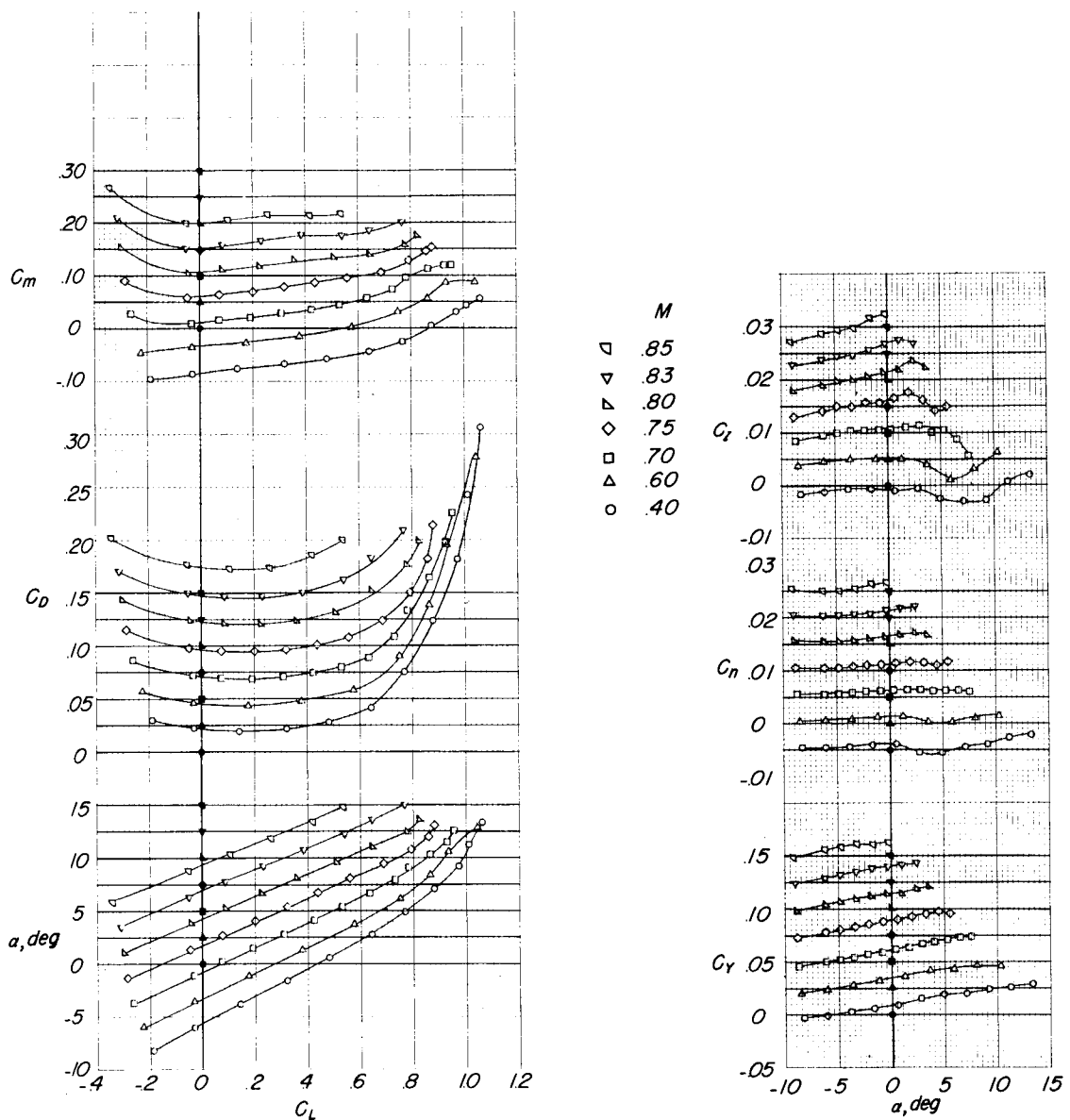
(d) Horizontal tail off.

Figure 9.- Concluded.
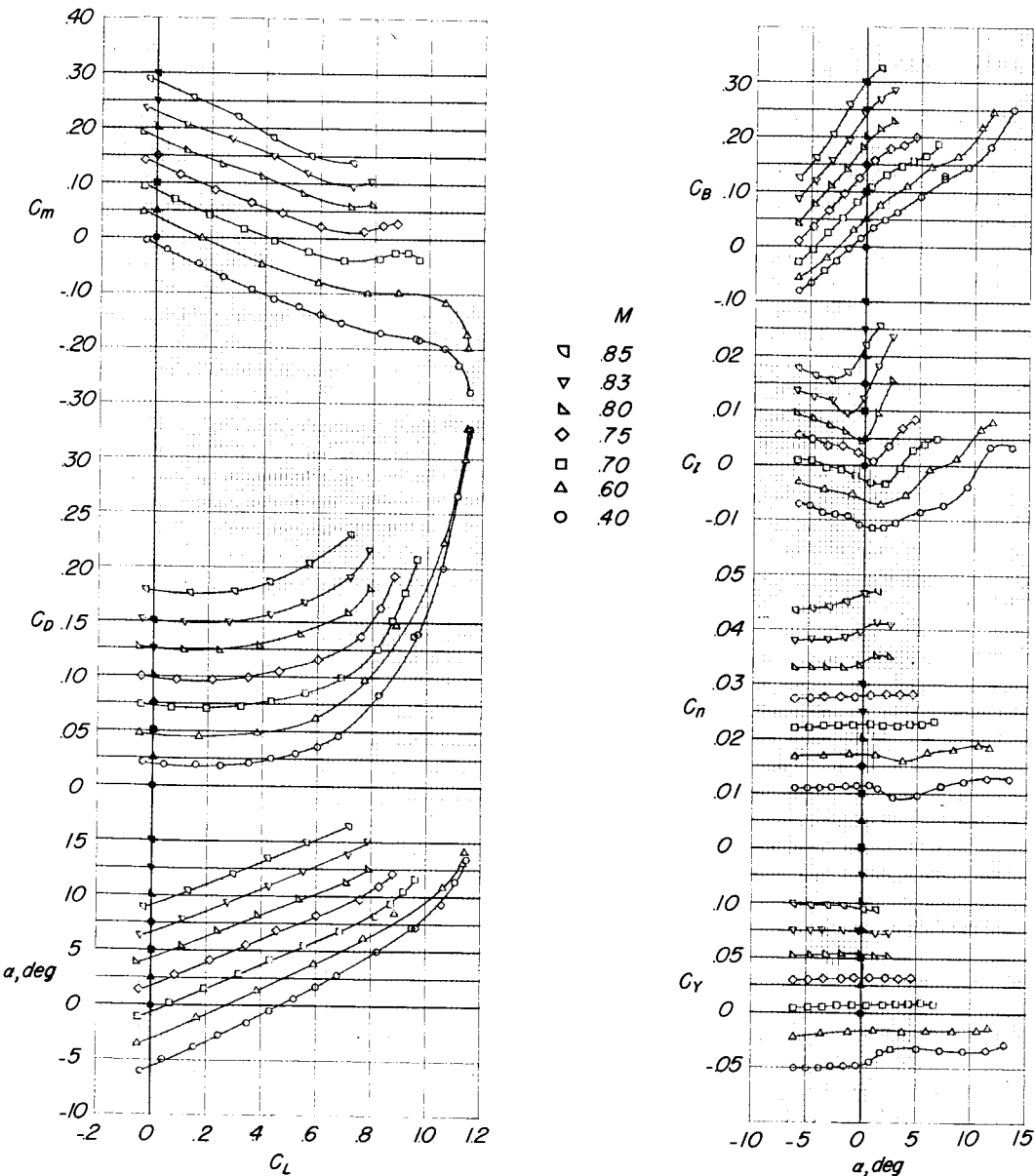
(a) $\beta = 4^{\circ}$.

Figure 10.- Aerodynamic characteristics of the B-52 airplane model with
the X-15 pylon mounted.  Wing slot A; effect of sideslip;
$\delta_a = \delta_e = \delta_r = 0^{\circ}$.
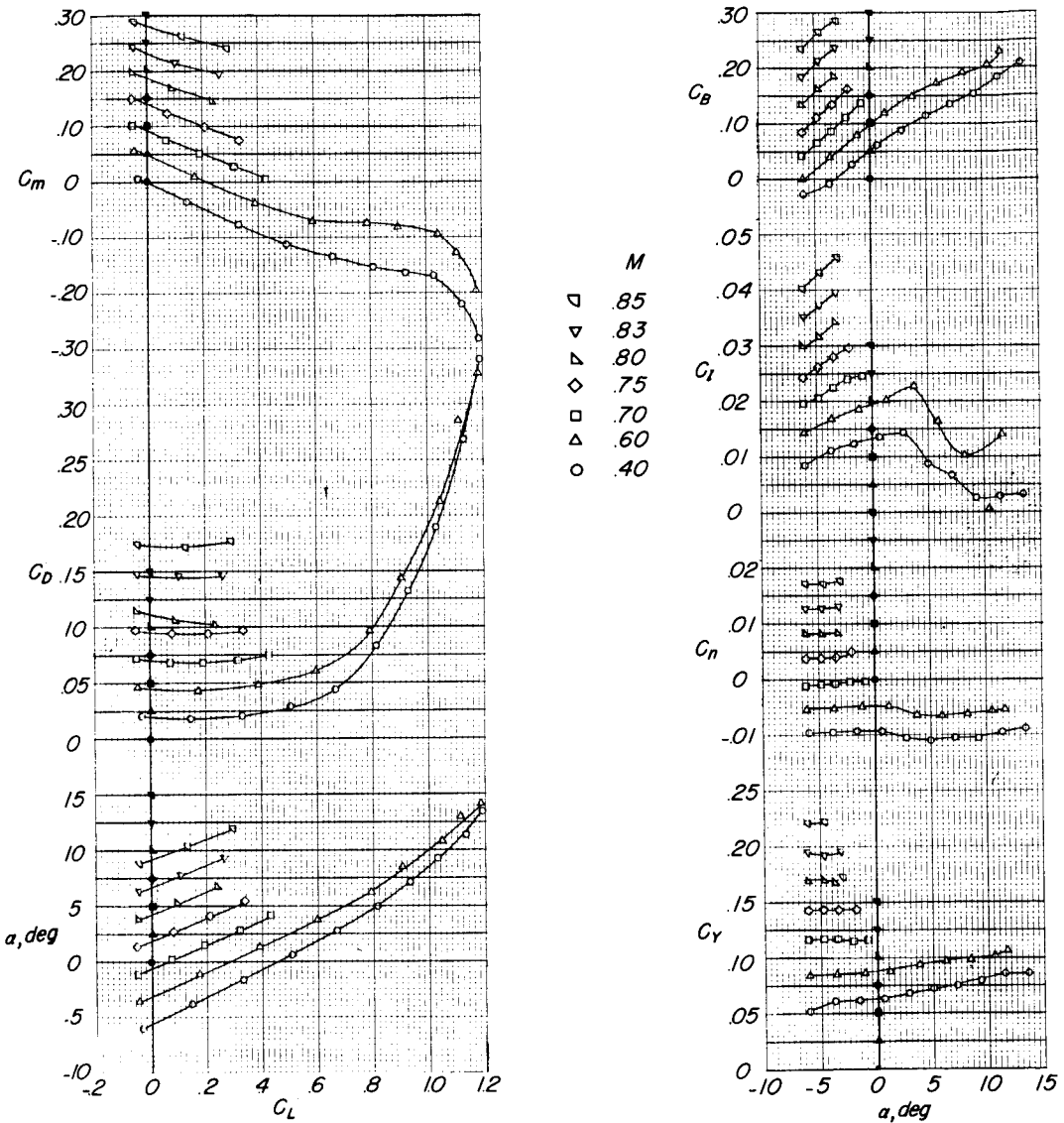
(b)  β = -4°.

Figure 10.- Concluded.

(a)  $\delta_e = 15^\circ$.
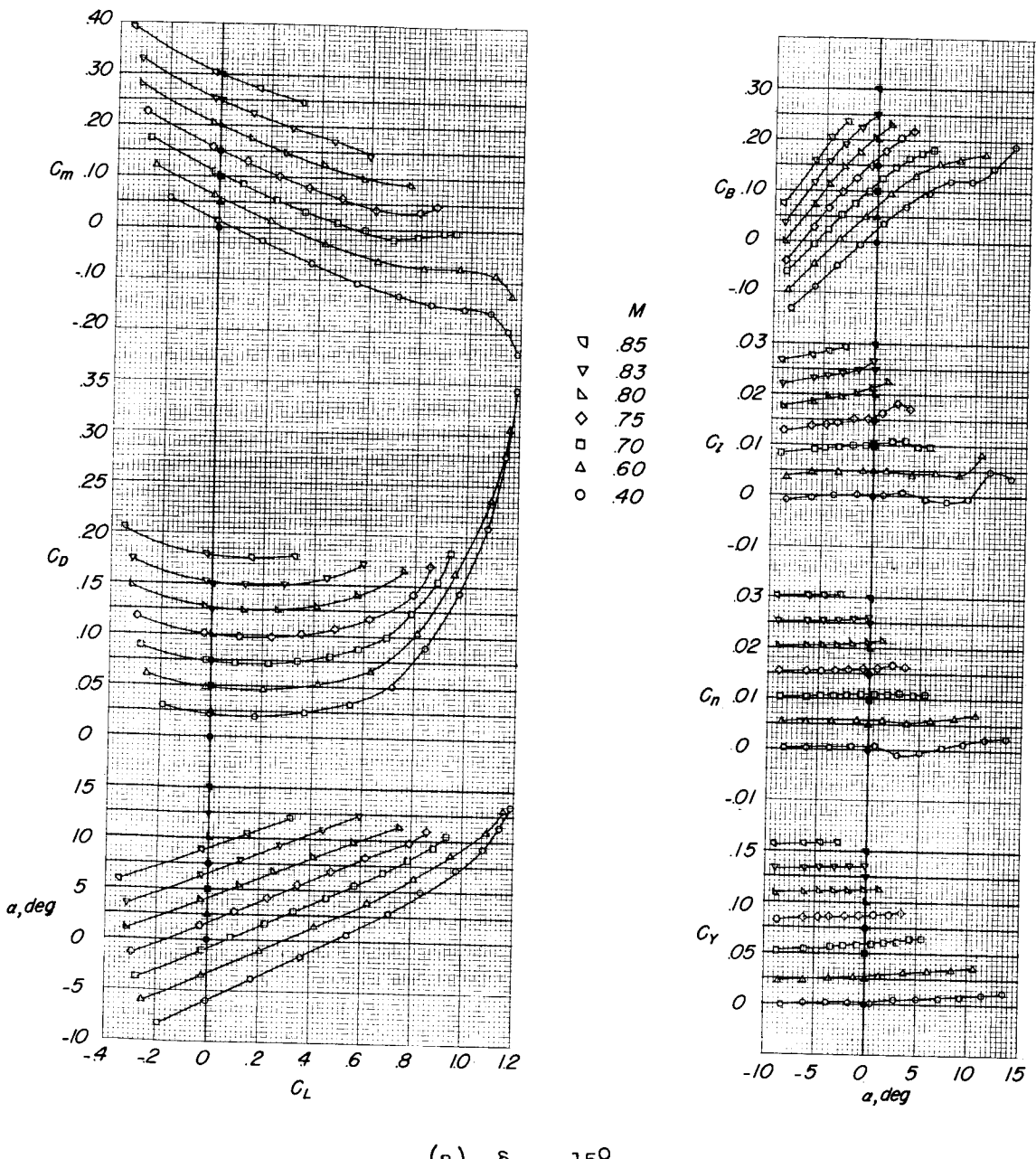
Figure 11.- Aerodynamic characteristics of the B-52 airplane model.  Wing
slot A; X-15 pylon mounted; effect of X-15 pitch control; $i_t = 3^\circ$;
$\beta = 0^\circ$; $\delta_a = \delta_r = 0^\circ$.
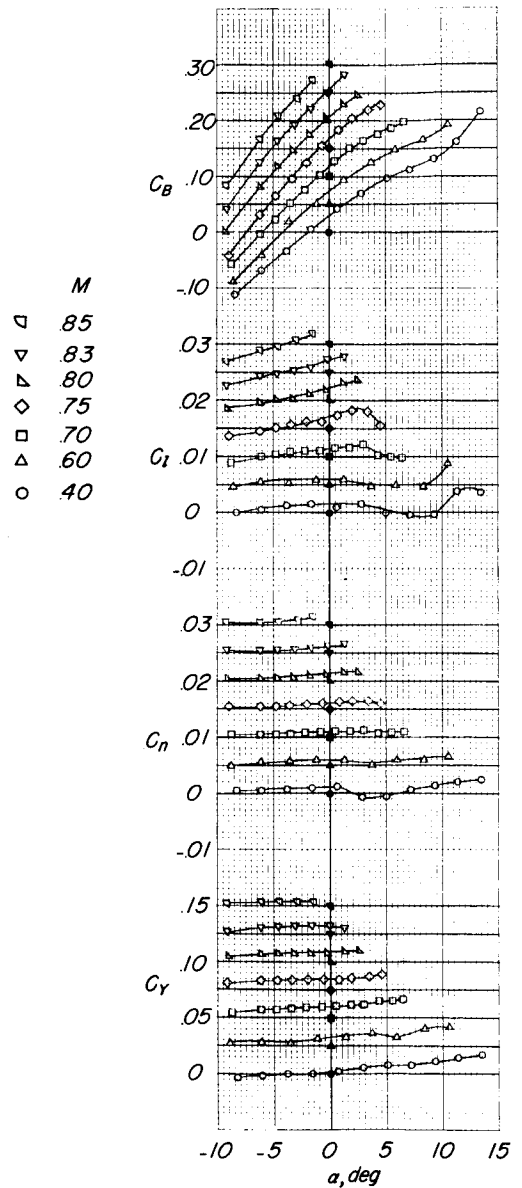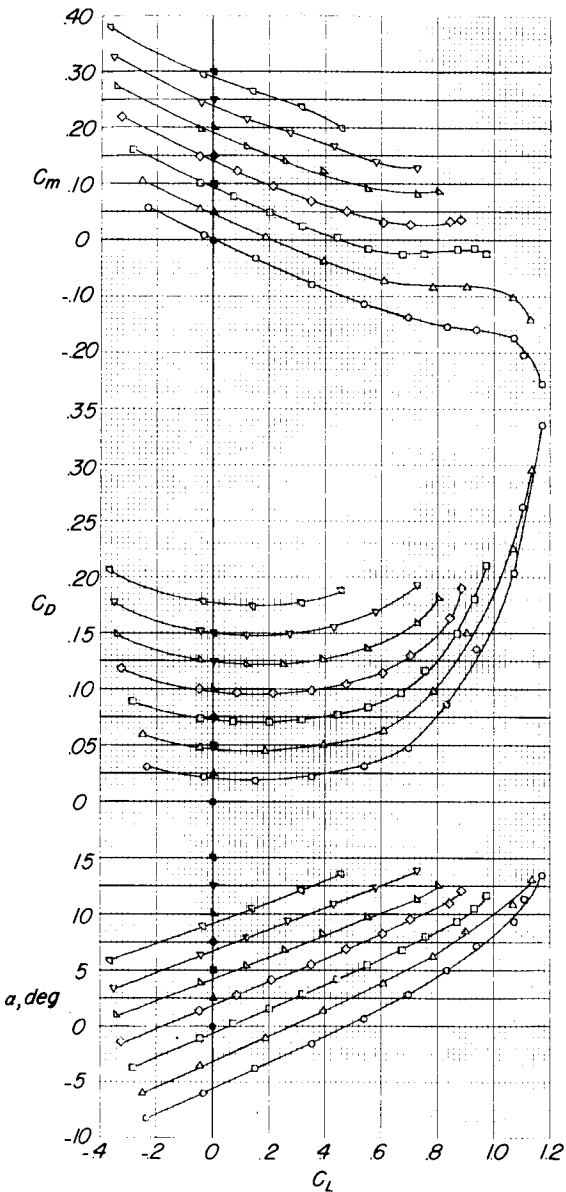
(b)  $\delta_e = 5°$.

Figure 11.- Continued.

(c) $\delta_e = -5°$.

Figure 11.- Continued.
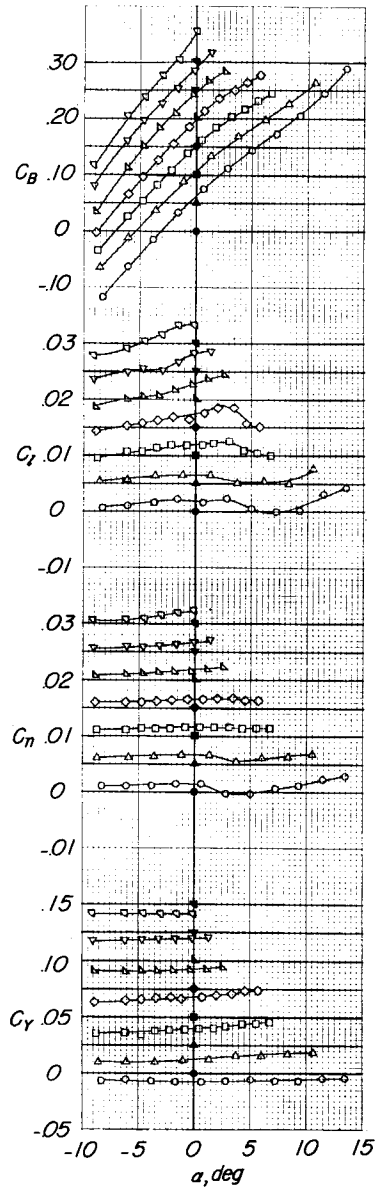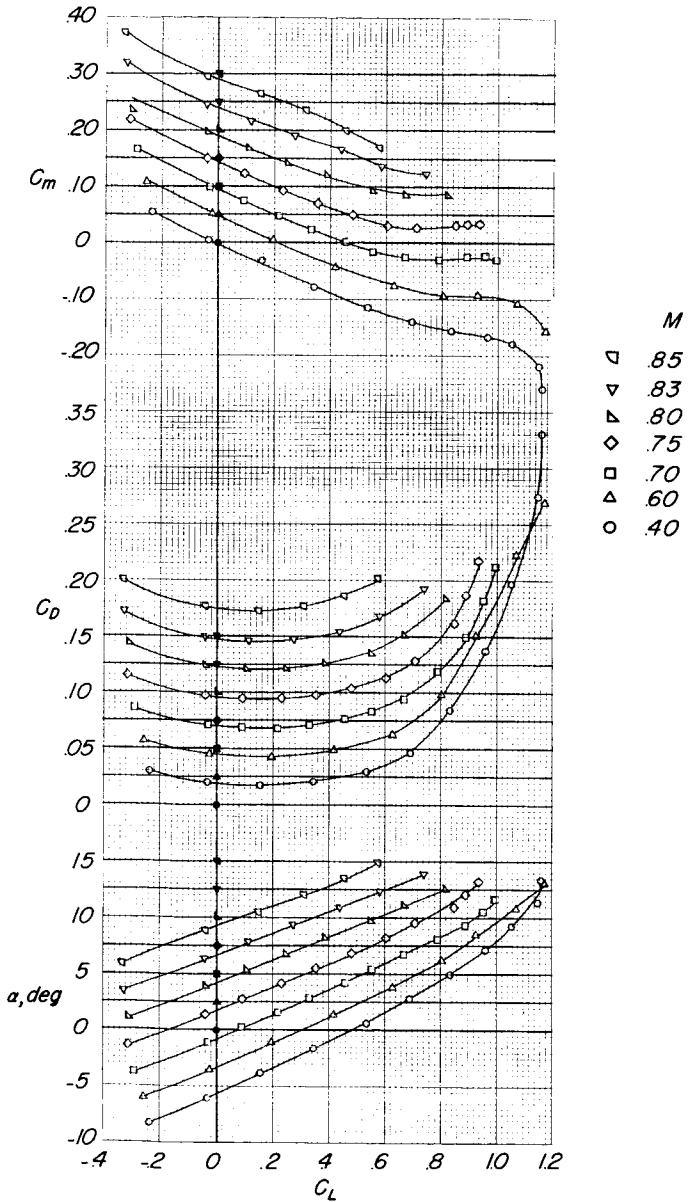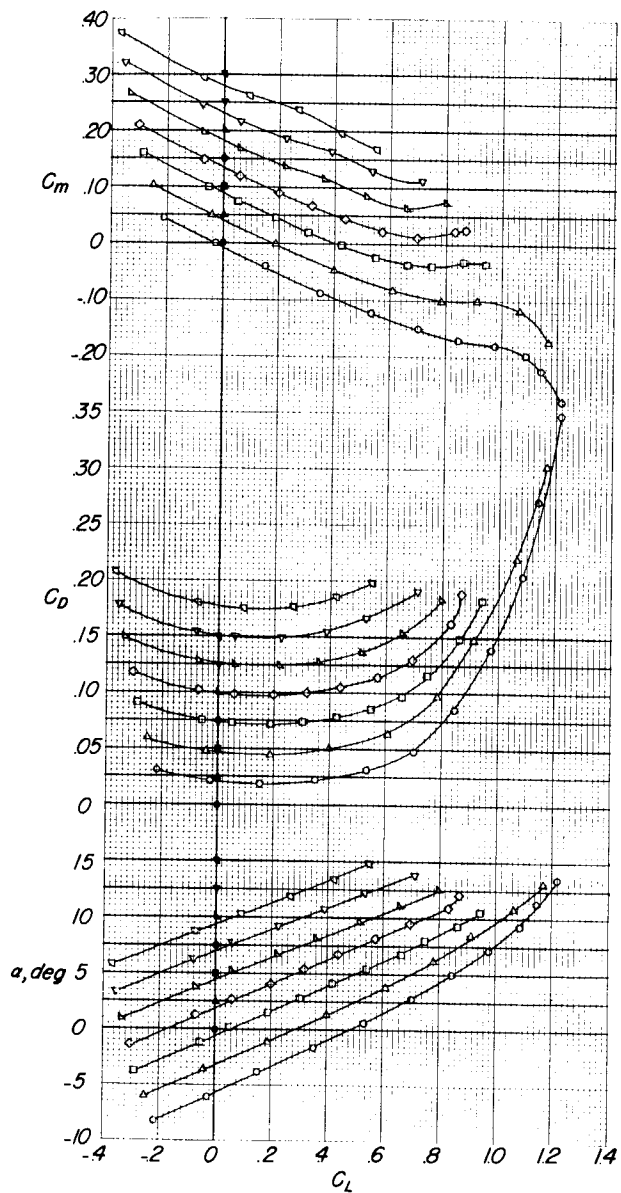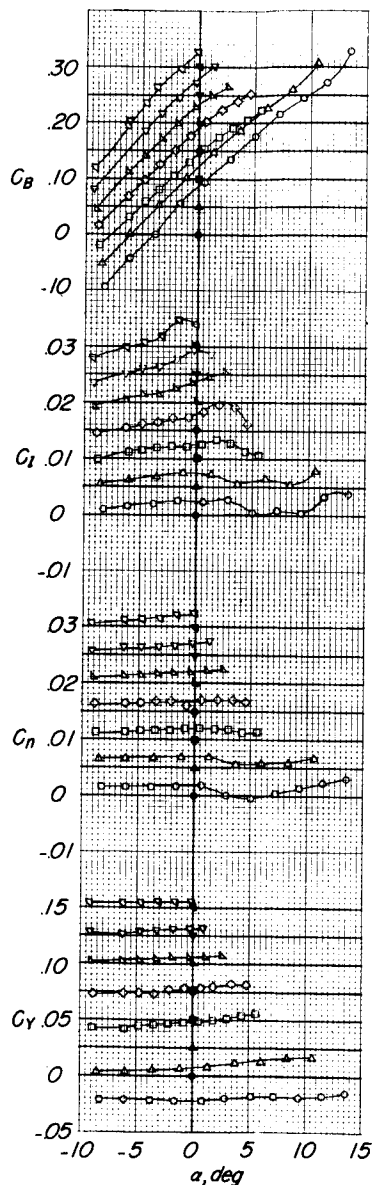
(d)  $\delta_e = -15°$.

Figure 11.- Continued.
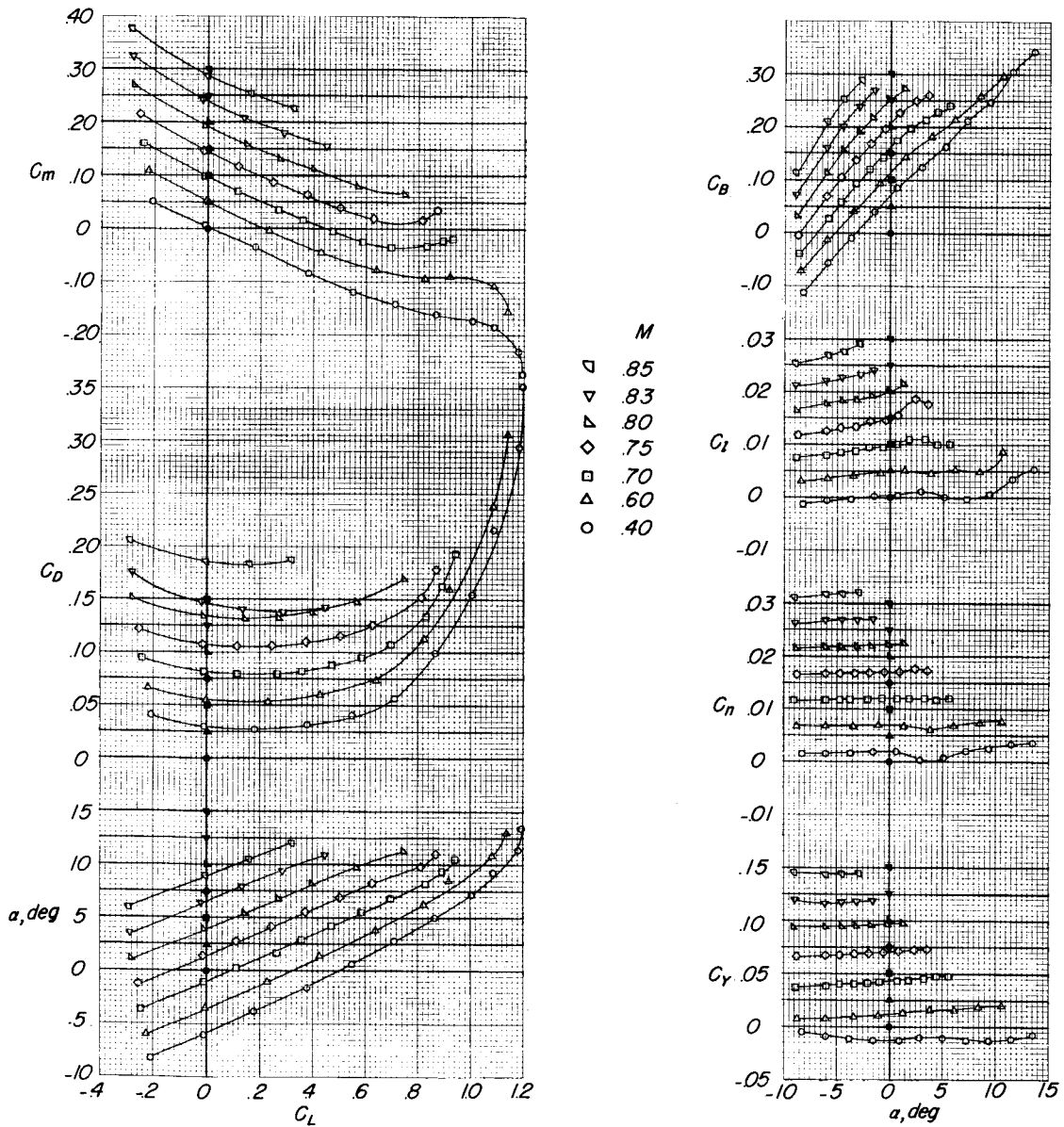
(e) $\delta_e = -45°$.

Figure 11.- Concluded.
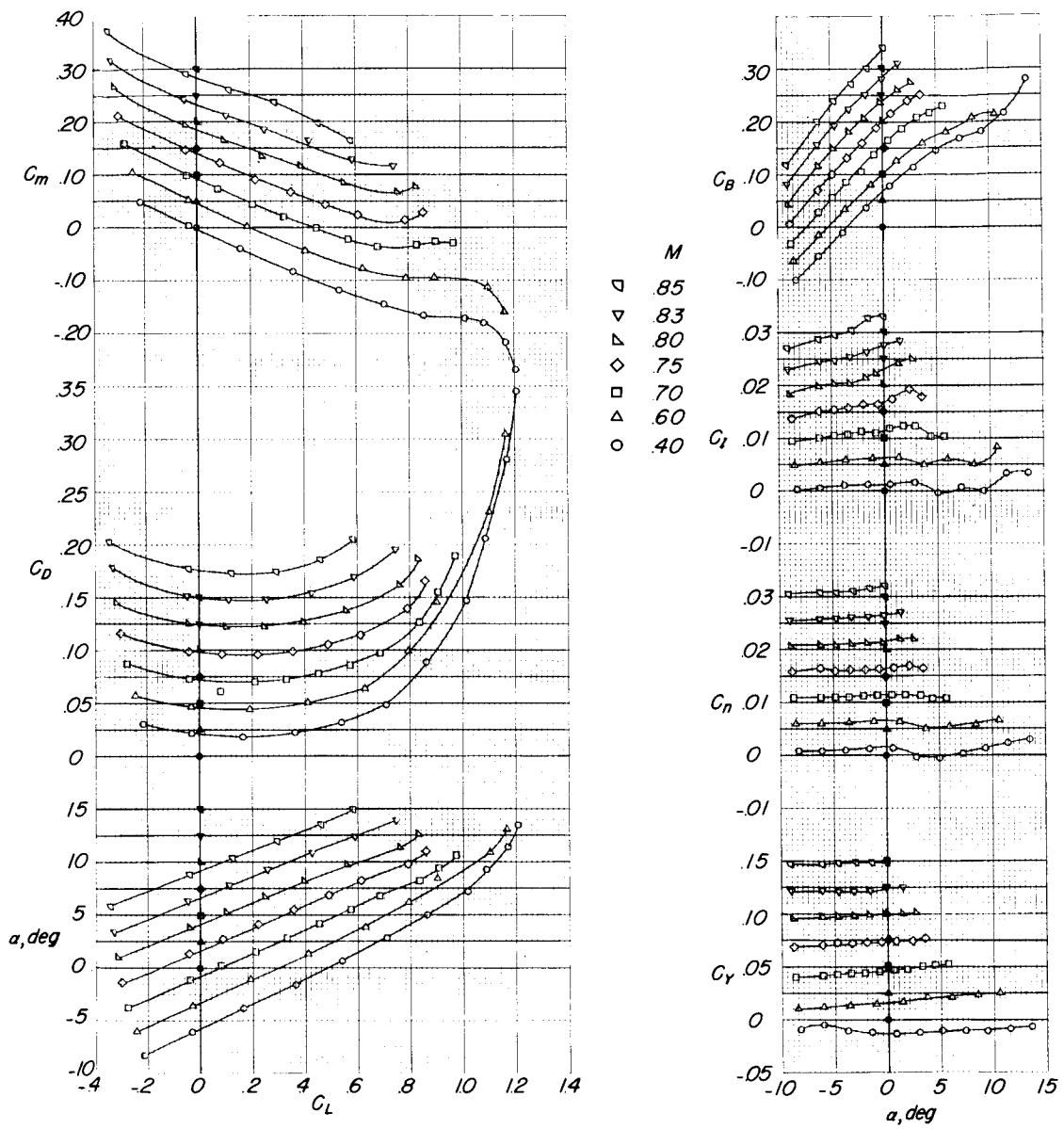
(a)  $\delta_a = 15^\circ$.

Figure 12.- Aerodynamic characteristics of the B-52 airplane model with the X-15 pylon mounted.  Wing slot A; effect of X-15 roll control; $i_t = 3^\circ$; $\beta = 0^\circ$; $\delta_e = \delta_r = 0^\circ$.
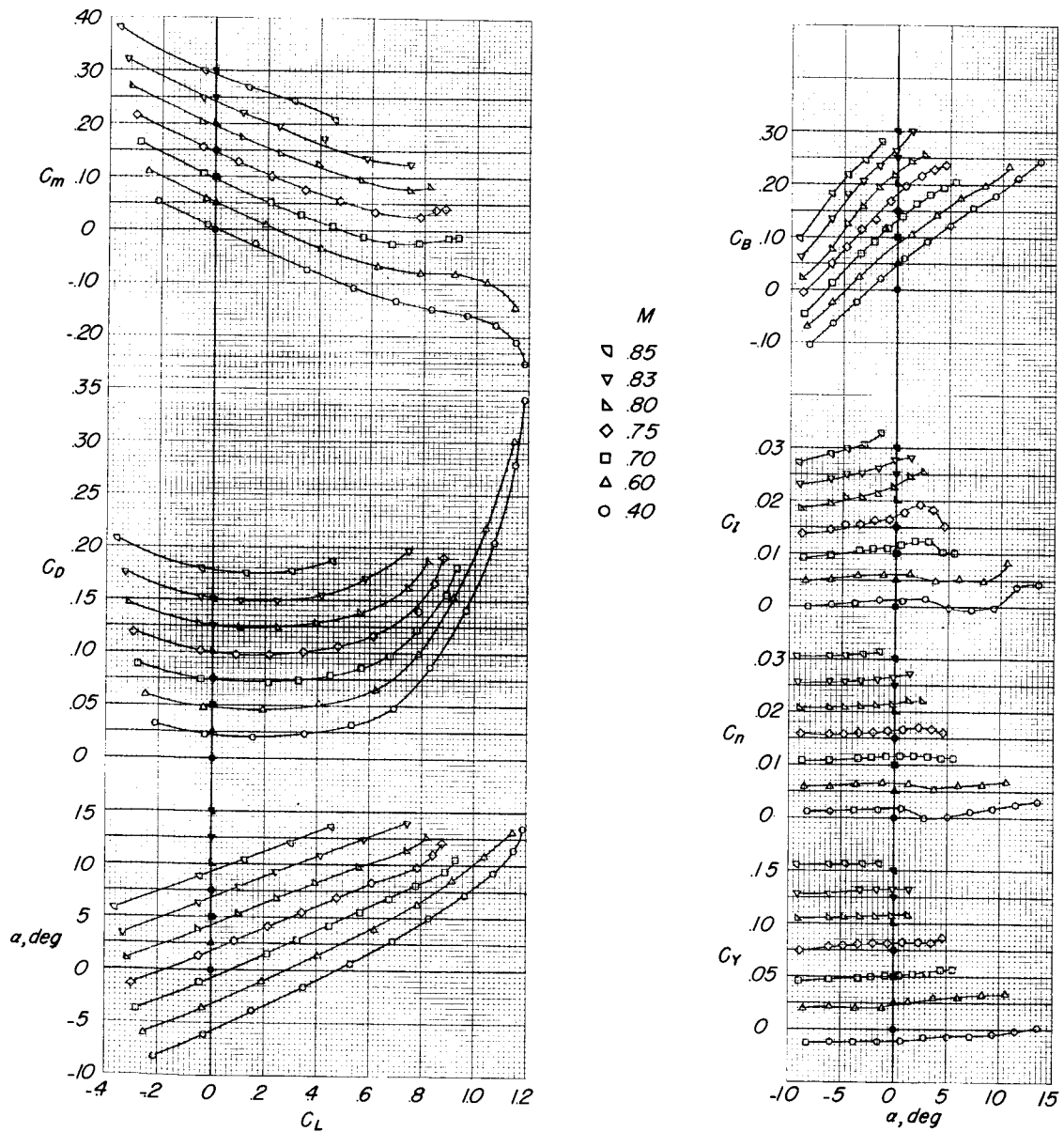
(b) $\delta_a = -15^\circ$.

Figure 12.- Concluded.

(a) $\delta_r = 7.5^o$.
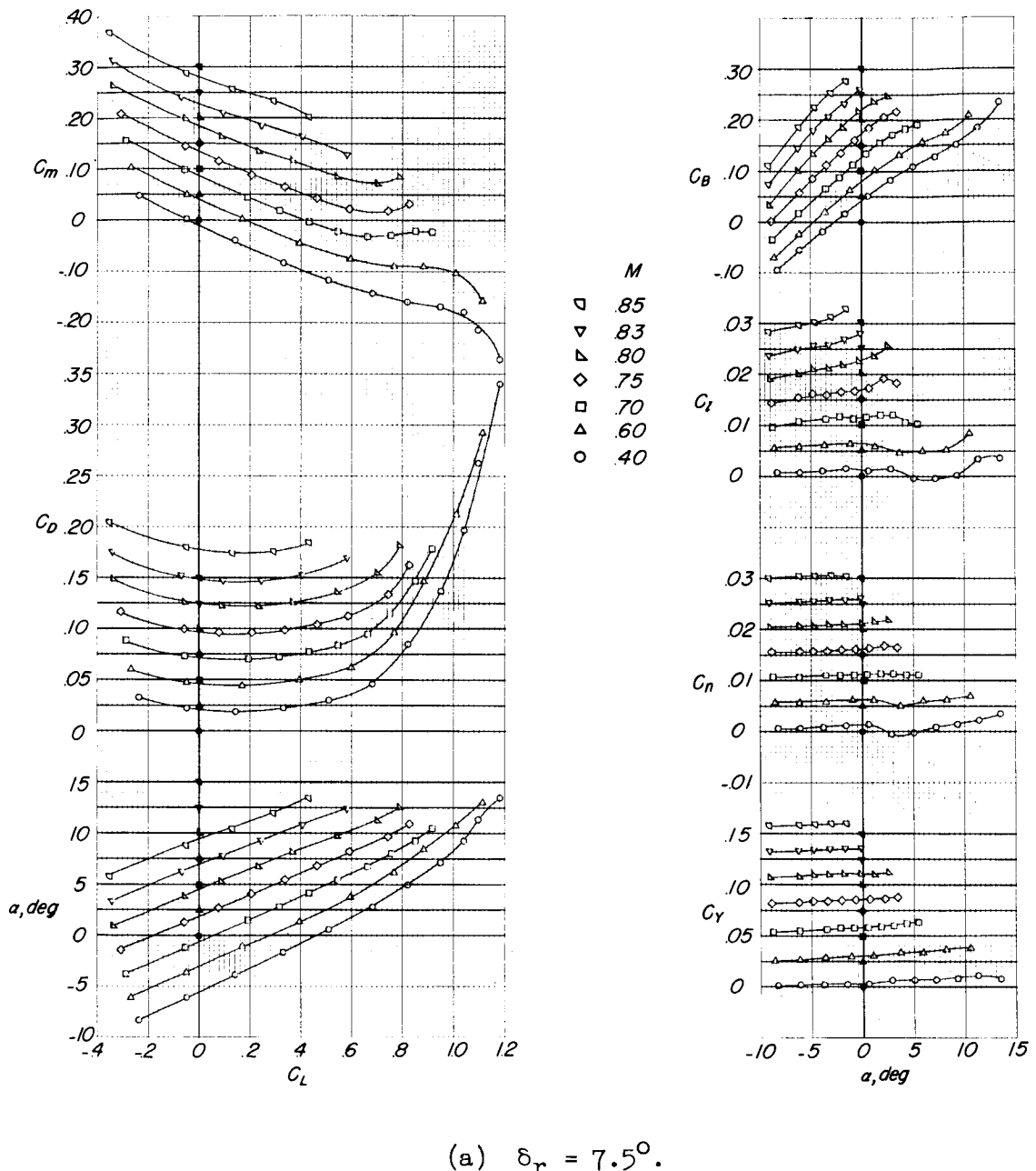
Figure 13.- Aerodynamic characteristics of the B-52 airplane model with the X-15 pylon mounted. Effect of X-15 vertical-tail deflection; $i_t = 3^o$; $\beta = 0^o$; $\delta_a = \delta_e = 0^o$.
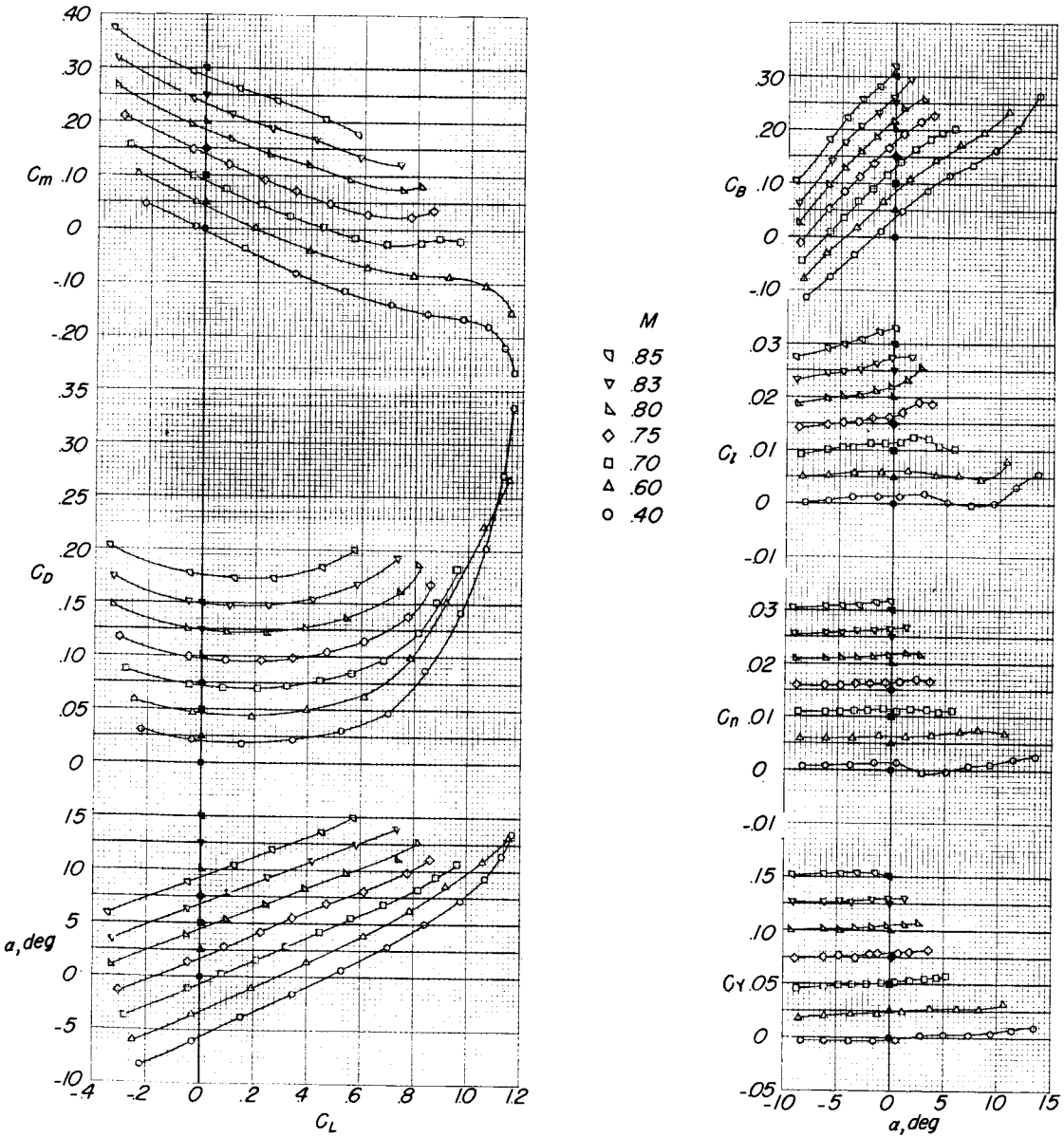
(b)  $\delta_r = -7.5^\circ$.

Figure 13.- Concluded.
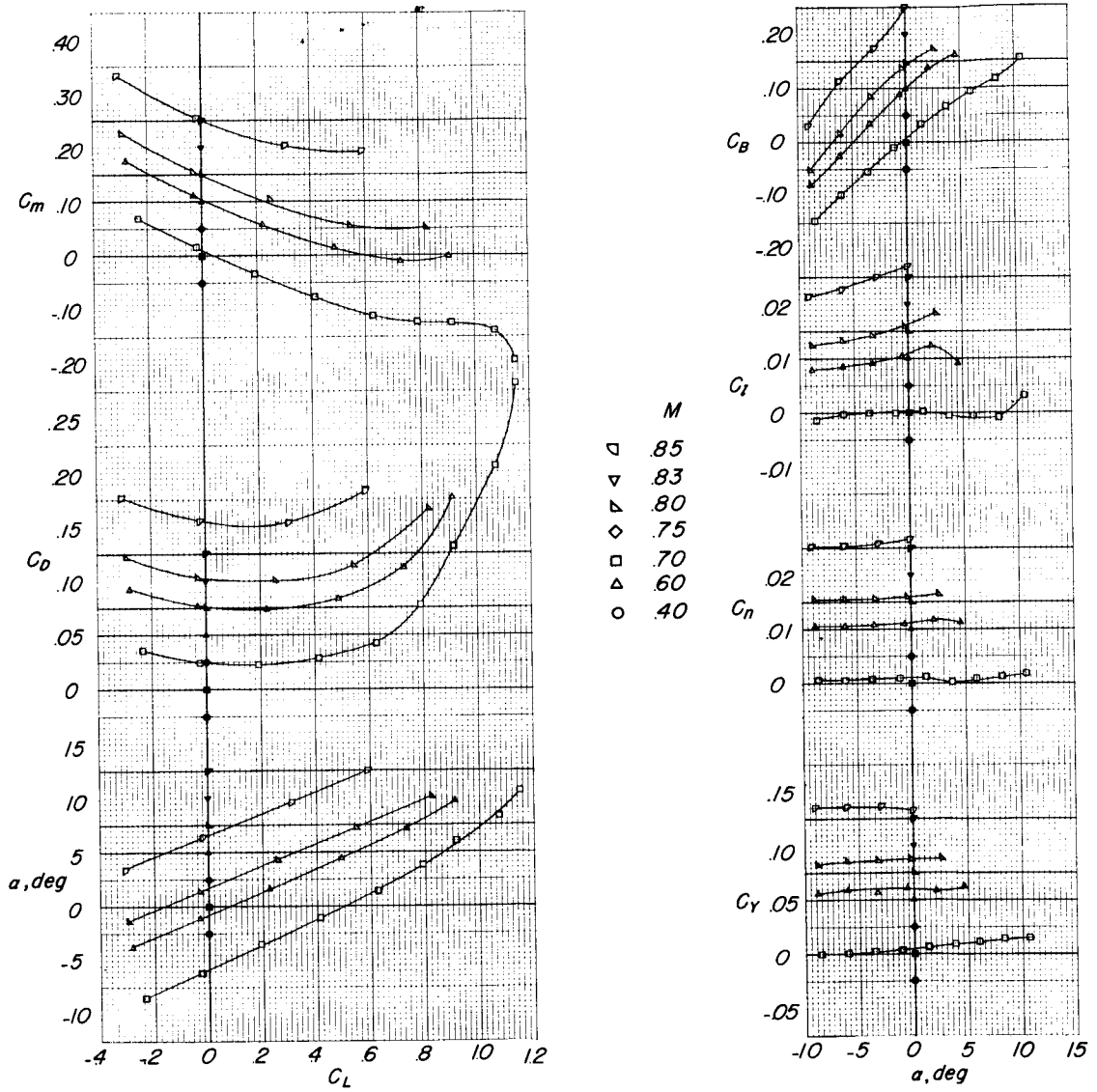
Figure 14.- Aerodynamic characteristics of the B-52 airplane model. X-15 pylon mounted; X-15 speed brakes deflected $35^\circ$; $\delta_a = \delta_e = \delta_r = 0^\circ$; $i_t = 3^\circ$; $\beta = 0^\circ$.

(a)  $i_t = 3^O$.
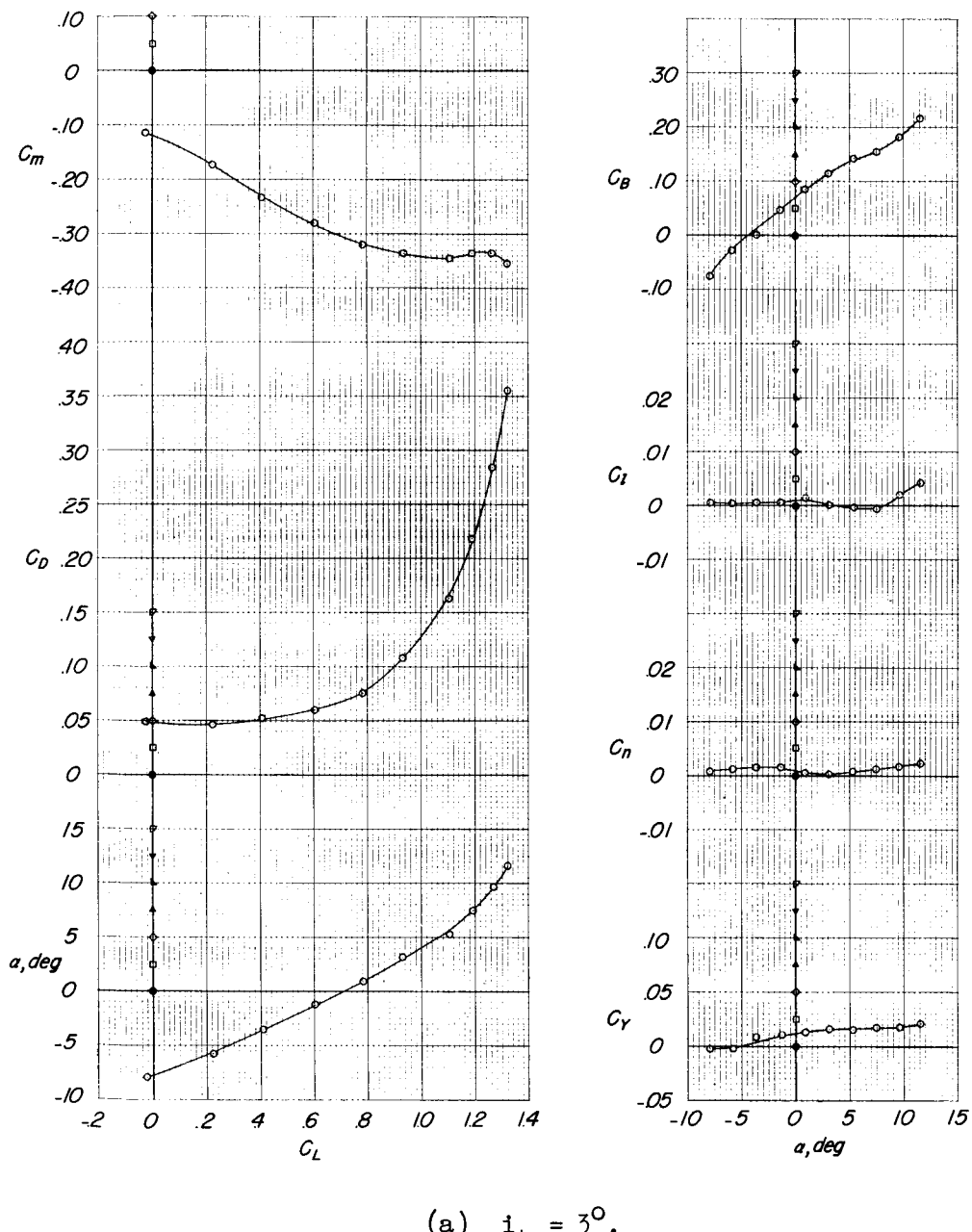
Figure 15.- Aerodynamic characteristics of the B-52 airplane model with the X-15 pylon mounted; effect of stabilizer deflection with outboard B-52 flaps deflected $30^O$; M = 0.40.
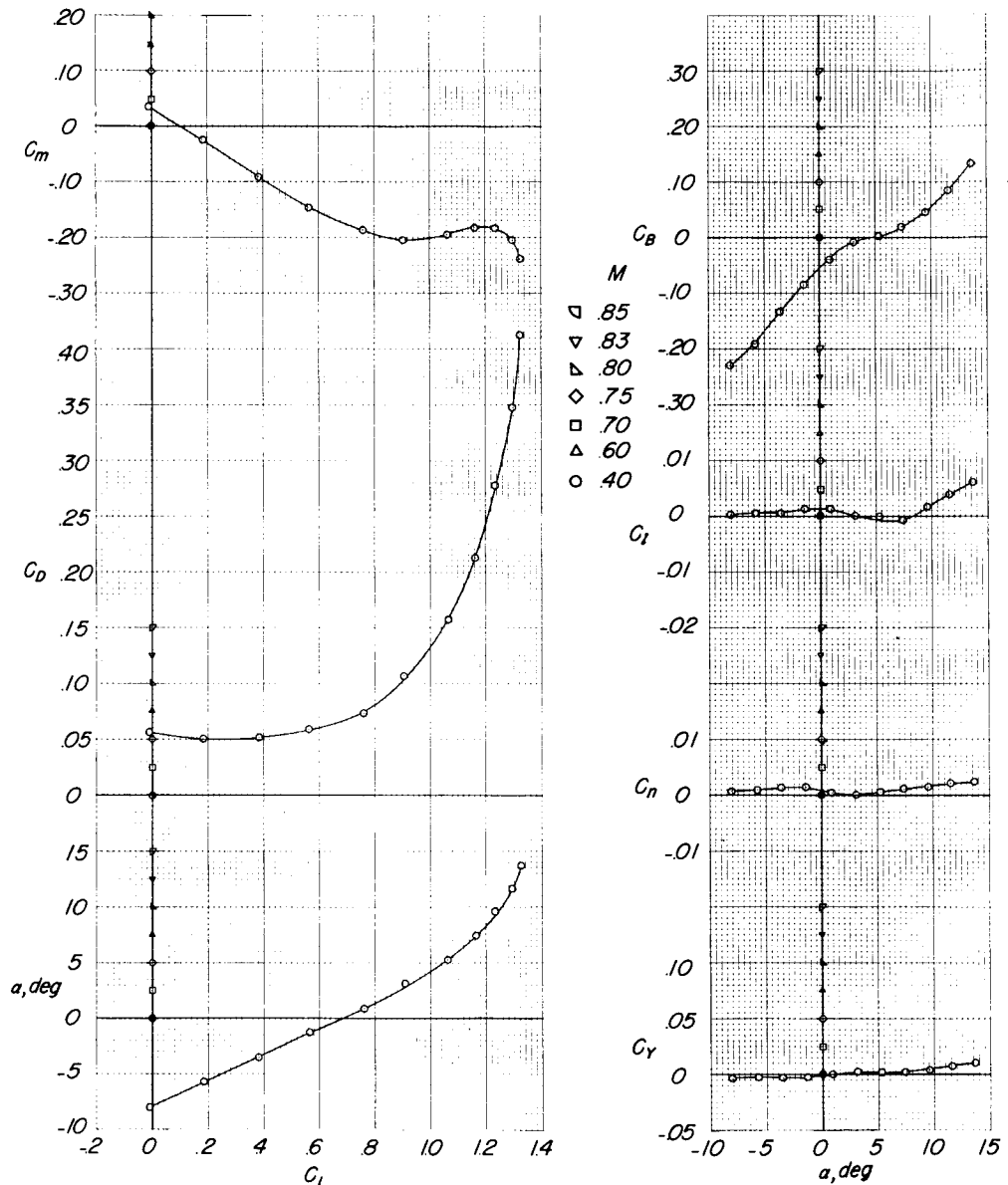
(b)  $i_t = -2^\circ$.

Figure 15.- Concluded.
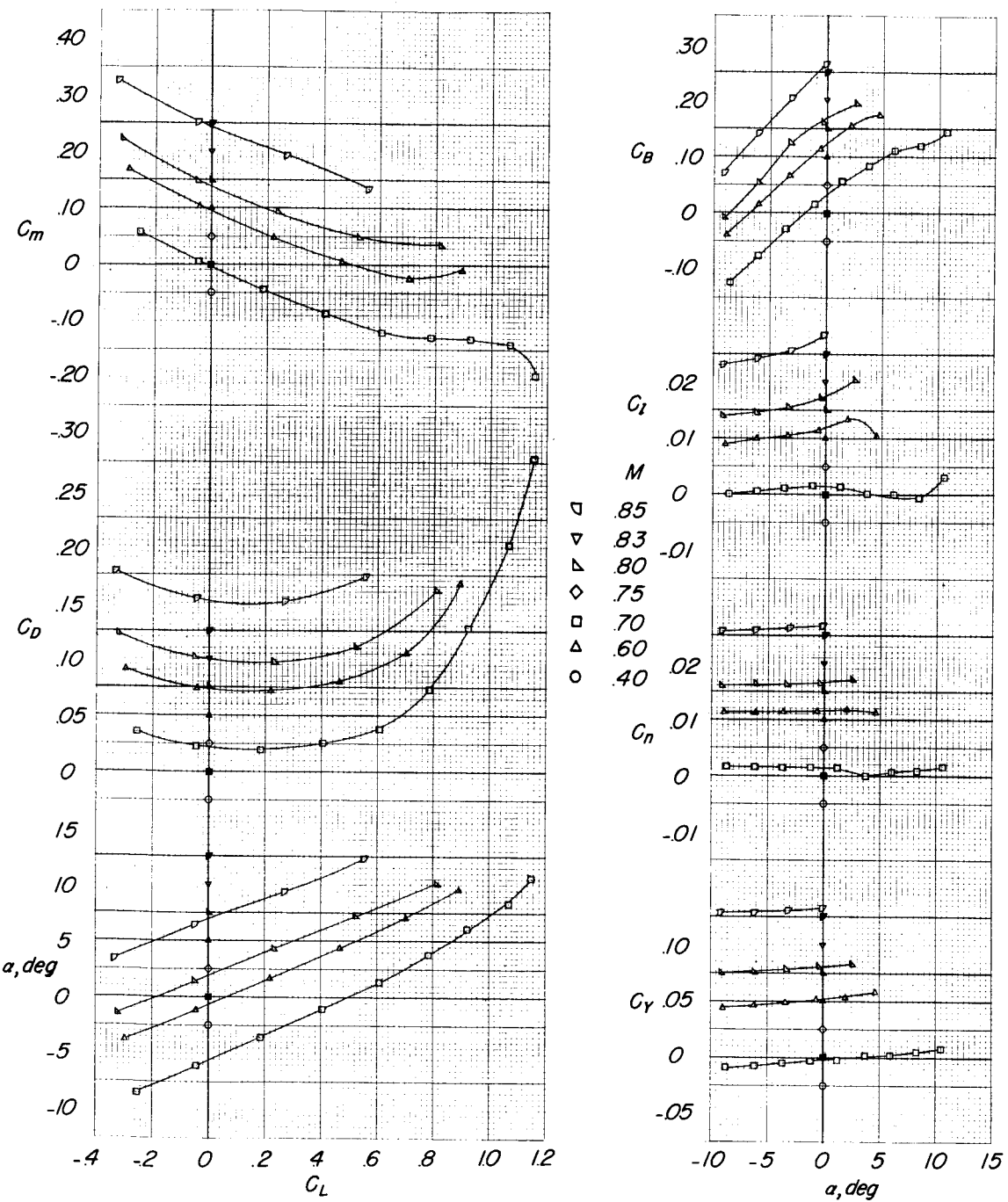
Figure 16.- Aerodynamic characteristics of the B-52 airplane model. X-15 pylon mounted; buffet fairing in place; $\delta_a = \delta_r = \delta_e = 0^\circ$; $i_t = 3^\circ$; $\beta = 0^\circ$.
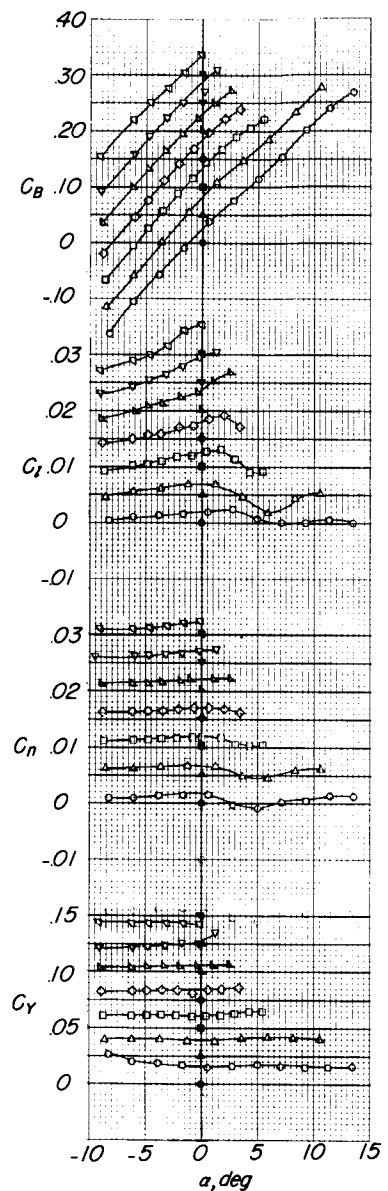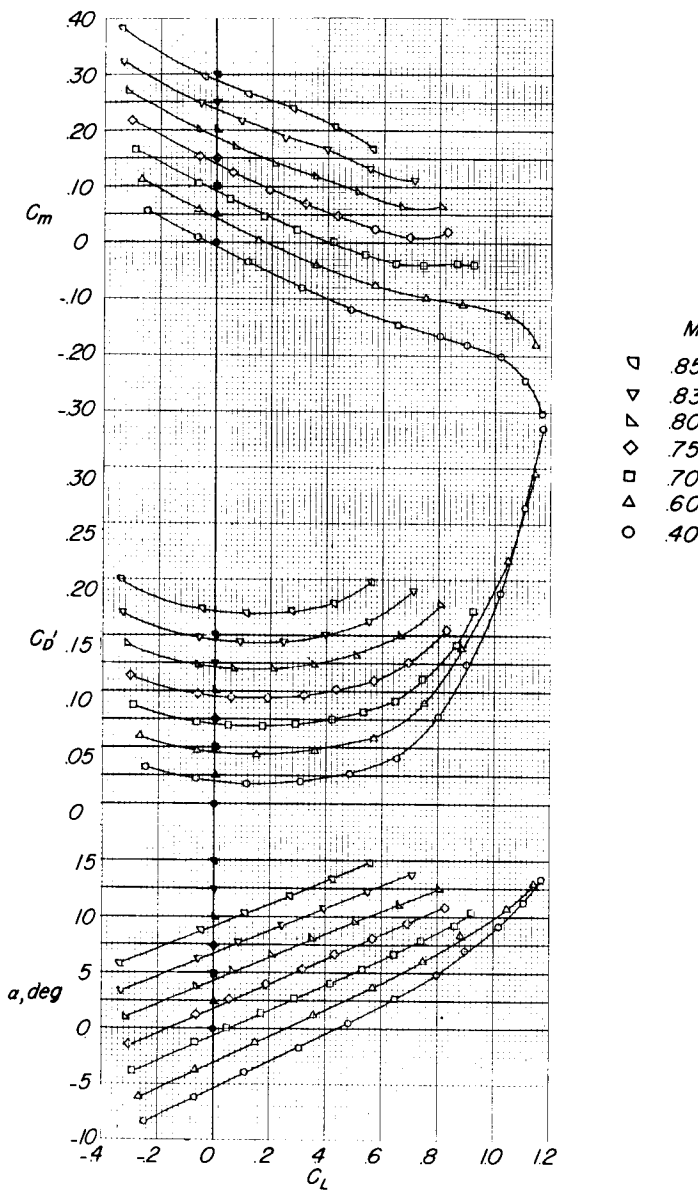
(a)  β = 0°.

Figure 17.- Aerodynamic characteristics of the B-52 airplane model with X-15 off and wing slot and pylon in place.  Effect of sideslip; $i_t$ = 3°.
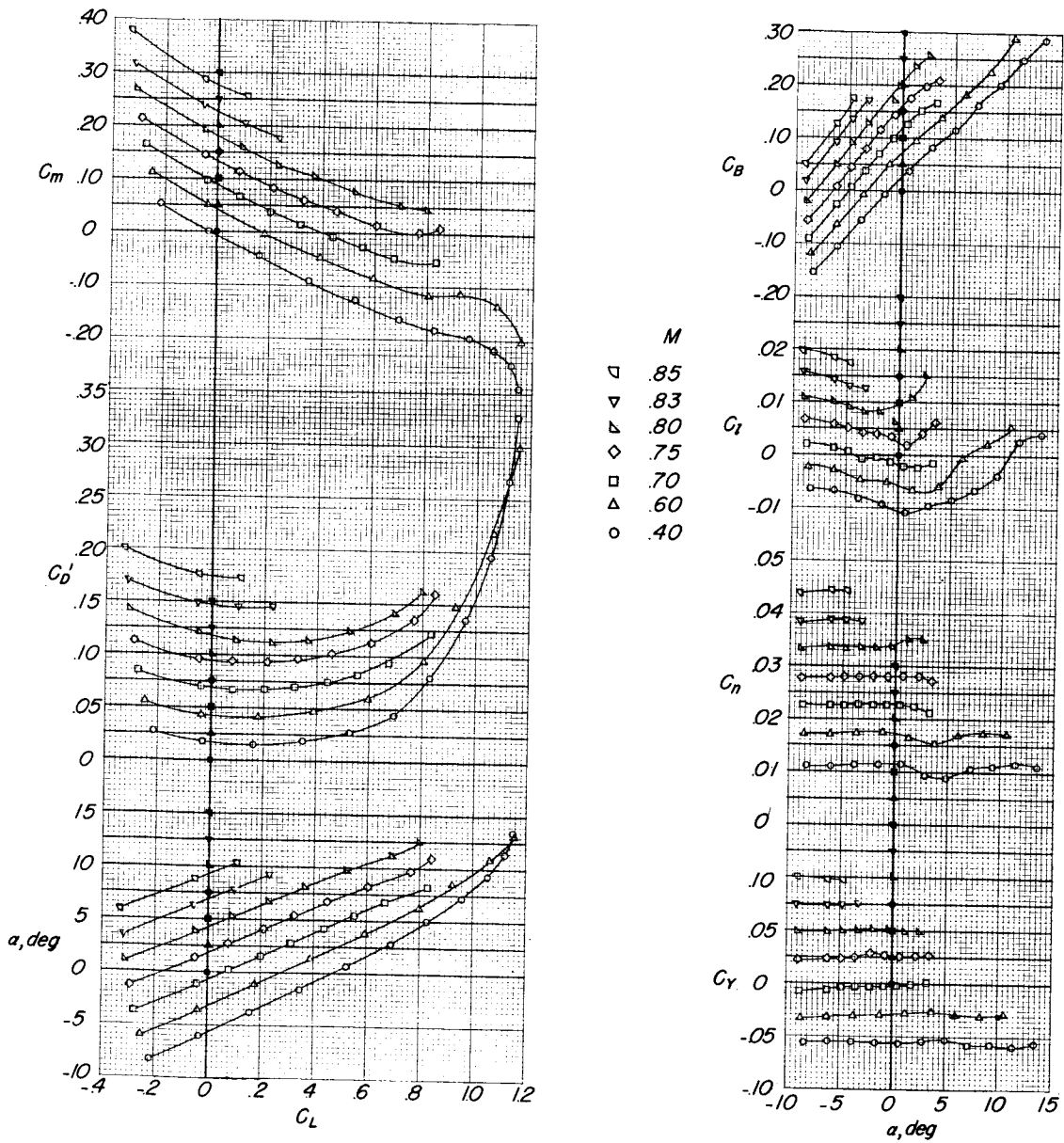
(b)  β = 4°.

Figure 17.- Continued.
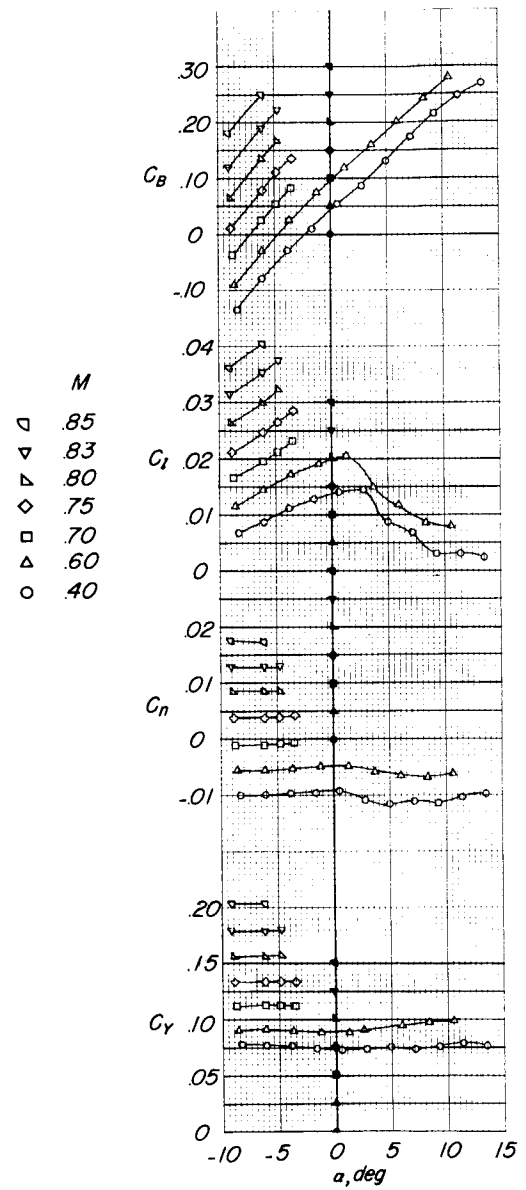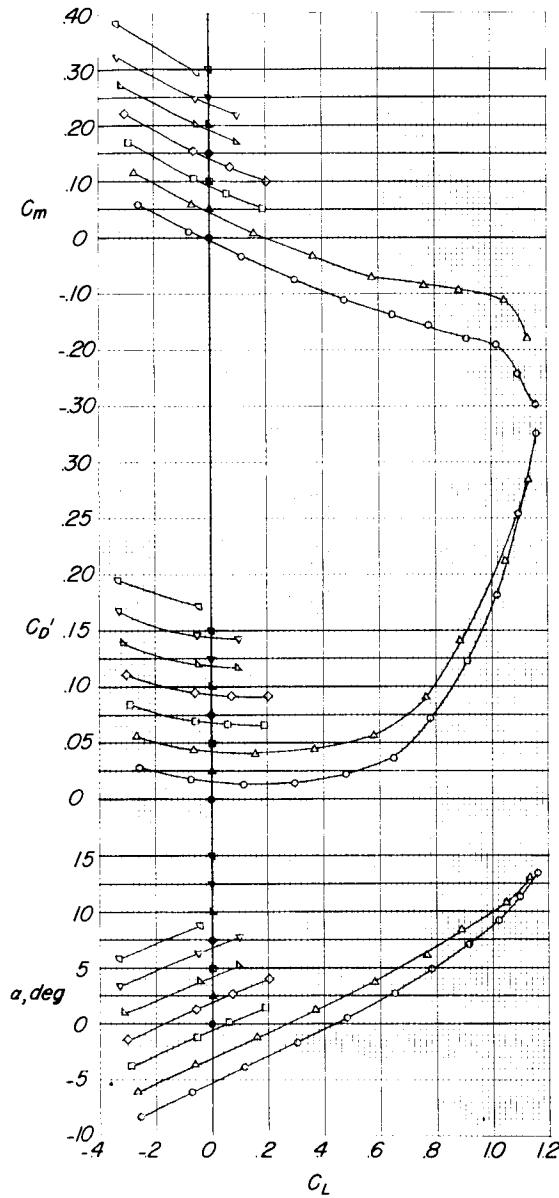
(c)  β = -4°.

Figure 17.- Concluded.
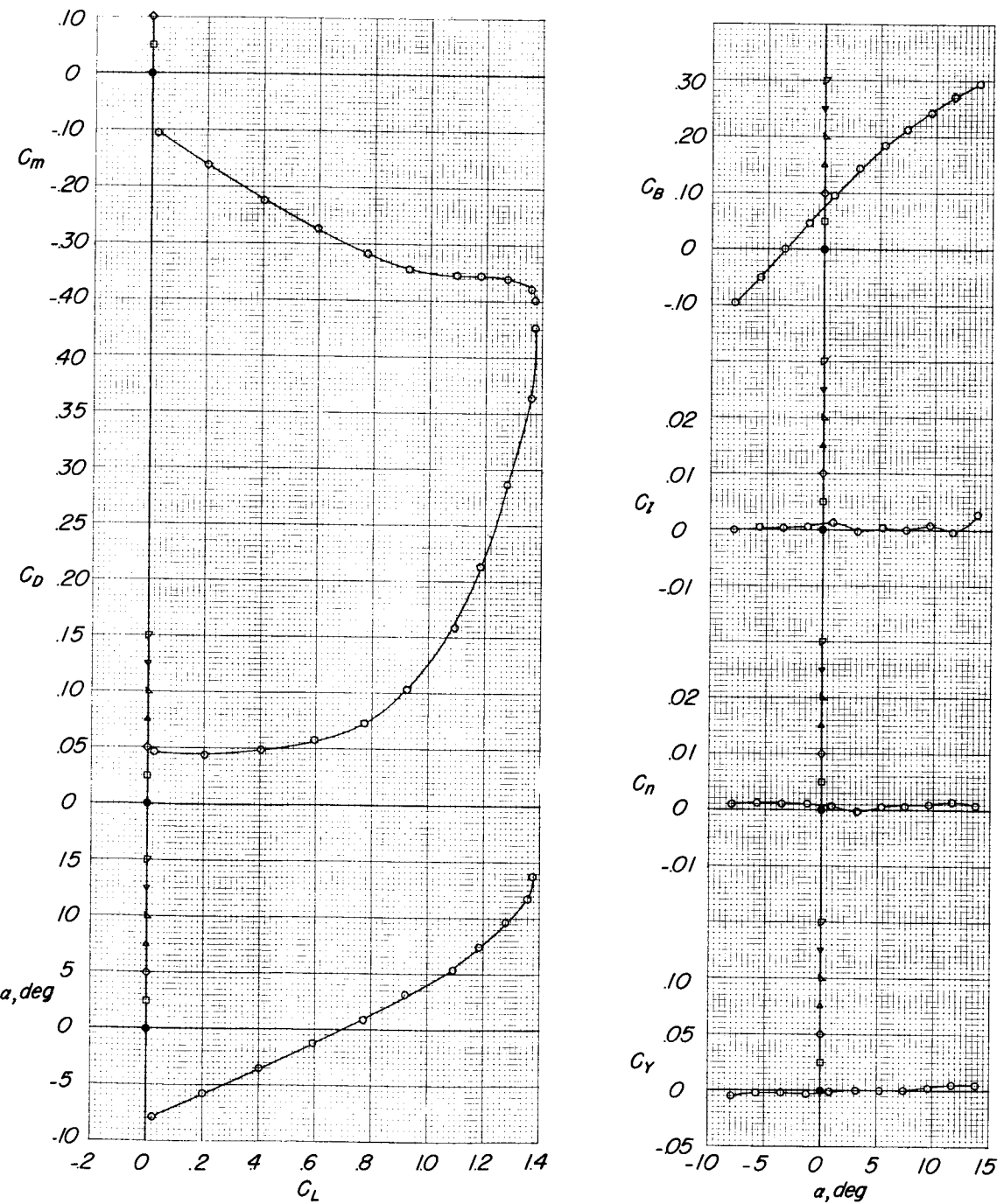
Figure 18.- Aerodynamic characteristics of the B-52 airplane model with the X-15 off and slot and pylon in place. Effect of outboard flap deflection; $\delta_f = 30°$; M = 0.40.
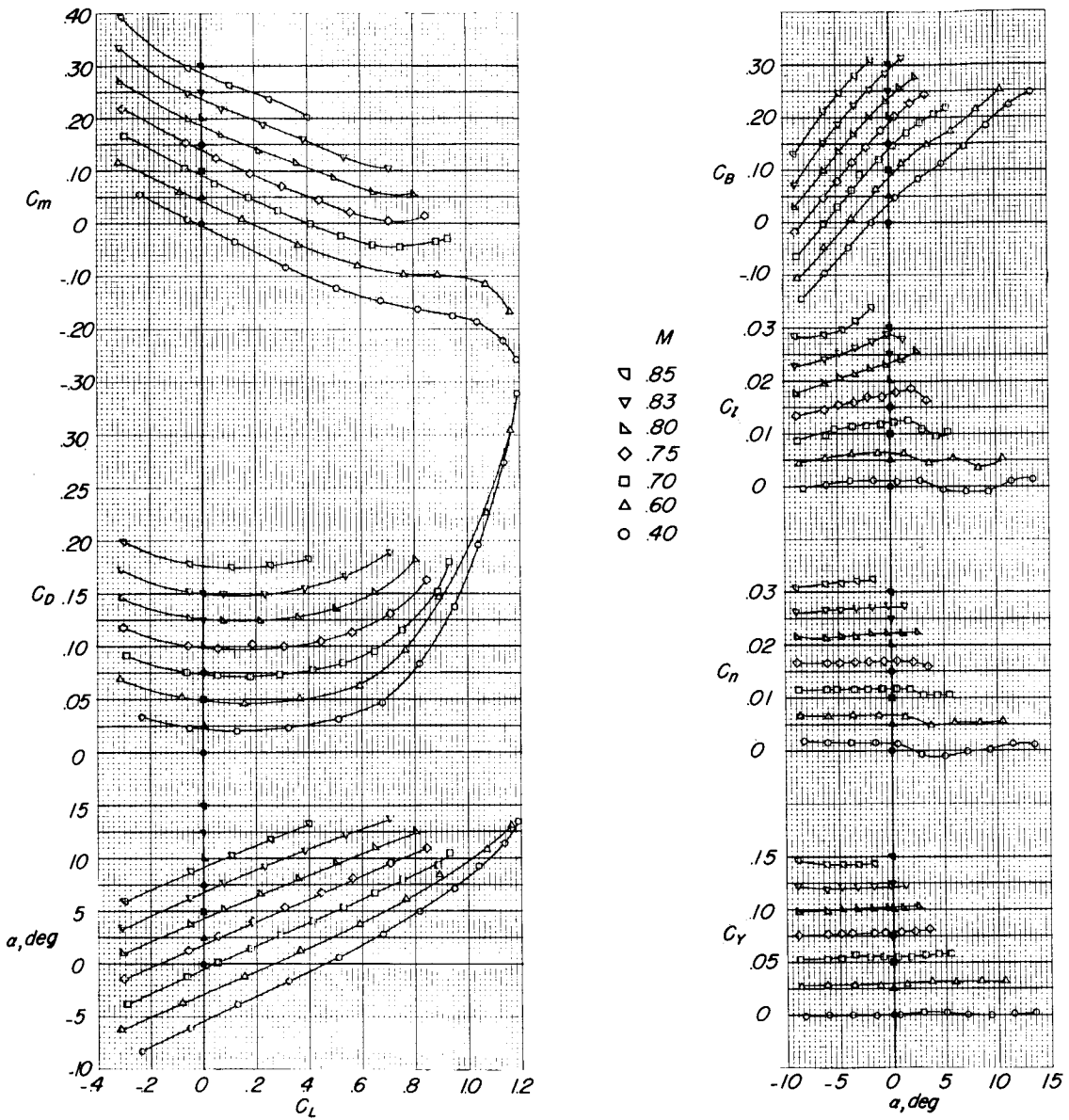
Figure 19.- Aerodynamic characteristics of the B-52 airplane model with X-15 off and slot and pylon in place. Buffet fairing on; $\beta = 0°$; $i_t = 3°$.
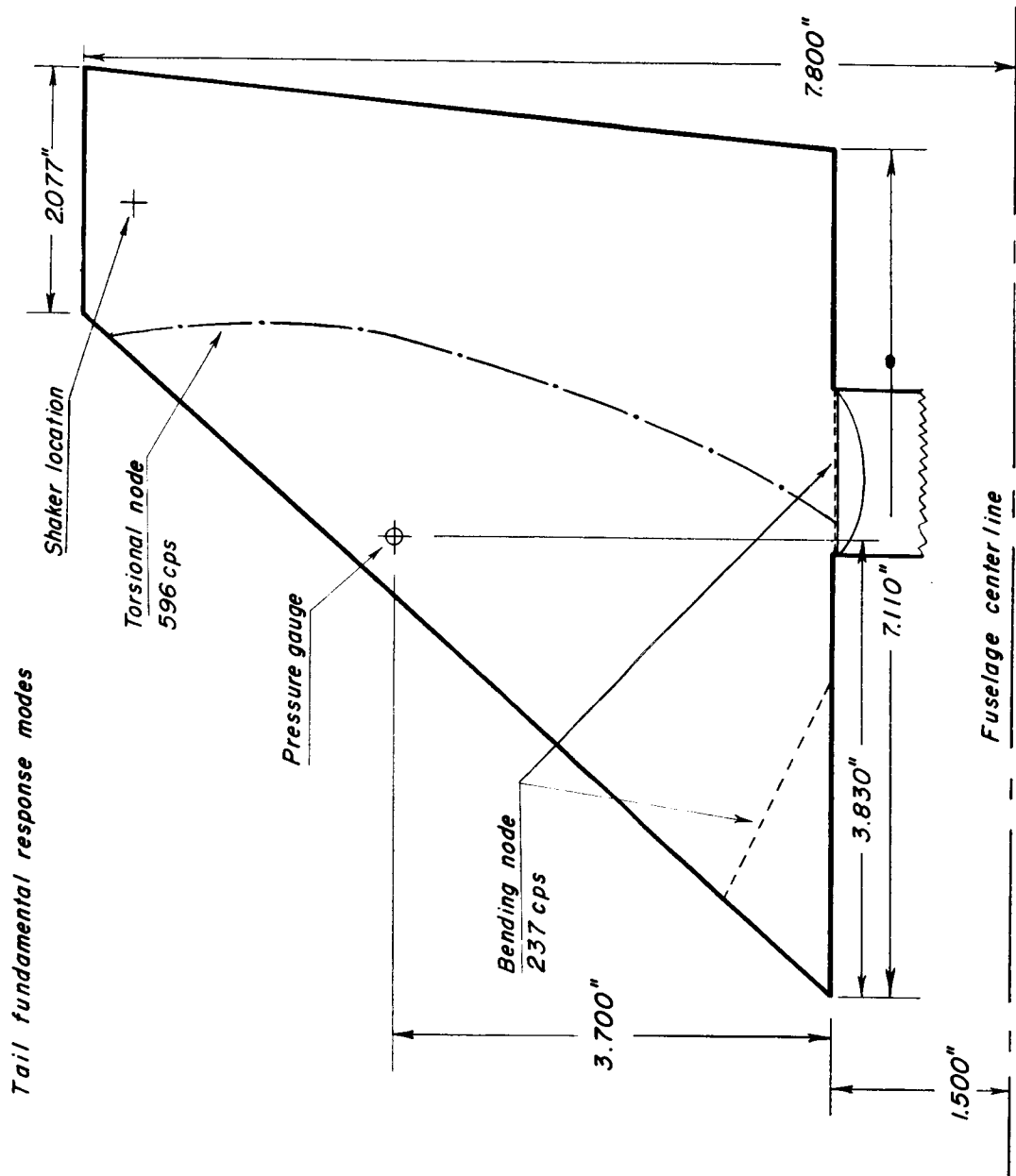
Figure 20.- B-52 horizontal-tail fundamental response modes.
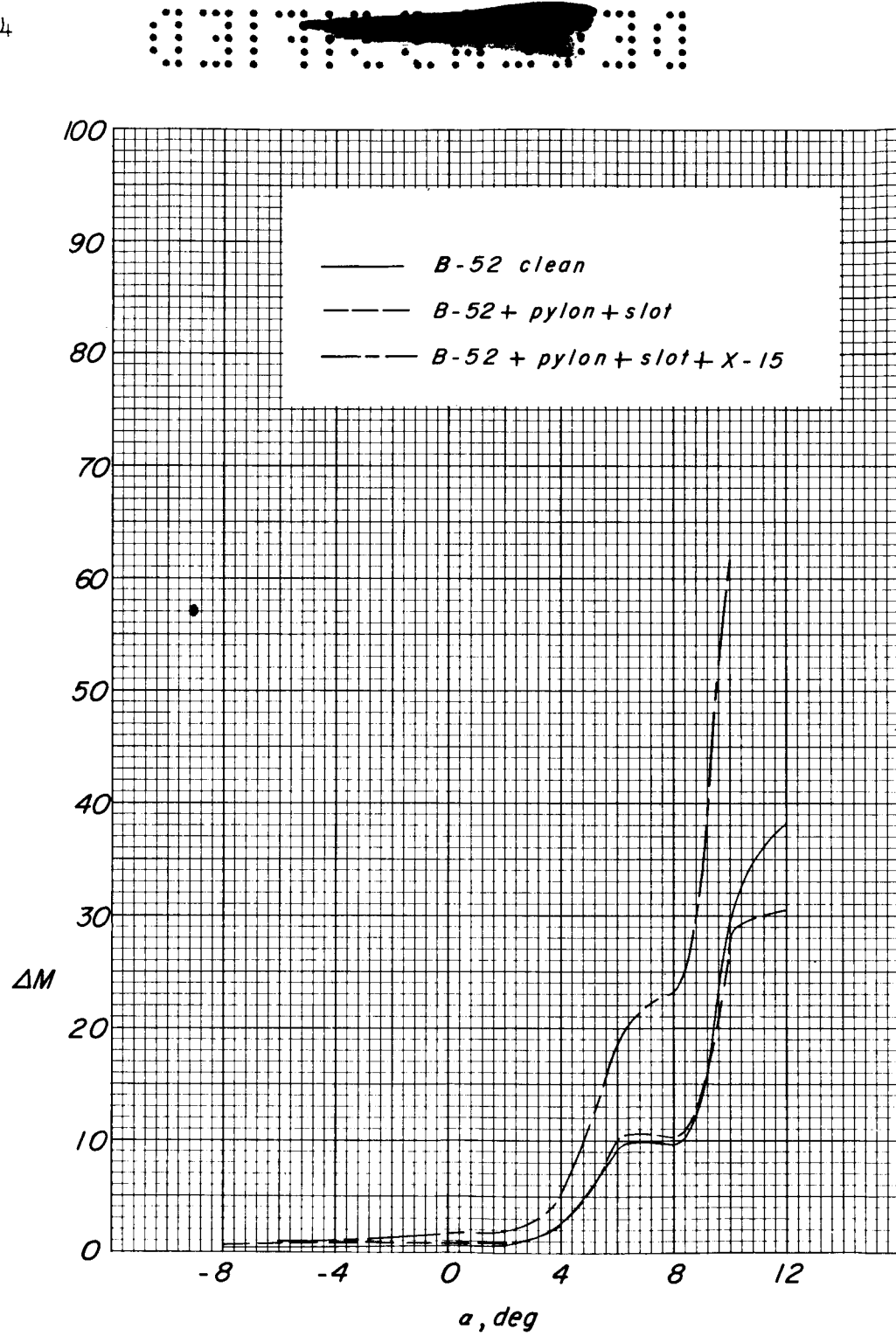
(a)  M = 0.40.

Figure 21.- Effect of the basic additions on horizontal-tail panel buffet.
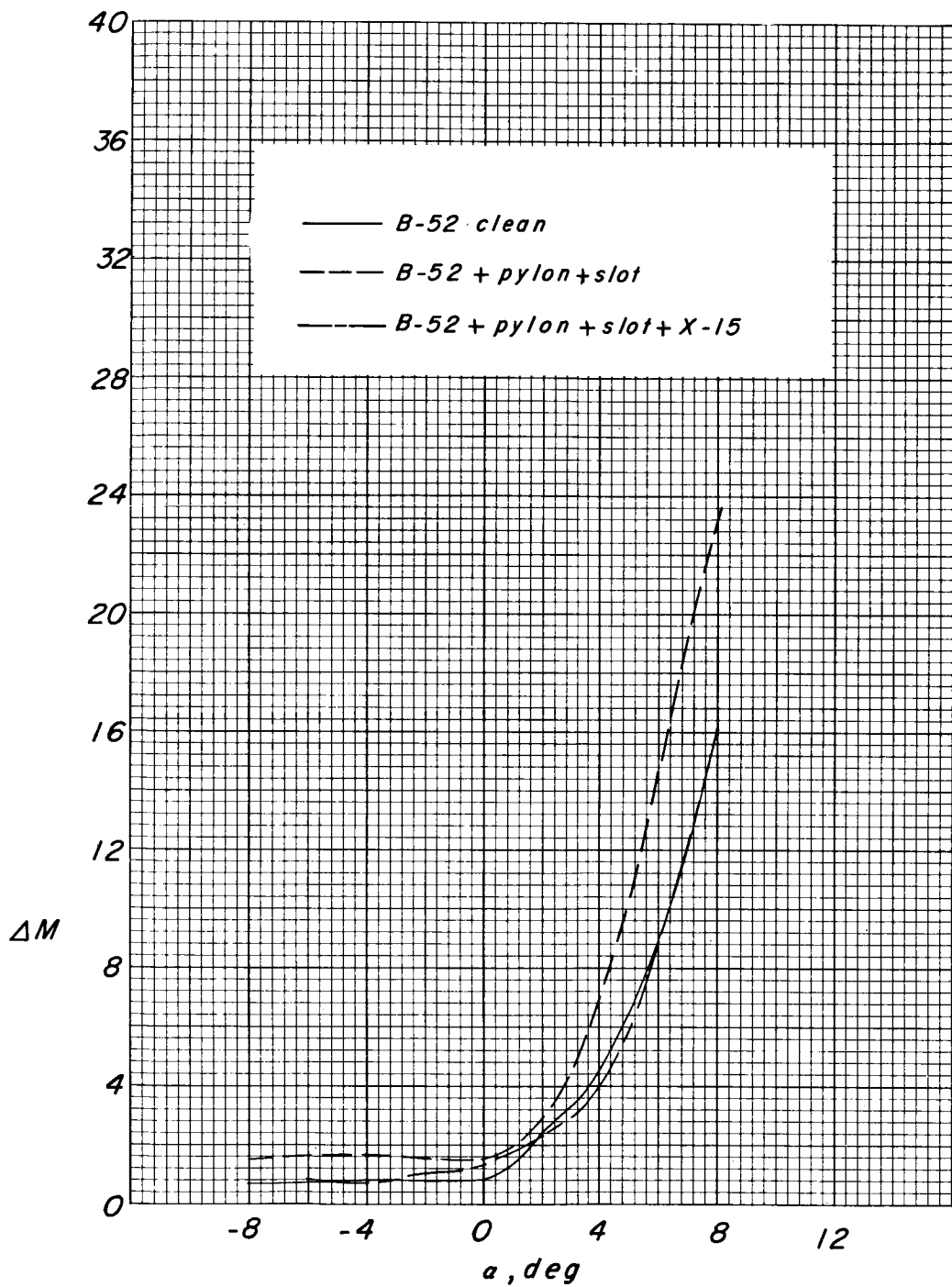
(b)   M = 0.60.

Figure 21.- Continued.
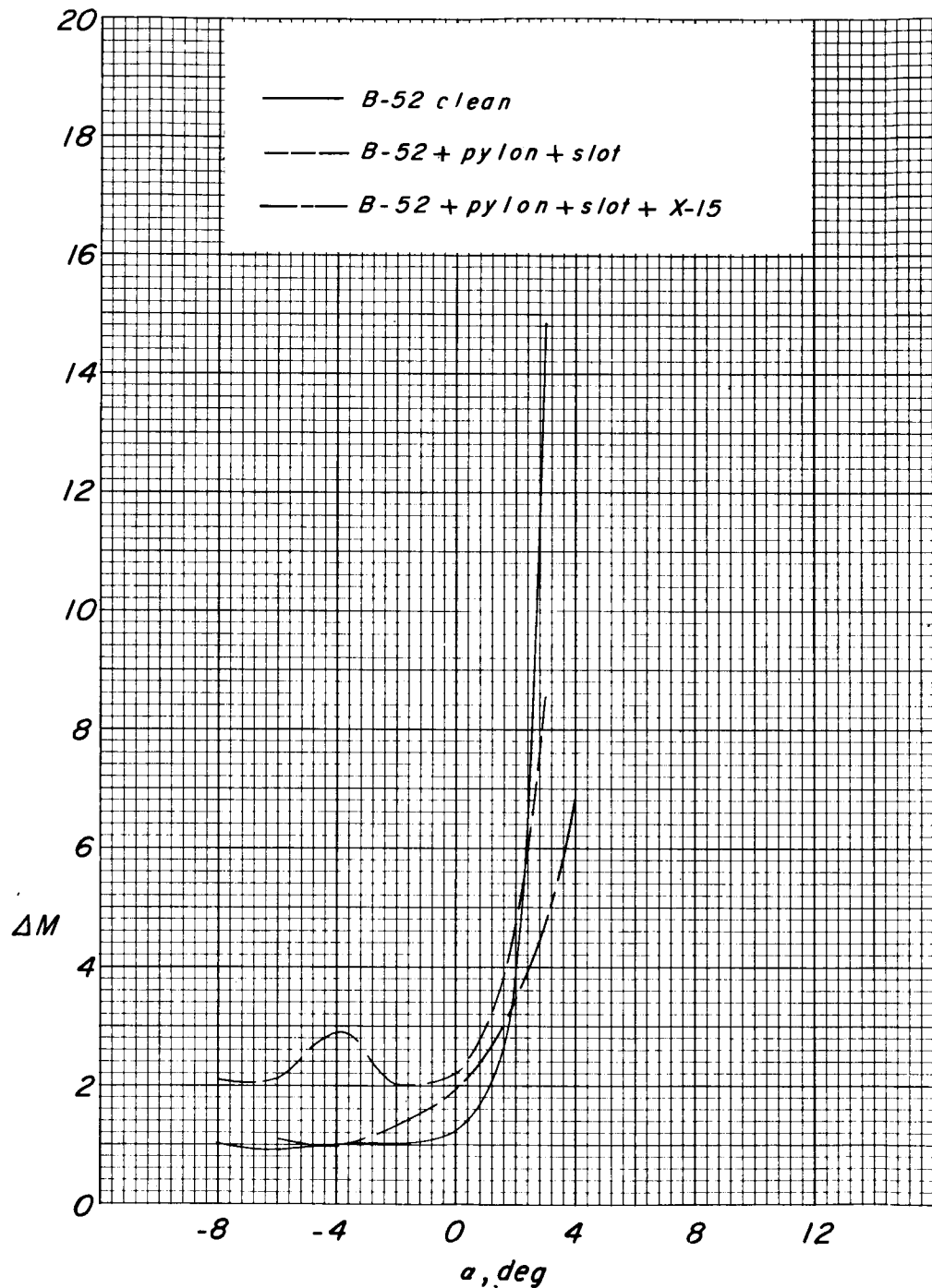
(c)  M = 0.70.

Figure 21.- Continued.
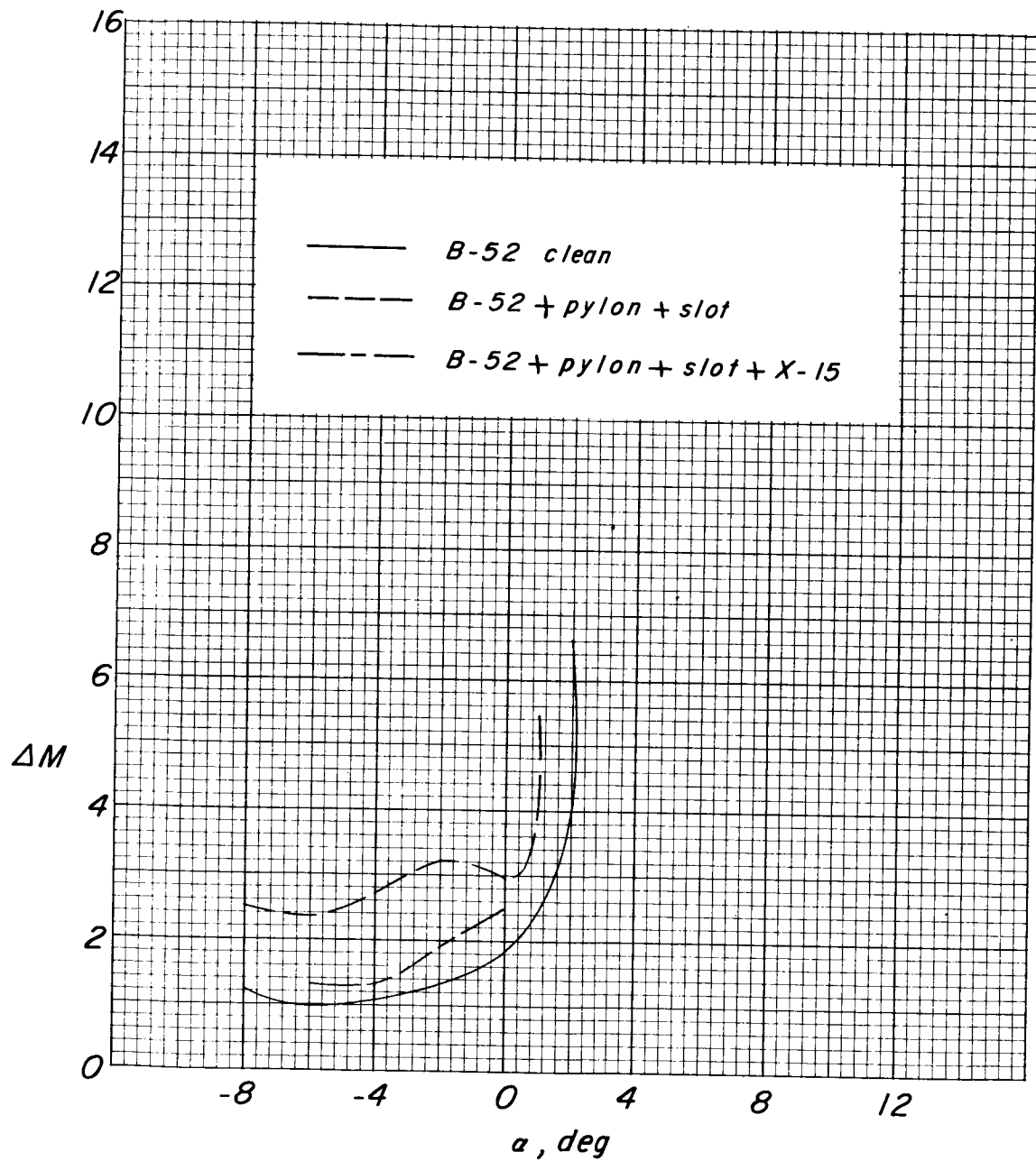
(d)  M = 0.75.

Figure 21.- Continued.
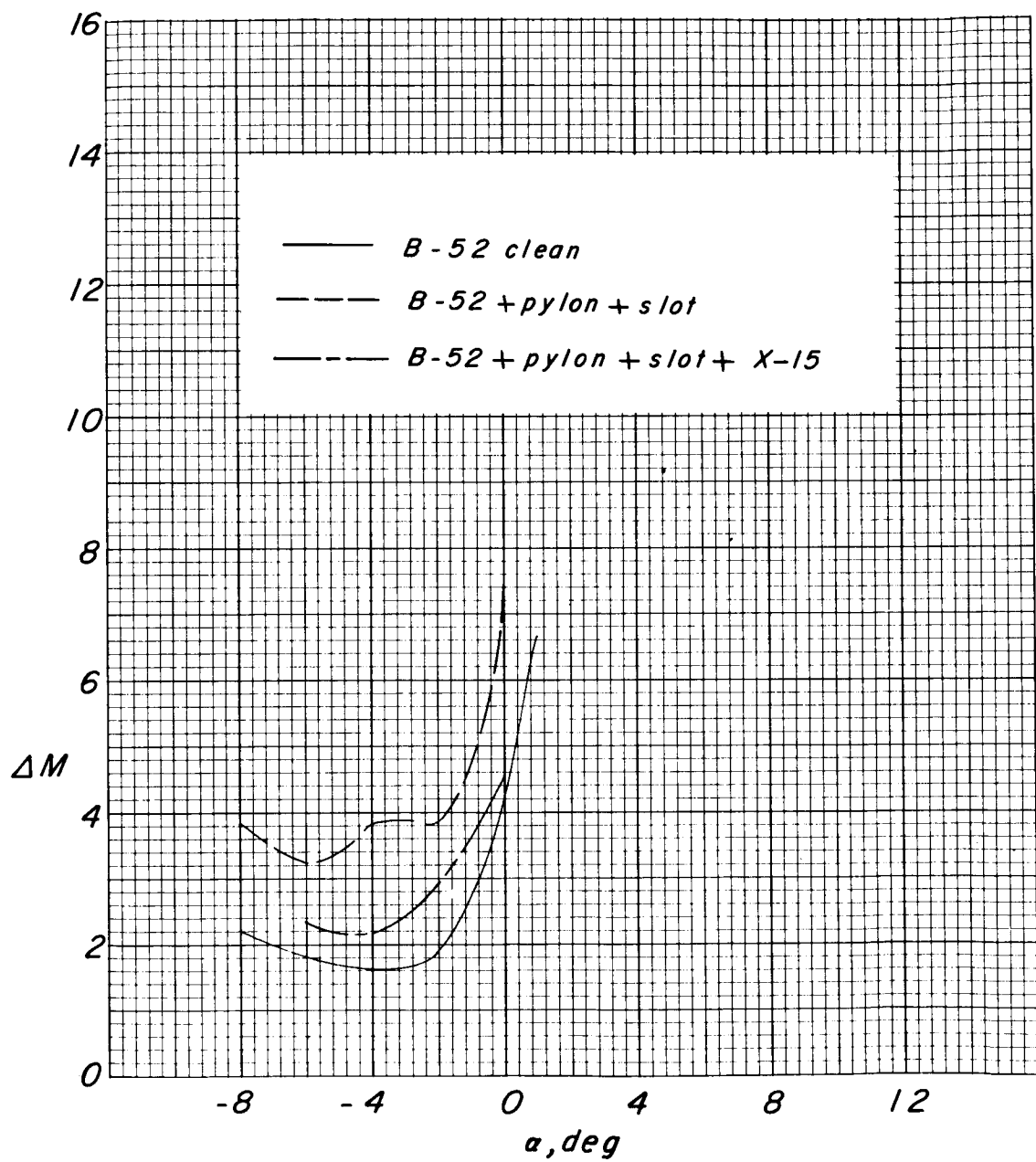
(e)  M = 0.80.

Figure 21.- Continued.
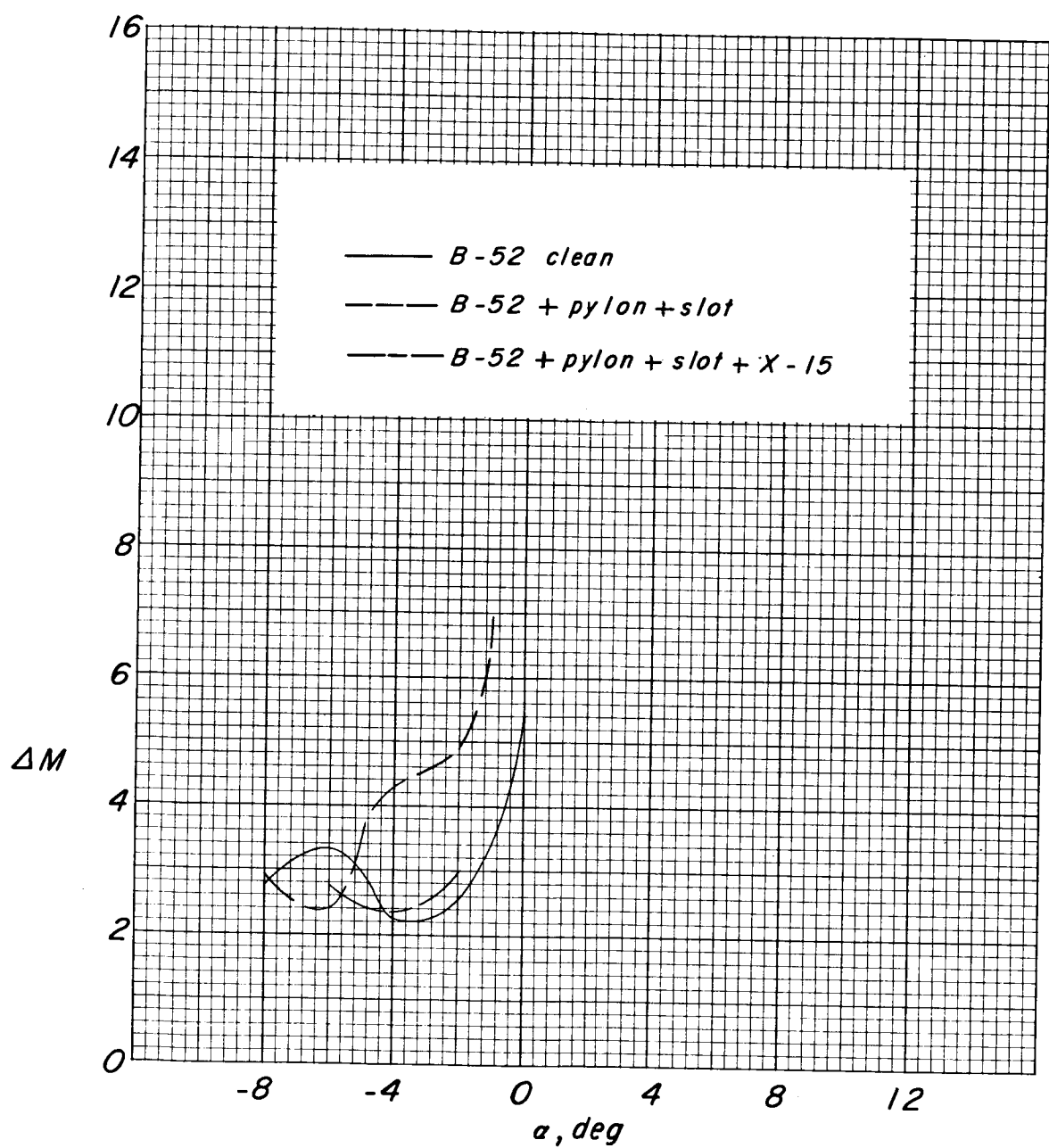
(f)  M = 0.83.

Figure 21.- Continued.
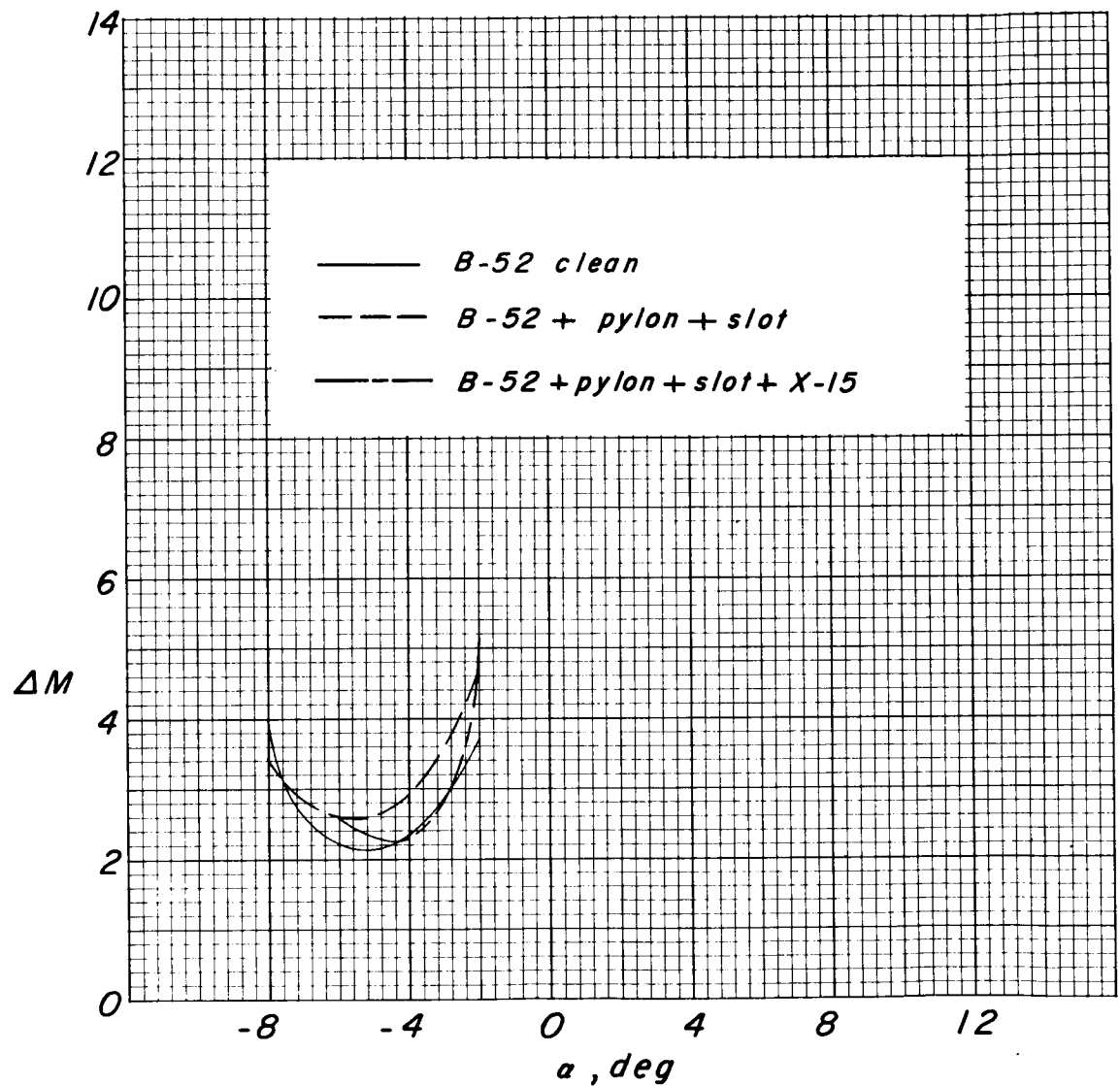
(g)  M = 0.85.

Figure 21.- Concluded.
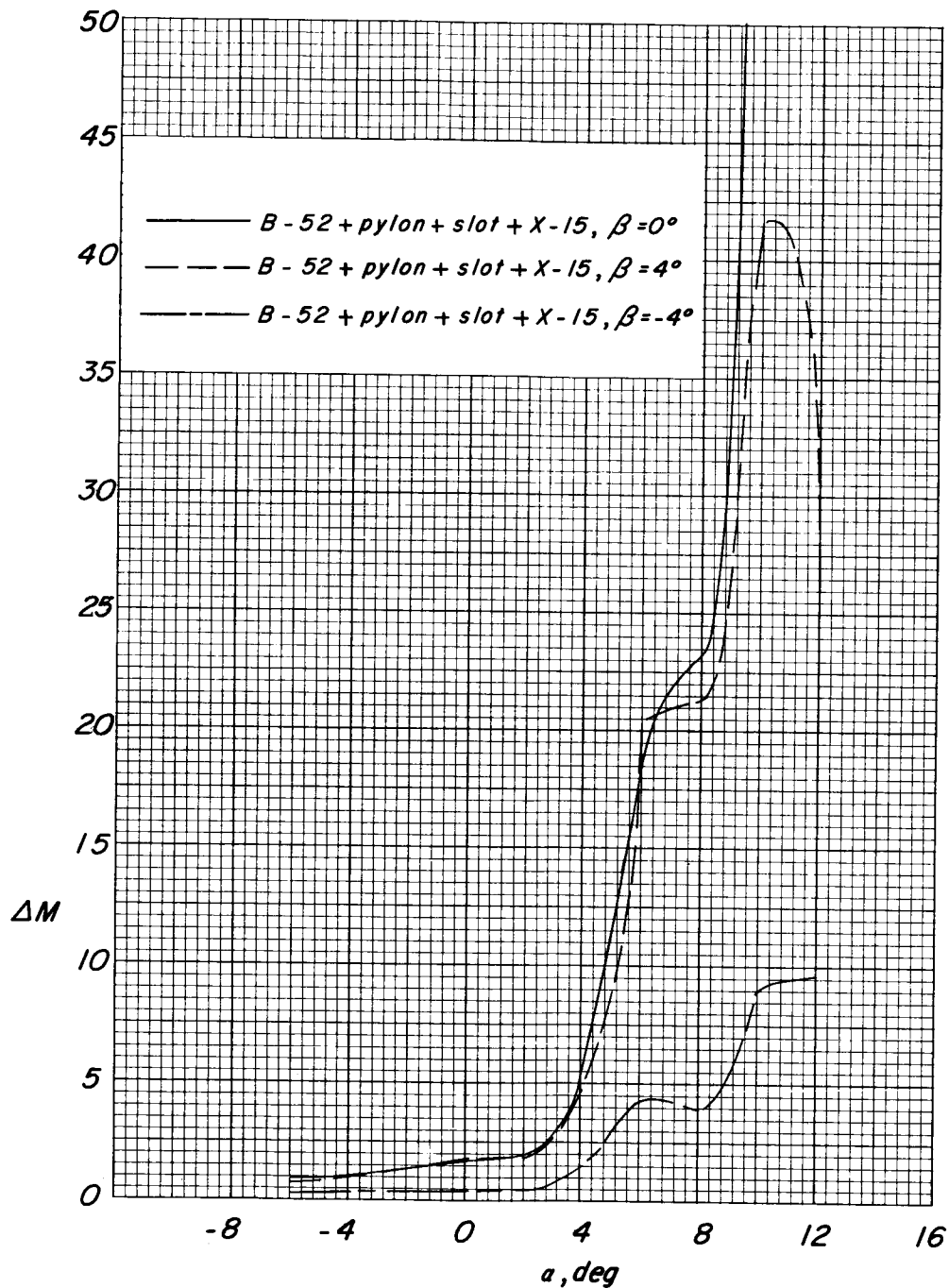
(a)  M = 0.40.

Figure 22.- Effect of the combination in sideslip on horizontal-tail panel
buffet.
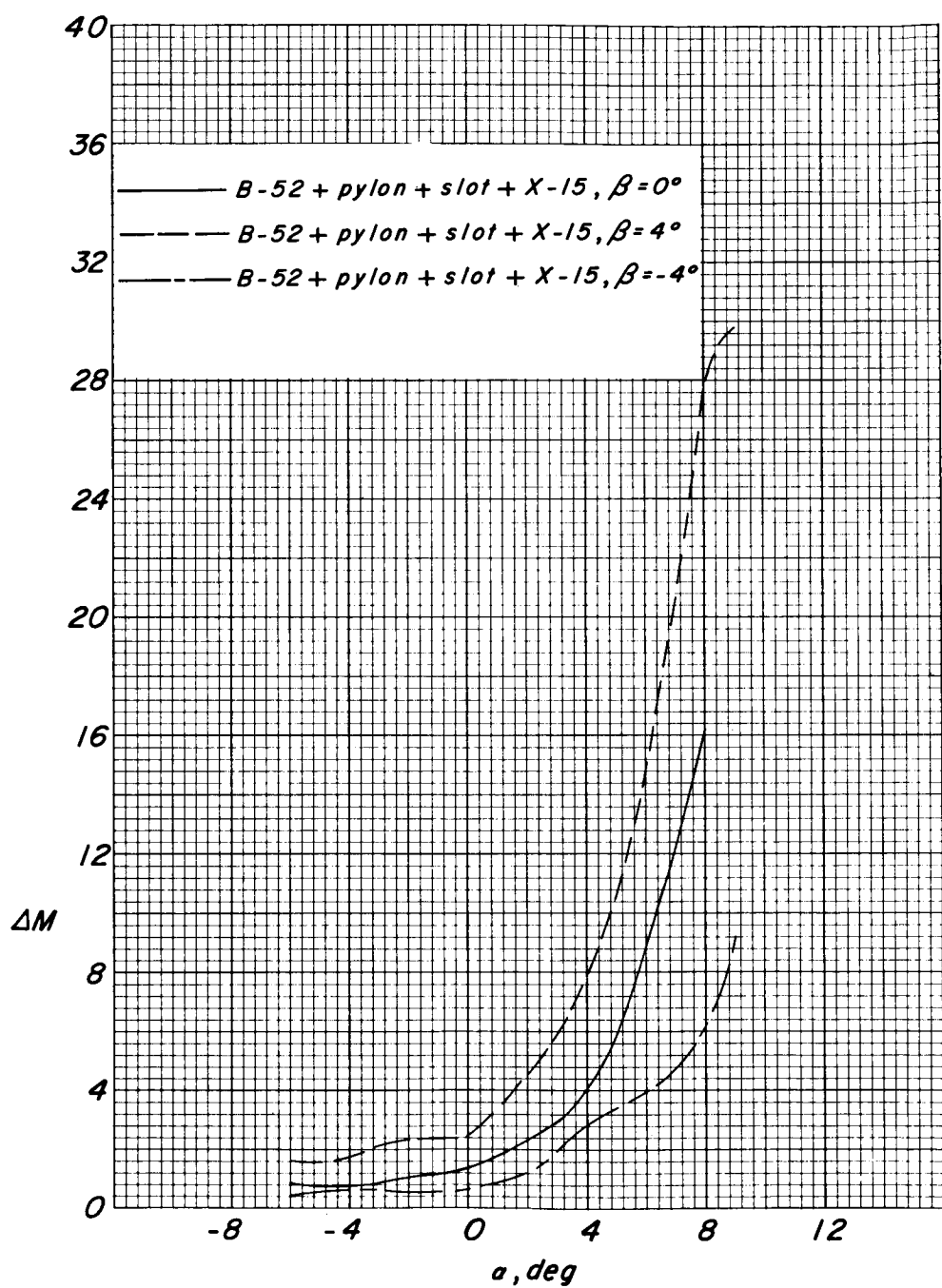
(b)  M = 0.60.

Figure 22.- Continued.
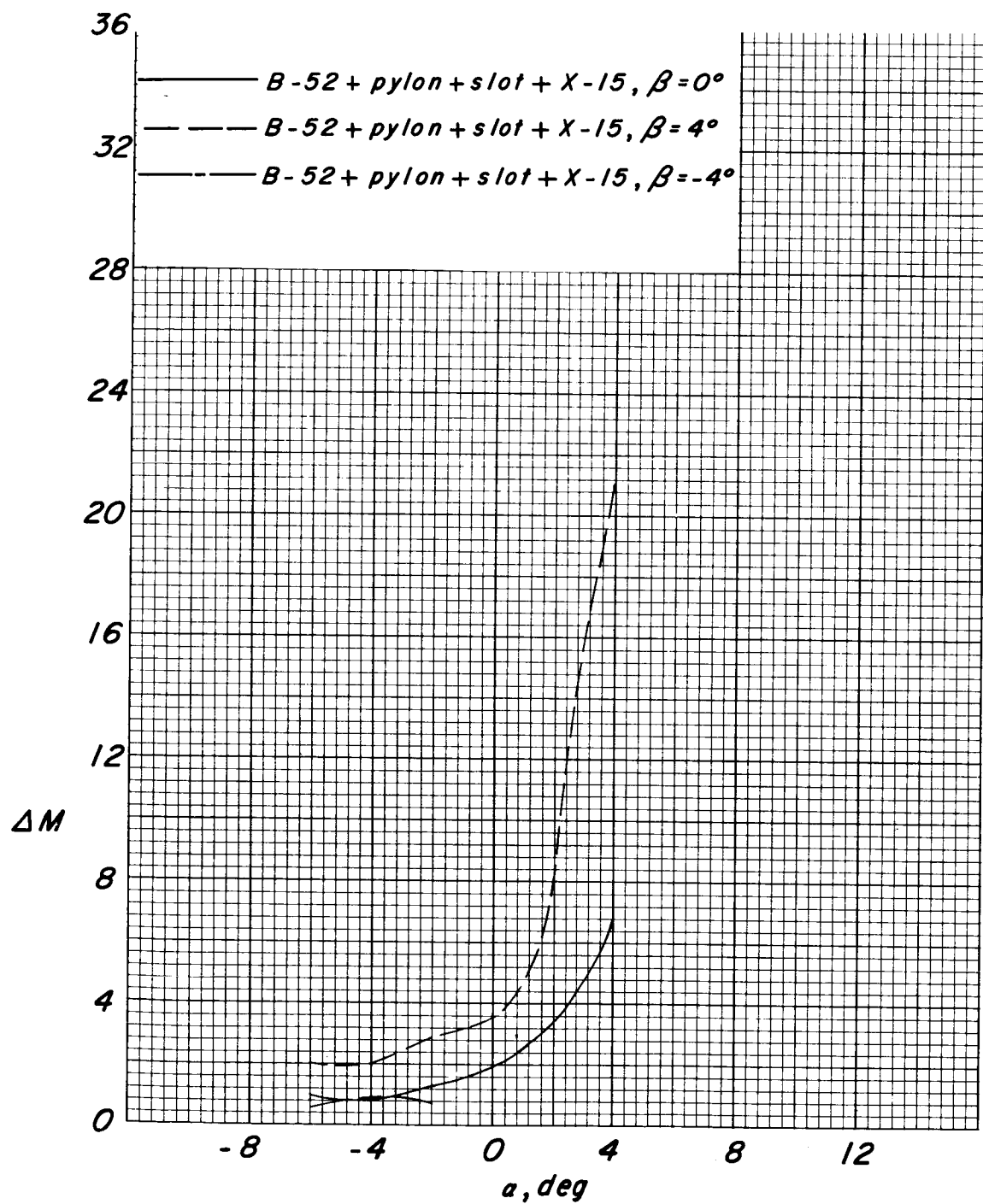
(c)  M = 0.70.

Figure 22.- Continued.
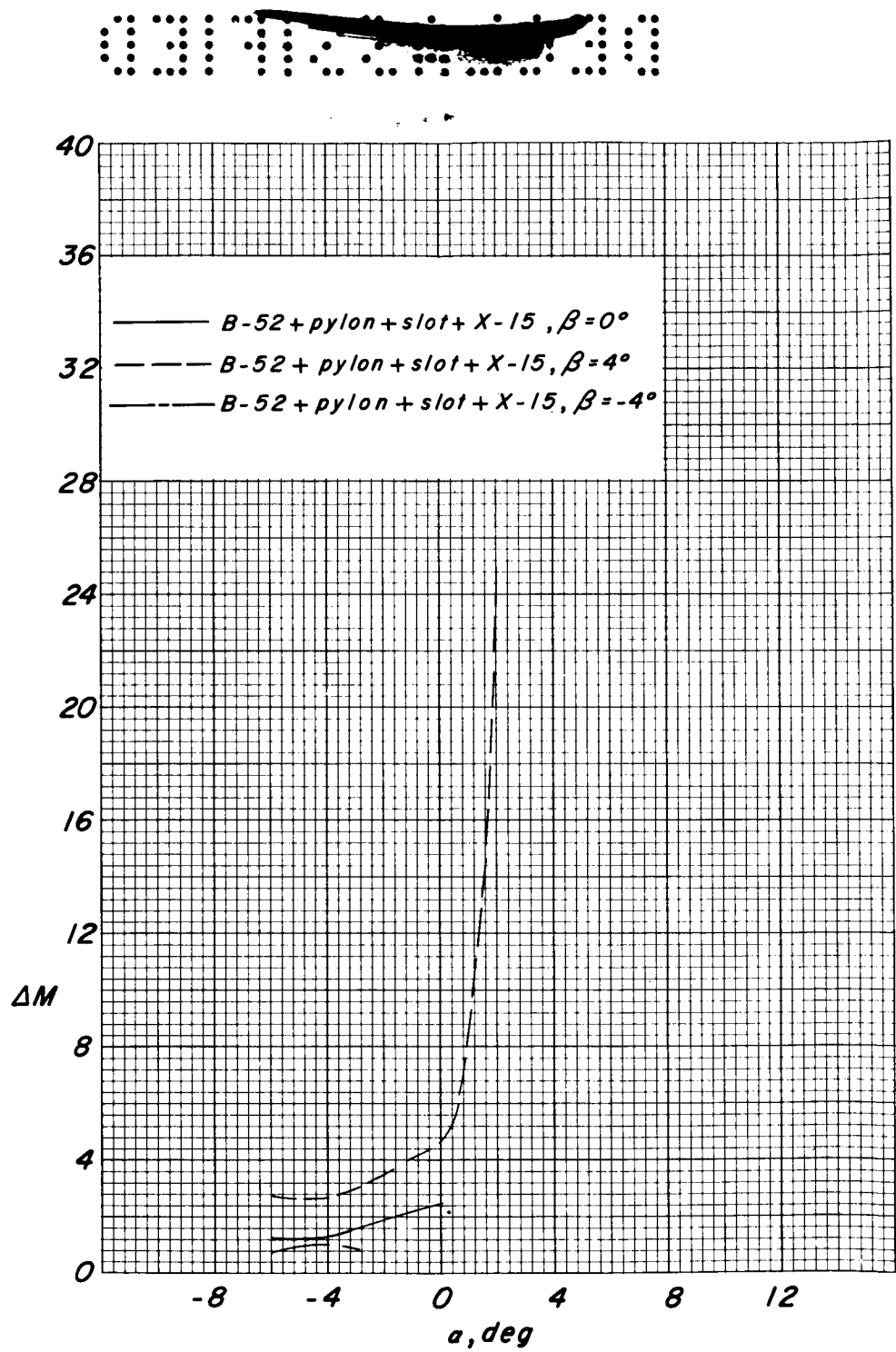
(d)  M = 0.75.

Figure 22.- Continued.
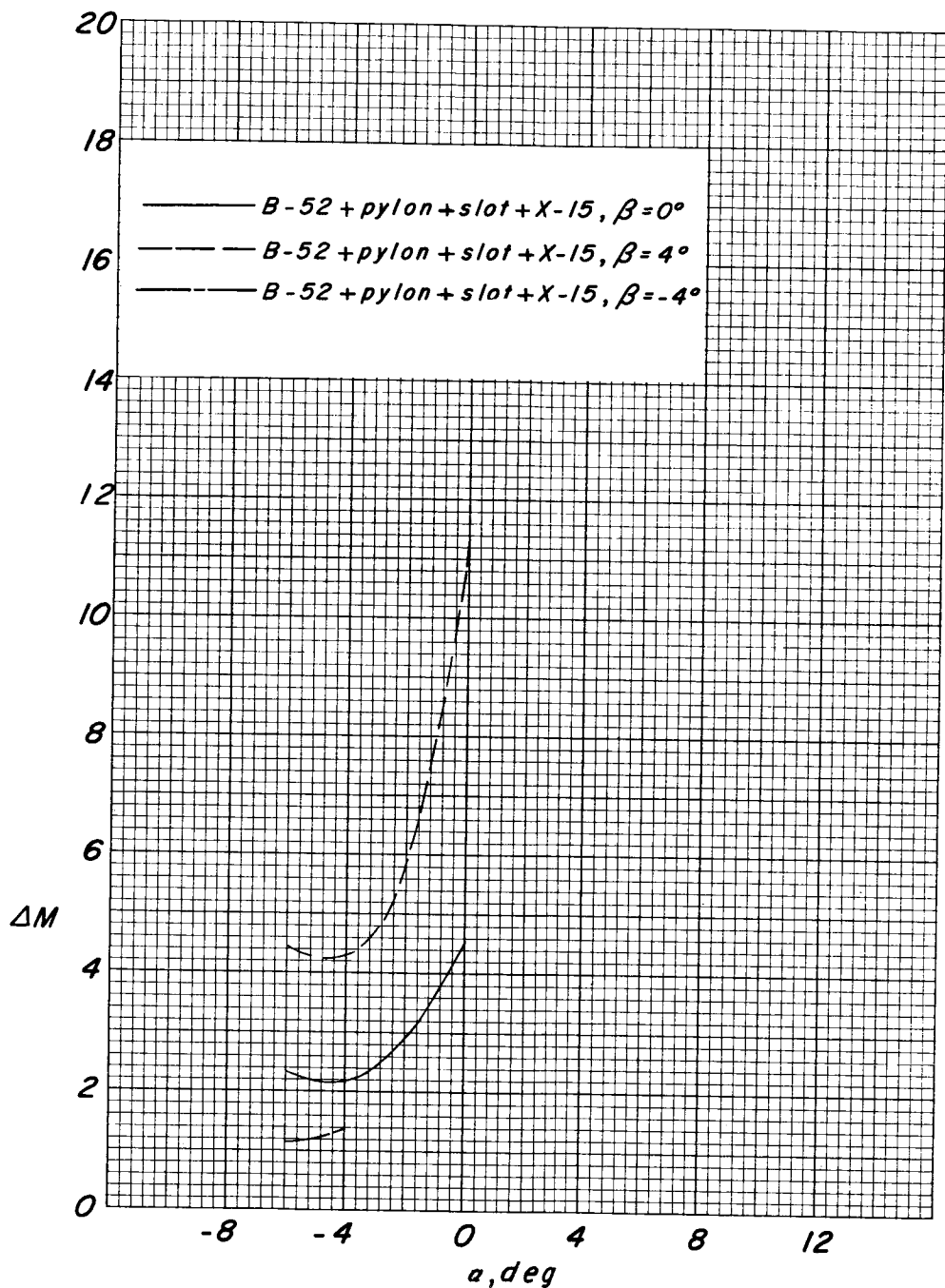
(e)  M = 0.80.

Figure 22.- Continued.
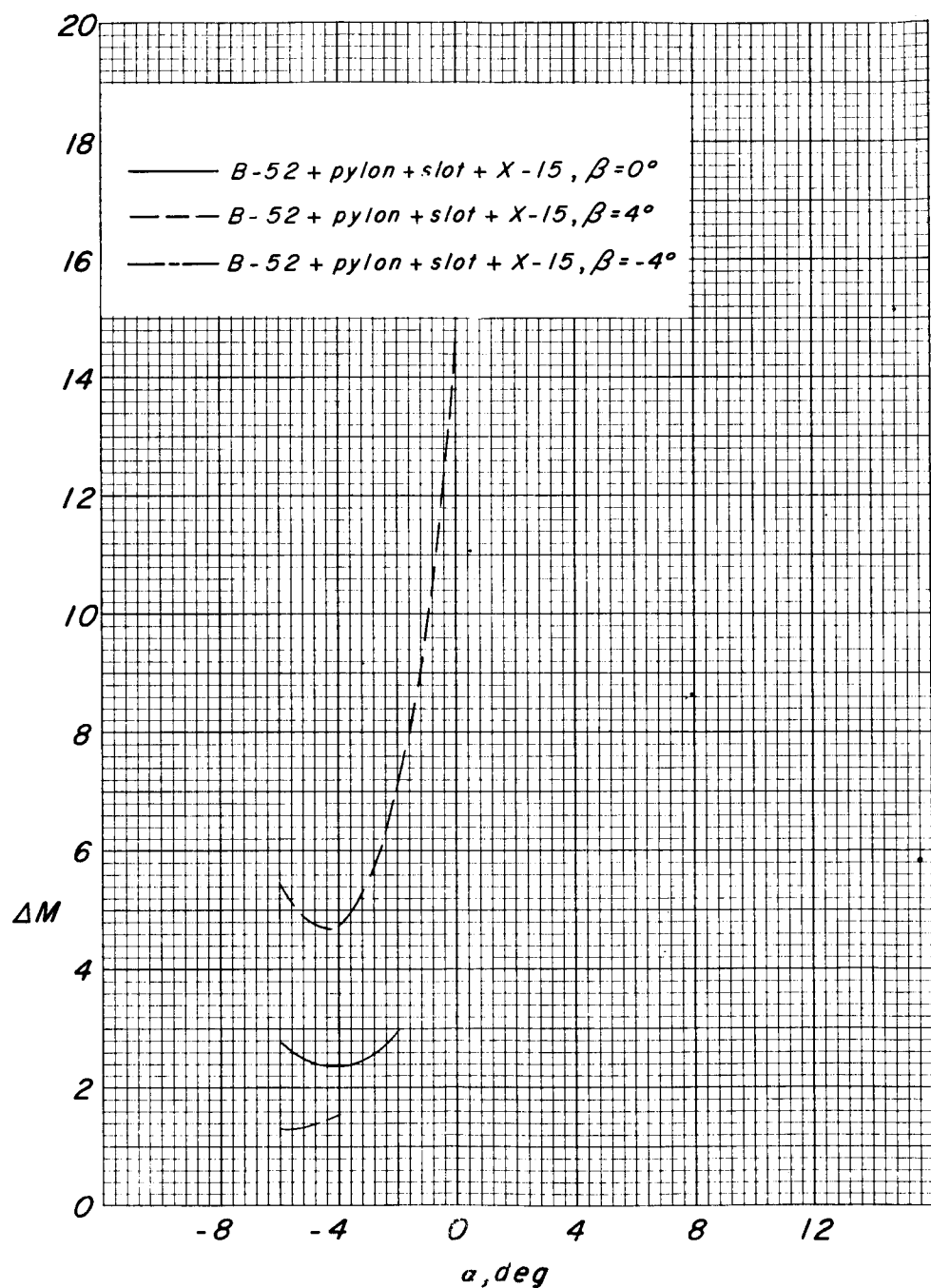
(f) M = 0.83.

Figure 22.- Continued.
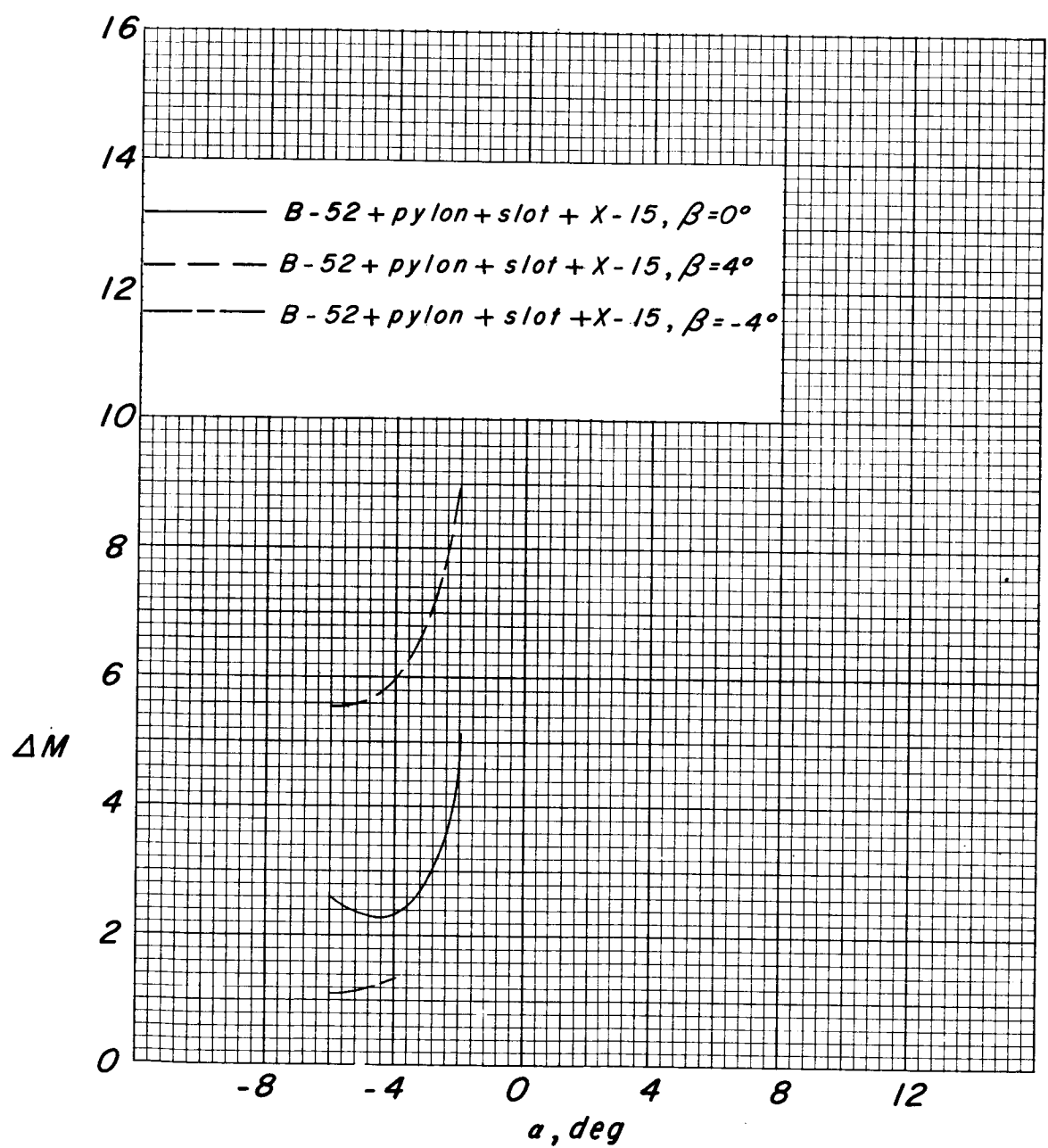
(g)  M = 0.85.

Figure 22.- Concluded.
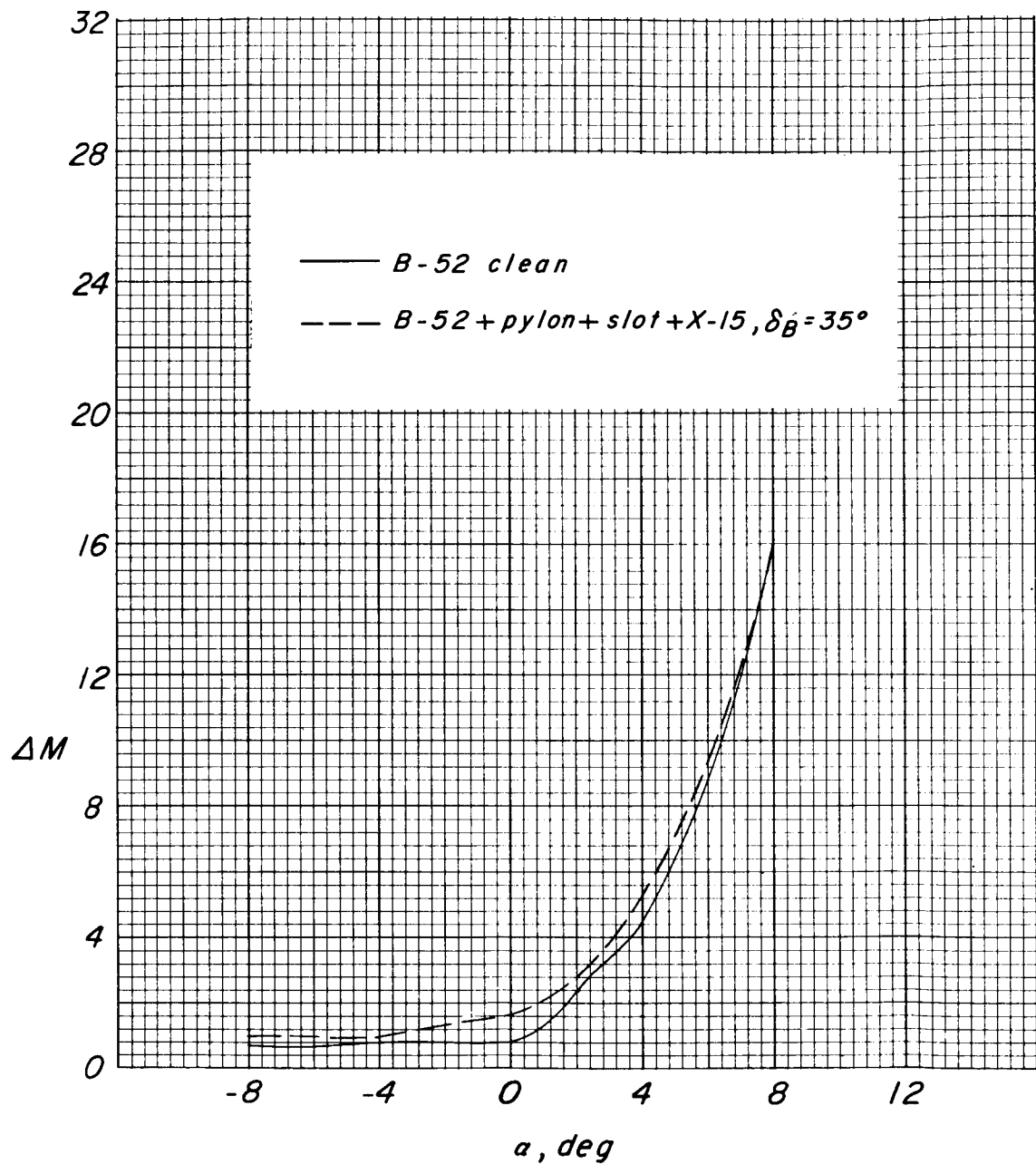
(a)  M = 0.60.

Figure 23.- Effect of X-15 speed-brake deflection on horizontal-tail panel buffet.
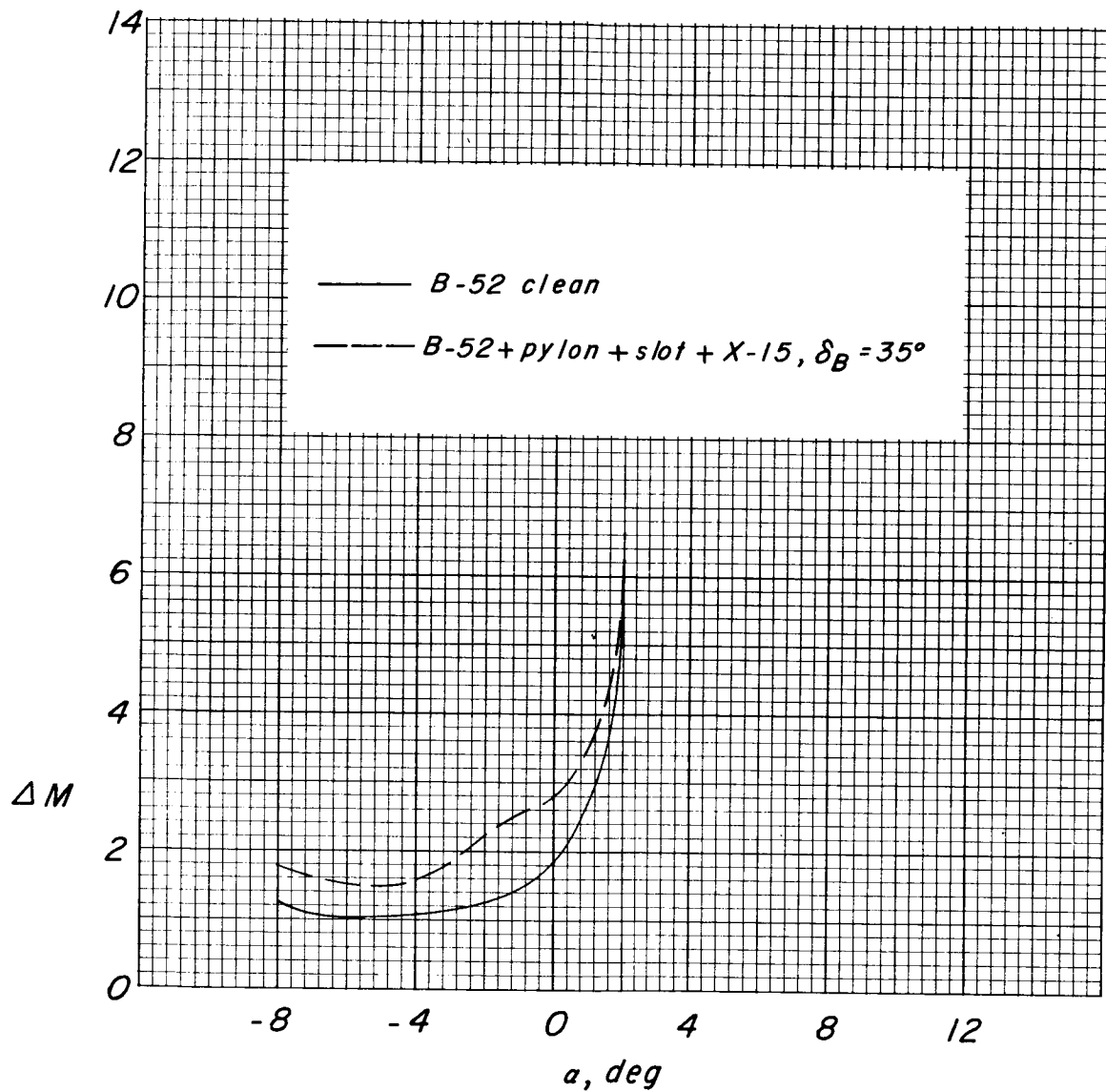
(b)  M = 0.75.

Figure 23.- Continued.
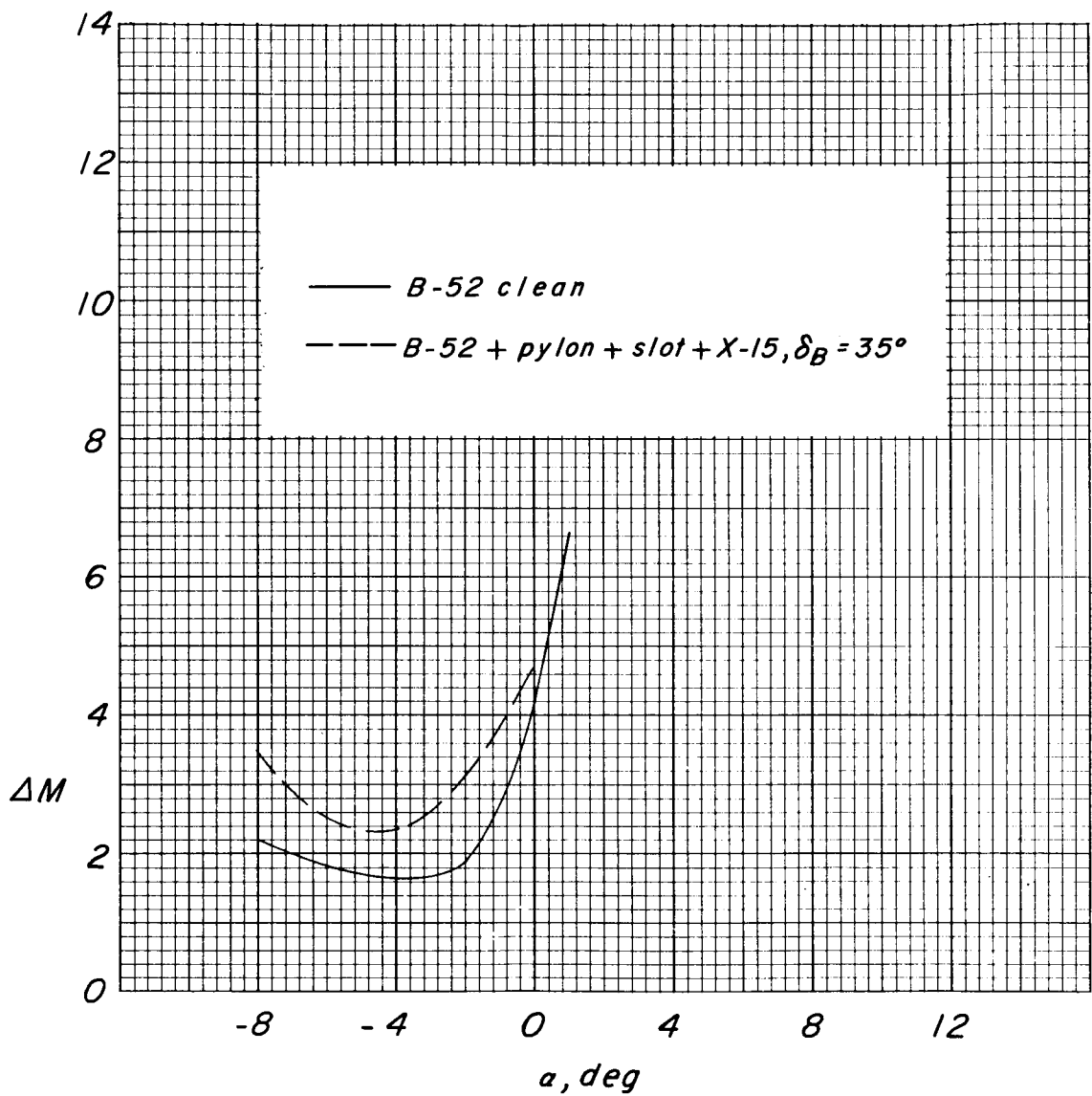
(c)  M = 0.80.

Figure 23.- Continued.
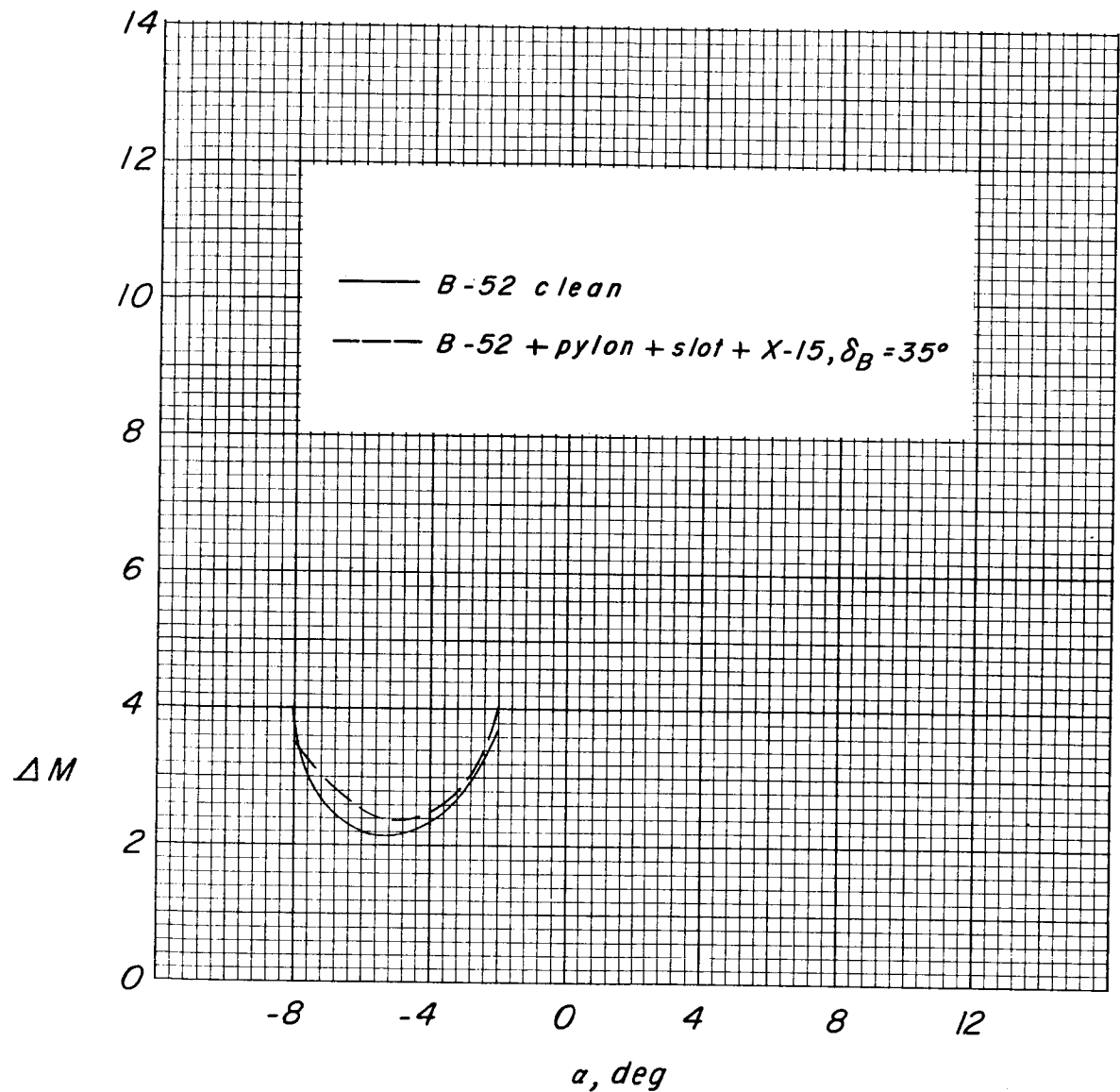
(d)  M = 0.85.

Figure 23.- Concluded.
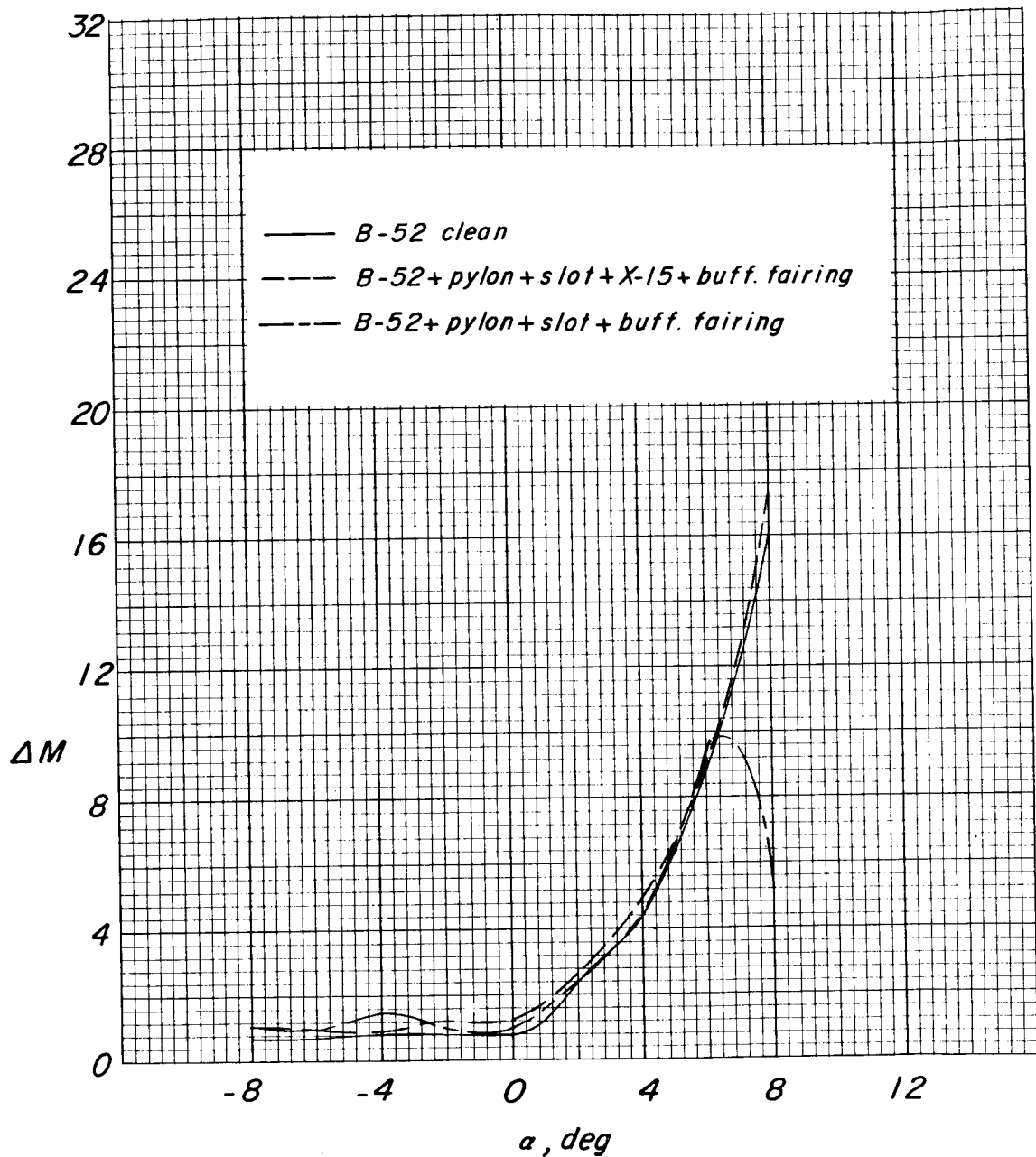
(a)  M = 0.60.

Figure 24.- Effect of buffet-fairing installation on horizontal-tail panel buffet.
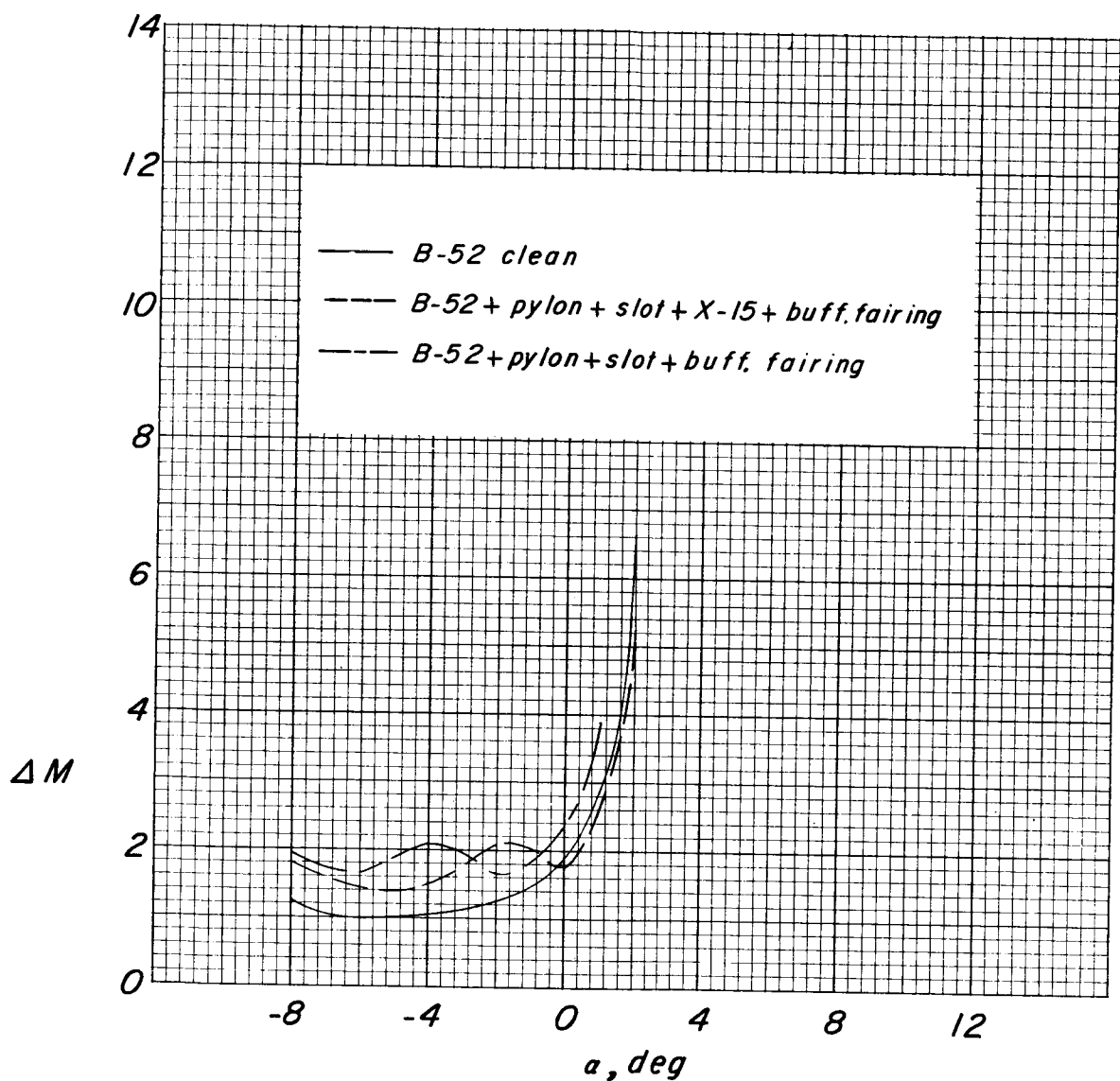
(b)  M = 0.75.

Figure 24.- Continued.
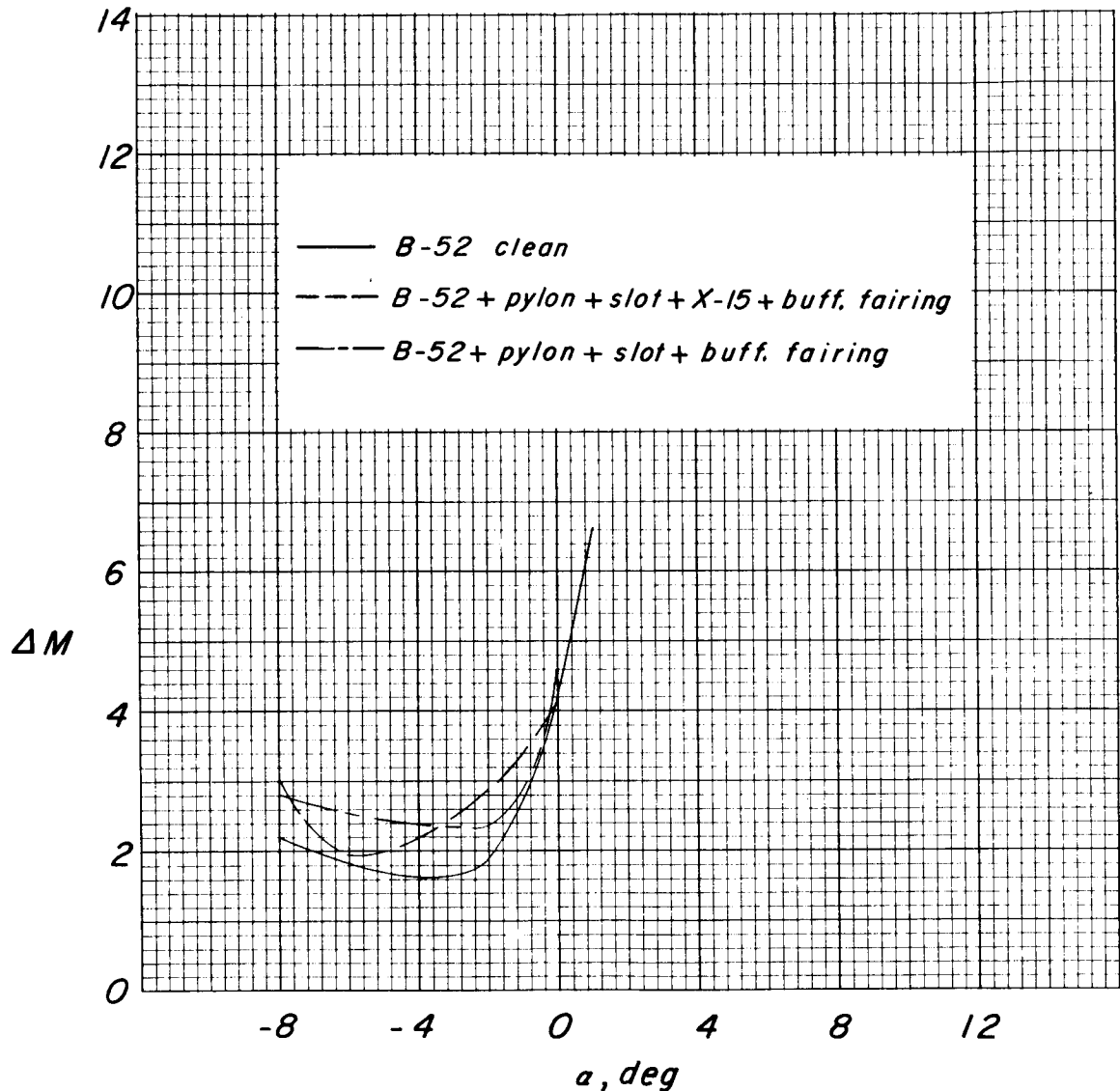
(c)  M = 0.80.

Figure 24.- Continued.
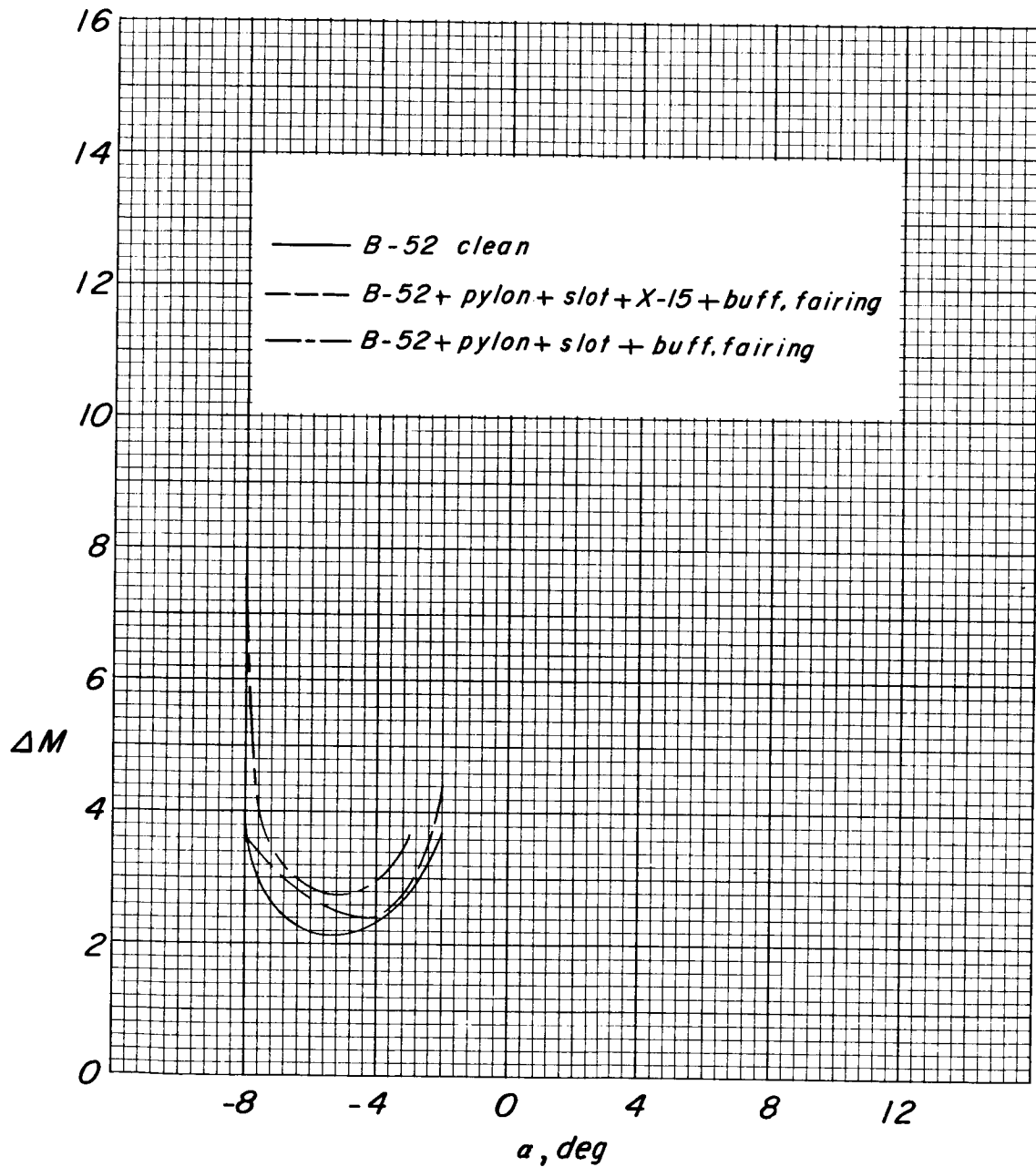
(d)   M = 0.85.

Figure 24.- Concluded.
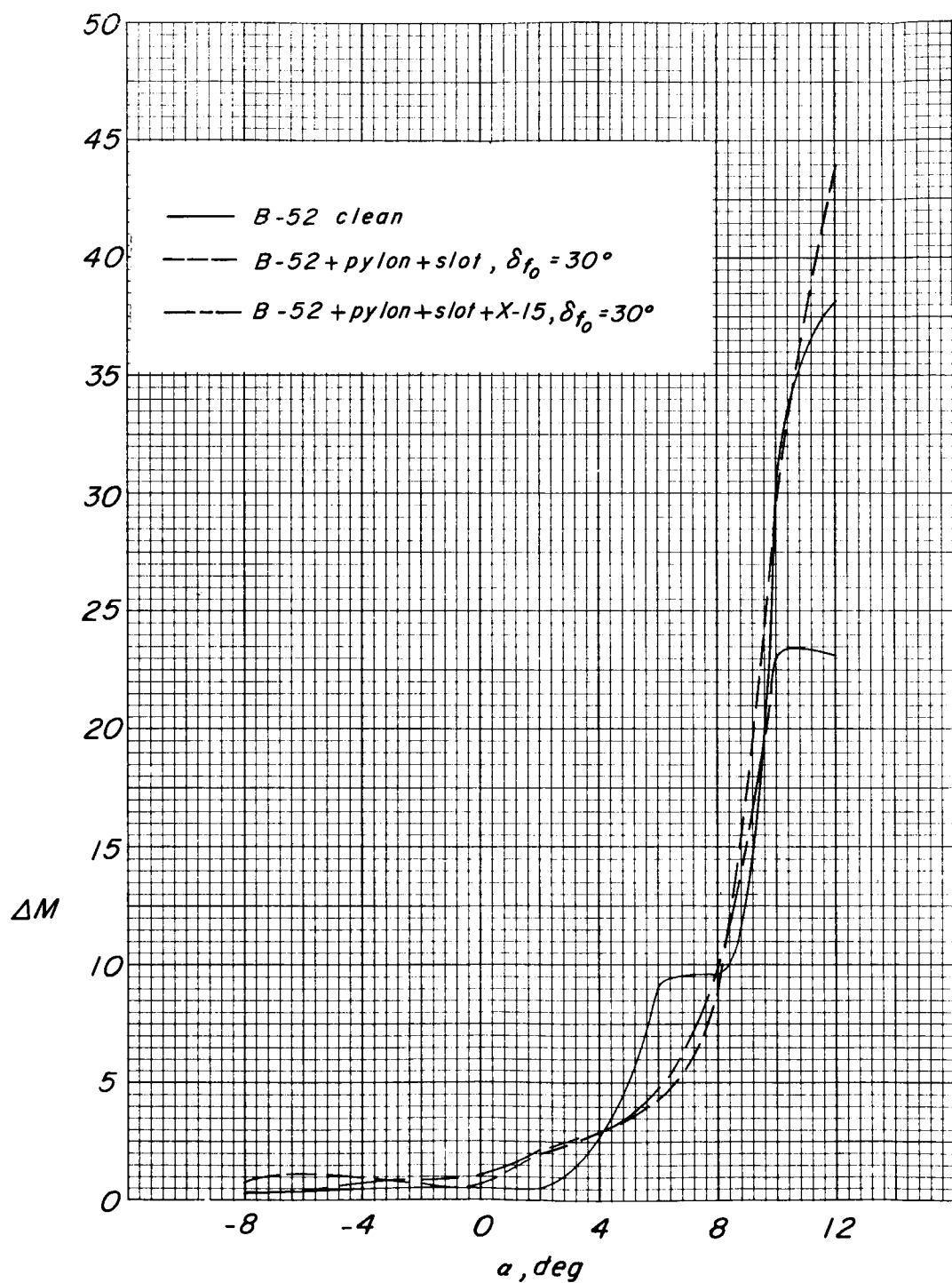
Figure 25.- Effect of B-52 outboard flaps on horizontal-tail panel buffet. M = 0.40.
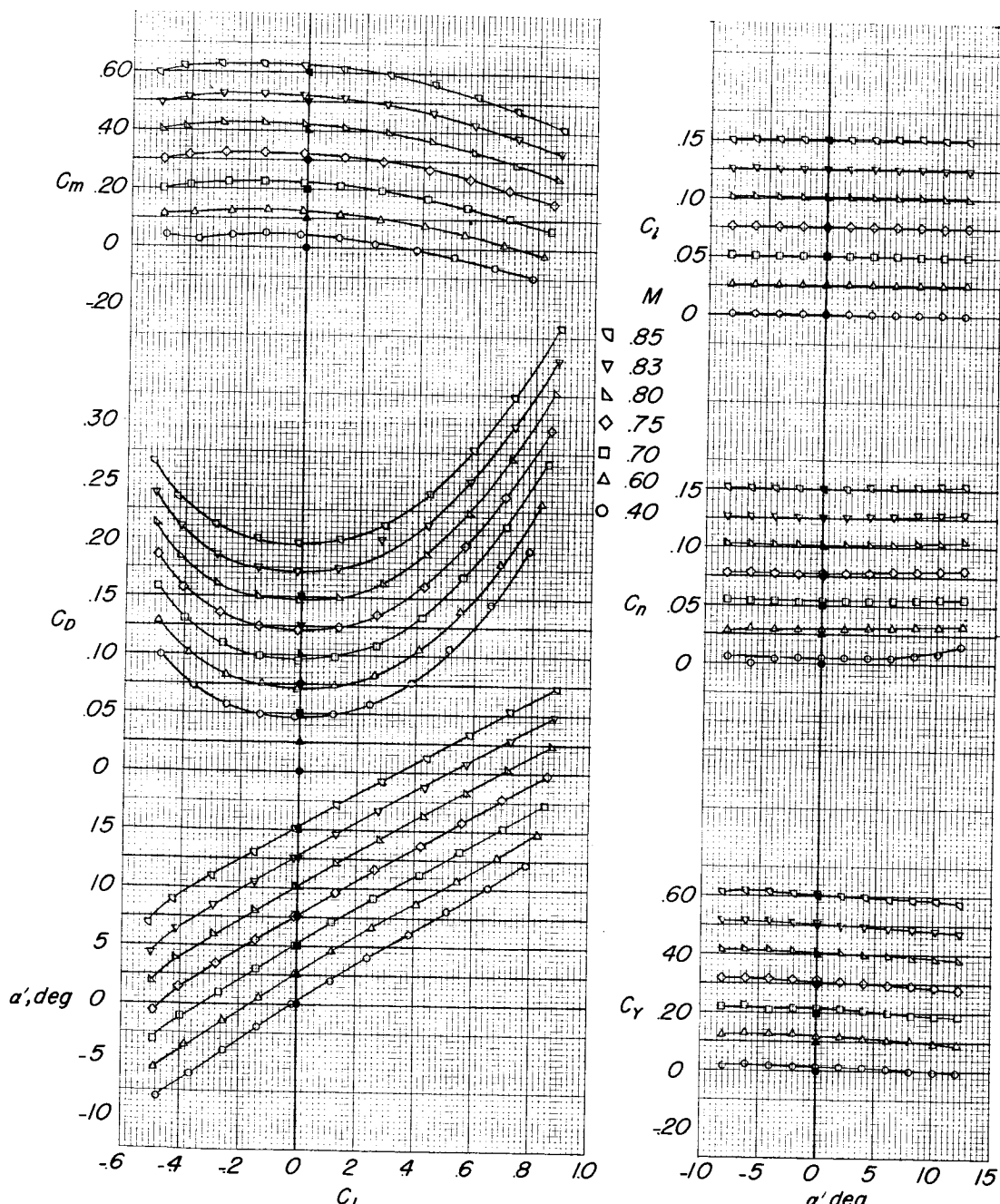
(a)  $\delta_e = 0°$;  $\delta_a = 0°$;  $\delta_r = 0°$.

Figure 26.- Aerodynamic characteristics of the X-15 model.  Effect of control deflection; $\beta = 0°$.
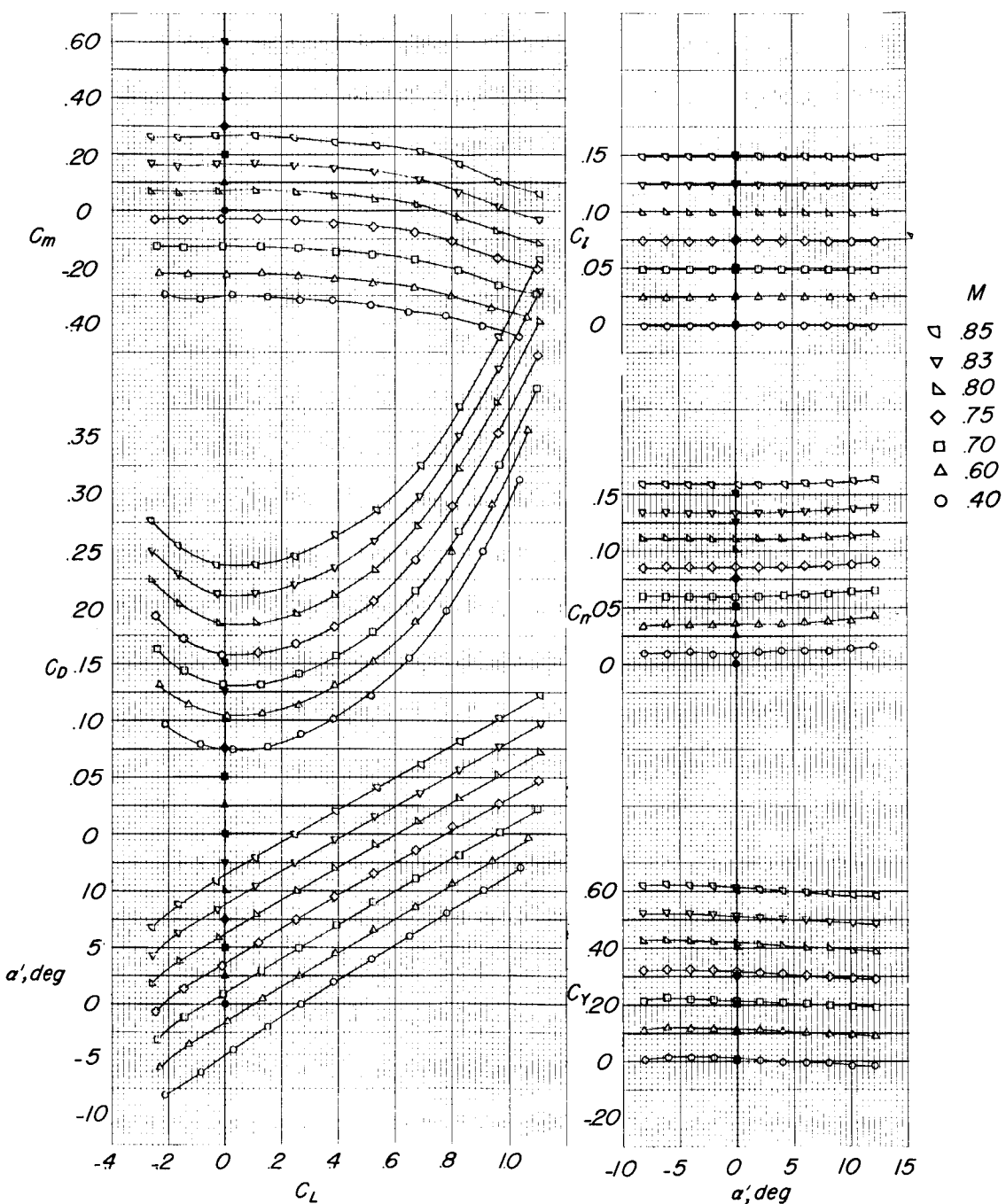
(b)  $\delta_e = 15°$; $\delta_a = 0°$; $\delta_r = 0°$.

Figure 26.- Continued.

(c)  $\delta_e = 5^o$;  $\delta_a = 0^o$;  $\delta_r = 0^o$.
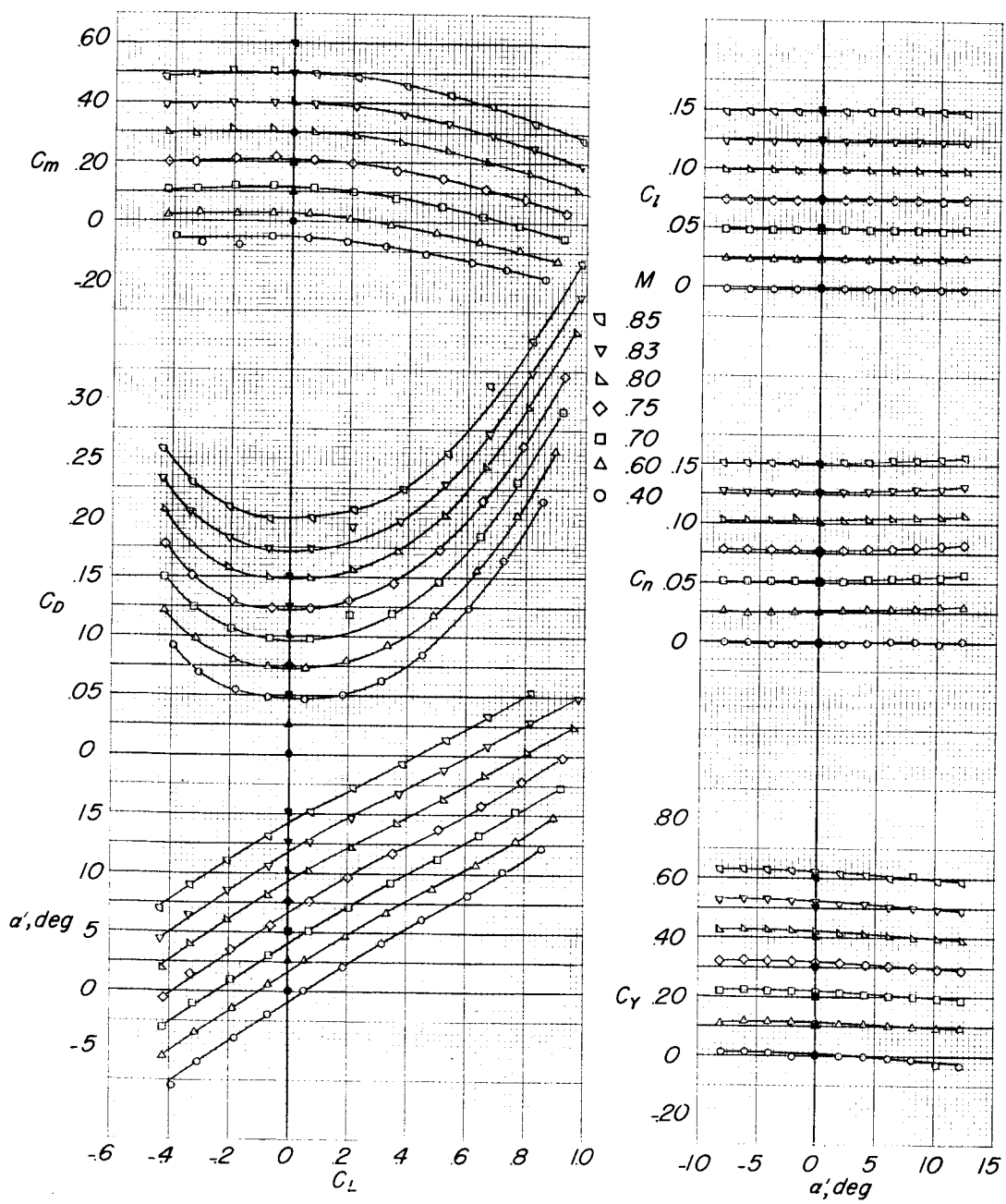
Figure 26.- Continued.

(d)  $\delta_e = -5°$; $\delta_a = 0°$; $\delta_r = 0°$.

Figure 26.- Continued.
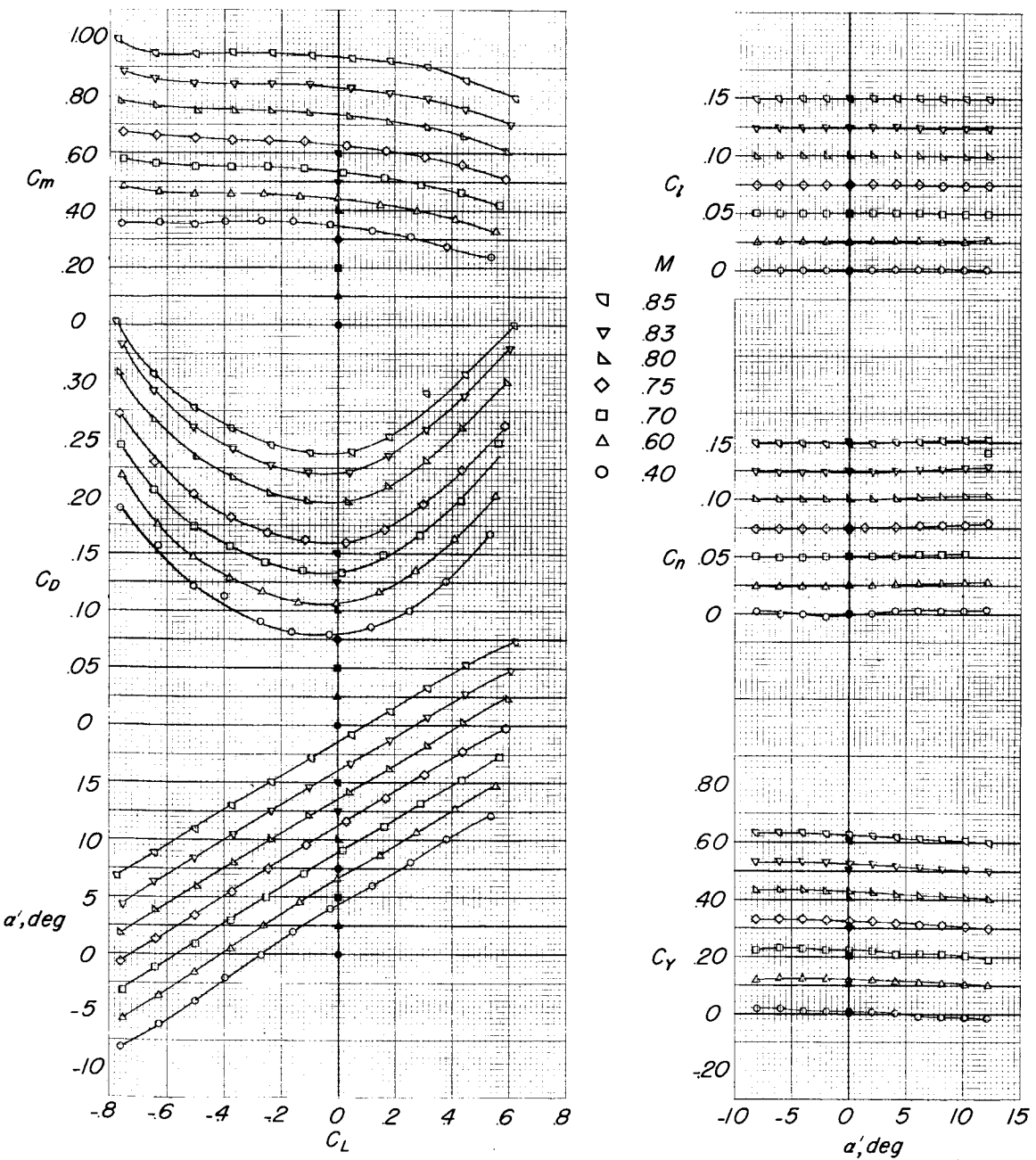
(e) $\delta_e = -15°$; $\delta_a = 0°$; $\delta_r = 0°$.

Figure 26.- Continued.
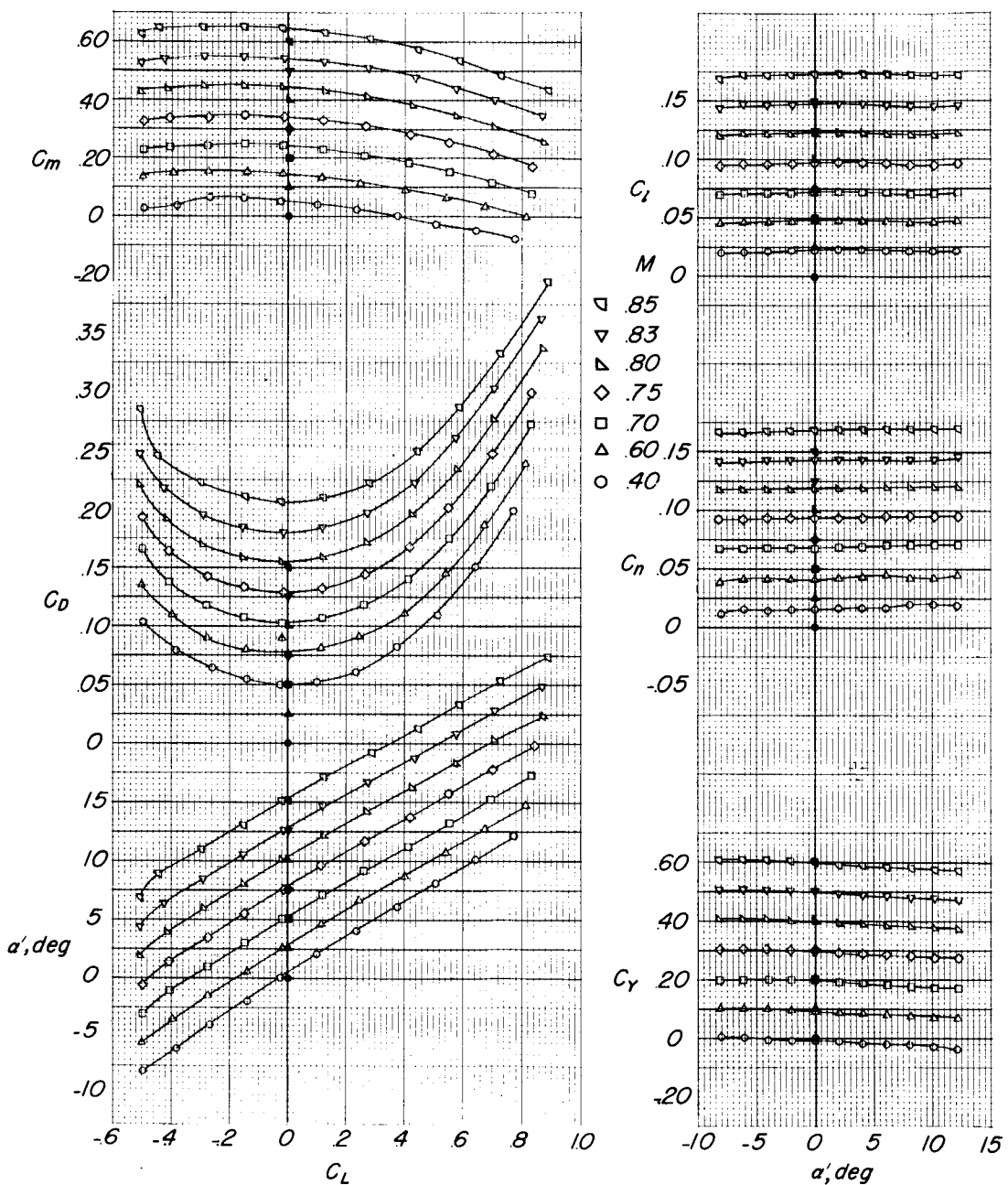
(f)  $\delta_e = 0°$;  $\delta_a = -15°$;  $\delta_r = 0°$.

Figure 26.- Continued.
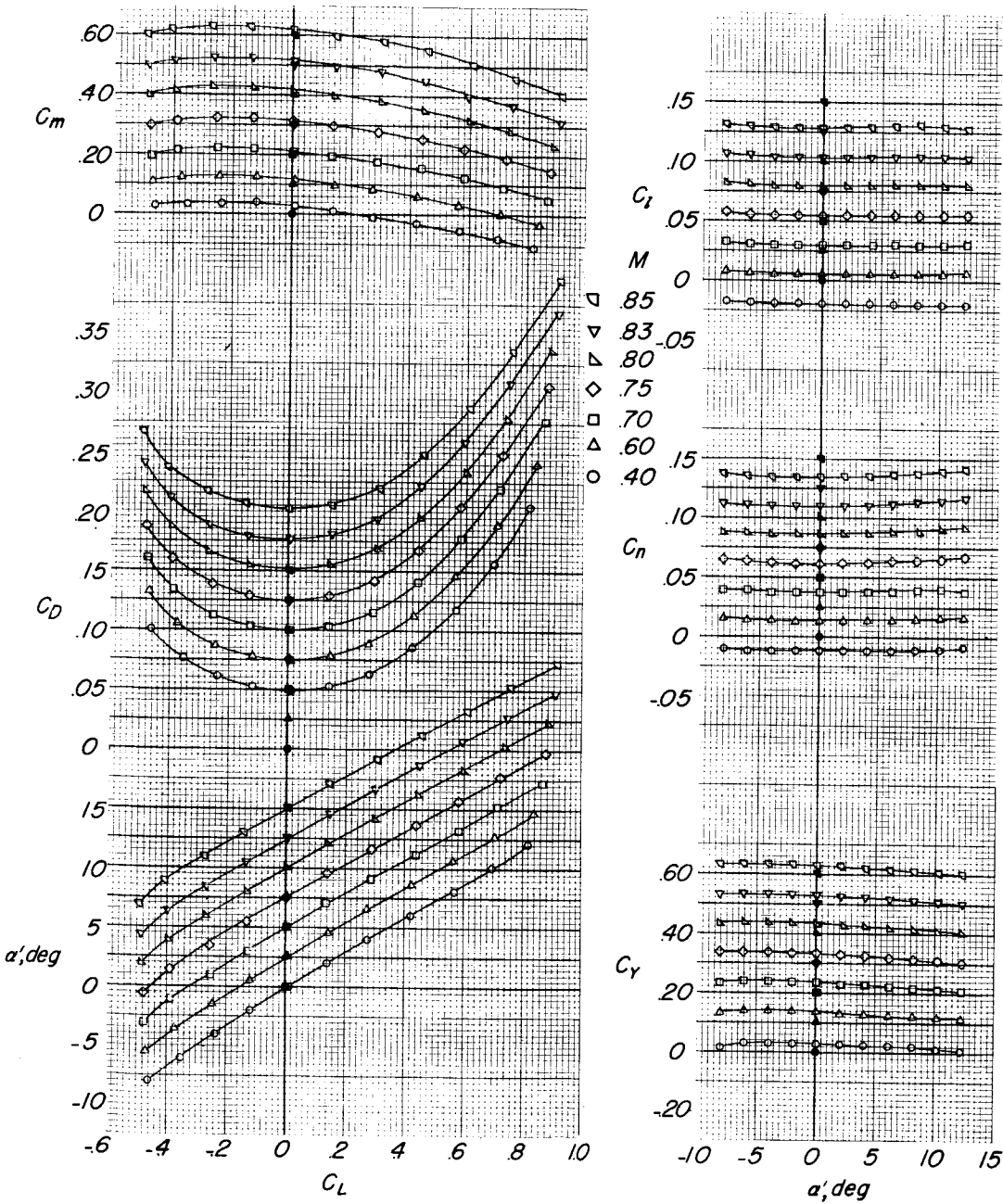
(g)  $\delta_e = 0^\circ$; $\delta_a = 15^\circ$; $\delta_r = 0^\circ$.

Figure 26.- Continued.

(h)  $\delta_e = 0^o$; $\delta_a = 0^o$; $\delta_r = -7.5^o$.
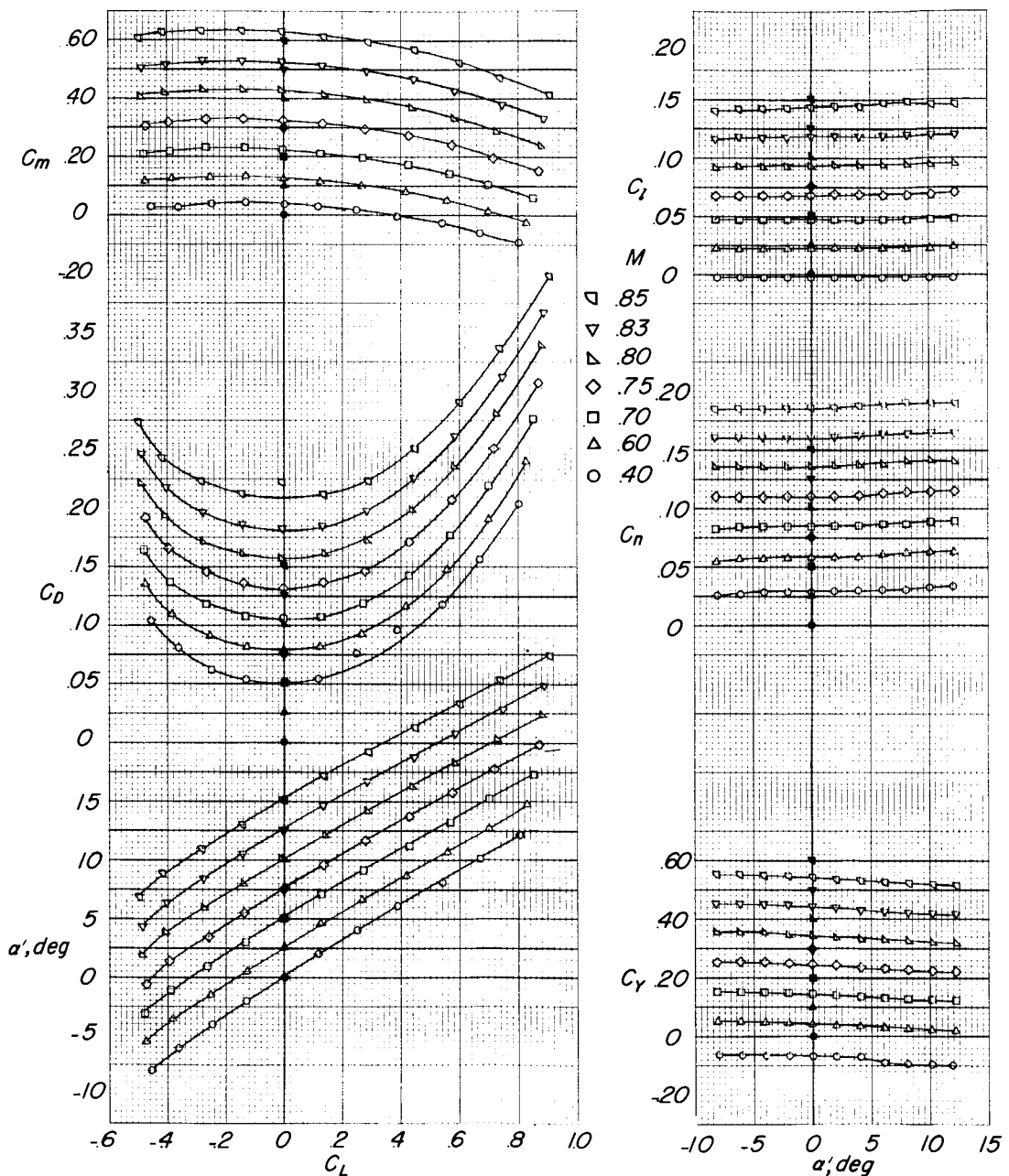
Figure 26.- Continued.

(i)  $\delta_e = 0^\circ$; $\delta_a = 0^\circ$; $\delta_r = 7.5^\circ$.

Figure 26.- Concluded.

(a) $\beta = 4^O$.
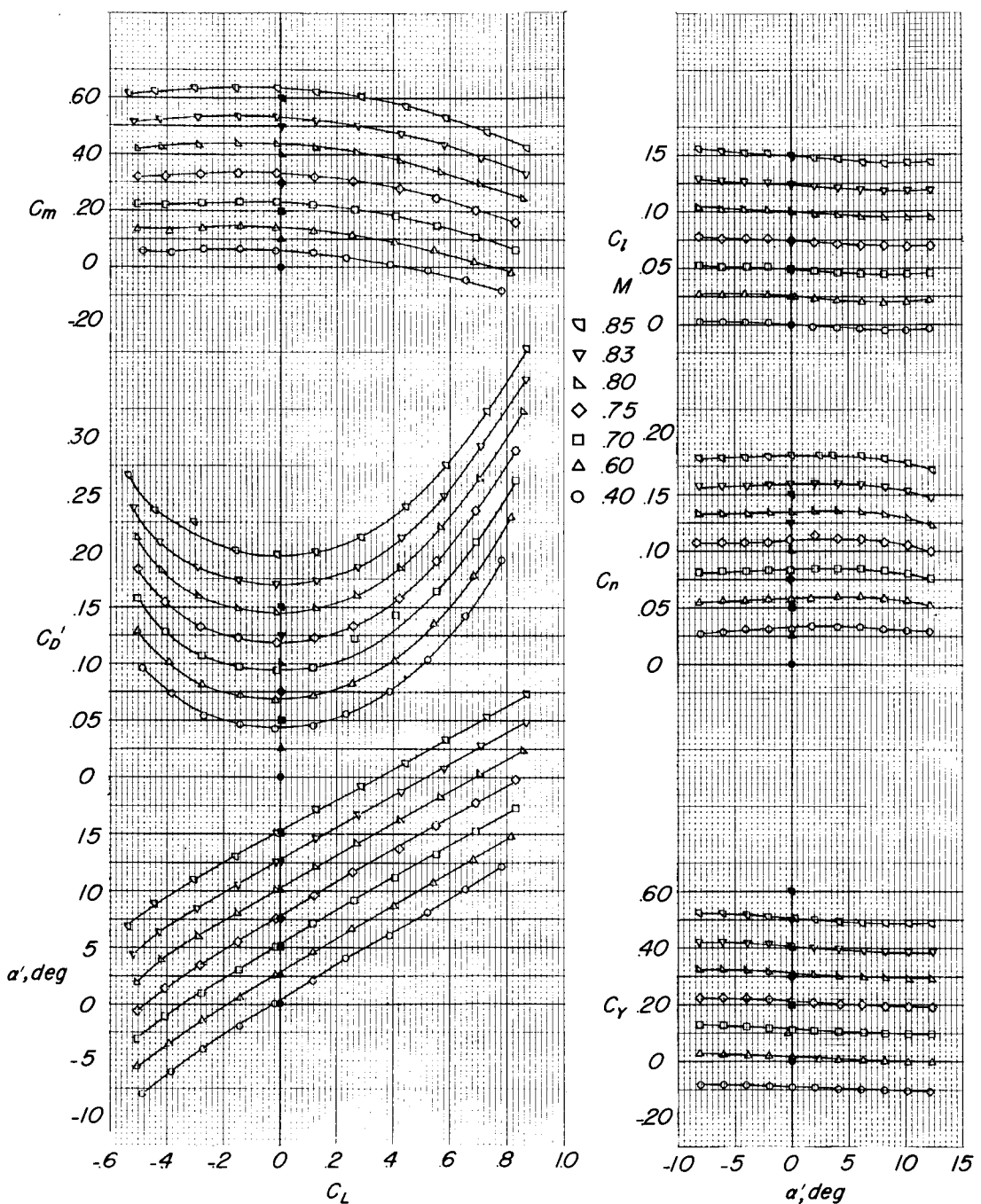
Figure 27.- Aerodynamic characteristics of the X-15 model. $\delta_e = 0^O$; $\delta_a = 0^O$; $\delta_r = 0^O$.

(b) β = -4°.
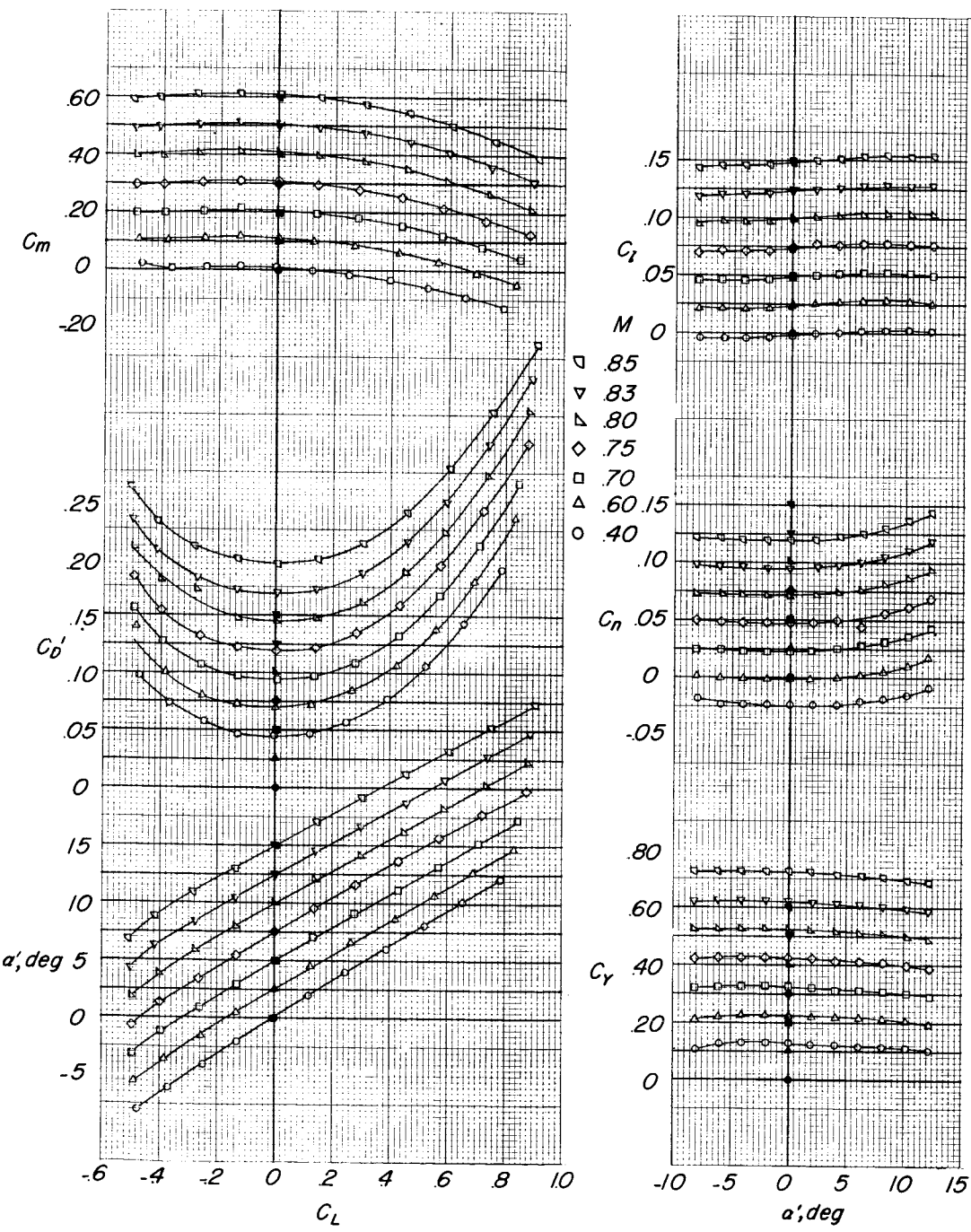
Figure 27.- Concluded.
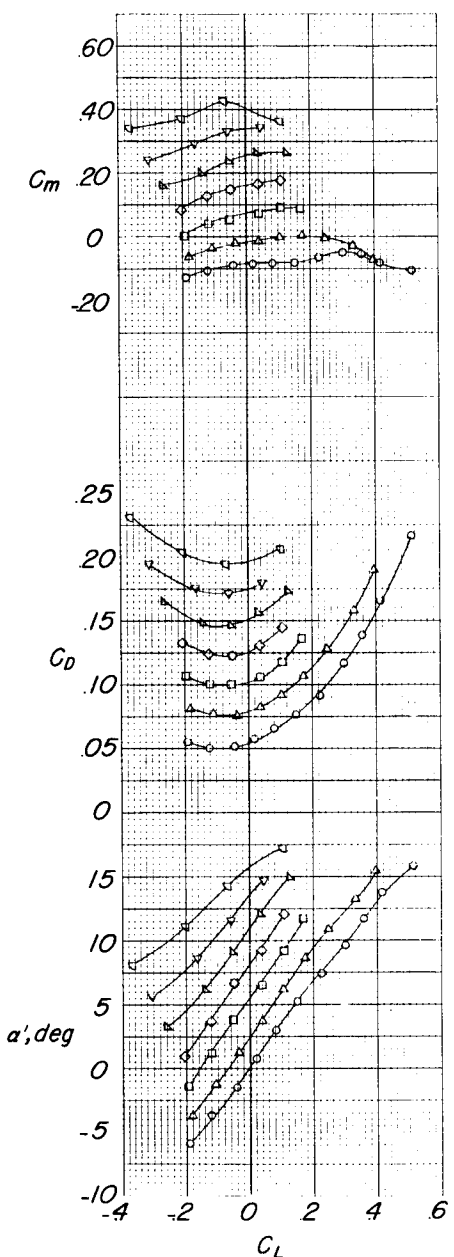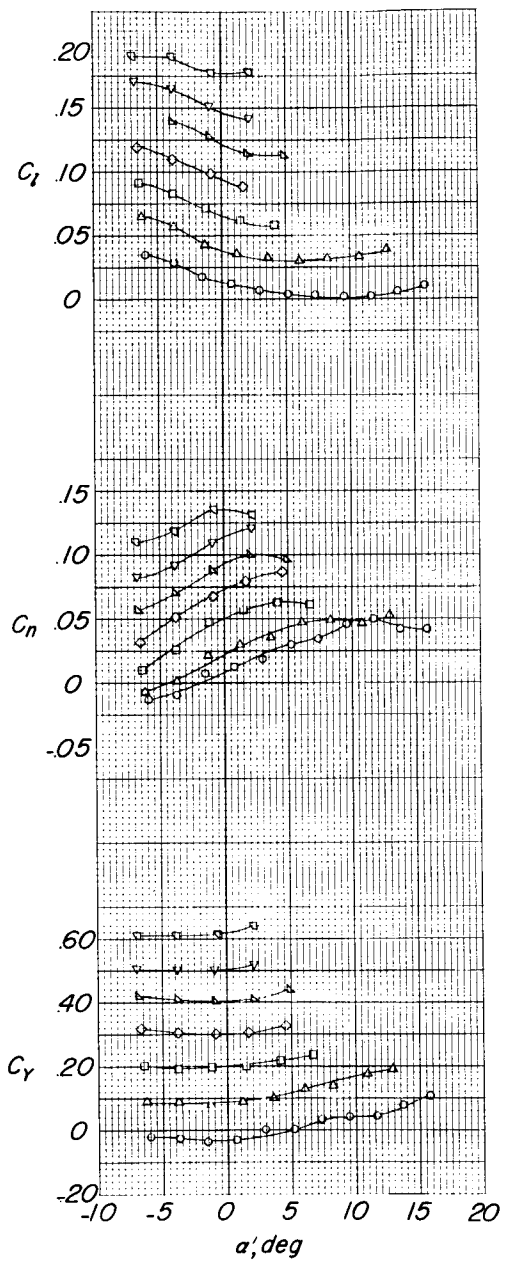
(a) $\delta_a = \delta_r = \delta_e = 0^\circ$.

Figure 28.– Aerodynamic characteristics of the X-15 model in the presence of the B-52 with X-15 pylon mounted. $\Delta\alpha = 2^\circ 15'$; $\Delta\beta = 0^\circ$; $\beta = 0^\circ$; $i_t = 3^\circ$.
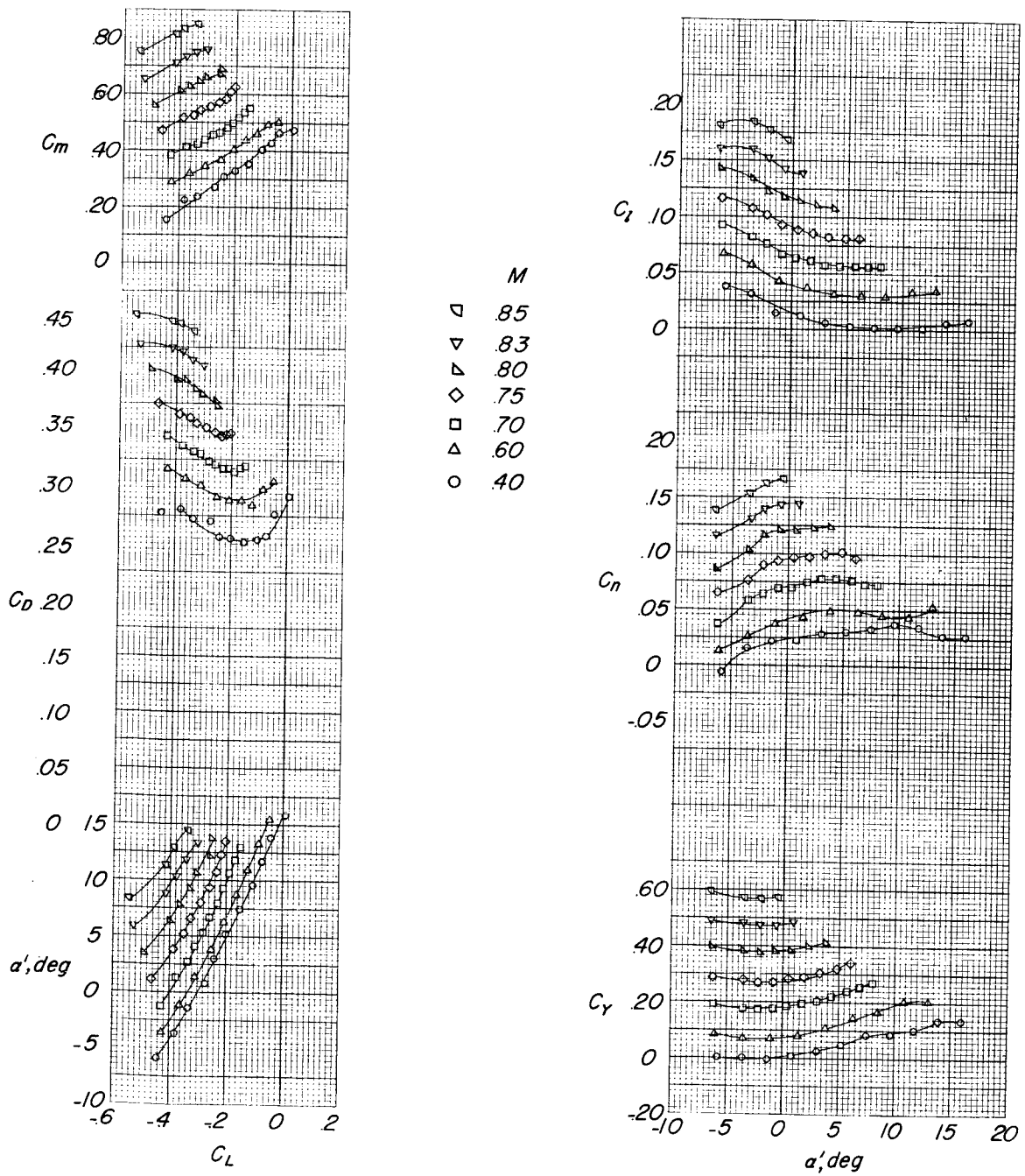
(b)  $\delta_e = -45°$;  $\delta_r = \delta_a = 0°$.

Figure 28.- Continued.
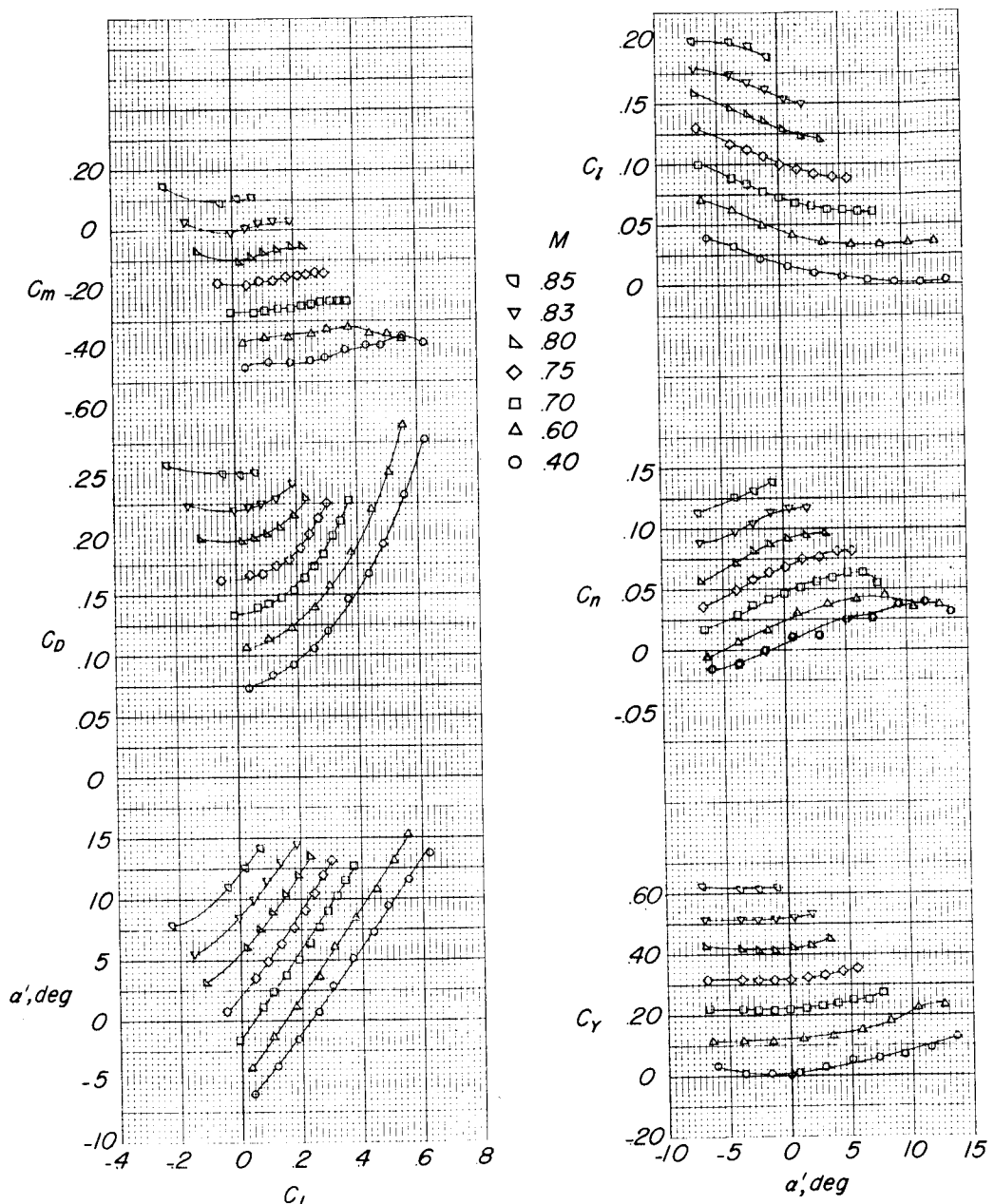
(c)  $\delta_e = 15°$;  $\delta_r = \delta_a = 0°$.

Figure 28.- Continued.

(d)  $\delta_e = 5^o$;  $\delta_r = \delta_a = 0^o$;  $i_t = 3^o$.
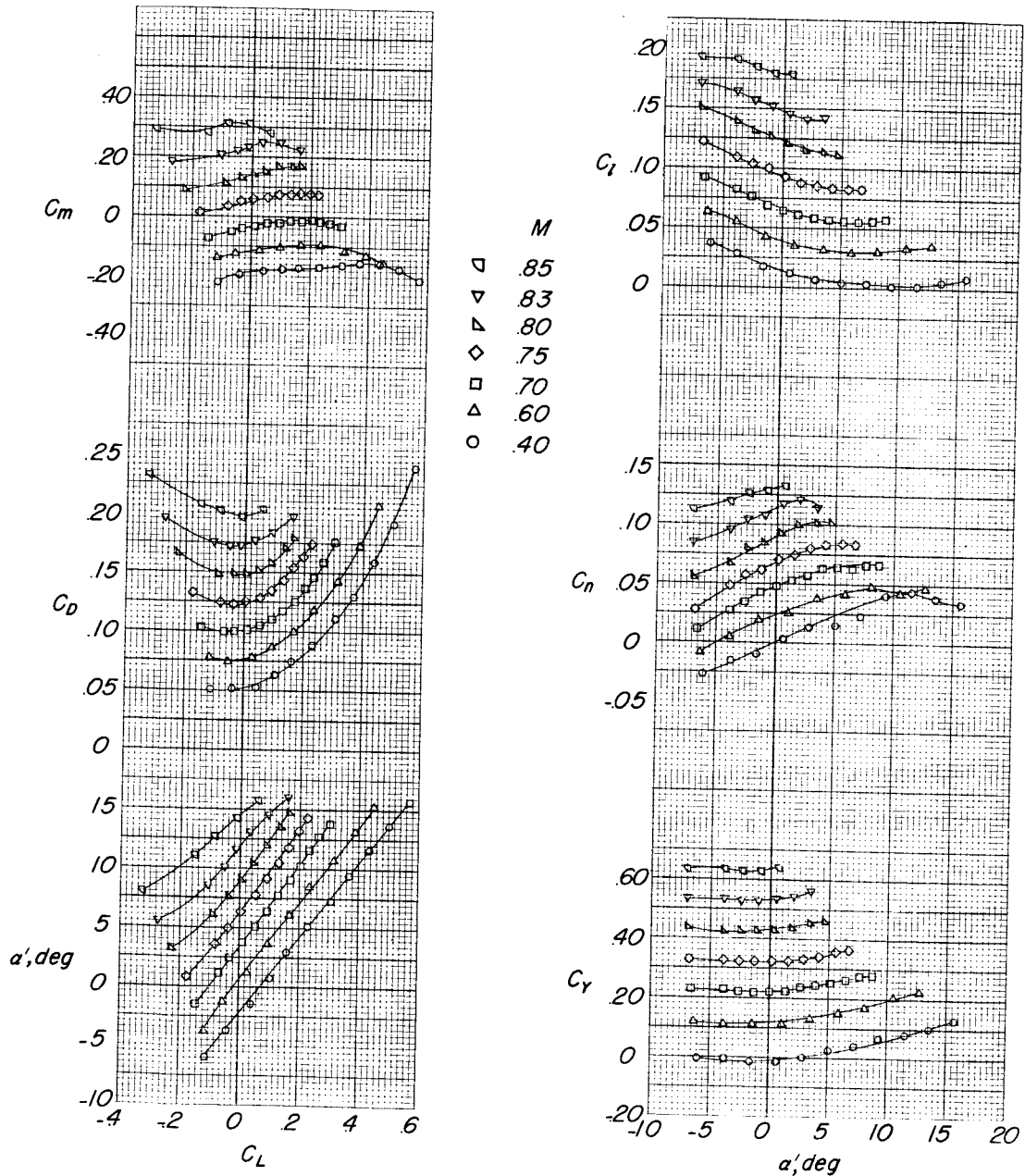
Figure 28.- Continued.
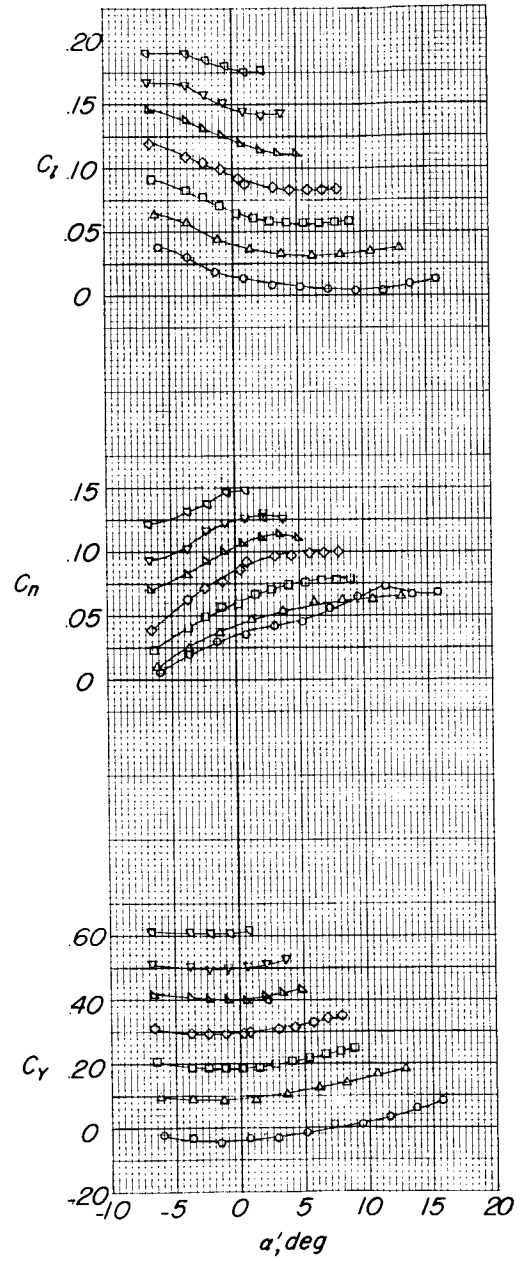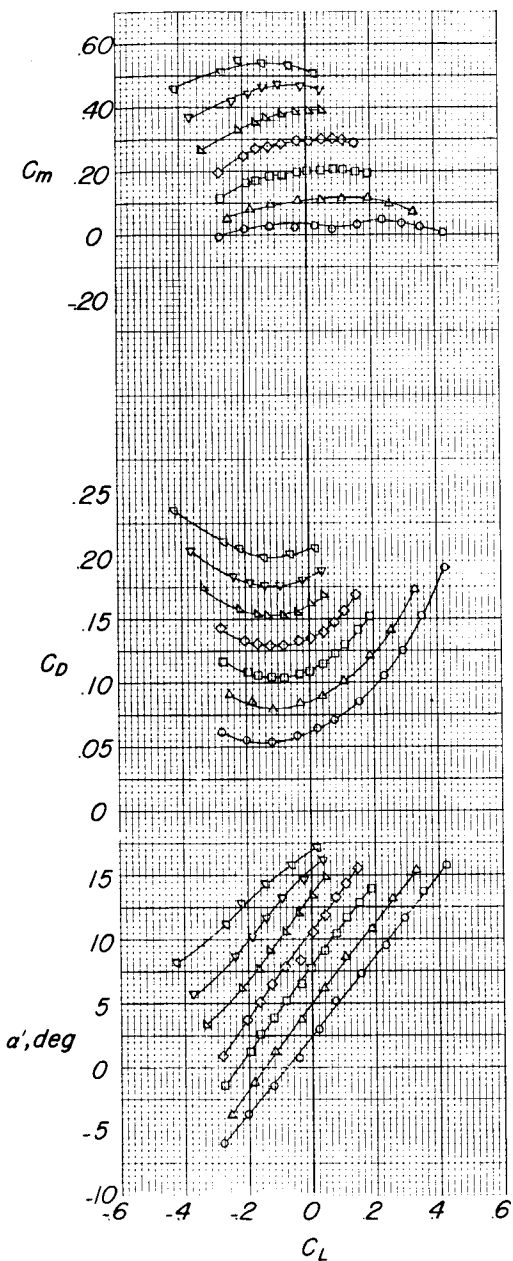
(e)  $\delta_e = -5°$;  $\delta_r = \delta_a = 0°$.

Figure 28.- Continued.
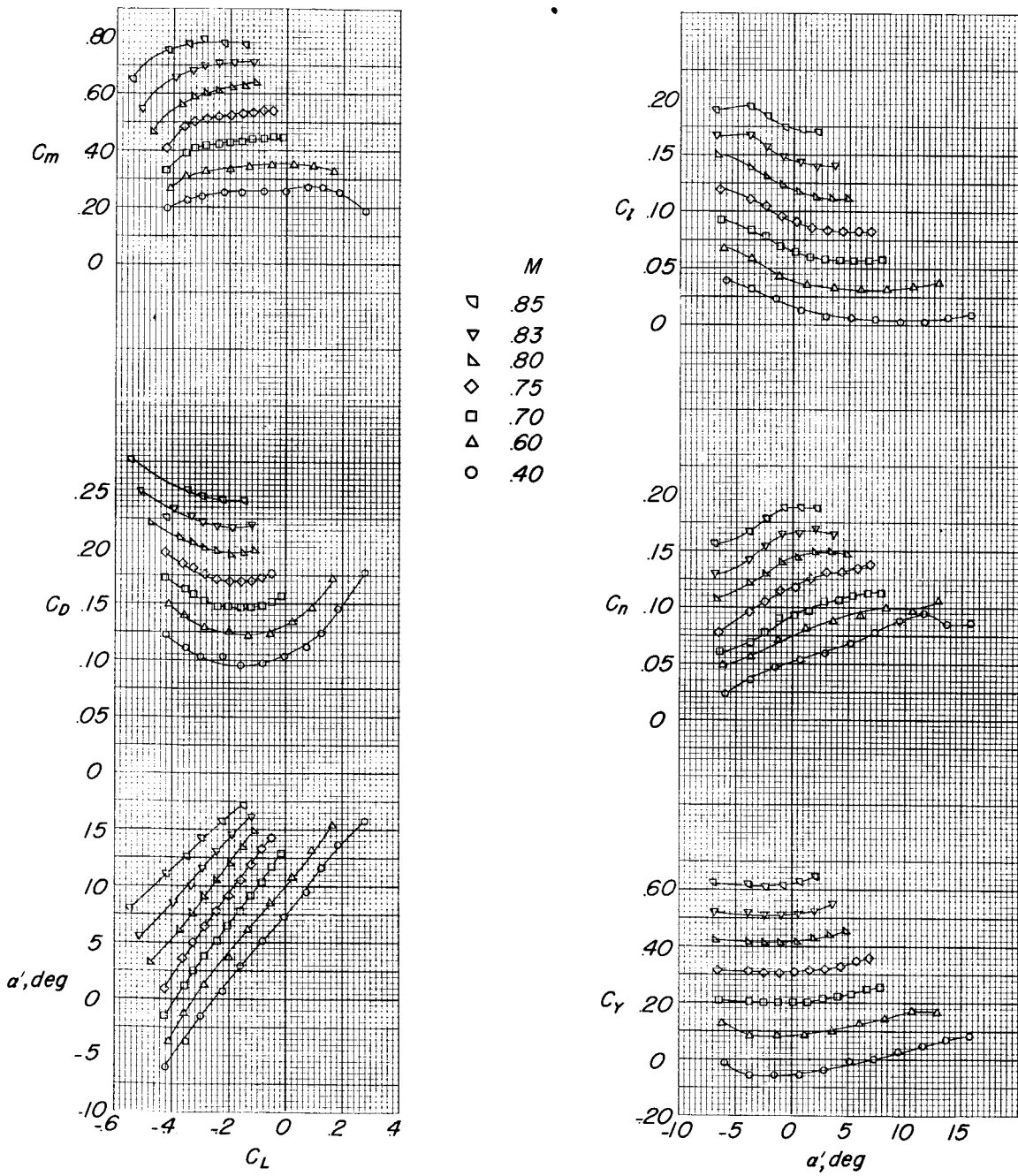
(f)  $\delta_e = -15°$;  $\delta_r = \delta_a = 0°$.

Figure 28.- Continued.
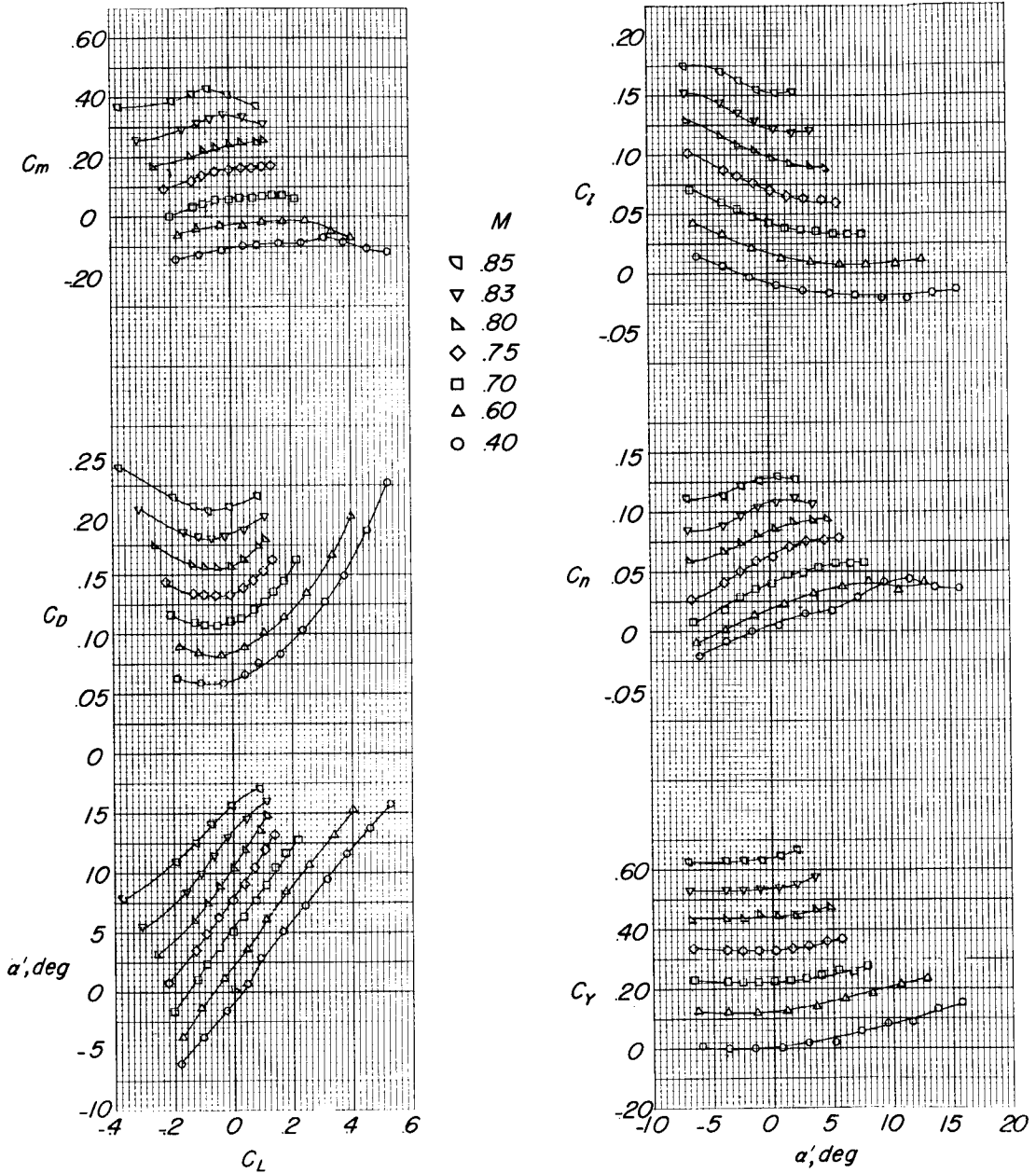
(g) Check control deflection.

Figure 28.- Continued.

DECLASSIFIED
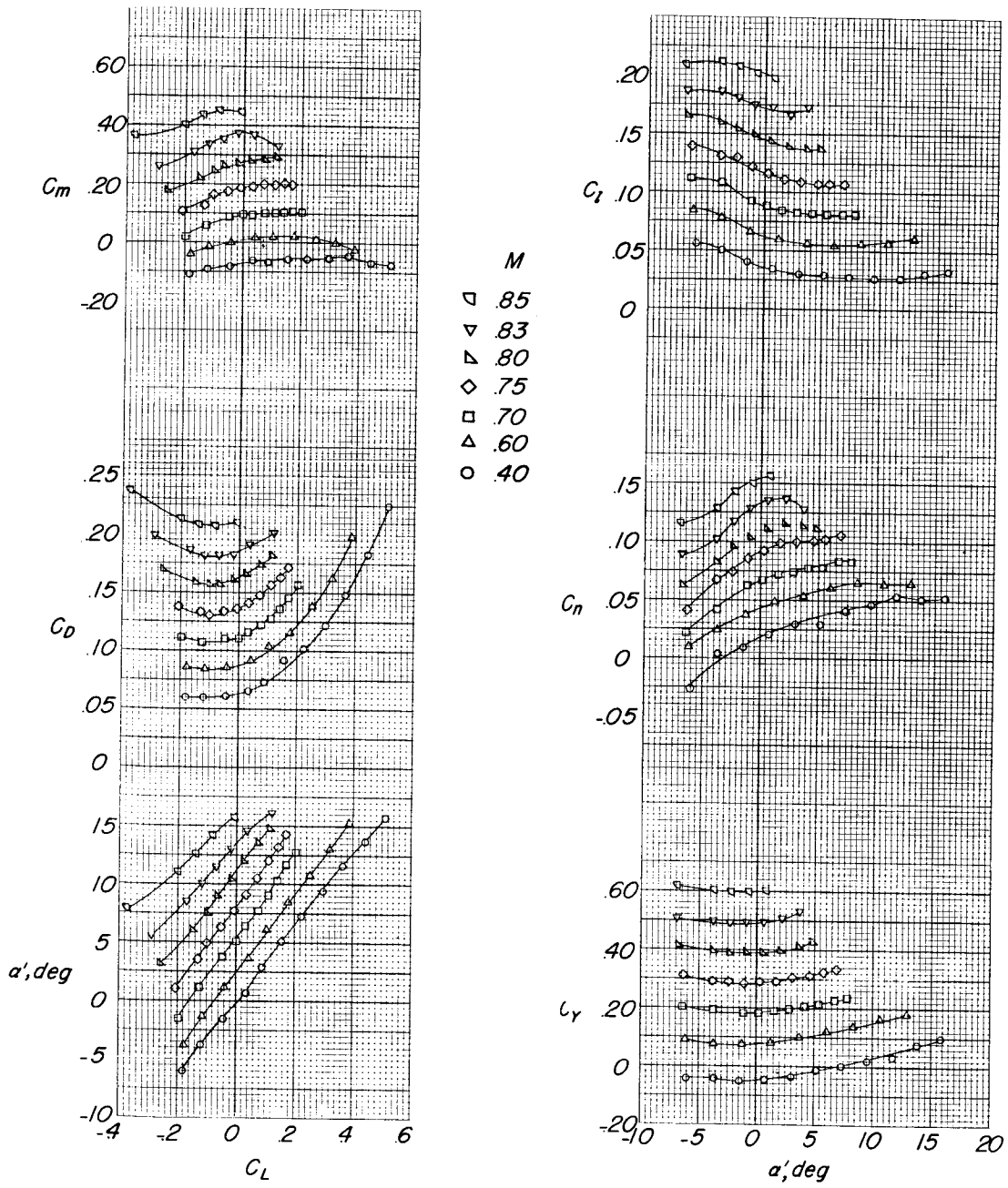


(h) $\delta_a = -15^\circ$; $\delta_e = \delta_r = 0^\circ$.

Figure 28.- Continued.
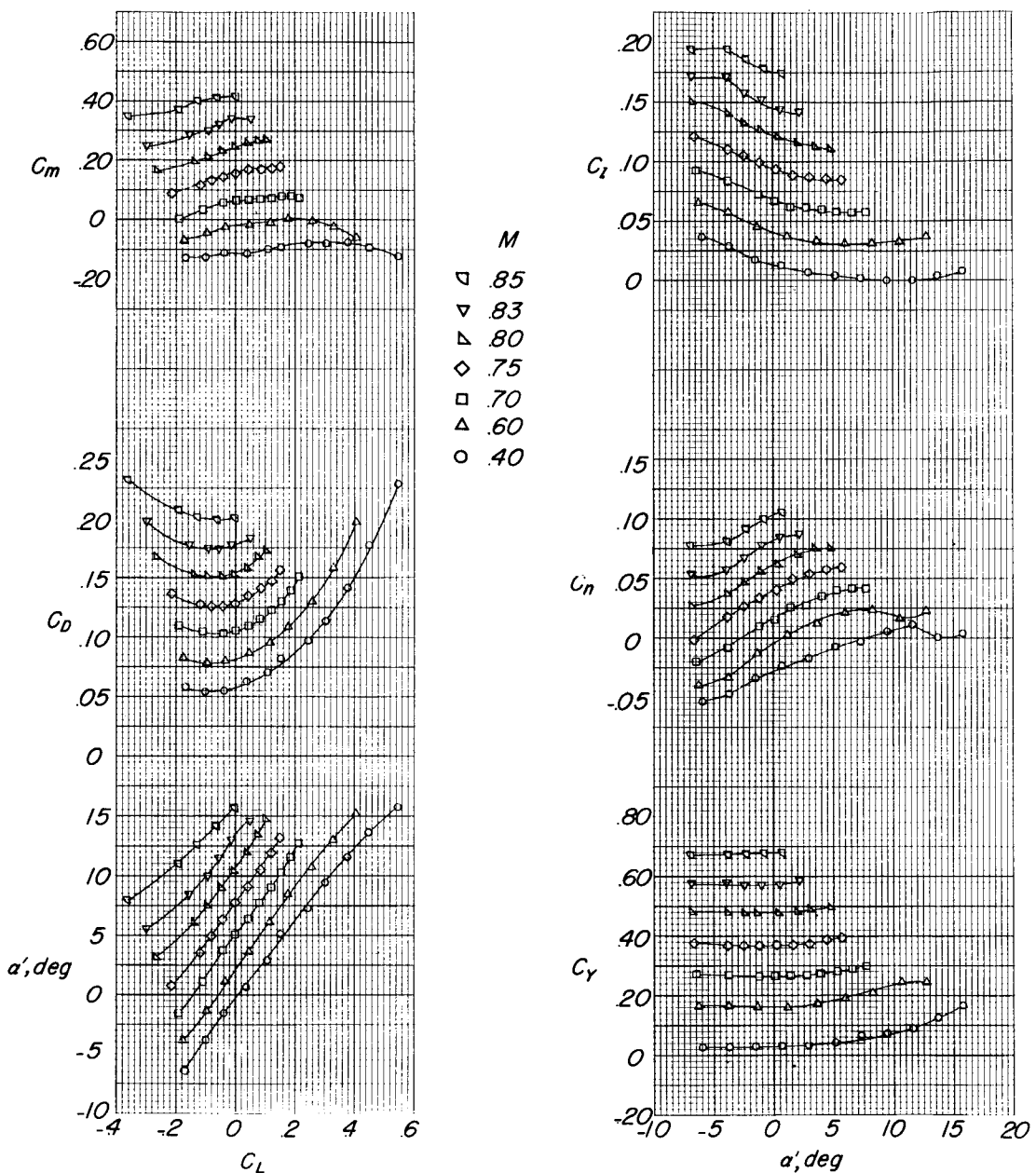
(i) $\delta_r = 7.5°$; $\delta_e = \delta_a = 0°$.

Figure 28.- Continued.
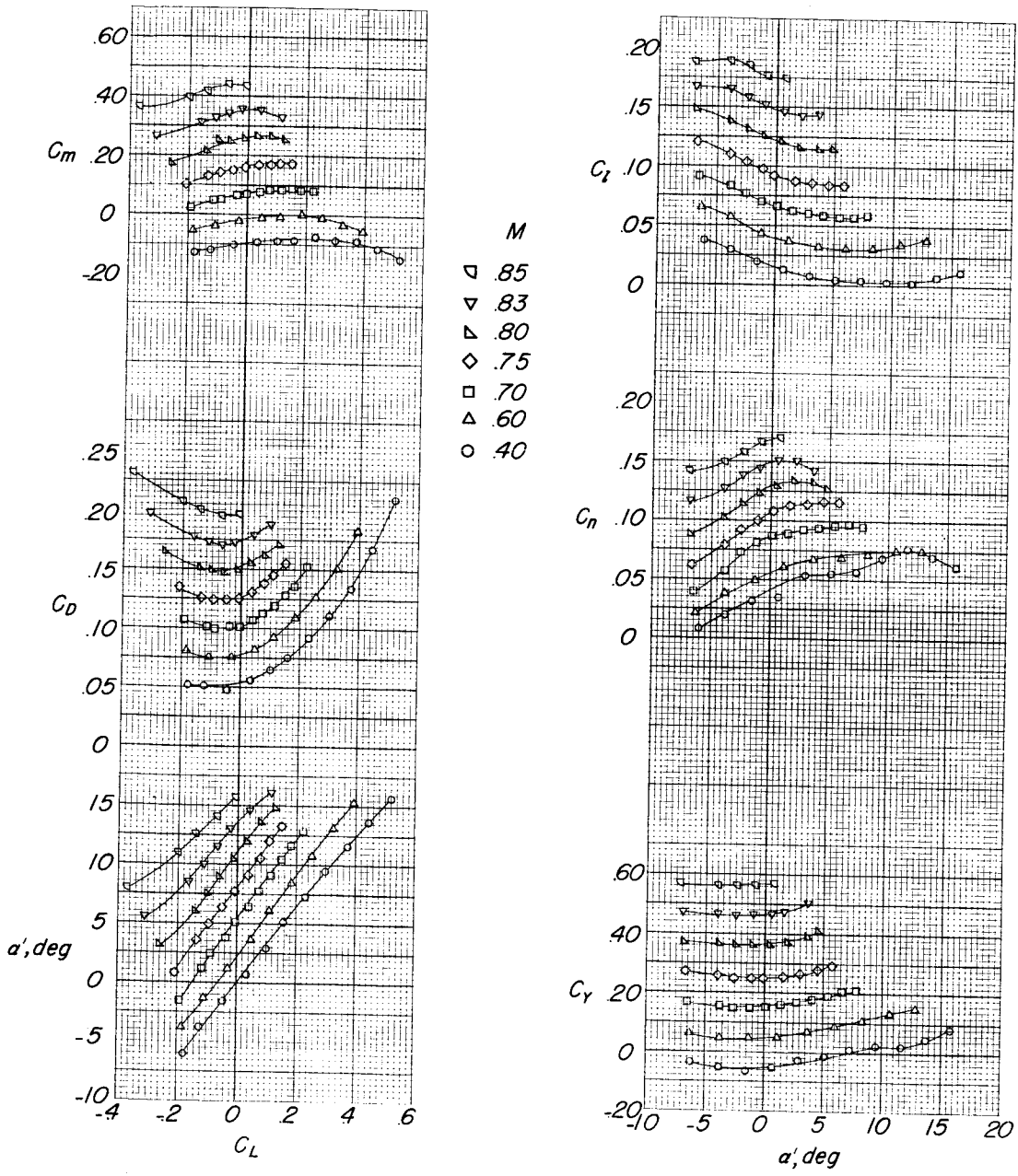
(j)  $\delta_r = -7.5°$;  $\delta_e = \delta_a = 0°$.

Figure 28.- Concluded.
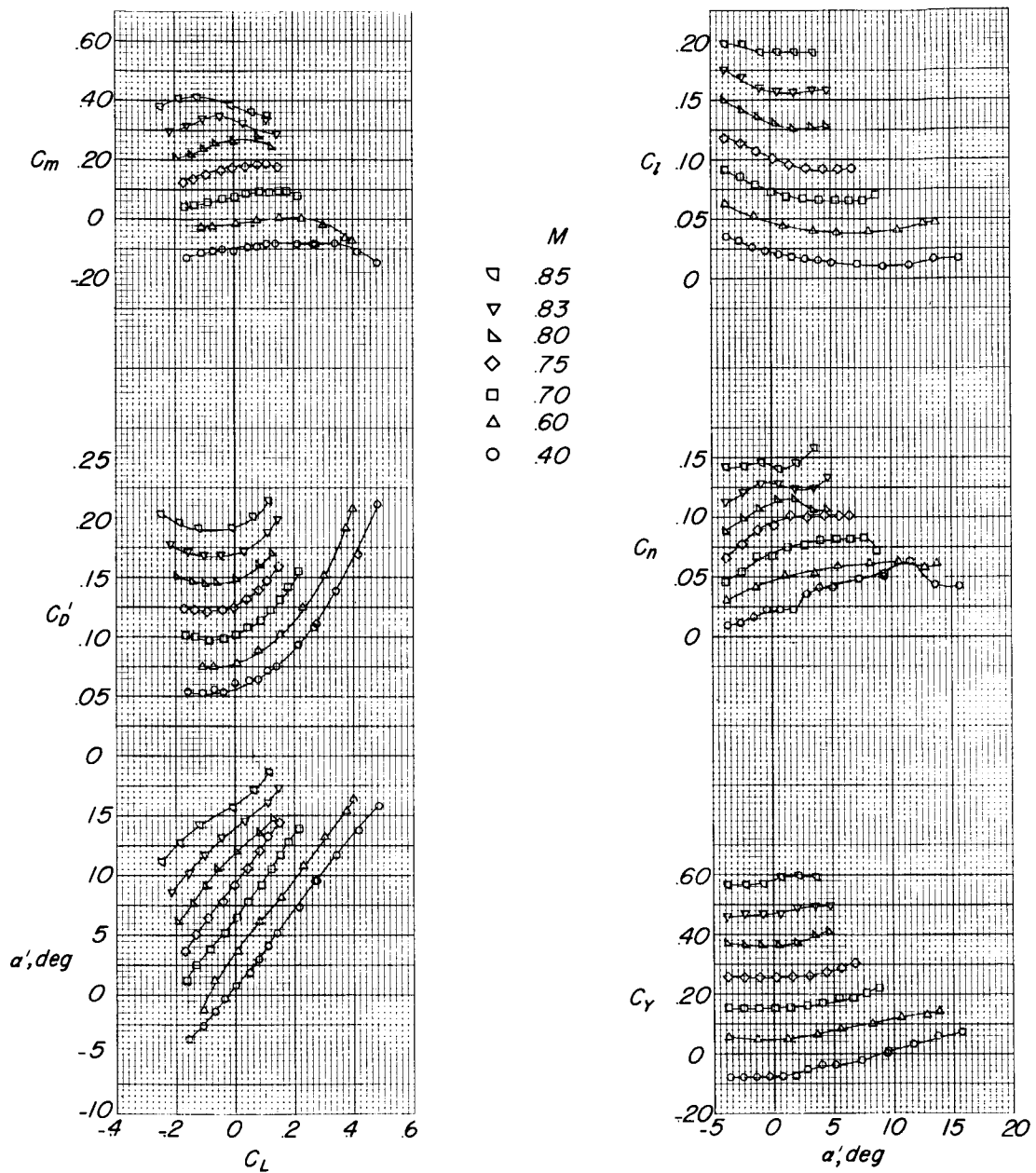
(a)  β = 4°.

Figure 29.- Aerodynamic characteristics of the X-15 airplane model in the presence of the B-52 model.  Pylon-mounted effect of sideslip of the combination; $i_t$ = 3°; $\delta_e$ = $\delta_r$ = $\delta_a$ = 0°.
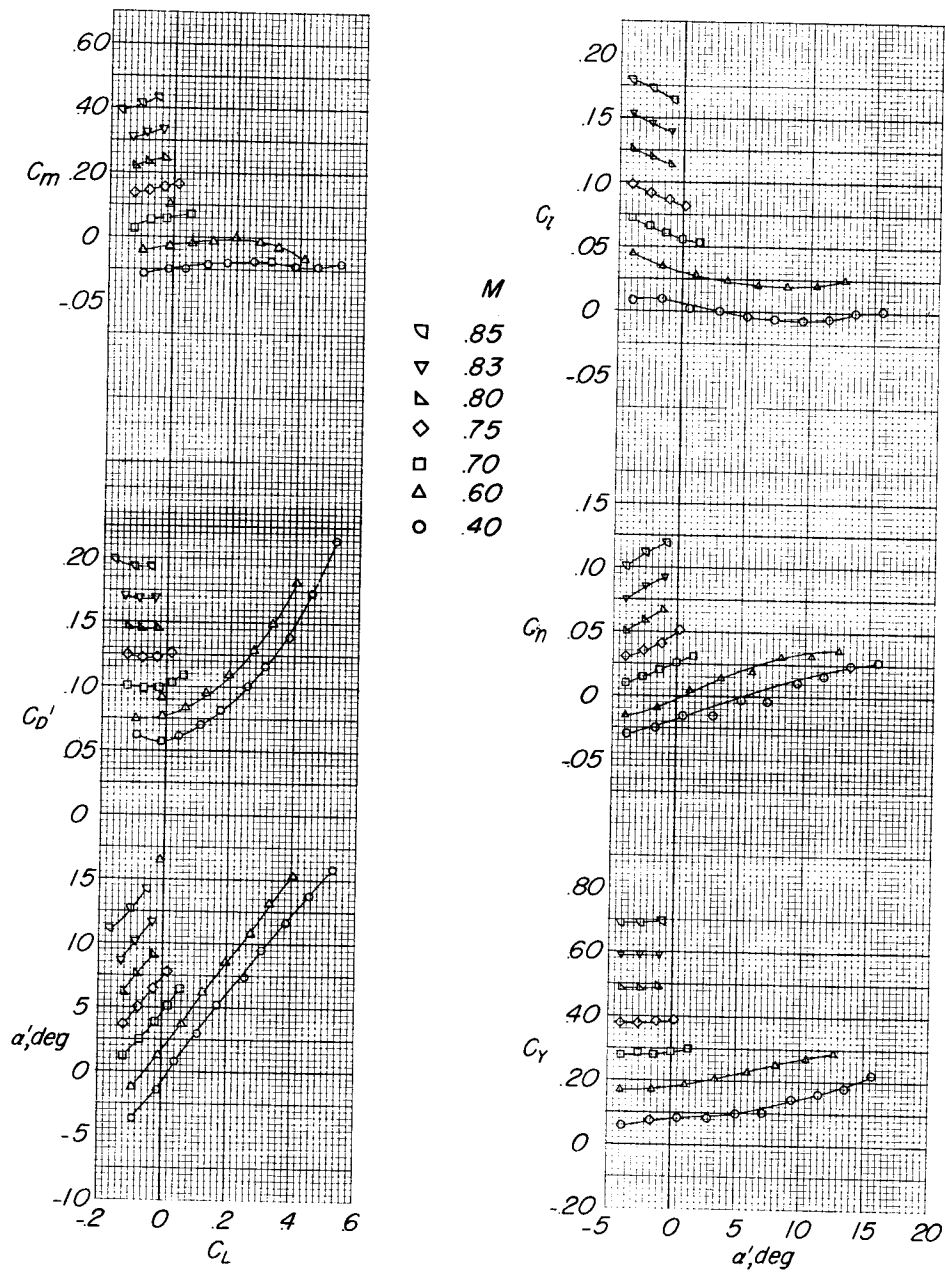
(b)  β = -4°.

Figure 29.- Concluded.
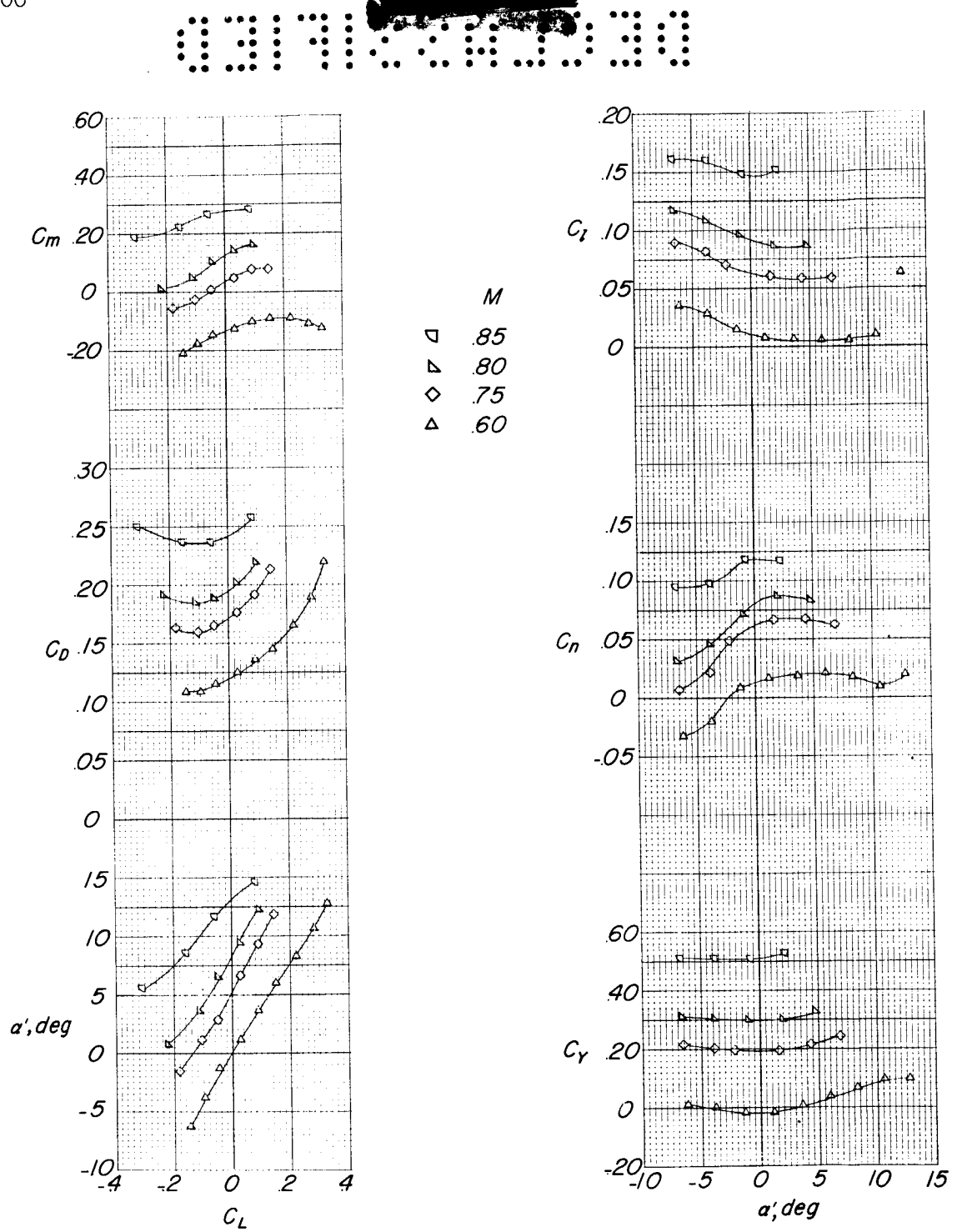
Figure 30.- Aerodynamic characteristics of the X-15 airplane model pylon mounted. Effect of speed-brake deflection.
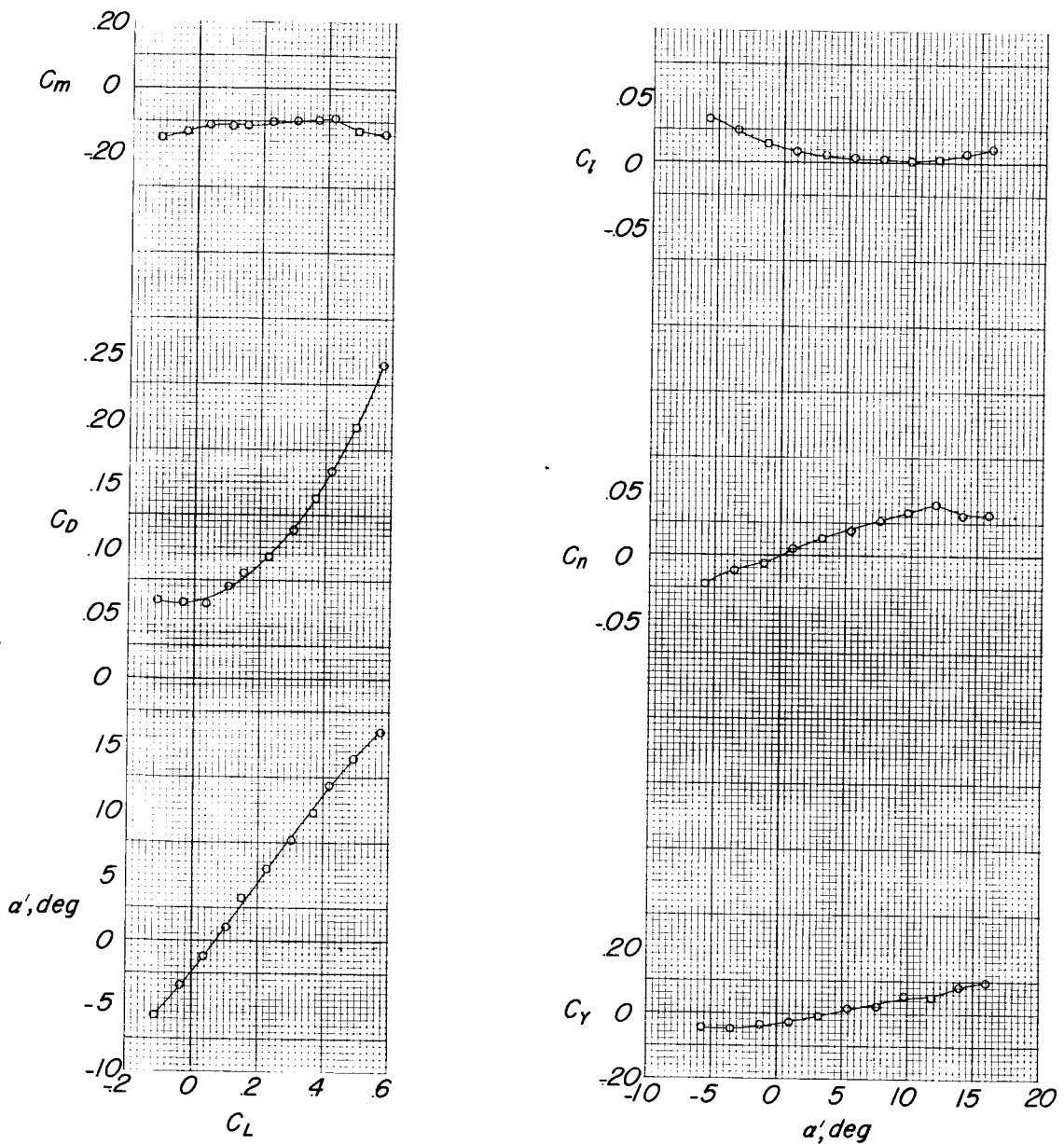
Figure 31.- Aerodynamic characteristics of the X-15 airplane model pylon mounted on B-52. Outboard flap deflected $30^\circ$; M = 0.40; $i_t = 3^\circ$; $\delta_e = \delta_r = \delta_a = 0^\circ$.
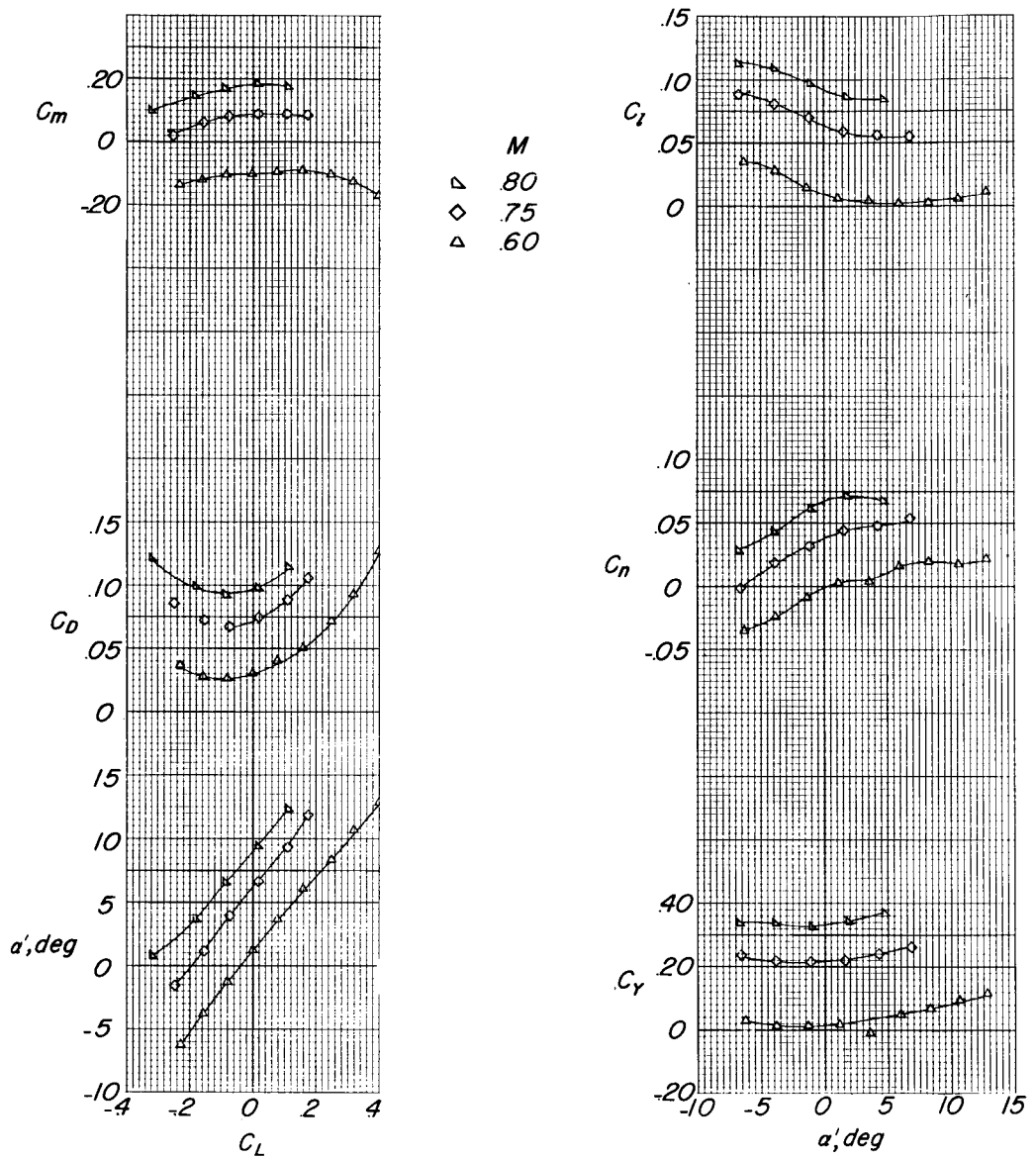
Figure 32.- Aerodynamic characteristics of the X-15 airplane model. Pylon-mounted buffet fairing in place; $\delta_e = \delta_r = \delta_a = \delta_B = \delta_f = \beta = 0°$; $i_t = 3°$.
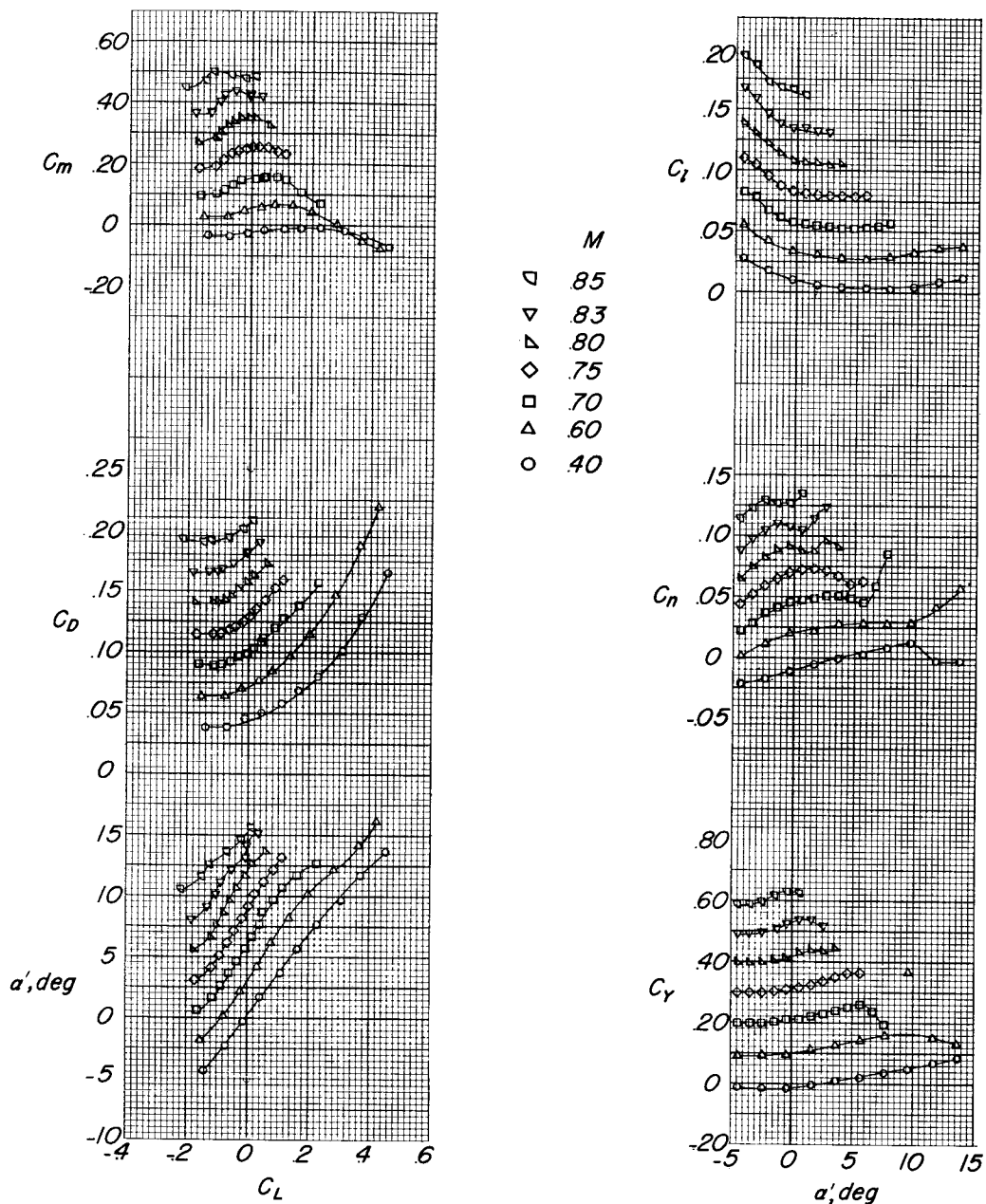
(a)  z = 0 inch.

Figure 33.- Aerodynamic characteristics of the X-15 model in the presence of the B-52 model.  Sting mounted; $\Delta\alpha = 1°30'$; $\Delta\beta = 0°$; $\Phi = 0°$; $\delta_e = \delta_a = \delta_r = 0°$.
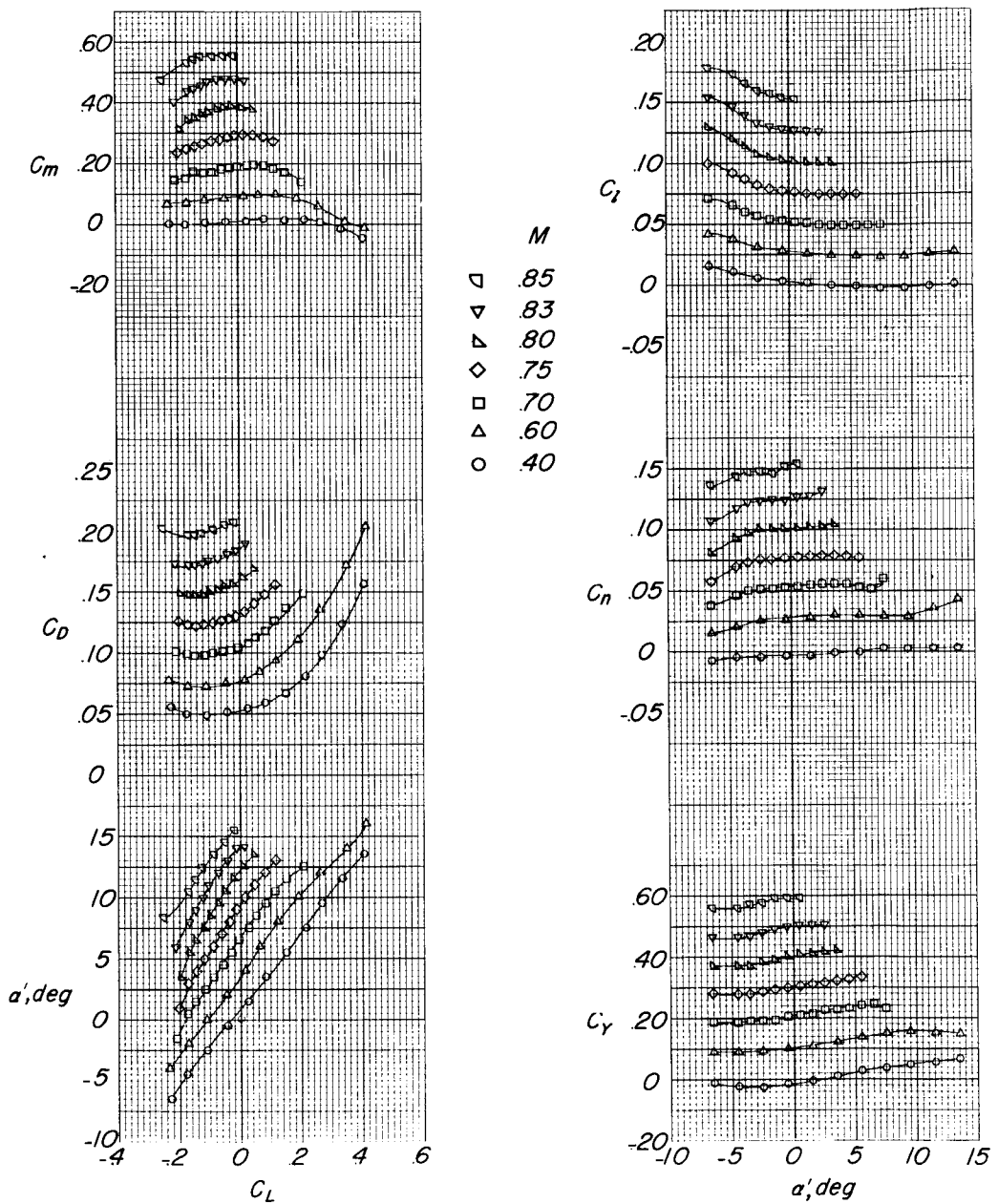
(b)   z = 1 inch.

Figure 33.- Continued.

DECLASSIFIED
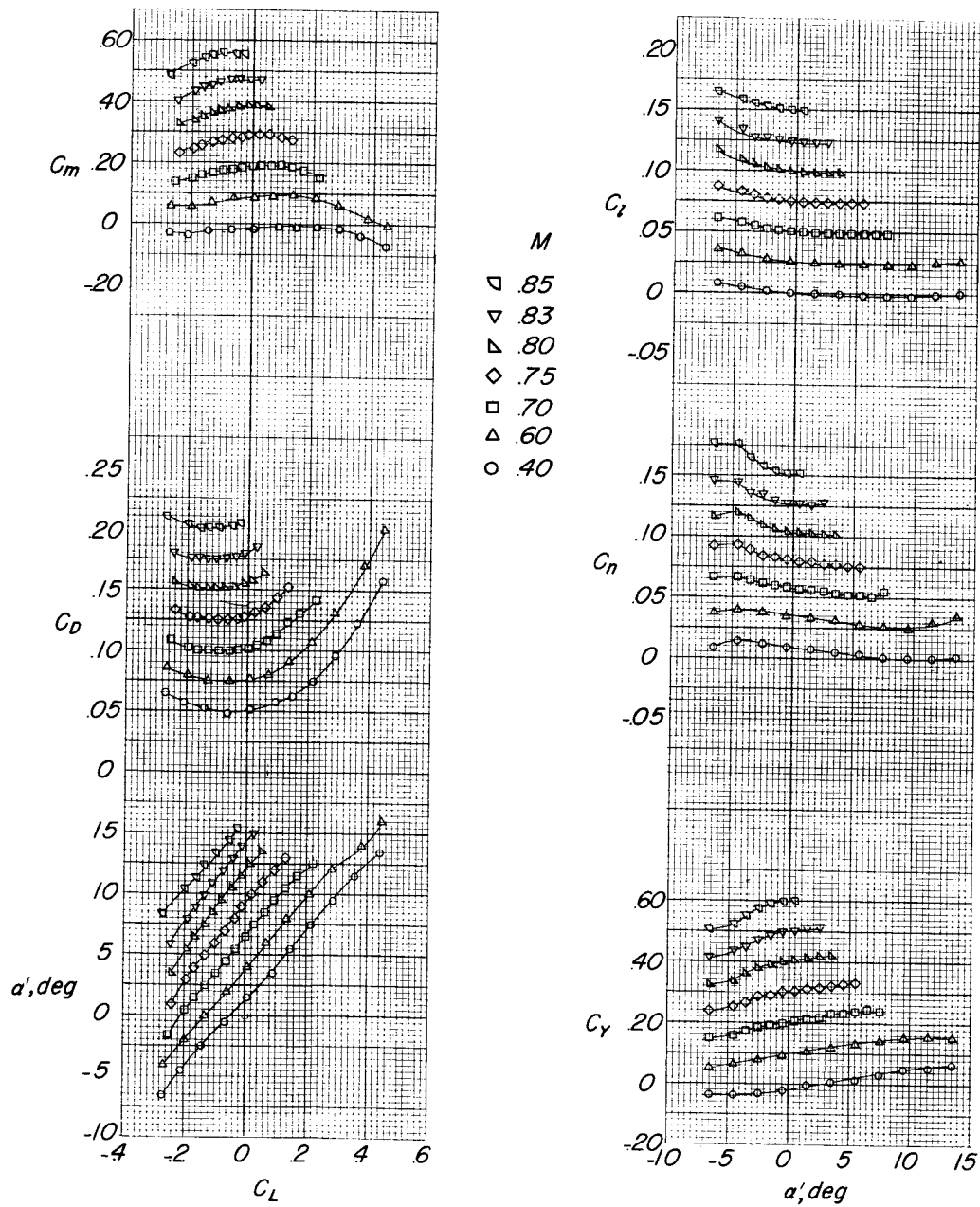


(c)  z = 2 inches.

Figure 33.- Continued.
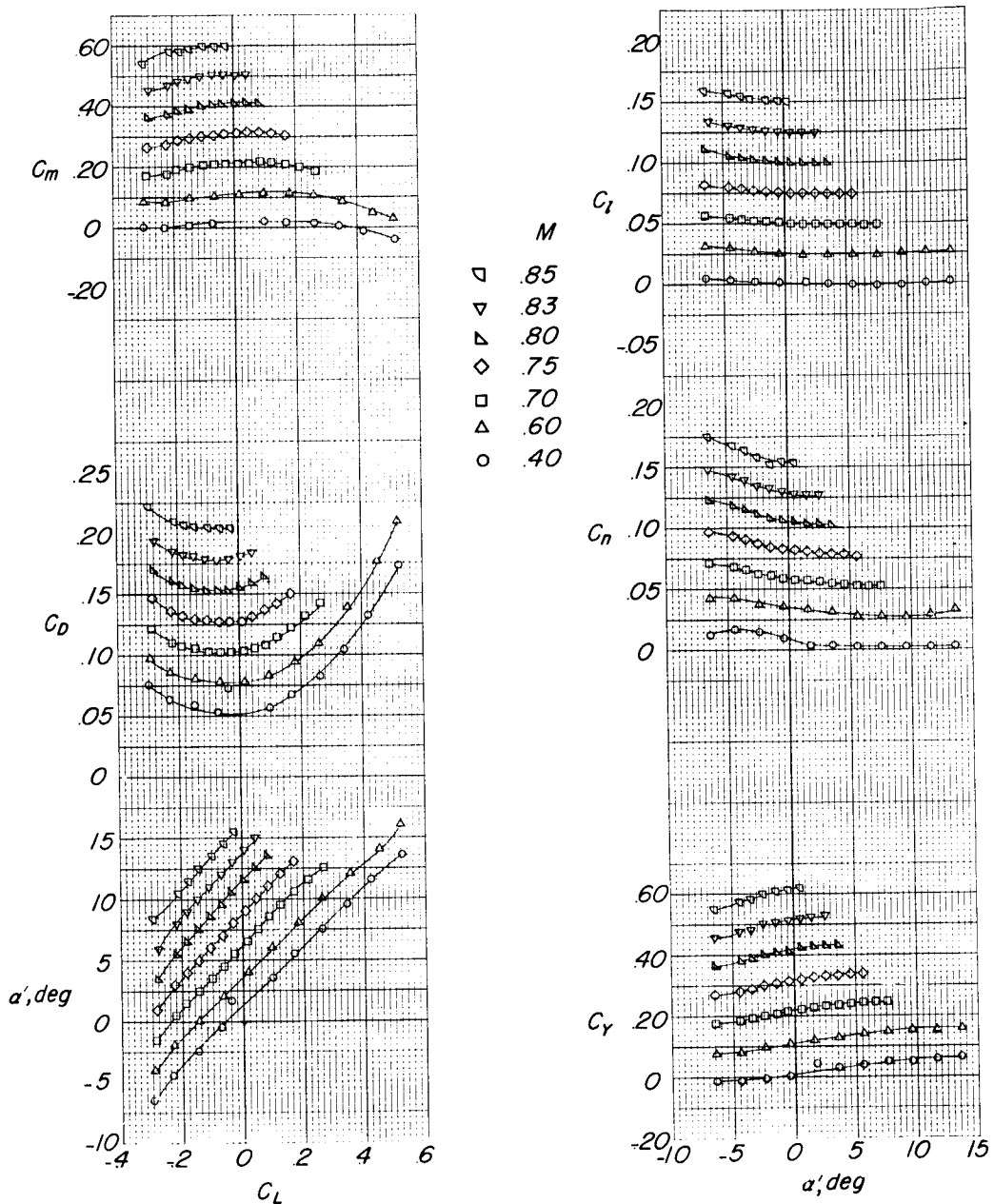
(d)   z = 4 inches.

Figure 33.- Continued.
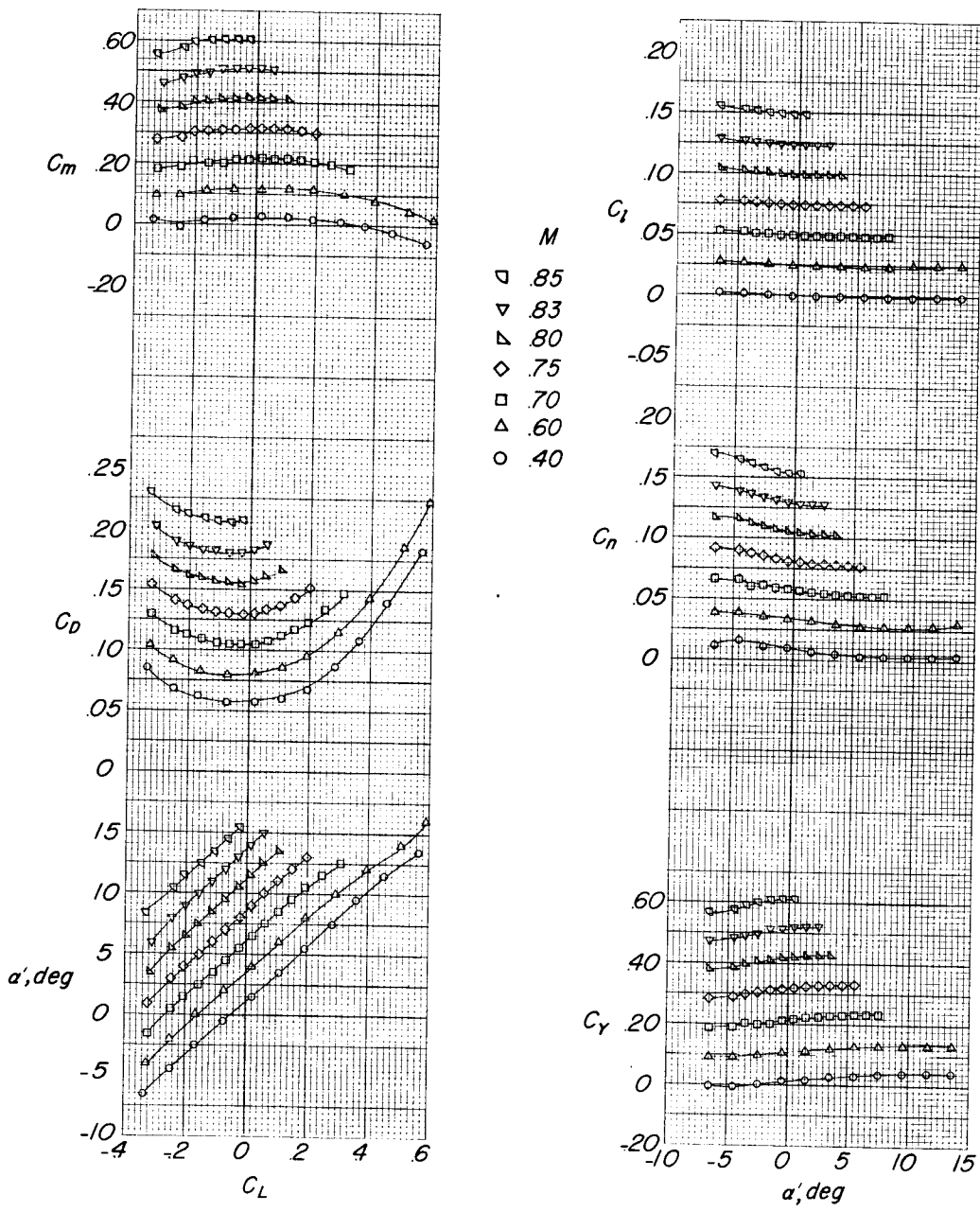
(e)  z = 5.75 inches.

Figure 33.- Continued.
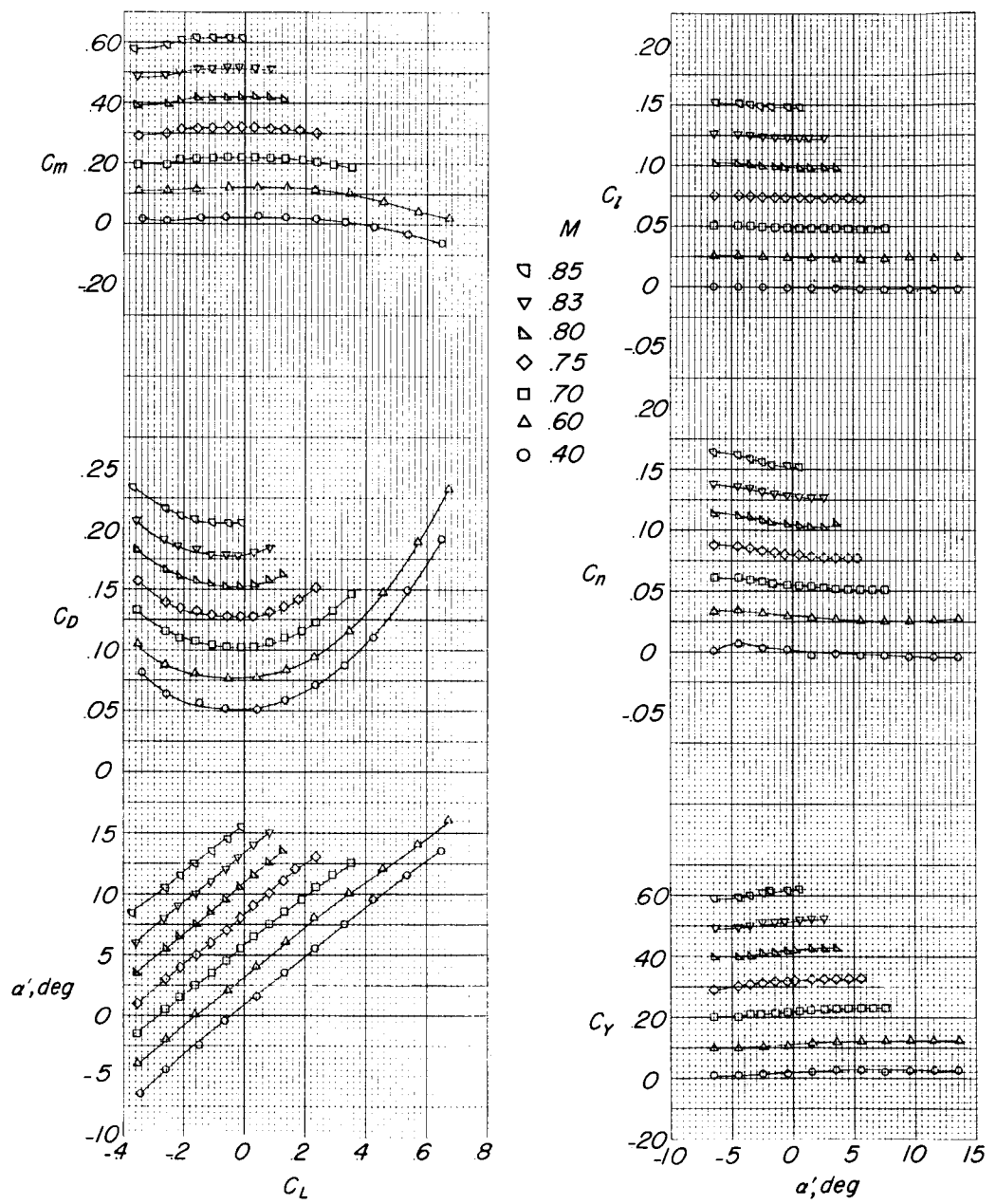
(f)  z = 8 inches.

Figure 33.- Continued.
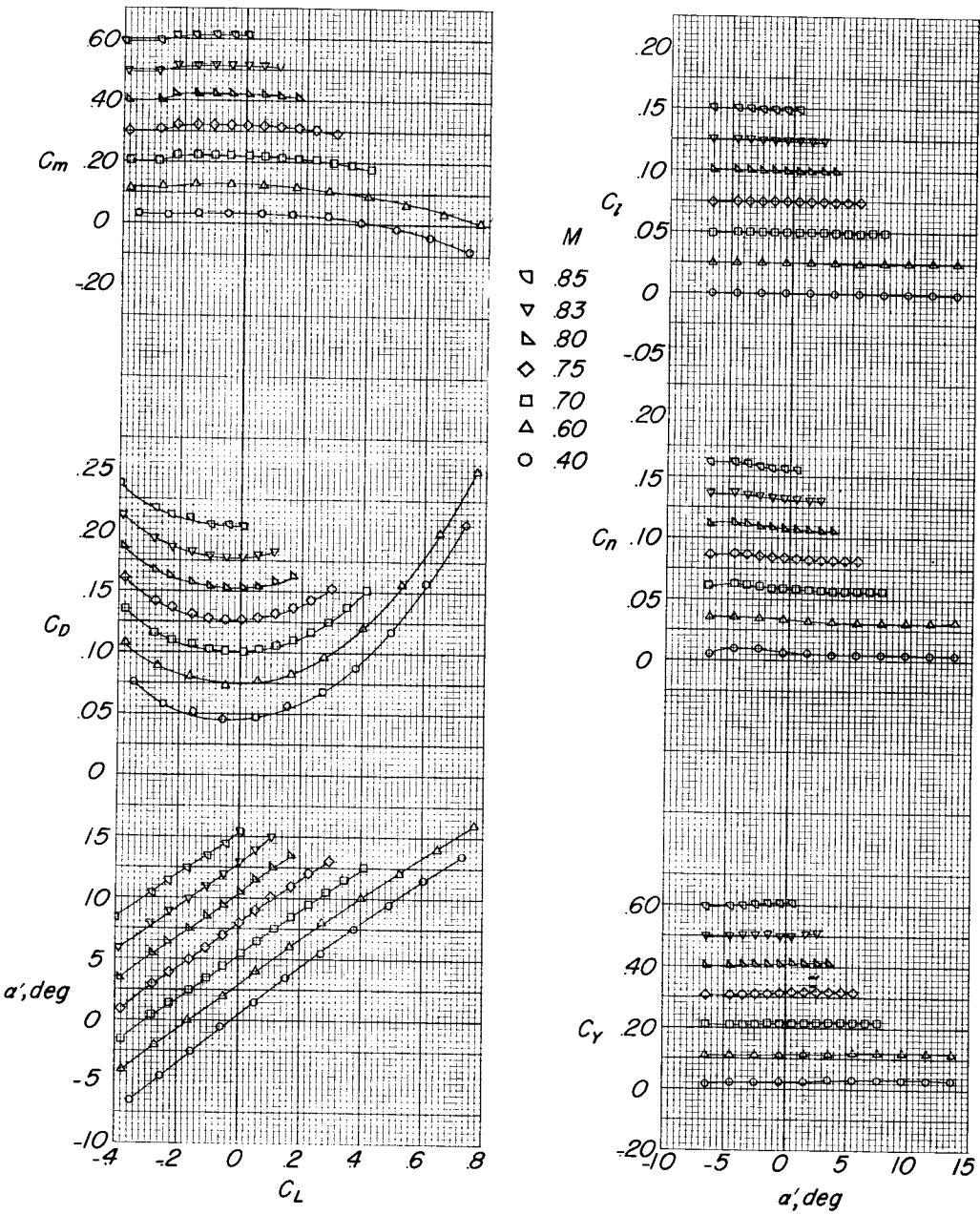
(g)  z = 12 inches.

Figure 33.- Concluded.
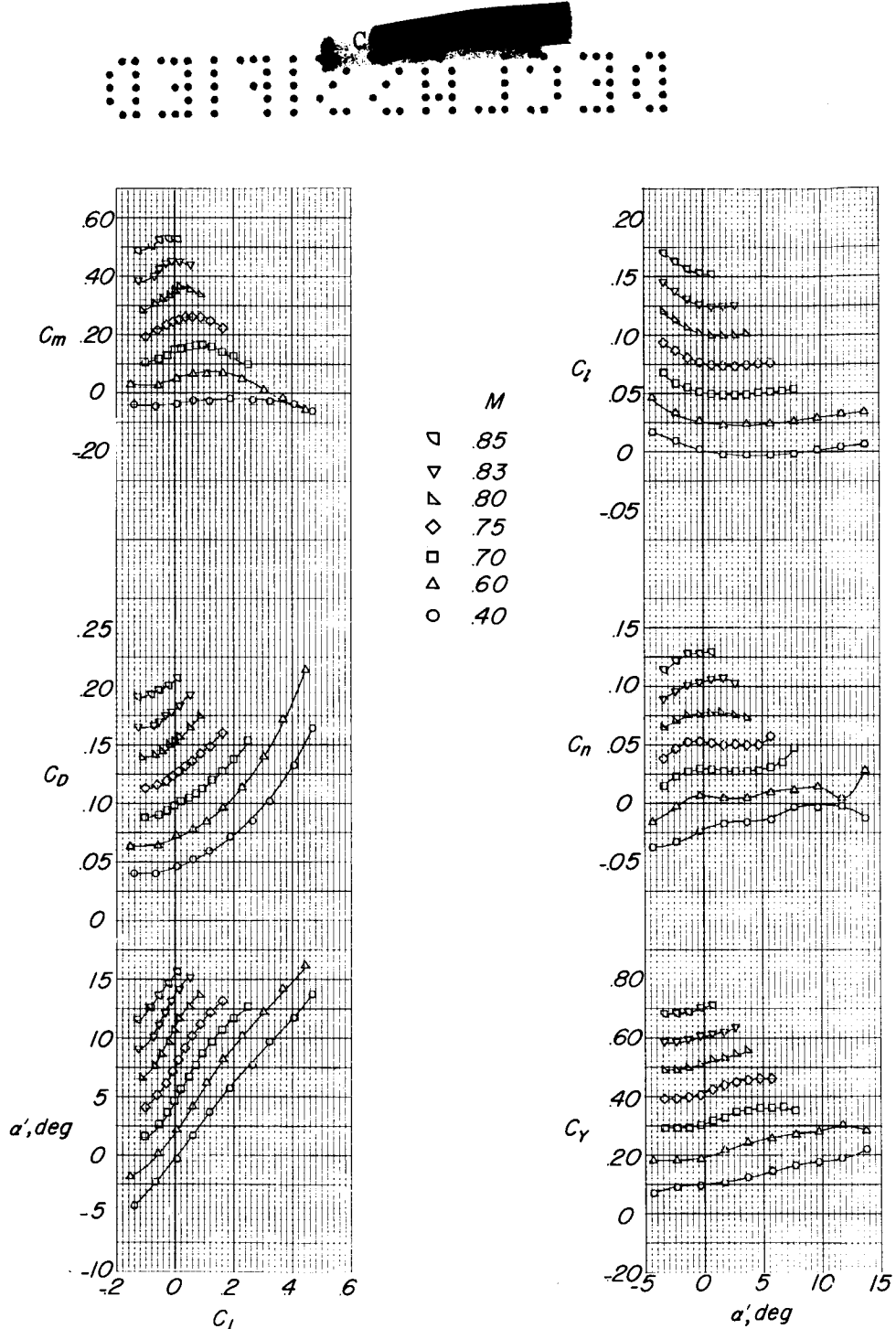
(a)  β = -4°.

Figure 34.- Aerodynamic characteristics of the X-15 model in the presence
of the B-52 model.  X-15 sting mounted; $\Delta\alpha$ = 1°40'; $\Delta\beta$ = 0°; $\Phi$ = 0°;
z = 0 inch; effect of sideslipping the combination.
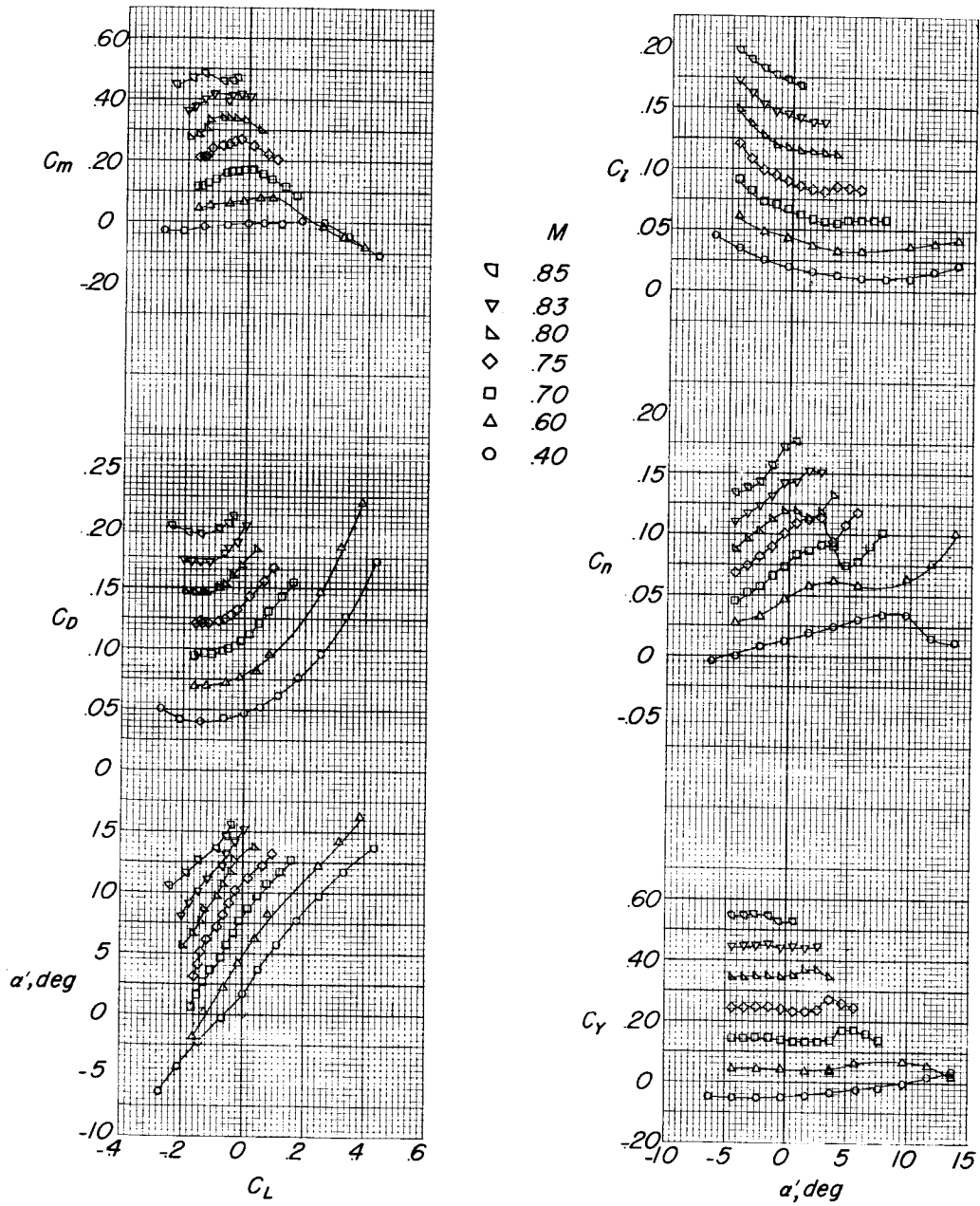
(b)  β = 4°.

Figure 34.- Concluded.
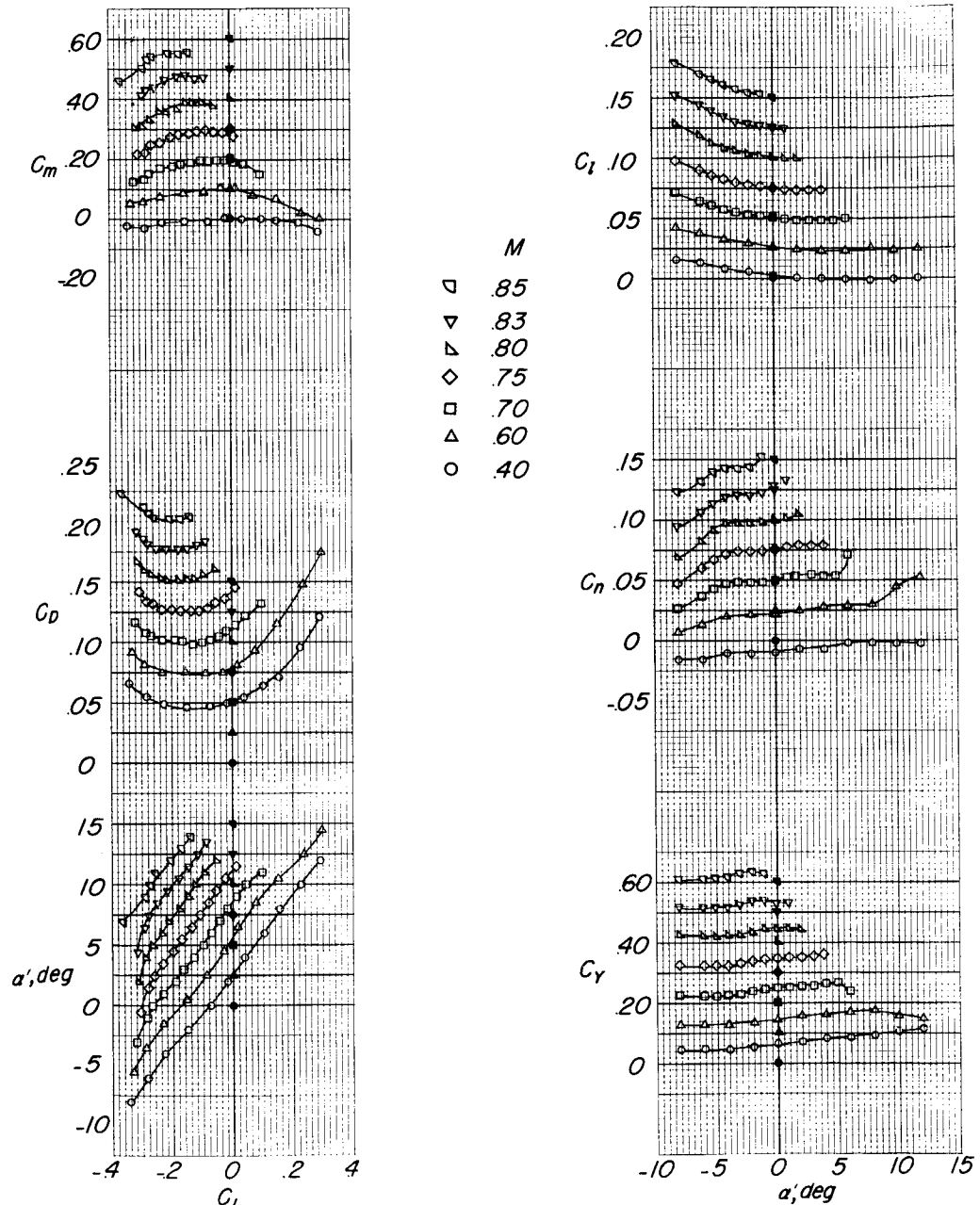
(a)  z = 1 inch.

Figure 35.- Aerodynamic characteristics of the X-15 model in the presence of the B-52 model.  Sting mounted; $\Delta\alpha = 0^O$; $\Delta\beta = 0^O$; $\Phi = 0^O$; $\delta_e = \delta_a = \delta_r = 0^O$.
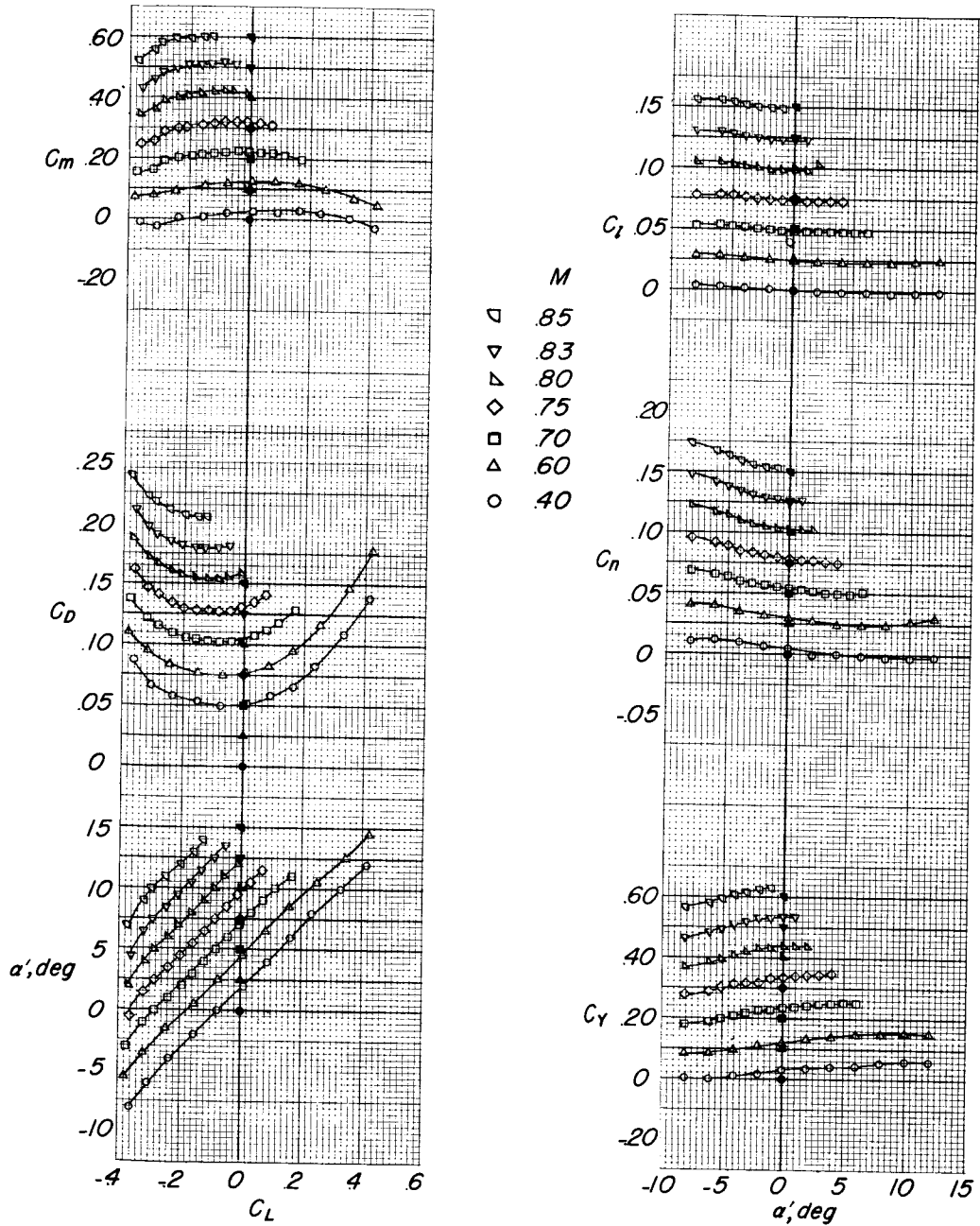
(b)  z = 4 inches.

Figure 35.- Continued.
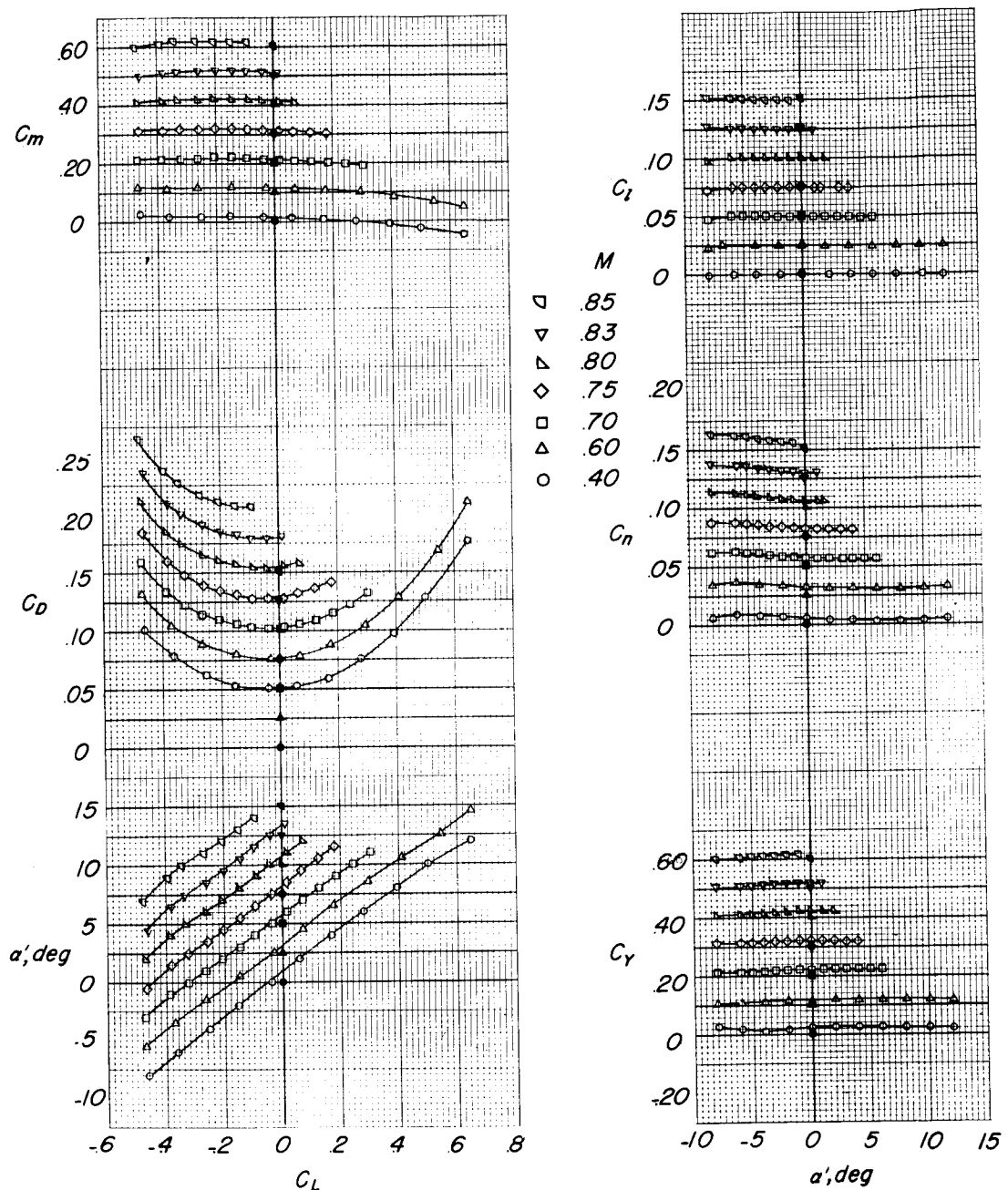
(c)   z = 12 inches.

Figure 35.- Concluded.
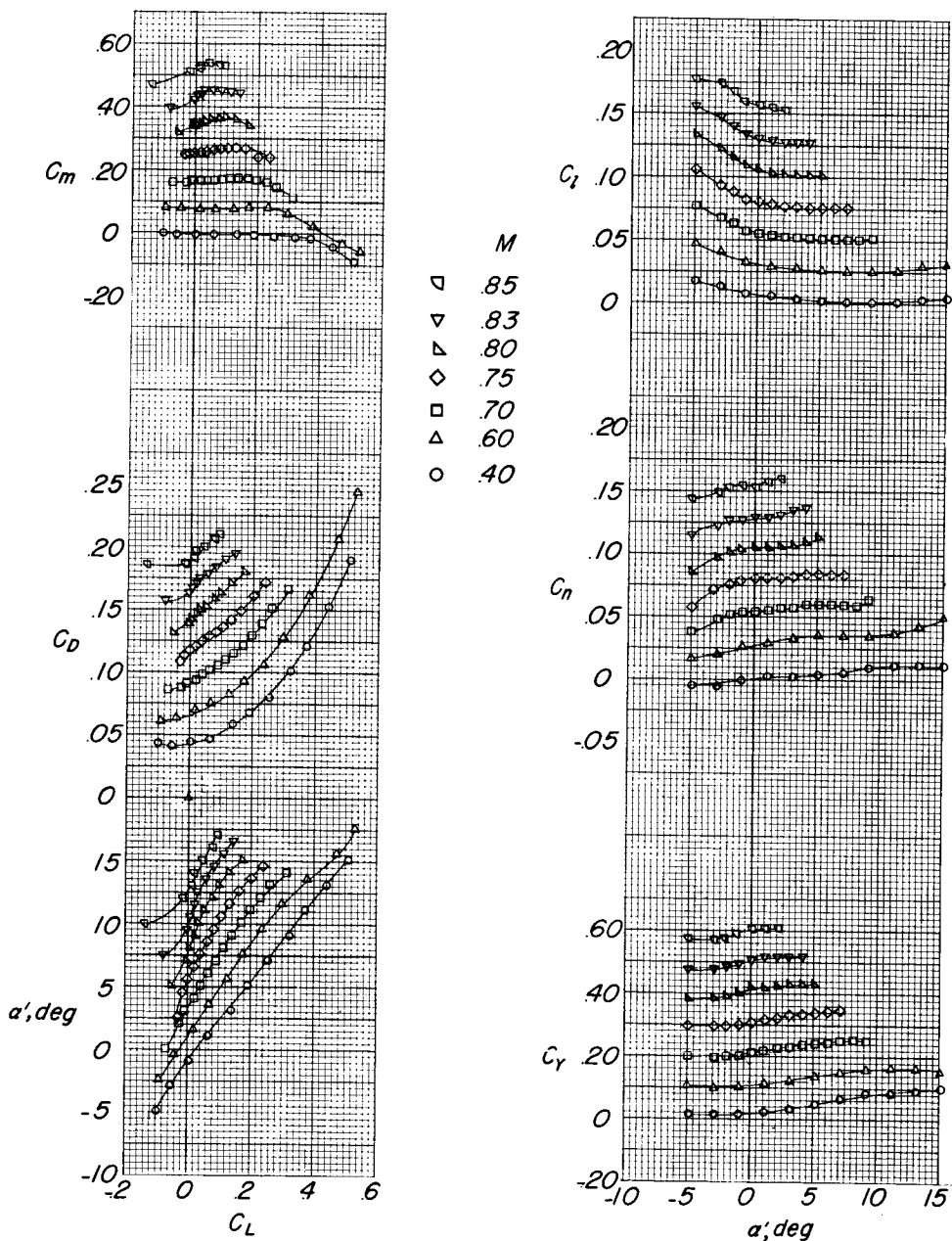
(a)  z = 1 inch.

Figure 36.- Aerodynamic characteristics of the X-15 model in the presence of the B-52 model.  Sting mounted; $\Delta\alpha = 3^\circ 5'$; $\Delta\beta = 0^\circ$; $\Phi = 0^\circ$.
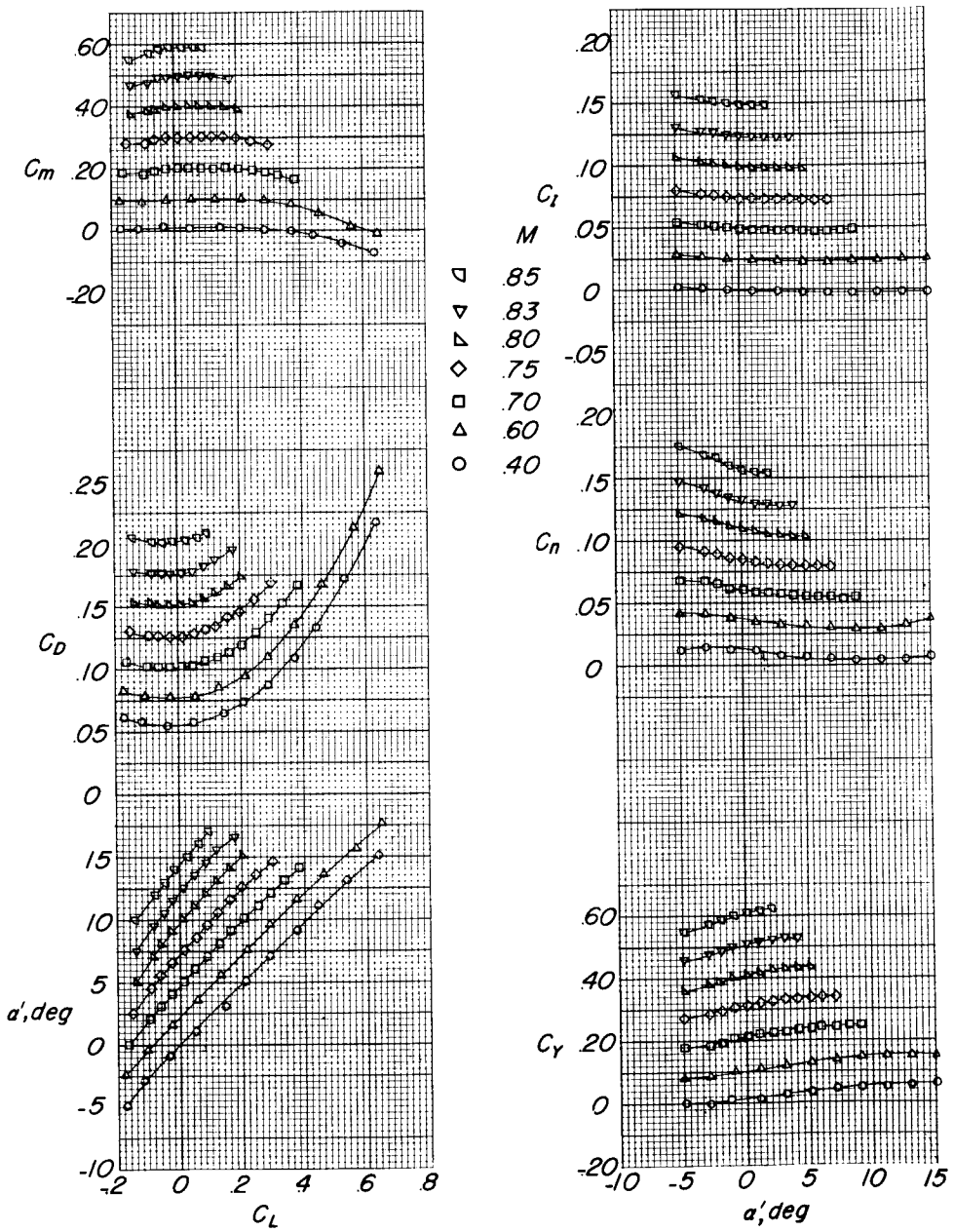
(b)  z = 4 inches.

Figure 36.- Continued.
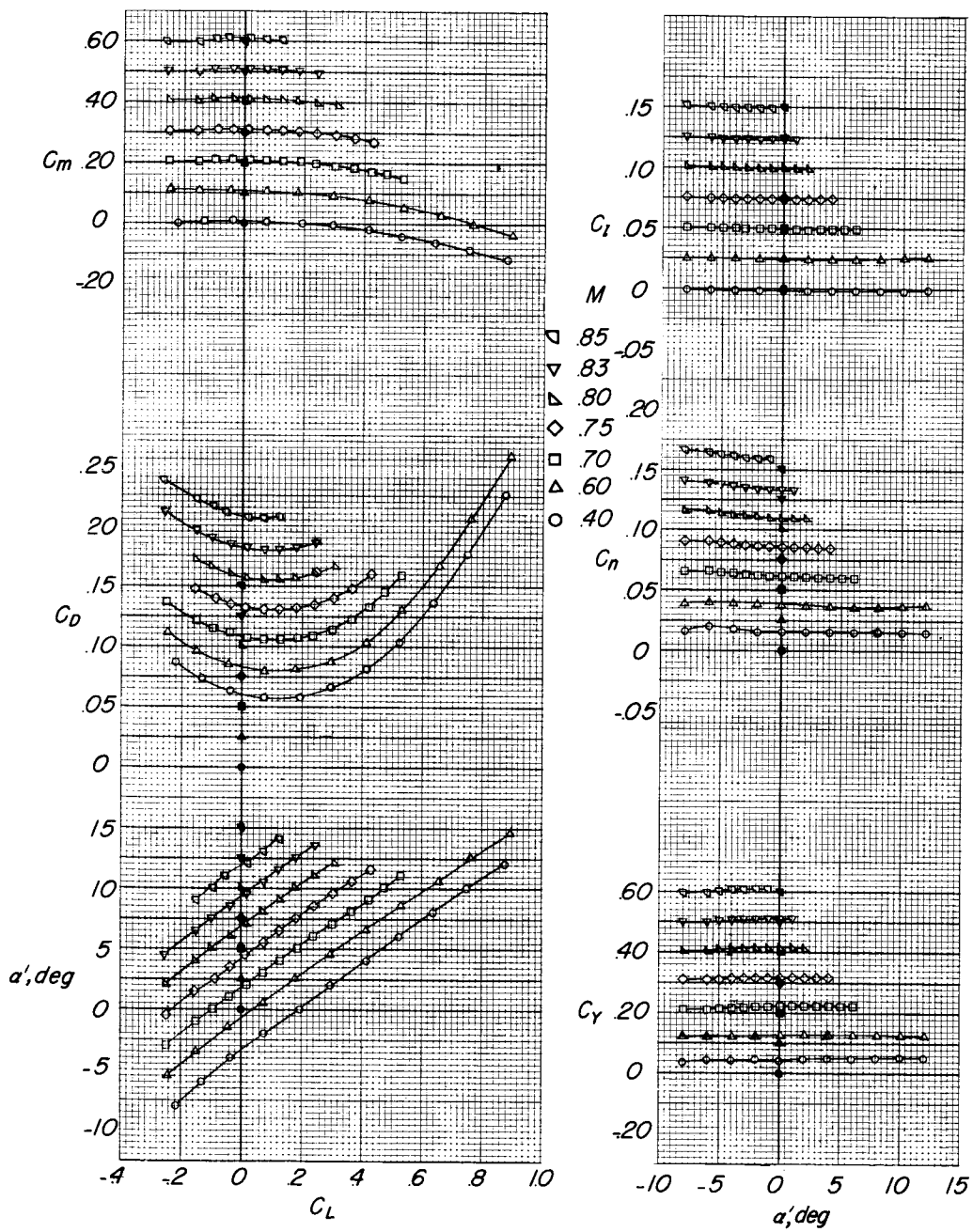
(c)   z = 12 inches.

Figure 36.- Concluded.

118
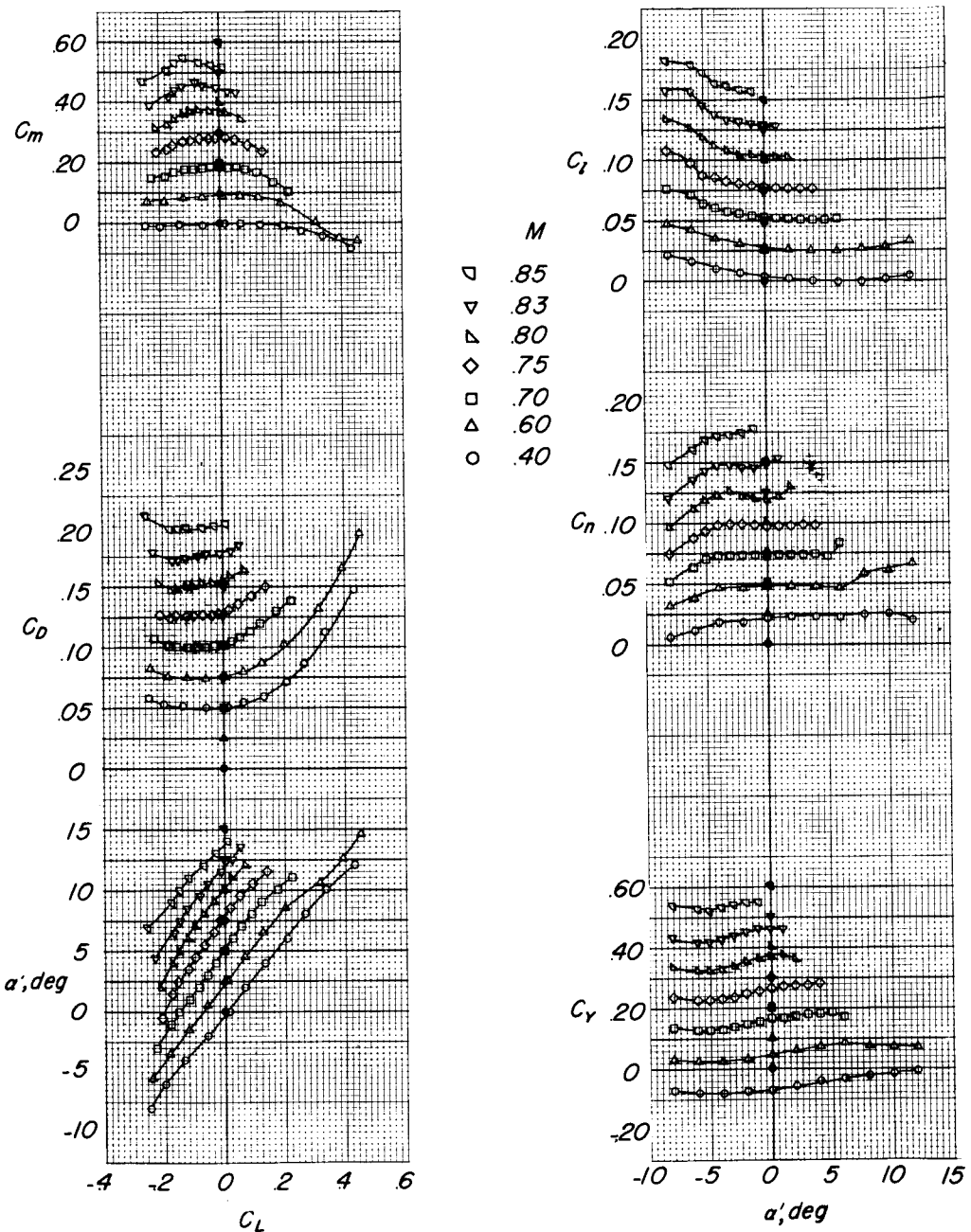


(a)  z = 1 inch.

Figure 37.- Aerodynamic characteristics of the X-15 model in the presence
of the B-52 model.  Sting mounted; $\Delta\alpha = 1^\circ 30'$; $\Delta\beta = 2^\circ 19'$; $\Phi = 0^\circ$.
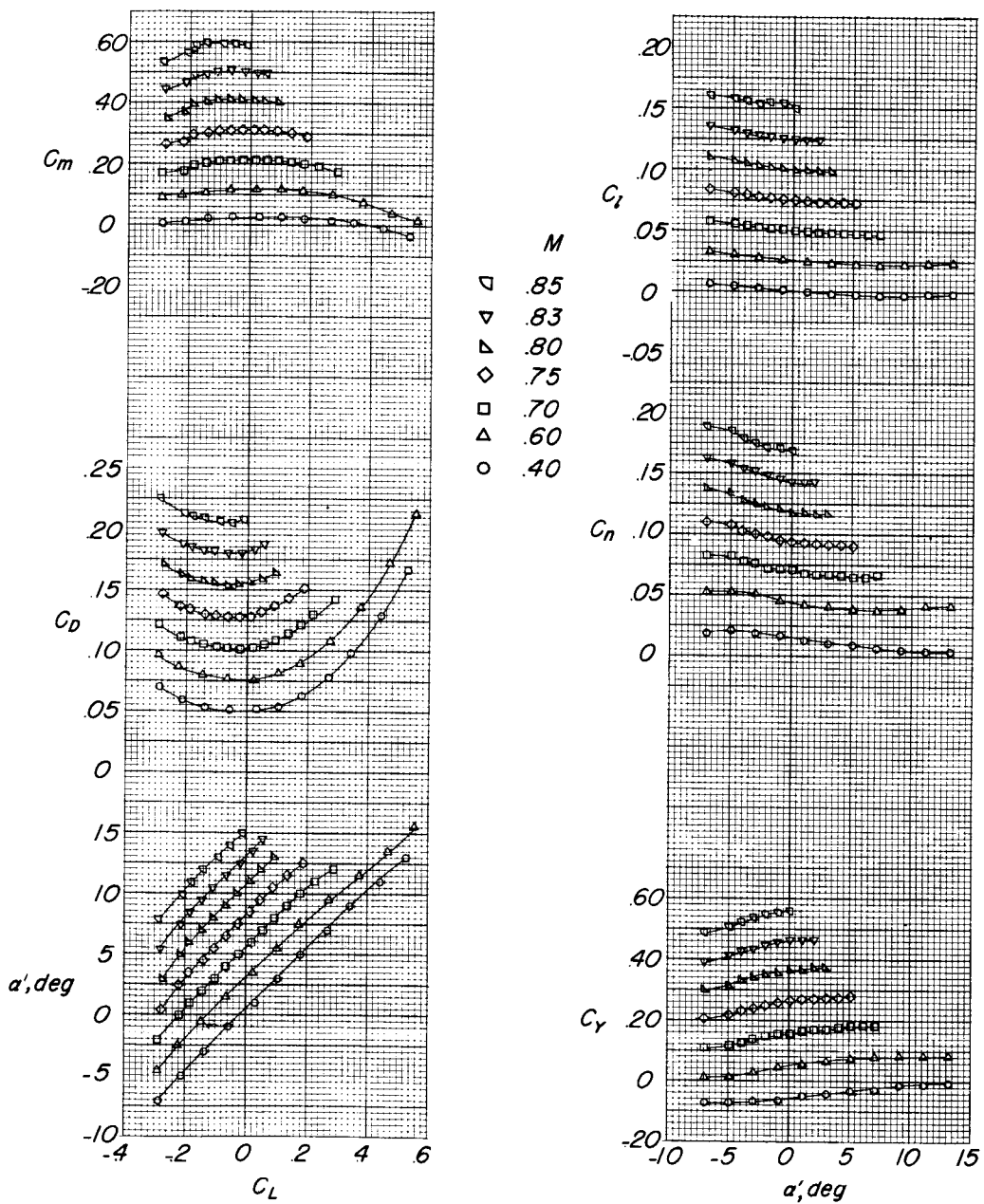
(b)  z = 4 inches.

Figure 37.- Continued.
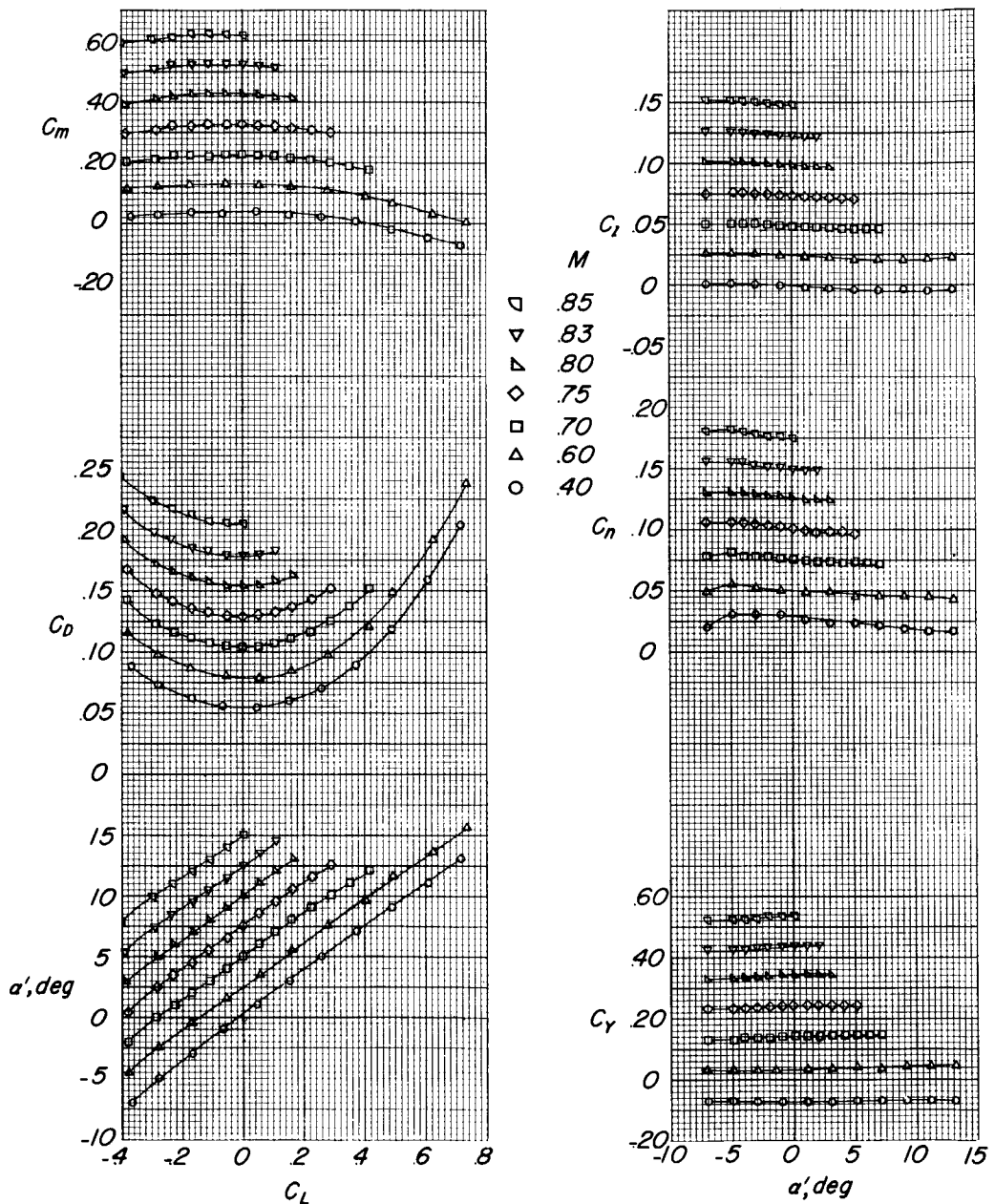
(c)   z = 12 inches.

Figure 37.- Concluded.
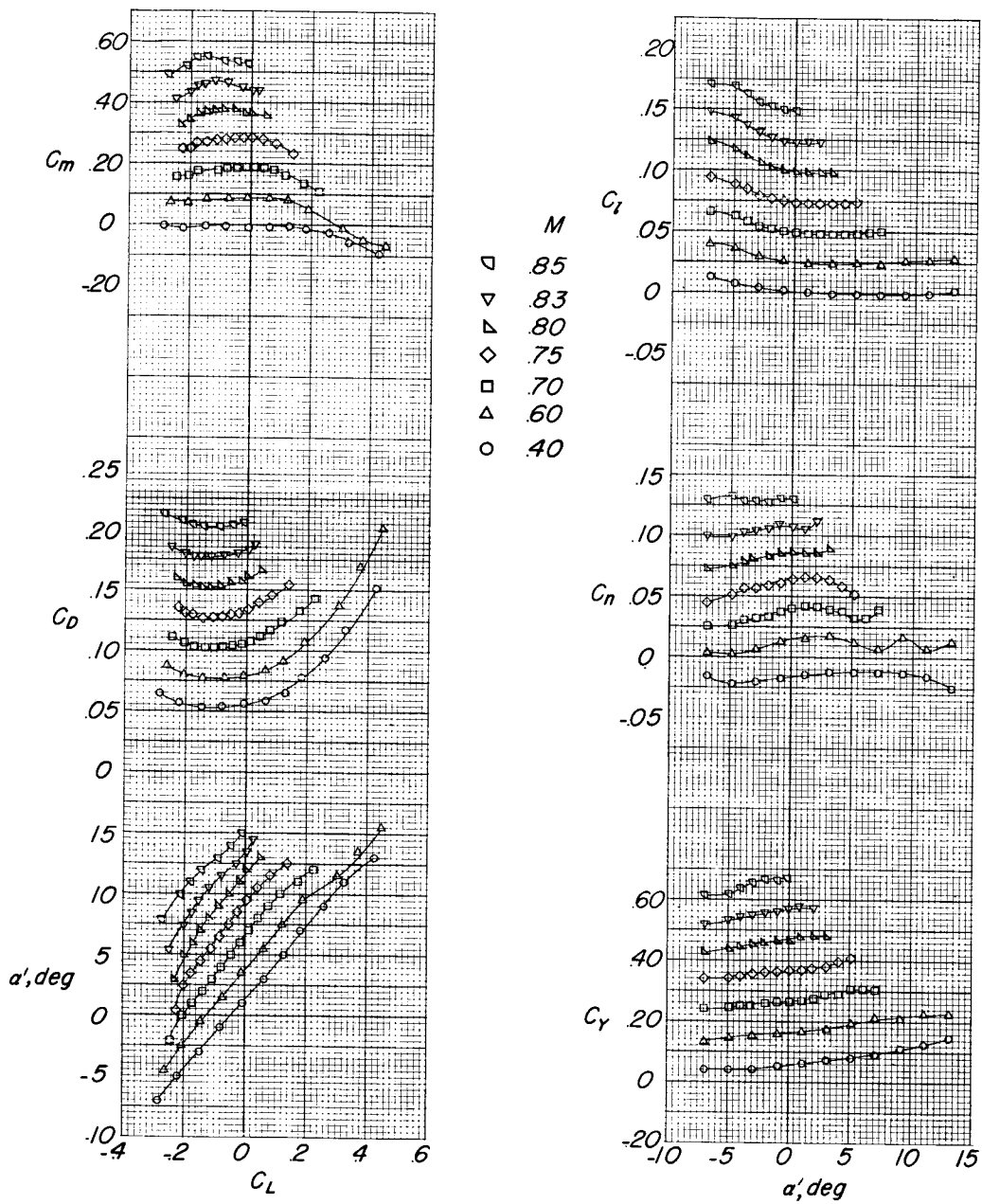
(a)  z = 1 inch.

Figure 38.- Aerodynamic characteristics of the X-15 model in the presence of the B-52 model.  $\Delta\alpha = 1°30'$; $\Delta\beta = -2°19'$; $\Phi = 0°$.
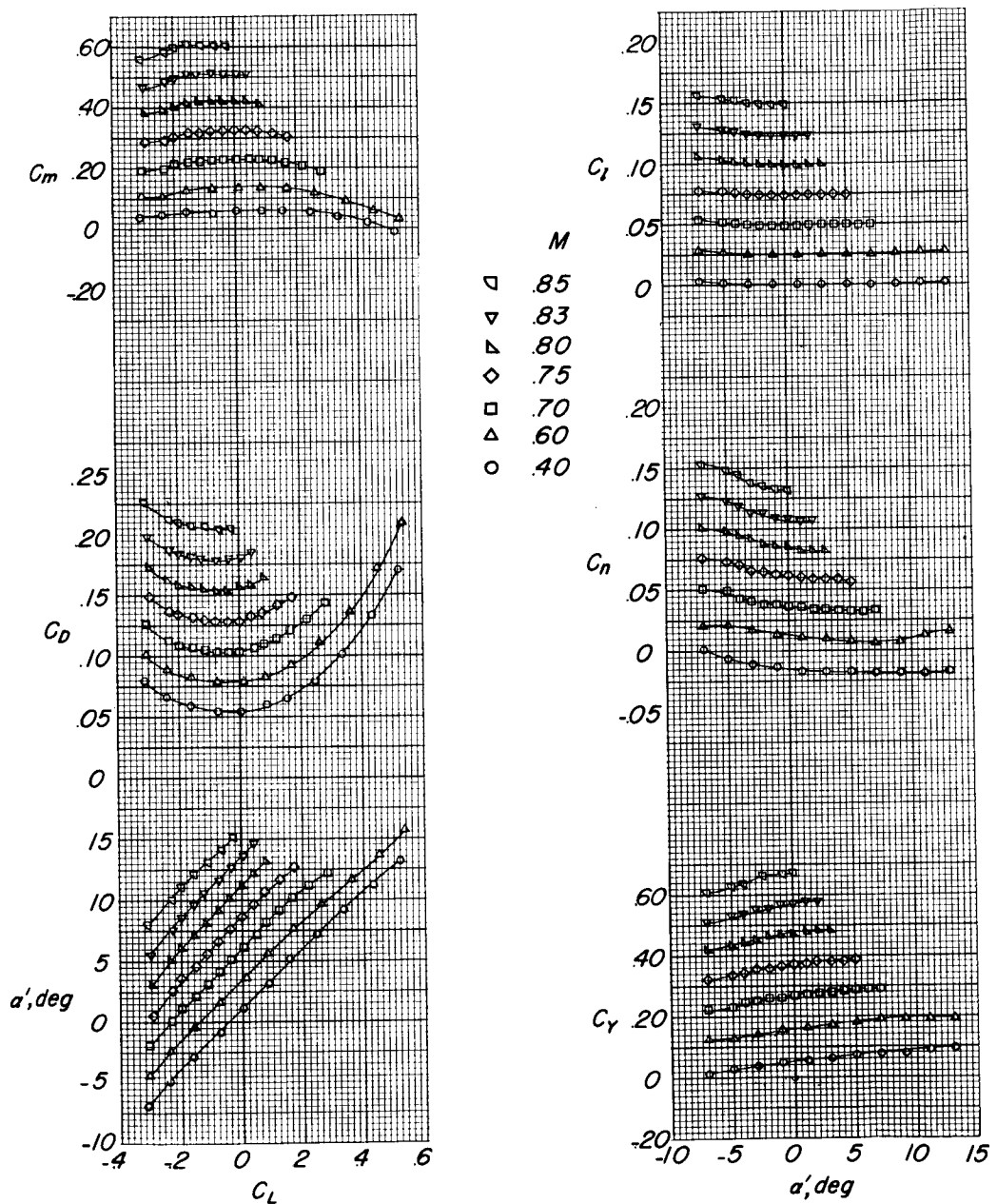
(b)  z = 4 inches.

Figure 38.- Continued.
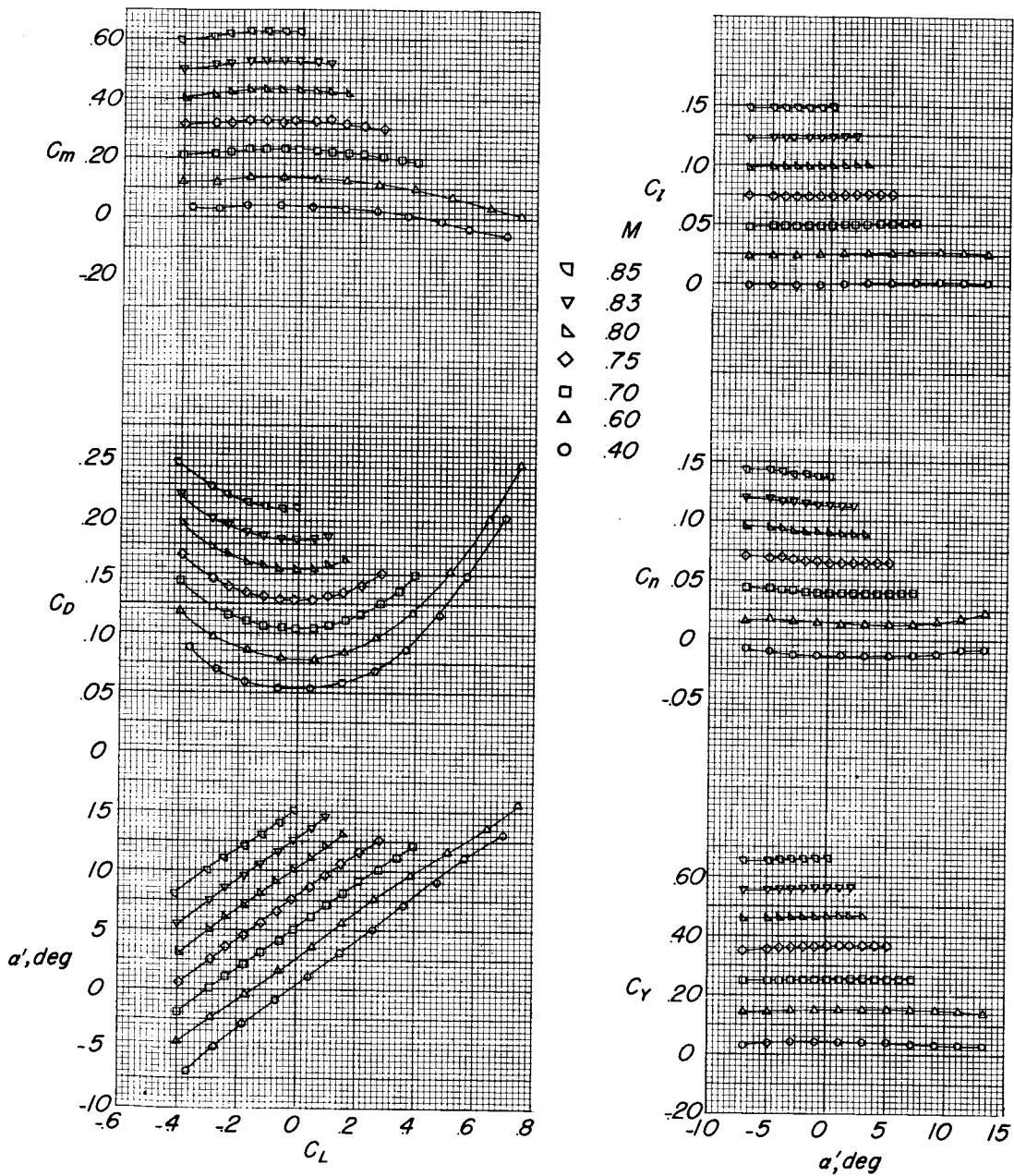
(c)  z = 12 inches.

Figure 38.- Concluded.
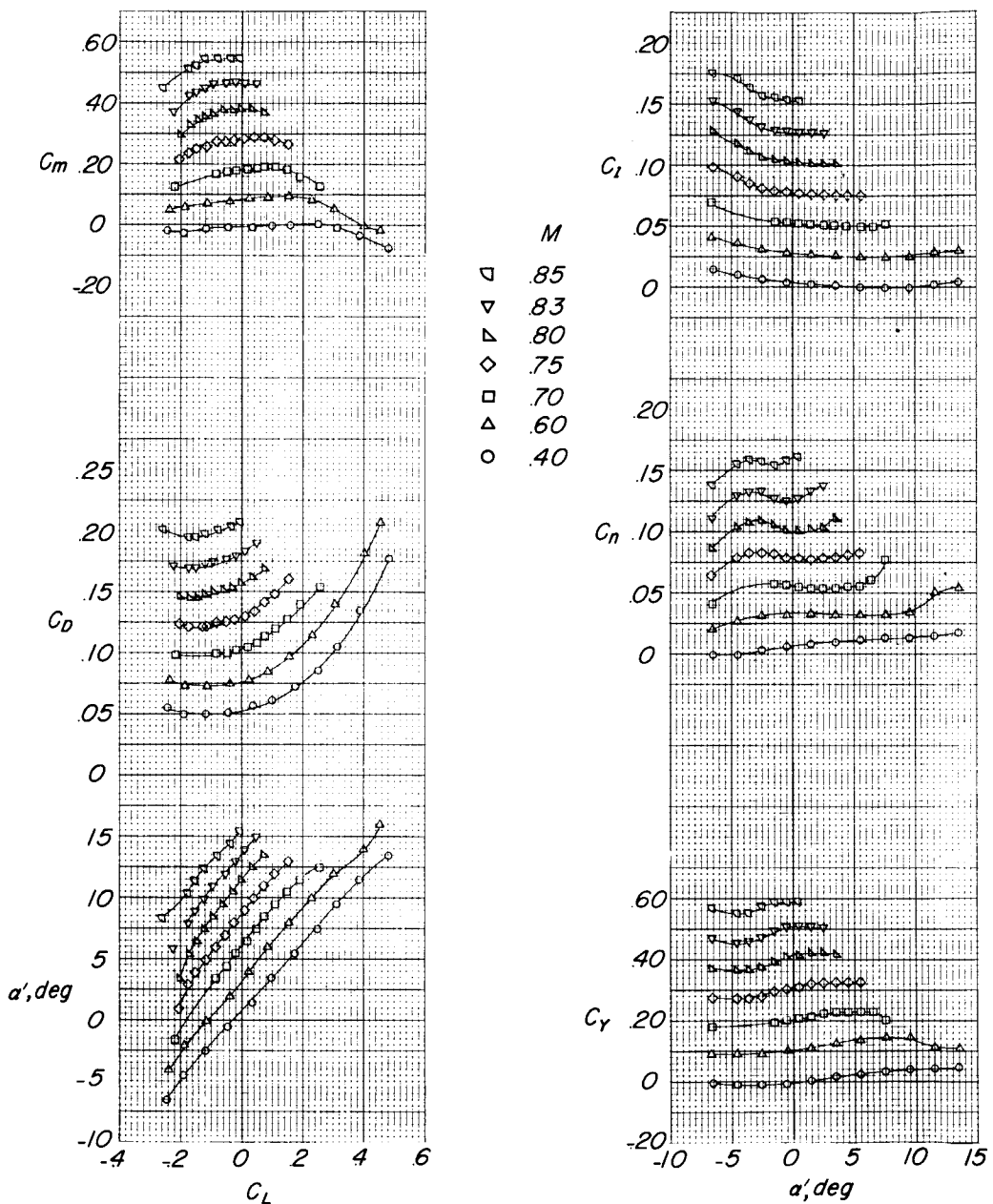
(a)   z = 1 inch.

Figure 39.- Aerodynamic characteristics of the X-15 model in the presence of the B-52 model.  Sting mounted; effect of X-15 bank angle; $\Delta\alpha = 1^\circ 30'$; $\Delta\beta = 0^\circ$; $\Phi = 9^\circ 50'$; $\delta_e = \delta_a = \delta_r = 0^\circ$.
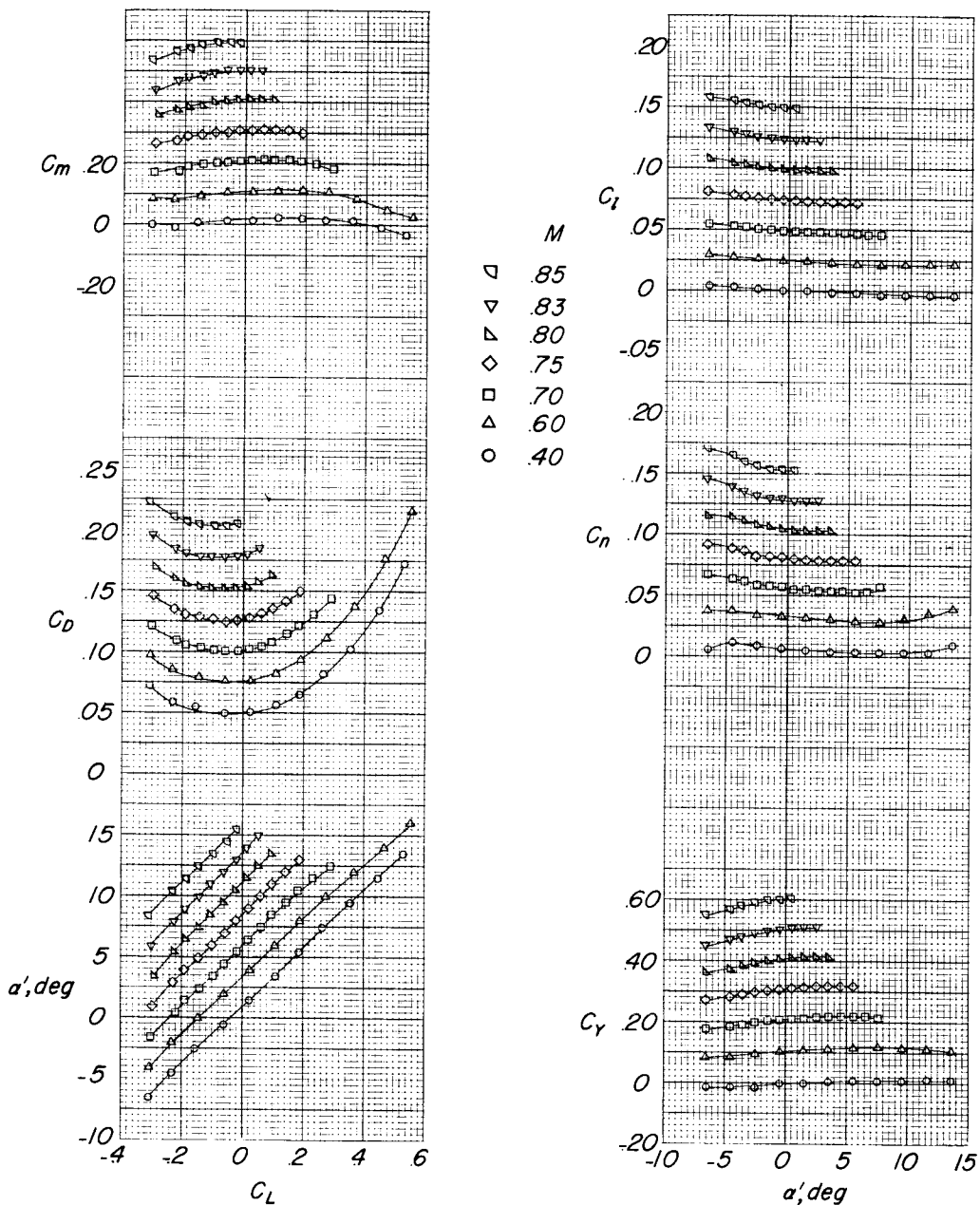
(b)  z = 4 inches.

Figure 39.- Concluded.
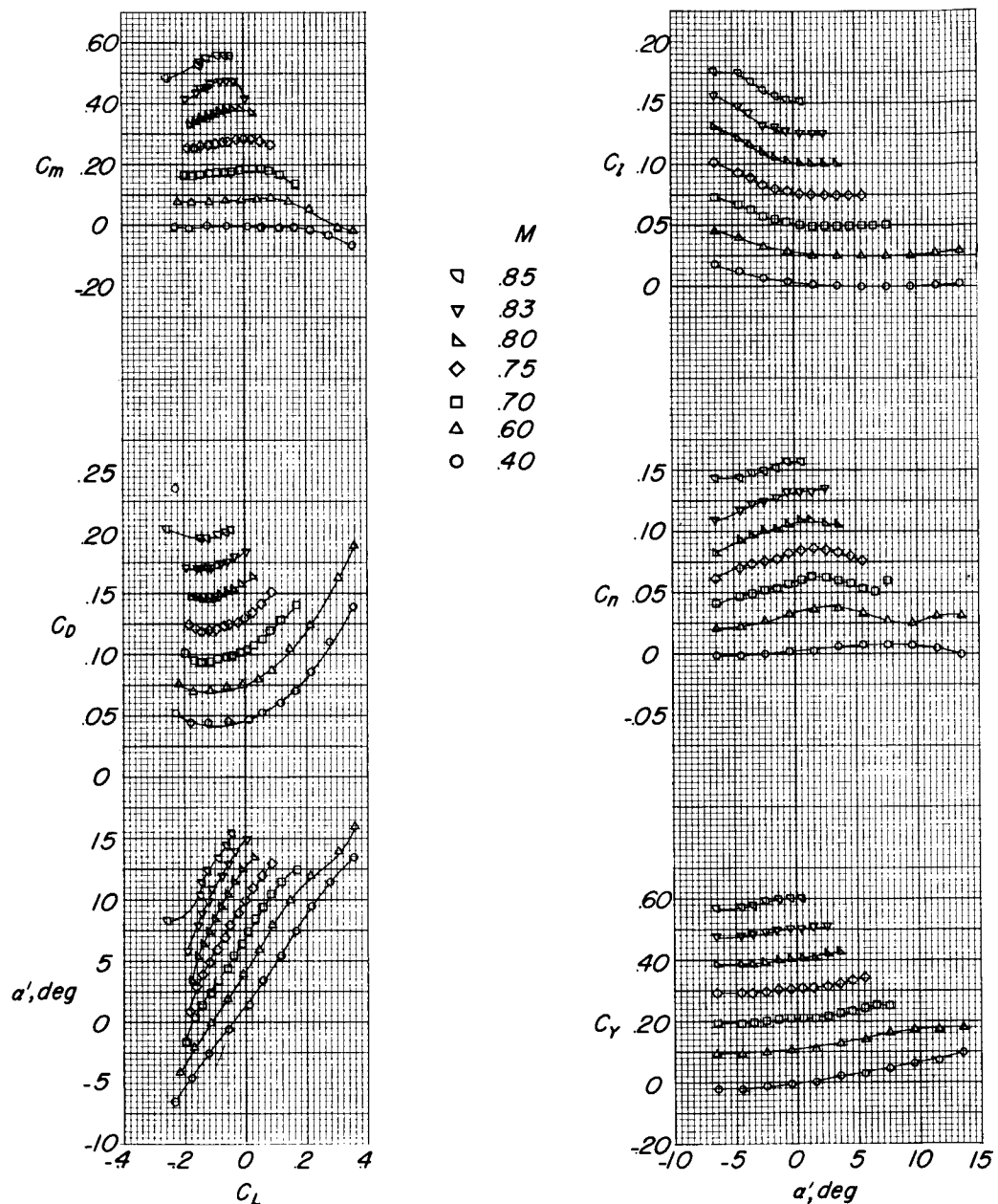
(a)  z = 1 inch.

Figure 40.- Aerodynamic characteristics of the X-15 model in the presence of the B-52 model.  Sting mounted; effect of X-15 bank angle; $\Delta\alpha = 1^\circ30'$; $\Delta\beta = 0^\circ$; $\Phi = -9^\circ50'$.  $\delta_e = \delta_a = \delta_r = 0^\circ$.
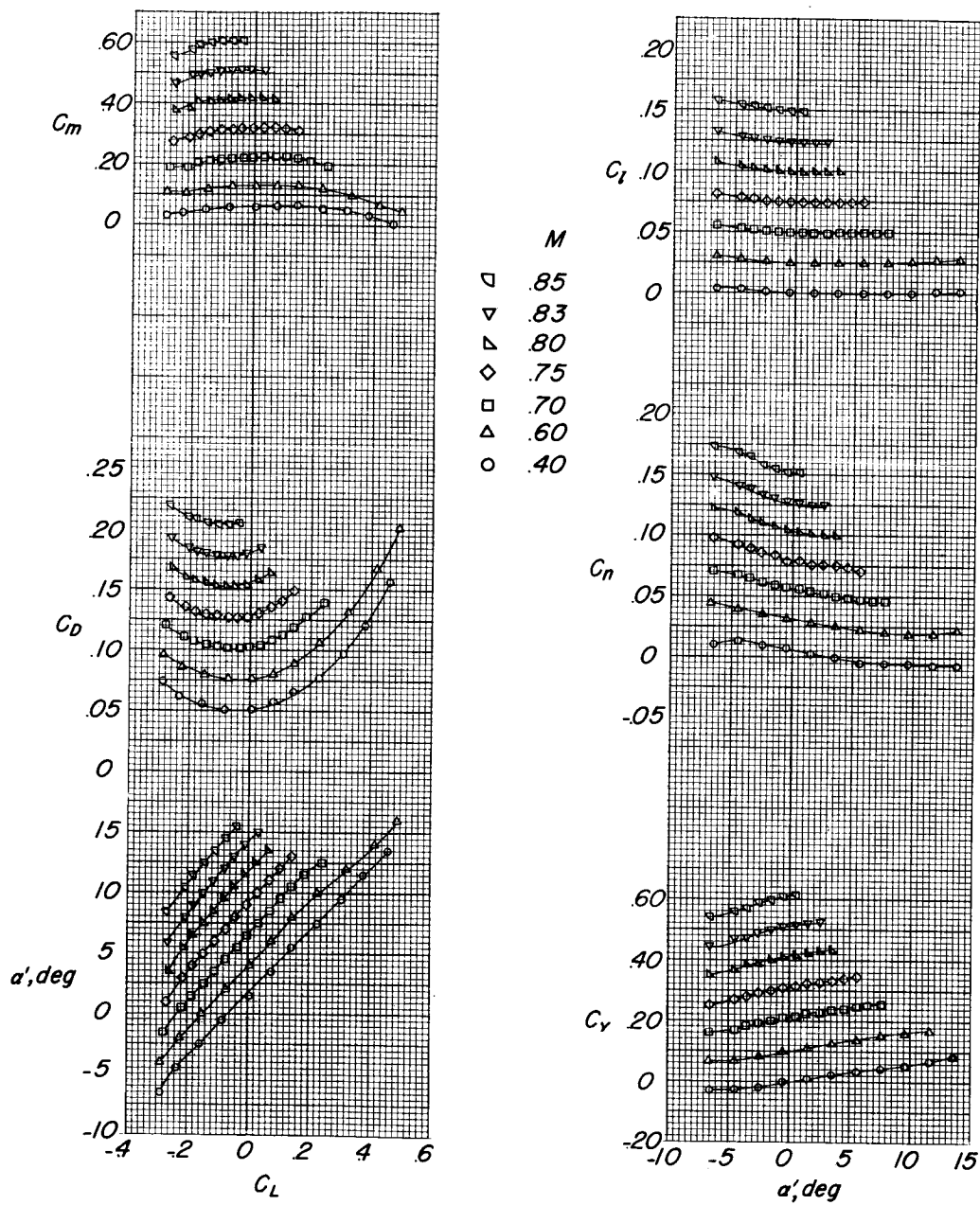
(b)   z = 4 inches.

Figure 40.- Concluded.
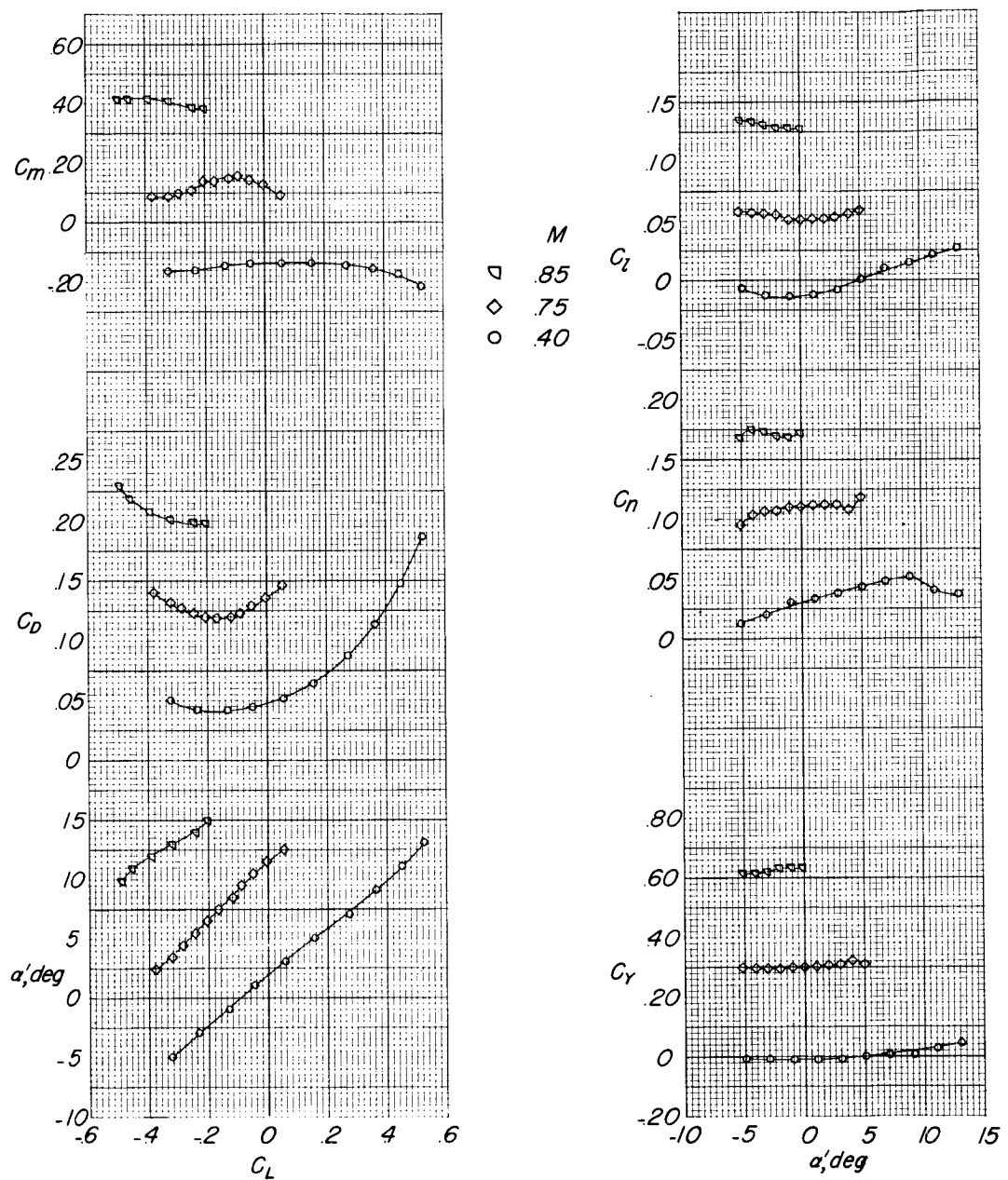
(a) Large B-52 wing fix $A_1$ in forward location.

Figure 41.- Aerodynamic characteristics of the X-15 model sting mounted in the presence of the B-52 model. Effect of wing fix; $\Delta\alpha = 1^\circ 30'$; $\Delta\beta = 0^\circ$; $\Phi = 0^\circ$; z = 0; small wing cutout.
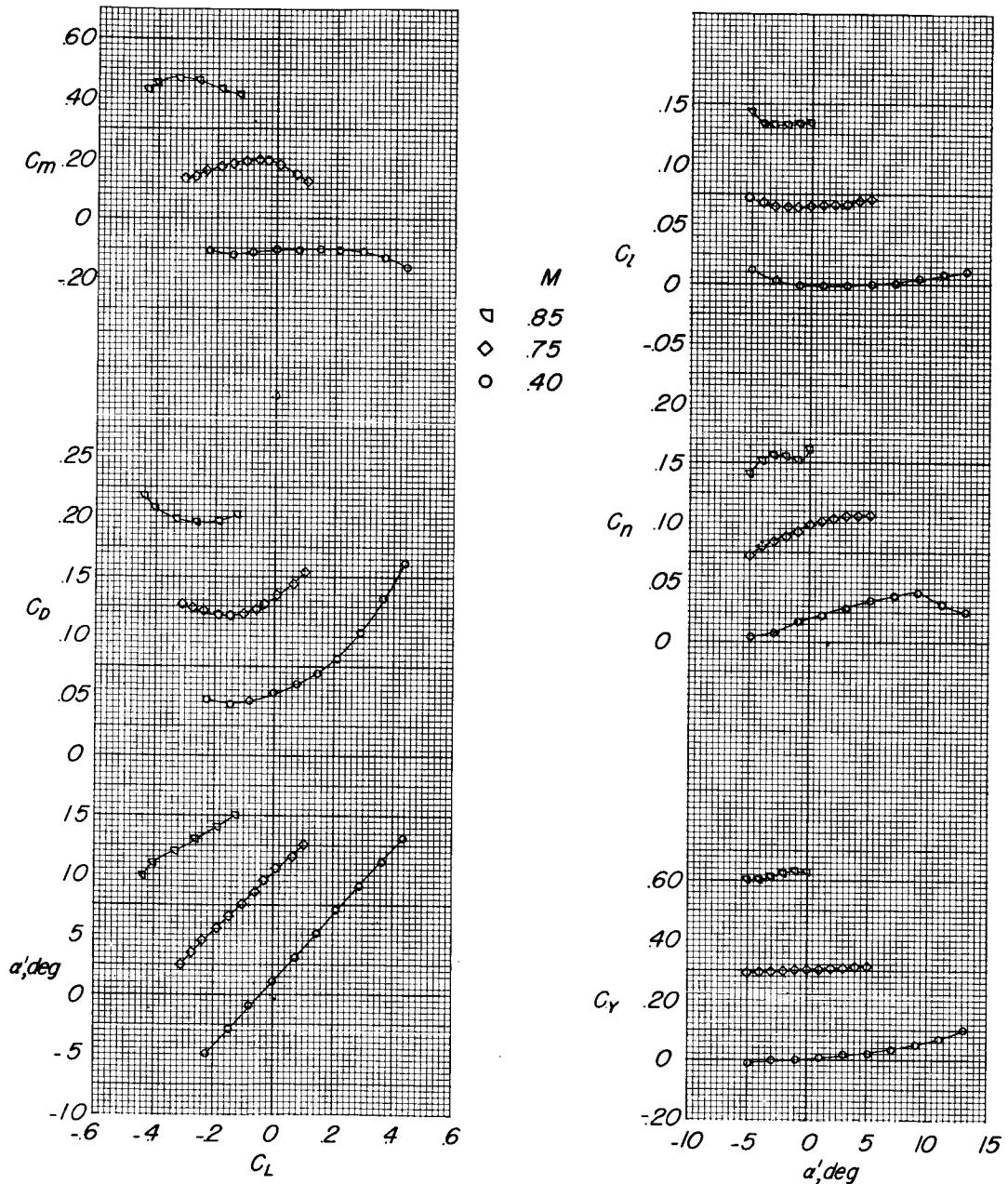
(b) Small B-52 wing fix in rearward location $B_2$.

Figure 41.- Continued.
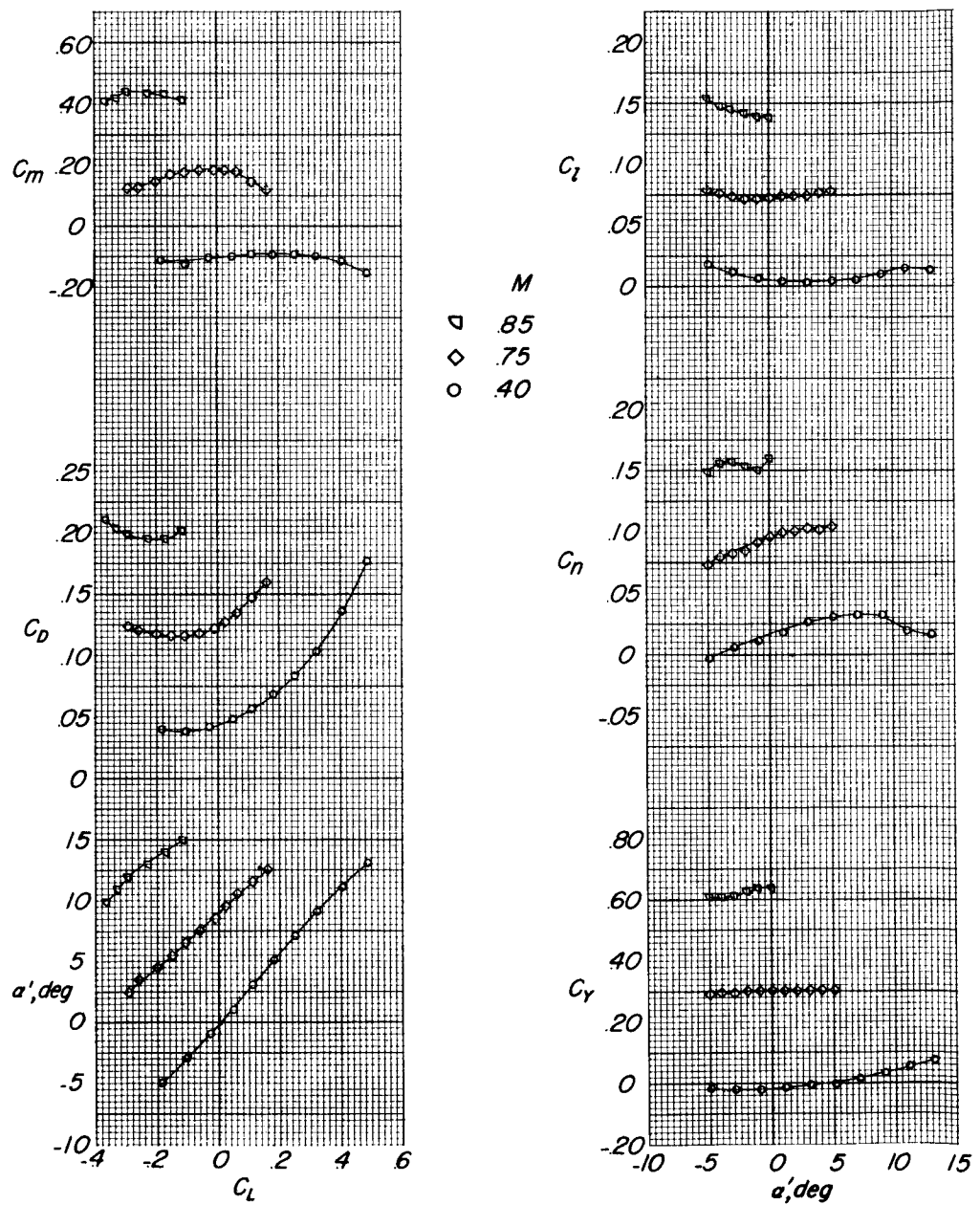
(c) Small B-52 wing-fix in forward location $B_1$.

Figure 41.- Concluded.
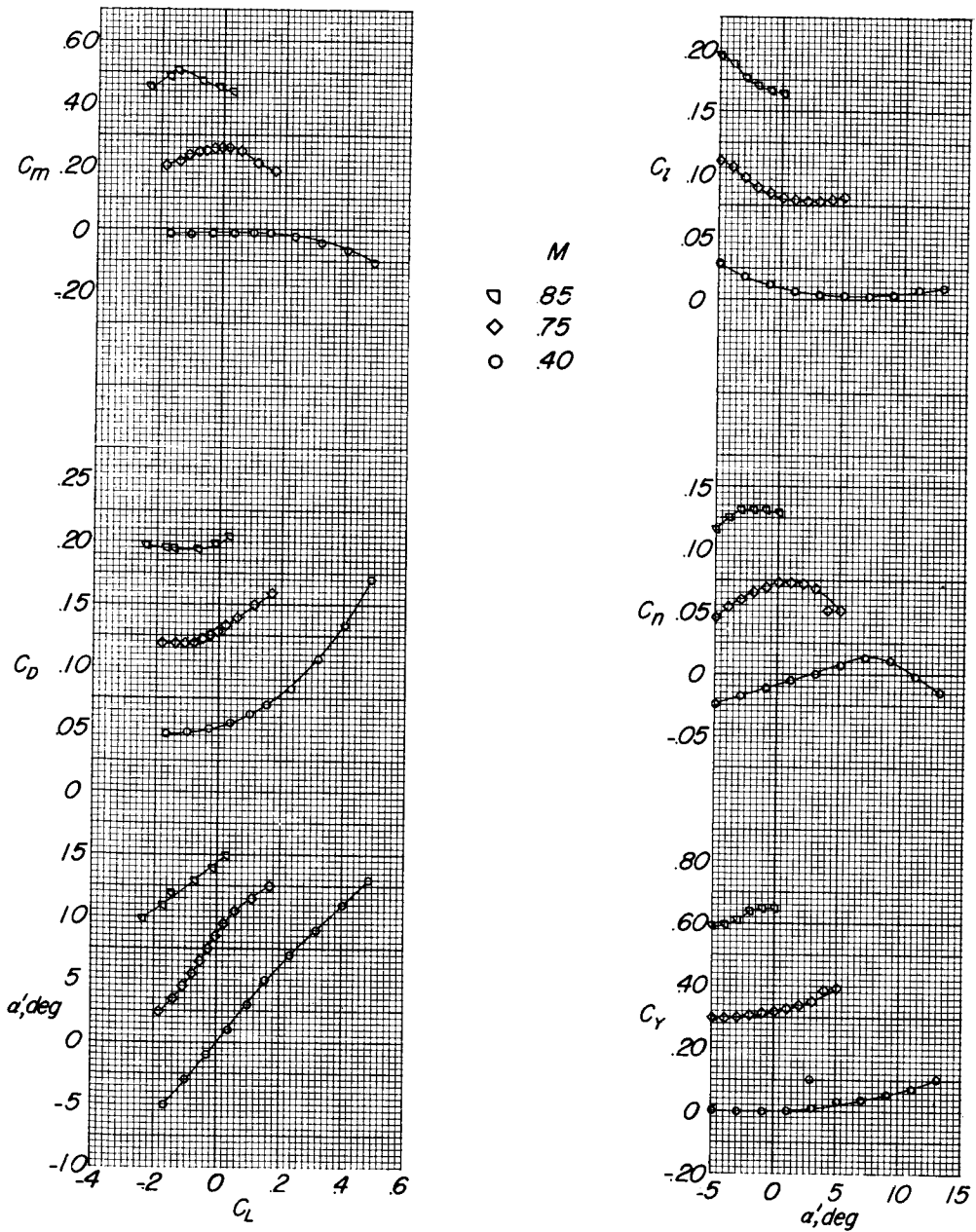
Figure 42.- Aerodynamic characteristics of the X-15 model in the presence of the B-52 model. Effect of large wing cutout B; $\Delta\alpha = 1^\circ 30'$; $\Delta\beta = 0^\circ$; $\Phi = 0^\circ$; z = 0. X-15 sting mounted.
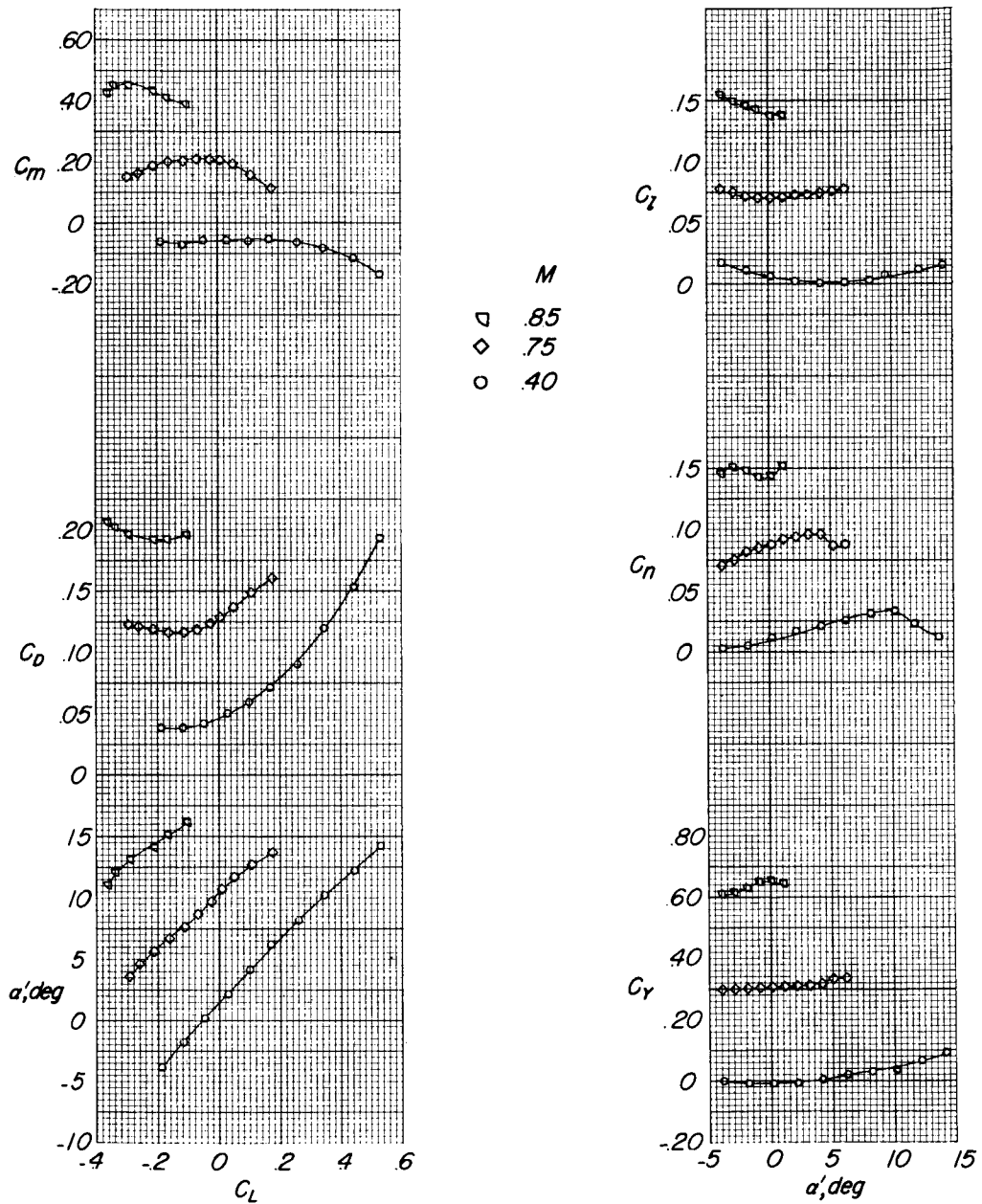
(a)  z = 0 inch; $\Delta\alpha = 1^\circ 4'$.

Figure 43.- Aerodynamic characteristics of the X-15 model in the presence of the B-52 model.  Small B-52 wing fix in forward location; large cutout in B-52 wing; $\beta' = 0^\circ$; $\Phi = 0^\circ$; $\delta_e = \delta_a = \delta_r = 0^\circ$.
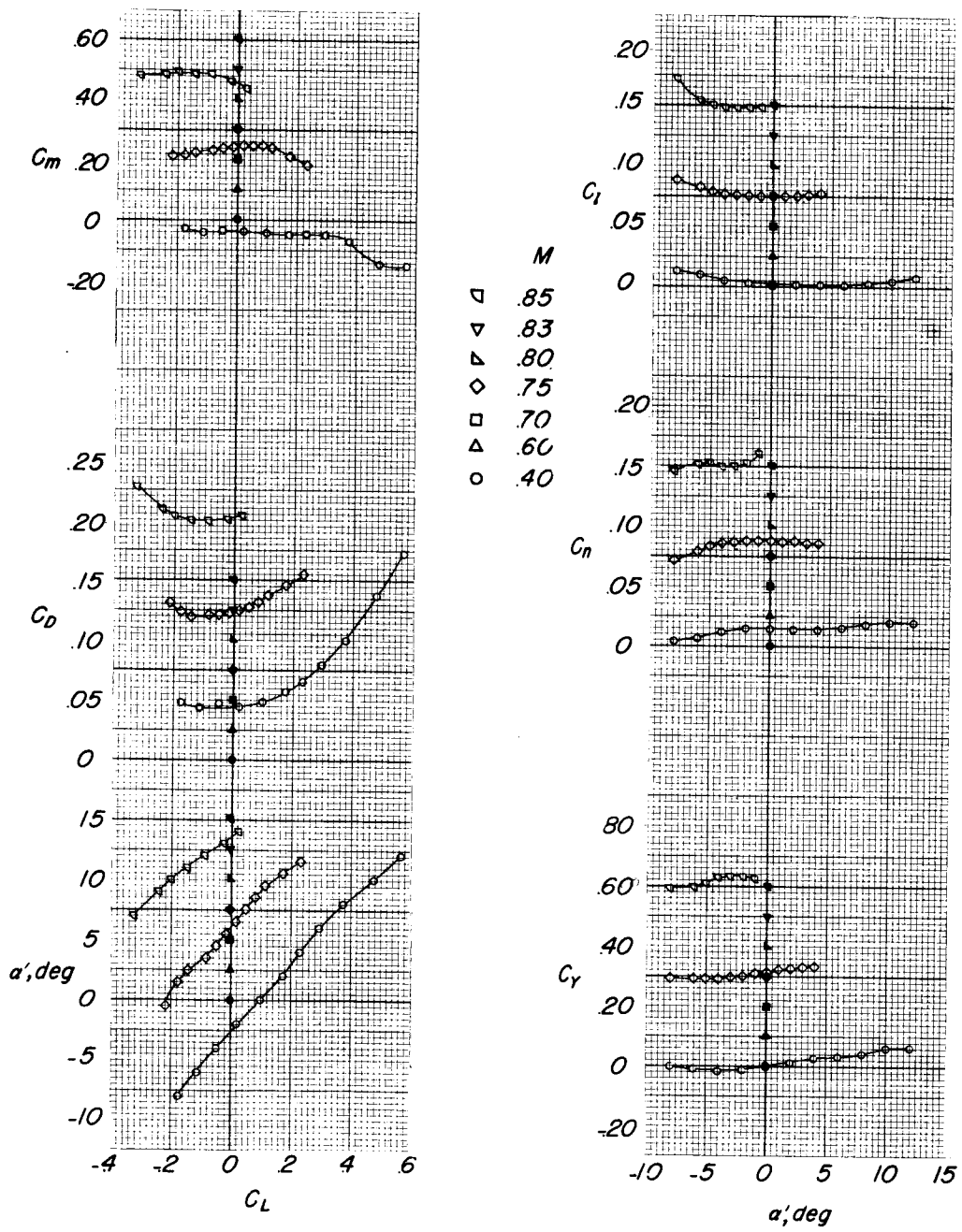
(b)  z = 1 inch; $\Delta\alpha = 2^\circ 10'$.

Figure 43.- Continued.
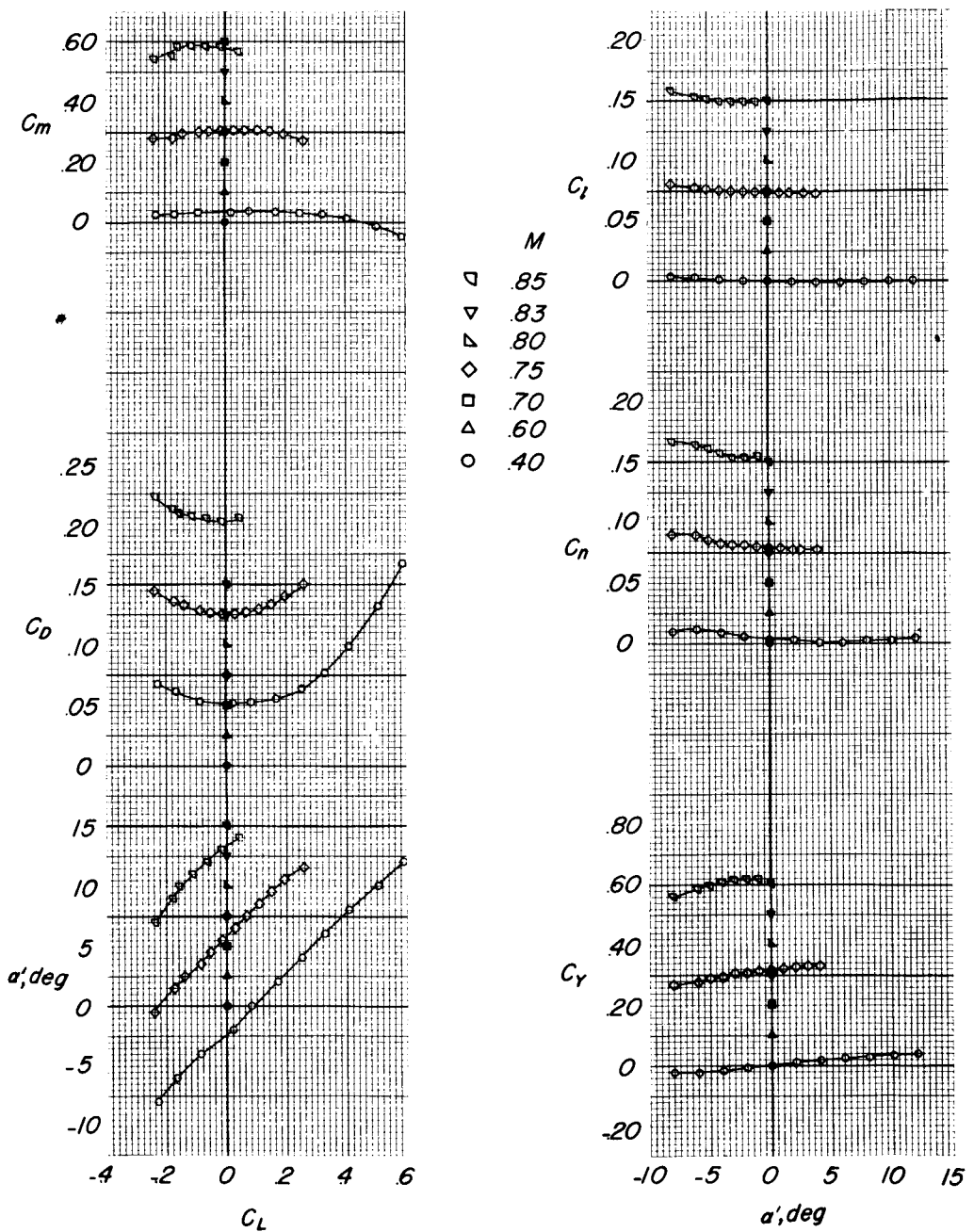
(c)  z = 4 inches; $\Delta\alpha = 2°10'$.

Figure 43.- Concluded.